Histological, ultrastructural, elemental, and molecular genetic characterization of 'Stabilstroh', a complex trait of rye (*Secale cereale* L.) determining lodging resistance.

Dissertation
zur Erlangung des Doktorgrades
der Agrarwissenschaften (Dr. agr.)

der
Naturwissenschaftlichen Fakultät III - Agrar- und
Ernährungswissenschaften, Geowissenschaften und Informatik
der Martin-Luther-Universität
Halle-Wittenberg

Vorgelegt von
Aleksandra Muszyńska
geb. am 05.11.1981 in Świętochłowice

Gutachter:

PD. Dr. Andreas Börner (IPK, Gatersleben)

Prof. Klaus Pillen (Martin-Luther-Universität Halle-Wittenberg)

Prof. Heinrich Grausgruber (Universität für Bodenkultur Wien)

Verteidigt am: 18.06.2018

HALLE (SAALE), GERMANY, 2018

Mojej mamie.

Acknowledgements

I would like to express my warmest gratitude to those, who helped me during this project, as well as those, whose paths crossed with mine and became a big part of my life during my PhD studies.

To my supervisors: Dr. Andreas Börner, Dr. Gilbert Melz, Dr. Michael Melzer, Prof. Klaus Pillen, and Dr. Marion Röder for giving me the opportunity to take part in this project, as well as constructive suggestions, valuable support, and indispensable help. Special thanks to Dr. Börner for his inspiring words, expert advice, patient guidance, encouragement, and constant support.

To all the members of SZB Group: Dr. Twan Rutten, Dr. Marek Marzec, Dr. Pooja Pandey, Monika Wiesner, Marion Benecke, Kirsten Hoffie, Theresa Engling, and Sibylle Freist for welcoming me warmly in the group, for all the things they taught me, and for giving me their time and advice.

To Dr. Kai Eggert, Dr. Yudelsy Antonia Tandron Moya, and Susanne Reiner for the establishment of the method and analysis of elements content.

To all wonderful technicians, who were always there whenever I needed, ready to share their experiences and to give me their time: Stefan Ortleb (AAN), Rosi Czihal (GGK), Anette Heber (GGK), Corinna Trautewig (PBP), and Anette Marlow (RGR).

To Dr. Ruonan Zhou and Dr. Ahmad Alqudah for giving me hints for the construction of genetic maps.

To Dr. Eva Bauer for kindly providing me sequences for the development of KASP markers.

To Dr. Borisjuk for encouraging me on every little step, giving me opportunities to grow, investing her time and resources in my development, showing me how to be strong, and for believing in me.

To Dr. Britt Leps, for saving me many times from a bureaucratic hassle, for your devotion, for giving me feeling I am not alone, and for taking care. I am sure I would not manage to finish this thesis without your support.

To all my friends: Twan, Alex, Rico, Monika, Karolina and Piotr, Damian and Ania, Ralf, as well as the IPK Polish community for offering me their friendship and emotional support, for sharing good times and hard times, and for letting me win at board games when things were not so great.

To my loving family, who always supported me in every decision, invested in my education, stood by my side, and let me doing what I loved. Thank you for your patience, love, and understanding.

Table of contents

List of figures

List of tables

List of abbreviations

10YR 4/2	Dark greyish brown soil according to Munsell soil colour description
10YR 4/3	Brown soil according to Munsell soil colour description
AGPs	Arabinogalactan proteins
AGs	arabinogalactans
Ara*f*	α-L-arabinofuranosyl
BC	Boron content
Bc1	*Brittle culm1* gene
Bk2	*Brittle stalk2* gene
bp	Base pairs
bs$_{1,2}$	Recessive *brittle stem* alleles
CaC	Calcium content
CCD	charge-coupled device
CesA	*Cellulose synthase A* gene
CIM	Composite Interval Mapping
CMS	Cytoplasmic Male Sterility
COMT	Caffeic acid 3-*O*-methyltransferase
CSI	Cellulose synthase interacting protein
Csl	*Cellulose synthase-like* gene
CSSL	Chromosome segment substitution line
ct	*compactum* gene
CuC	Copper content
CW	Cell wall
CWT	Culm wall thickness
DArT	Diversity Arrays Technology
DArTseq	Diversity Arrays Technology deploying sequencing of the representations on the Next Generation Sequencing platforms
DBI	Diameter of the basal internode
DEC	Diameter of epidermal cell
DEP1	*Dense and Erect Panicle1*
DNA	Deoxyribonucleic acid
DSC	Diameter of sclerenchymal cell
dw	Recessive *dwarf* gene
Dw/Ddw	*(Dominant) Dwarf* gene
DWC	Dry weight of culms

DWS	Dry weight of a single culm
ECW	Inner periclinal cell wall of the epidermis
EDTA	Ethylenediaminetetraacetic acid
EpI	Epidermal invaginations
EXTC	Extensin type gamma
F_2	Second filial generation of offspring
FA	formaldehyde
FeC	Iron content
FRET	fluorescence resonance energy transfer
GA	Glutaraldehyde
GA	Gibberellic acid
GAX	Glucuronoarabinoxylans
GPI	Glycosylphosphatidylinositol
GRPs	Glycine-rich proteins
HCl	Hydrochloric acid
HRGPs	Hydroxyproline-rich glycoproteins
ICP-OES	Inductively coupled plasma optical emission spectrometry
IPA1	*Ideal Plant Architecture1*
IVB	Inner vascular bundles
KASP	Kompetitive Allele Specific PCR
KC	Potassium content
KCl	Potassium chloride
LBI	Length of the second basal internode
LDL	Low-density lipoprotein
LM	Light microscopy
LOD	logarithm of the odds
lx	Lux
MAS	Marker Assisted Selection
MgC	Magnesium content
$MgCl_2$	Magnesium chloride
miRNA	microRNA
MnC	Manganese content
Moc	Molybdenum content
MOT1	Molybdate transporter1
MT	*Metallothionine* gene
NaC	Sodium content
NaCl	Sodium chloride
NGS	Next Generation Sequencing

NiC	Nickel Content
NoT	Number of tillers
np	*nana postratum* gene
OVB	Outer vascular bundles
PbC	Lead citrate
PC	Phosphorus content
PCC	Pearson correlation coefficient
PCR	Polymerase chain reaction
PGA	Polygalacturonic acid
PGRs	Plant growth regulators
PH	Plant height
pH	Potential of hydrogen
PO	Propylene oxide
PRPs	Proline-rich proteins
PTFE	Polytetrafluoroethylene
QTL	Quantitative Trait Locus/Loci
REMS	Rye Expressed MicroSatellites
RFLP	restriction fragment length polymorphism
RG	Rhamnogalacturonan
Rht	*Reduced height* genes
RIL	recombinant inbred line
RMS	Rye MicroSatellites
SAM	S-adenosyl methionine binding domain in COMT proteins
SC	Sulfur content
ScL	Sclerenchymal tissue layer
SCM	Secale cereale Microsatellites
ScR	The ratio of the thickness of sclerenchyma to the diameter of the internode
SCW	Sclerenchymal cell wall
SD	standard deviation
SDS	Sodium dodecyl sulfate
SEM	Scanning electron microscopy
SiC	Silicon content
SIM	Simple Interval Mapping
SNP	Single-Nucleotide Polymorphism
SSR	Single Sequence Repeat
TaCM	Wheat caffeic acid 3-*O*-methyltransferase gene
Taq	*Thermus aquaticus* thermostable DNA polymerase
TBE	Tris/Borate/EDTA buffer

T E	Tris/EDTA buffer
TEM	Transmission electron microscopy
THRGPs	Threonine-hydroxyproline-rich glycoproteins
UA	Uranyl acetate
UV	Ultraviolet
WFP	*Wealthy Farmer's Panicle*
WMS	Wheat MicroSatellites
XET	Xyloglucan endotransglycosylase
XTHs	Xyloglucan transglycosylases/hydrolases
XyGs	Xyloglucans
Xyl*p*	B-D-xylopyranosyl
ZnC	Zinc content

1. Introduction

1.1 | Rye

Rye (*Secale cereale* L.) belongs to the grass family, Poaceae (syn. Gramineae), in the tribe of Triticeae (Tang *et al.,* 2011). This crop plant is adapted to a wide range of environmental and climatic conditions, thus capable of producing higher yields than wheat and barley under adverse conditions, what enabled it to become a staple food grain at higher altitudes, in tropical and subtropical latitudes, and in regions with poor sandy or rocky soils and severe winters (Karpenstein-Machan and Maschka, 1996; Geiger and Miedaner, 2009; Tang *et al.,* 2011). Rye is also known for its low pH and aluminium tolerance (Geiger and Miedaner, 2009; Tang *et al.,* 2011). Additionally, rye bears genes associated with: high protein content, resistance to many cereal diseases, sprouting, drought, winter hardiness, and other morphological and biochemical traits, which can be transferred to closely related crops (Rakowska, 1996; Geiger and Miedaner, 2009; Tang *et al.,* 2011). Moreover, rye is known to have the lowest requirements for fertilisers, herbicides, and pesticides, proving the plant as being the most ecologically pure product for the direct bread production (Madej, 1996; Rakowska, 1996).

1.1.1 | Rye production and its uses

Referring to the database of the Statistics Division of the Food and Agriculture Organization of the United Nations (FAOSTAT, 2016), rye is the ninth major cereal grain worldwide and the fifth in the European Union (after wheat, maize, barley, and triticale) by its production. In Germany, rye is even more popular, being the fourth most cultivated cereal grain, after wheat, barley, and maize (FAOSTAT, 2016). Most of the rye produced worldwide is grown in the cool temperate zone, known as 'the rye belt', which is spreading from the Netherlands, through the North and East European Plain, to the Ural Mountains (Bushuk, 2001). The world production of rye in 2014 was 15,337,075 tonnes, and 8,804,588 tonnes in the European Union, which corresponds to 57.41% of the world production (FAOSTAT, 2016). The largest producers of rye in 2014 were Germany with 3,854,400 tonnes (25.13% of world production), Russian Federation with 3,280,759 tonnes and Poland with 2,792,593 tonnes (Fig.1; FAOSTAT, 2016).
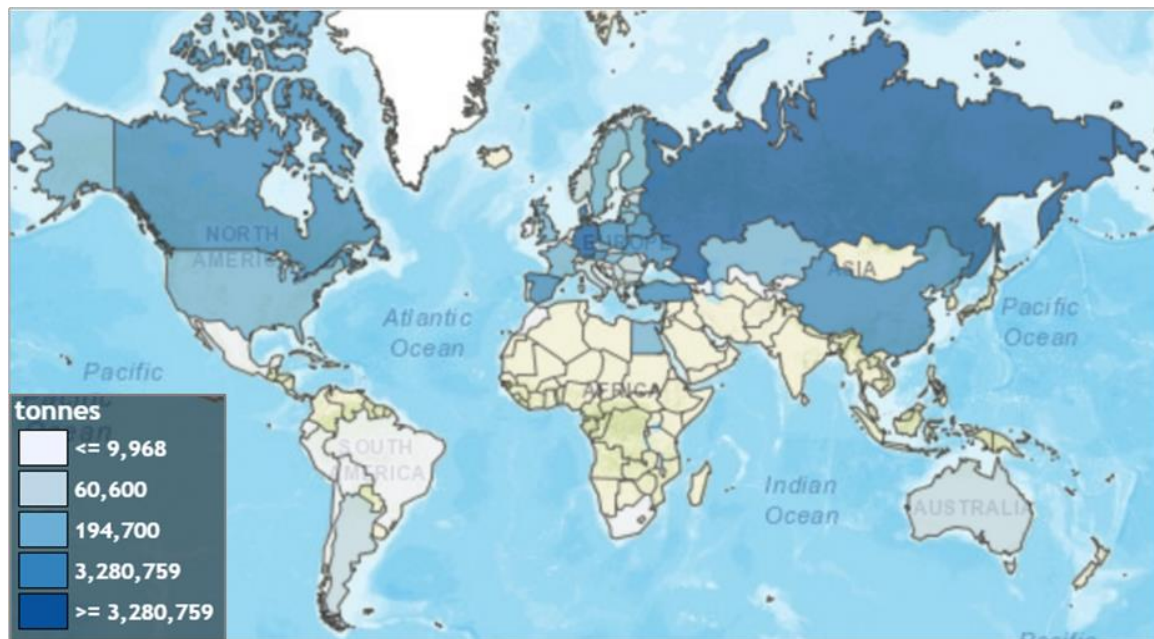
FIGURE 1 World production of rye in 2014 by countries (FAOSTAT, 2016).

Over the years 1961-2014, there has been a clear downward tendency in the rye production and its harvested area in the world and the European Union (Fig.2; FAOSTAT, 2016). The decrease in the cultivated area was substantial since the 1970s, mainly as an offset by an increase in yield (Bushuk, 2001). Nowadays, the decreasing rye harvested area is the result of low prices of such cereal in the previous years, strongly affecting the profitability of its production. Additionally, rye production has lost to more lucrative triticale over the years since 1975 (Fig.3; FAOSTAT, 2016).

Nevertheless, because of the winter hardiness of rye and its ability to grow on soils with marginal fertility and consumer demand for its products, rye should keep its role as an essential crop (Bushuk, 2001; Geiger and Miedaner, 2009). New high yielding population and hybrid varieties have taken yielding potential, lodging resistance, and baking quality, offering the yield comparable to other cereals, regardless of the level of field management intensity (Madej, 1996). In Northern and Eastern Europe, rye is the second after wheat, yet the most commonly used cereal grain in the production of soft and crisp bread (Nilsson *et al.,* 1997; Bushuk, 2001; Tang *et al.,* 2011). Rye grain is also used for the production of groat, porridge, breakfast cereals, and bran, as well as for sprouts or even pasta (Bushuk, 2001; Tang *et al.,* 2011; Schlegel, 2014). Additionally, it is an important crop for the production of mixed animal feeds and as green manure in crop rotation (Bushuk, 2001; Tang *et al.,* 2011).

FIGURE 2 Agricultural parameters of rye over the years 1961-2014 (FAOSTAT, 2016): production (**A**), area harvested (**B**), and yield (**C**).
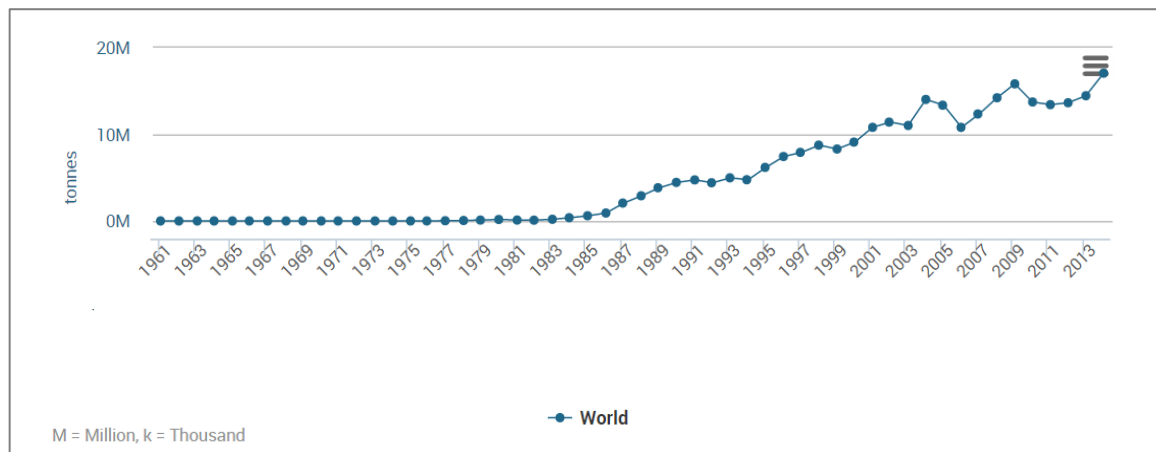
FIGURE 3 World production of triticale over the years 1961-2014 (FAOSTAT, 2016).

Rye grain contains dietary phytosterols, which inhibit cholesterol absorption, decreasing plasma levels of low-density lipoprotein (LDL) cholesterol, and thereby decreasing the risk of developing cardiovascular diseases (Schlegel, 2014). Rye grain is also rich in iron, B and E vitamins, and dietary phenolic antioxidants (Schlegel, 2014). Moreover, it is known to contain a high content of dietary fibre (150-170 g kg^{-1} in whole grain flour) and rye bread contains about three times more fibre than white wheat bread, since the endosperm of rye contains twice as much cell wall components than wheat (Rakowska, 1996; Nilsson *et al.,* 1997; Bushuk, 2001; Tang *et al.,* 2011). These characteristics of rye bread positively influence bowel activity, metabolism, and the quantity, quality, and composition of the intestinal flora, as well as offer a practical dietary means of hypocholesterolemic effects in men with moderately elevated serum cholesterol (Leinonen *et al.,* 2000; Schlegel, 2014). The protective cholesterol-lowering effect of water-soluble fibre is due to binding of bile acids in the small intestine, what enhances synthesis of bile acids from cholesterol in the liver (Leinonen *et al.,* 2000). Moreover, a diet rich in high-fibre cereal is associated with a reduced risk of colorectal cancer (Hill, 1997). By consuming whole grain bread it is also possible to reduce the absorption of biliary oestrogens and increase the faecal output of these hormones, and together with high amounts of lignans in rye, they have been shown to reduce breast cancer risk (Cade *et al.,* 2007; Aubertin-Leheudre *et al.,* 2008).

A substantial quantity of rye production is used for distilling grain into vodka, gin, and whiskey (Bushuk, 2001; Tang *et al.,* 2011). Rye is also used for the production of non-potable alcohols and biomethane used in industry for chemical engineering, pharmaceuticals, cosmetics, and fuel (Tang *et al.,* 2011; Geiger and Miedaner, 2009; Schlegel, 2014). Additionally, in the Eastern European countries, a traditional fermented drink, called kvass, is produced from rye grain (Tang *et al.,* 2011; Schlegel, 2014).

Rye can also be grown for erosion control, to add organic matter, to enhance soil life, and for weed suppression (Barnes and Putnam, 1986; De Baets *et al.,* 2011). Rye straw is highly desirable for livestock bedding and increasingly valuable for the production of traditional thatched roofs, becoming more popular nowadays (Bushuk, 2001). Small quantities of it are also used in the manufacture of strawboard and paper (Bushuk, 2001). The straw can be successfully used for bioenergy systems, such as the production of bioethanol since it has relatively high cellulose and hemicellulose content, vigorous growth, high nutrient- and water-use efficiency, and low input production (Sun and Cheng, 2005). The varieties with high growth rate, maximal biomass yield, good field resistance, and finally good lodging resistance, like Helltop and Hellvus, are desirable for biofuel production (Schlegel, 2014; Welker *et al.,* 2015).

1.1.2 | Morphology of rye

Rye is an allogamous herbaceous plant, with culms up to 150 cm high and an extensive root system (Fig.4A; Sheng and Hunt, 1991; Kutschera *et al.,* 2009; Tang *et al.,* 2011), enabling it to be the most drought-tolerant annual cereal crop and less prone to root lodging (Neenan and Spencer-Smith, 1975; Tang *et al.,* 2011). The total root length in rye depends on the density of plants: if the distance between two plants is 15 cm, the total length of roots is equal to 0.975 km, and increases to 79.03 km for plants growing every 3 m (Kutschera *et al.,* 2009). The length of the roots also depends on the type of the soil and the climate: in dry climates and poor and sandy soils, the plant develops longer and denser roots to obtain necessary nutrients and water (Kutschera *et al.,* 2009).

The culm of rye consists of several internodes, which length is the smallest at the base and increases considerably towards the top (Tang *et al.,* 2011). The nodes are smooth (Fig.4B) and internodes hollow (Tang *et al.,* 2011). Leaf blades are blue-green, flat, linear, 2.5 – 20 mm wide, long, pointed with truncate ligules, without cross venation, and hairy on the lower surface (Tang *et al.,* 2011). The leaf sheaths play an essential role in strengthening the stem, particularly when the tissues are still green and weak (Mulder, 1954). Spikes are 7-15 cm long, slender, and nodding, composed of several spikelets, one at each node (Fig.4B; Tang *et al.,* 2011). The rachis is non-shattering, hollow, and its segments are densely covered with white hairs on the edges (Tang *et al.,* 2011). Spikelets are comprised of two hermaphroditic florets, placed flatwise against the rachis (Fig.4B; Tang *et al.,* 2011). The glumes are rigid and narrow, 8-18 mm long and awned (Fig.4B; Tang *et al.,* 2011). The lemmas are broader and longer, 10-19 mm long, sharply keeled and tapering into a long awn (Fig.4B; Tang *et al.,* 2011). Palea is relatively long and apically notched, two-nerved and 2-keeled (Tang *et al.,* 2011). Three stamens and two lodicules

are present, free, membranous, and ciliate (Tang *et al.,* 2011). The anthers are 2.3-12 mm long, not penicillate, and the ovaries are hairy (Tang *et al.,* 2011). The rye kernel is ellipsoid, longer and more slender than in wheat, neither attached to the lemma, nor palea (Tang *et al.,* 2011).
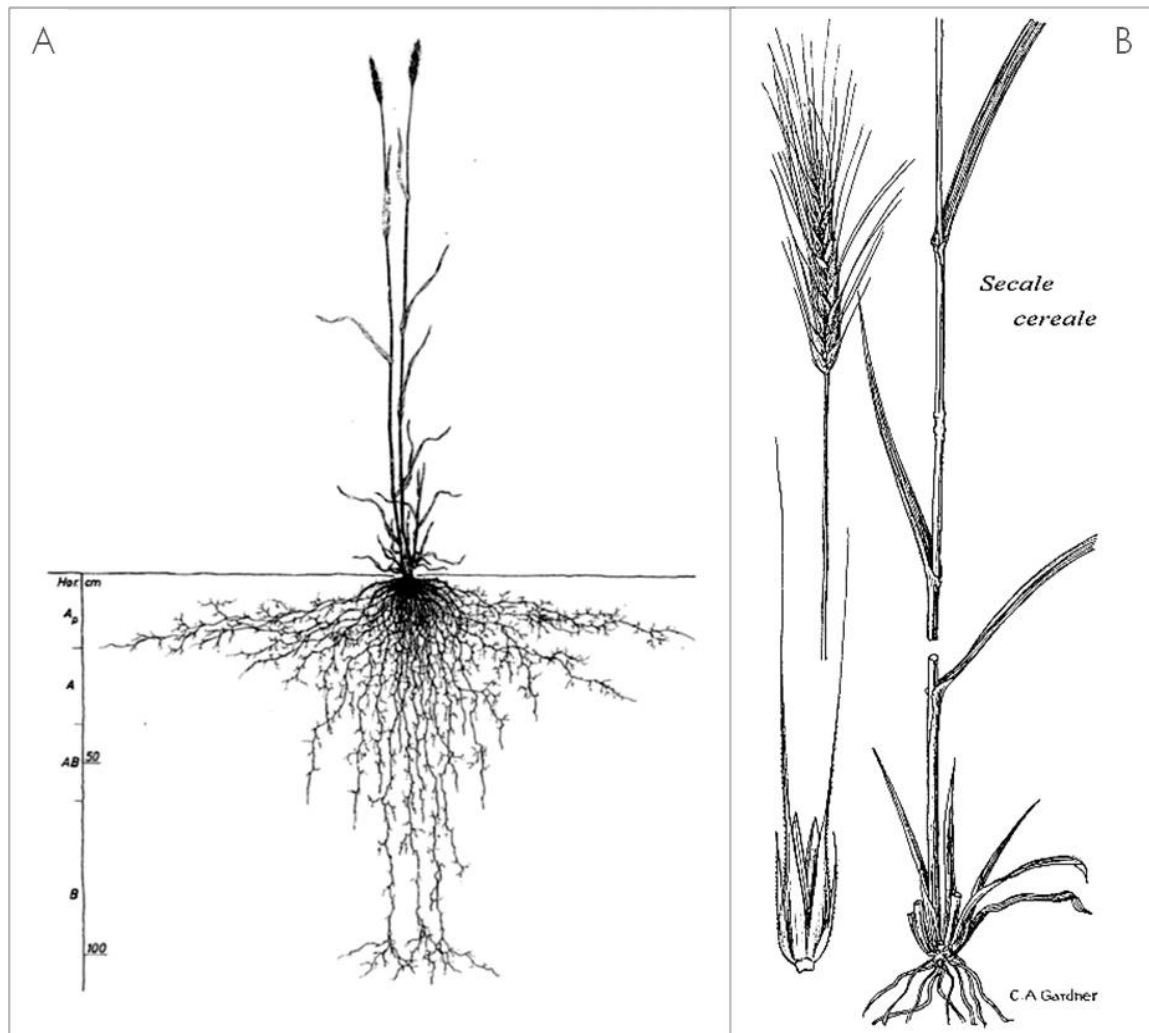
FIGURE 4 Rye morphology: root system of winter rye grown on brown soil (10YR 4/2 to 10YR 4/3) (**A**; Kutschera *et al.,* 2009), rye tillers, spikes, and florets (**B**; Gardner, 1952).

1.1.3 | Anatomy of the internode

The stem of rye is around 0.5 cm thick at the base, dictyostele type, with a large central cavity, which is the typical anatomy of internodes in the Pooideae subfamily, and from the mechanical point of view plants with the greatest diameter of lower internodes are the most desirable (Hayward, 1938; Mulder, 1954; Metcalfe, 1960).

The internode is covered with epidermal cells, compactly organised into a single continuous layer, which is uninterrupted, except for stomatal openings (Fig.5A; Hayward, 1938; Metcalfe, 1960; Rovenská, 1973). The outer and radial walls of the epidermis are thicker than the inner ones, being cutinized or suberized (Hayward, 1938; Metcalfe, 1960).

On the surface of the epidermal cells a well-developed cuticle is deposited, impregnated with cuticular waxes and covered with epicuticular waxes, what provides waterproof protection for a plant, prevents evaporation, and also functions in defence, forming a physical barrier that resists penetration by viruses, bacterial cells, and the spores or growing filaments of fungi (Hayward, 1938; Metcalfe, 1960; Freeman, 2005).
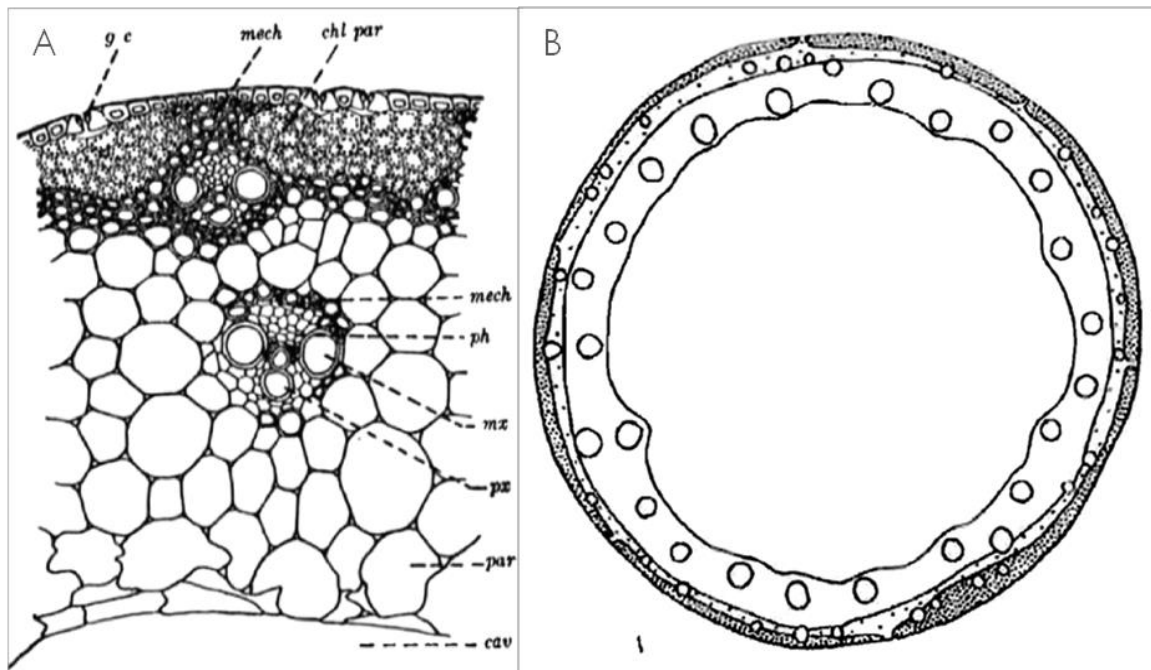
FIGURE 5 The anatomy of rye internode: scheme of a transverse section through rye internode (**A;** Hayward, 1938), distribution of outer and inner vascular bundles in the internode (**B;** Rovenská, 1973).
cav - central cavity of the stem; chl par - chlorophyll parenchyma; g c - guard cells; mech - mechanical tissue; mx – metaxylem; par - parenchyma; ph - phloem; px – protoxylem

The epidermis is subtended by a thick-walled ring of the sclerenchyma (6-8 cell layers, sometimes called hypoderm; Mulder, 1954) with flattened columns of thin-walled, circular in transection, chlorenchymal cells embedded in it, which run parallel along the stem (Fig.5A; Hayward, 1938; Metcalfe, 1960; Rovenská, 1973). The highest degree of lignification, an essential factor for lodging resistance is found in the lower internodes (Mulder, 1954). On the sides of the assimilating parenchyma, in stripes of sclerenchyma, small collateral type peripheral vascular bundles are located with phloem oriented outside, and xylem inside the axis of the culm (Fig.5A-B; Hayward, 1938; Metcalfe, 1960; Rovenská, 1973).

Under the sclerenchyma, around 12 cell layers of large thin-walled ground parenchyma are present, extending from the zone of the mechanical tissue to the central cavity (Fig.5A-B; Hayward, 1938; Metcalfe, 1960; Rovenská, 1973). The cell walls of these cells can be sometimes lignified (Mulder, 1954). Large inner collateral vascular bundles are

embedded in the parenchyma, with the phloem at the pole of the bundle towards the periphery of the culm, (Fig.5A-B; Hayward, 1938; Metcalfe, 1960; Rovenská, 1973). A sheath of mechanical tissue consisting of slender, elongated fibres (Fig.5A; Hayward, 1938; Metcalfe, 1960) surrounds these bundles. The protoxylem consists of one or two annular or spiral vessels, and the innermost element is reinforced with a combination of rings and spiral thickenings (Fig.5A; Hayward, 1938; Metcalfe, 1960). Protoxylem elements usually break down quite early in the life of the bundle and are replaced by longitudinal, intercellular cavities, in which the annular or spiral thickenings of the original vessel elements are sometimes to be seen (Metcalfe, 1960). The large, laterally placed, metaxylem vessels are pitted with several small tracheids between them (Fig.5A; Hayward, 1938; Metcalfe, 1960). The phloem is comprised of slender thin-walled sieve tubes and companion cells (Fig.5A; Hayward, 1938; Metcalfe, 1960).

1.1.4 | Rye breeding

Lodging resistance is one of the main objectives for rye breeding, next to grain yield and 1000-kernel weight, higher crude protein content, resistance to frost, drought, diseases (mildew, *Rhynchosporium*, leaf and stem rust, ergot, *Fusarium*), and preharvest sprouting (Geiger and Miedaner, 2009; Schlegel, 2014). The identification and selection of the traits determining lodging resistance has been an important goal for breeders, and many of them have found differences among lodging resistant and susceptible genotypes for various morphological and anatomical culm traits.

Population breeding is carried by random fertilisation since rye gametophytic self-incompatibility prevents self-fertilisation under open pollination and usually leads to the production of self-incompatible varieties (Geiger and Miedaner, 2009; Schlegel, 2014). The population varieties, which are open-pollinated and synthetic varieties, are steadily improved by recurrent half- or full-sib selection (Geiger and Miedaner, 2009). Before 1850, landraces were developed by natural selection and until 1900 mass selection was a standard procedure for rye grain, spikes shape, and plant habits improvement (Schlegel, 2014). From 1885 to 1921, the phenotypic recurrent selection was used to develop better rye populations, which was a significant improvement for rye breeding (Schlegel, 2014). In 1910, the separation breeding method was developed for rye, which supported the development of directed pollination (Schlegel, 2014). Since 1920 the method of overstored seeds ('half-sib progeny selection'), including regulated cross-fertilisation and progeny testing, became the standard before hybrid breeding was introduced (Schlegel, 2014). Breeding for bread making traits began in 1928, and a strong selection in the 1930s led to a significant increase of protein content in Petkus derivatives

(Schlegel, 2014). During the 1930s, several inbreeding methods were applied with no significant progress achieved in the selection and only for more distinct and primitive lines, the selection progress was better (Schlegel, 2014). Systematic hybrid studies in rye started in 1970 at the University of Hohenheim with the discovery of the so-called P-cytoplasm and the Cytoplasmic Male Sterility (CMS) became the cornerstone of hybrid production (Schlegel, 2014). Nowadays hybrid populations are more popular, and a good example is the case of Germany, where hybrid rye is grown on about 70% of total rye acreage (Geiger and Miedaner, 2009). 'Helltop' and 'Hellvus, rye hybrids developed by Dieckmann Seeds, combine the highest plant height among German collection of rye hybrids, high yield and large seeds with remarkable stability and lodging resistance.

1.2 | Lodging

Lodging is the phenomenon of the displacement of small-grained cereals shoots from their vertical stance, which occurs after the ear or panicle has emerged, and results in shoots permanently leaning horizontally on the ground, sometimes involving breakage of the stems (Mulder, 1954; Pinthus, 1973; Berry *et al.*, 2003; Berry *et al.*, 2004; Kelbert *et al.*, 2004). Lodging as a limiting factor causes significant economic losses and strongly affects the final yield of grain. It can reduce yield by up to 80% and can cause additional undesirable effects, including reduced grain size and number, reduced quality, greater drying costs, and problematic harvesting (Atkins, 1938; Mulder, 1954; Pinthus, 1973; Berry *et al.*, 2003; Berry *et al.*, 2004; Kelbert *et al.*, 2004; Kong *et al.*, 2013). Hence, the development of varieties resistant to lodging is an important objective in the most breeding programs. Lodging can be influenced by several factors, such as wind, rain, topography, soil type, previous crop, husbandry, and disease (Mulder, 1954; Pinthus, 1973; Kubicka and Kubicki, 1988; Berry *et al.*, 2003; Berry *et al.*, 2004). It is also associated with conditions that promote plant growth, such as an abundant supply of nutrients (Mulder, 1954; Pinthus, 1973; Kubicka and Kubicki, 1988; Berry *et al.*, 2004). Lodging resistance depends mostly on the morphology of plants, tiller anatomy, and root system (Mulder, 1954; Kubicka and Kubicki, 1988; Berry *et al.*, 2003; Berry *et al.*, 2004; Milczarski, 2008).

1.2.1 | Types of lodging

Lodging can be a result of buckling or breaking of the basal internodes, typically near the base of the stem, described as stem lodging (Pinthus, 1973; Berry *et al.*, 2004). Root lodging results from the failure of the anchorage system, and is characterised

by permanent displacement of the stem without any observable stem buckling, involving a specific disturbance of the root system (Mulder, 1954; Pinthus, 1973, Crook and Ennos, 1993; Berry *et al.,* 2004). In the small-grained crops, lodging is usually caused by one of the bottom two internodes buckling rather than by the loss of anchorage (Neenan and Spencer-Smith, 1975). That especially applies to rye, which has a larger proportion of root dry weight in the upper soil layer than other cereal crops (Sheng and Hunt, 1991). Buckling of the middle internodes, known as brackling, is common in barley and oats (Neenan and Spencer-Smith, 1975; White *et al.,* 2003), and susceptibility to brackling increases towards harvest (White, 1991). Buckling of the peduncle just below the ear is known as necking and is a common problem in barley (Berry *et al.,* 2004).

1.2.2 | Causes of lodging

The influence of wind, rain, hail, soil type, previous crop, an abundant supply of nutrients, and diseases on lodging are well-documented (Mulder, 1954; Miller and Anderson, 1963; Bremner, 1969; Pinthus, 1973; White, 1991; Easson *et al.,* 1993; Wong *et al.,* 1994; Baker, 1995; Crook and Ennos, 1995; Baker *at al.,* 1998; Chalmers *et al.,* 1998). Baker *et al.* (1998) assumed that the dominant parameter affecting lodging is the wind-induced bending moment of the stem base, which can be calculated from the wind speed acting upon the ear, the area and drag of the ear together with shoot natural frequency, height at the centre of gravity, and the damping ratio. The severity, which a region experiences lodging with, depends upon the season (Mulder, 1954; Pinthus, 1973). However, wet summers not always result in wide-spread lodging and summer rainfall is not the only determinant of a widespread lodging year (Mulder, 1954; Berry *et al.,* 2004). Lodging tends to be more common close to harvest, indicating cereals more prone to lodging as they develop (Mulder, 1954; Berry *et al.,* 2004). It also depends on the topography of a region, affecting local wind speeds (Berry *et al.,* 2004). Moreover, the differences can be seen within a field: the margins frequently show lodging, where it is associated with higher plant density and/or fertiliser supply (Easson *et al.,* 1993; Berry *et al.,* 2004). The wind-induced force acting on the upper sections of a shoot results in a bending moment at the plant base, what can be described as the shoot leverage (Berry *et al.,* 2004). Stem lodging is expected when the bending moment of a shoot exceeds the strength of the stem base, while root lodging is expected when the bending moment of all the shoots of the plant exceeds the strength of the root/soil system (Berry *et al.,* 2003; Berry *et al.,* 2004). Therefore, a key parameter for understanding the mechanics of lodging is the wind-induced base bending moment experienced by an individual shoot and the whole plant. The mentioned wind induced-base bending moment is dependent on: wind-induced force, the height

at the centre of gravity of a shoot, the frequency at which the shoot oscillates, the acceleration due to gravity, the mass of the shoot canopy, the Young's modulus, second moment of area of the stem, the density of air, the projected ear area for an individual shoot, the drag coefficient of an ear, the wind speed, and the rotational stiffness of the root-soil complex (Baker, 1995; Berry *et al.,* 2004). Lodging resistance also depends on the stem failure moment, which is influenced by stem failure yield stress (material strength), the external radius of the stem, and the culm wall thickness (Baker, 1995). Experiments in wind tunnels indicate high wind velocities of 15-30 m s^{-1} (54-108 km h^{-1}) are necessary to cause stem lodging (Pinthus, 1973). Baker (1995) concluded that the natural frequency of oscillation, averaging time, and turbulence intensity were basic parameters in determining plant stability, and mean failure wind speed of 11.6 m s^{-1} (41.76 km h^{-1}) was predicted for the cereal canopy case.

An abundant supply of available nitrogen for the plant (mainly NO_3^- ions) has been shown to increase lodging in rye, wheat, barley, and oats (Mulder, 1954; Miller and Anderson, 1963; Bremner, 1969; White, 1991; Easson *et al.,* 1993; Chalmers *et al.,* 1998). The most significant increase in lodging is usually observed in response to early applications of fertiliser (except oats; Chalmers *et al.,* 1998), before stem elongation (Mulder, 1954; Miller and Anderson, 1963), while the application after anthesis does not have this adverse effect (Webster and Jackson, 1993). The reason the application of fertilizer makes plants prone to lodging is increased length of basal internodes, as well as the reduced strength of the stem base, and the anchorage system as a consequence of reduced amount of lignified tissue within the sclerenchyma zone and reduced thickness of sclerenchyma cell walls (Welton, 1928; Mulder, 1954; Crook and Ennos, 1995; Berry *et al.,* 2004). Moreover, a greater nitrogen supply almost always reduces stem diameter and stem wall thickness, affecting their strength (Welton, 1928; Mulder, 1954), and also decreases the dry weight per unit length of the basal internodes in wheat, barley, oats, and rye (Welton, 1928; Mulder, 1954; White, 1991; Crook and Ennos, 1995). The effects of potassium, phosphorus, and trace elements are less pronounced and there is no or mixed effect of an additional supply of those fertilizers on lodging risk, except the soils with nutrient deficiency, where the supply can reduce lodging causing by increasing the diameter and strength of the stem (Mulder, 1954; Pinthus, 1973). It was shown for barley that potassium deficiency causes weaker lower internodes as a result of poor lignification of parenchyma cells (Tubbs, 1930). On the other hand, phosphorus-deficient plants and those with nitrogen deficiency had the strongest lower internodes (Tubbs, 1930). Silicon is reported to affect lodging with regularity, improving the breaking strength of stems, as shown for rice (Wong *et al.,* 1994; Berry *et al.,* 2004).

Insects, foot-rot, and root-rot diseases are another causes promoting lodging by weakening the anchorage of plants and affecting the lower stem internodes (Pinthus, 1973). The main diseases, which induce lodging of cereals, are root-rot caused by *Ophiobolus graminis,* and 'eyespot' foot-rot caused by *Cercosporella herpotrichoides* (Pinthus, 1973). Moreover, a higher density of plants with earlier and increased application of nitrogen fertiliser increases the occurrence of 'sharp eyespot' (*Rhizoctonia solani*) in winter wheat (Bremner, 1969).

1.2.3 | Determinants of stem lodging resistance

Since the XIXth century, beginning with Sir Davy's investigations, lodging of cereals has been associated with a low silicon content of the straw (Davy, 1836; Atkins, 1938). Afterwards, Liebig (1843) mentioned that all grasses require particular amounts of silicate of potash in the soil to strengthen the plant culm. Garber and Olson (1919) found the number of vascular bundles and the thickness of sclerenchyma cell walls to be a distinguishing trait for lodging and non-lodging cereals to determine promising selections. Additionally, both traits were found to be the most independent of soil variations (Garber and Olson, 1919). In 1928, Welton reported that lodging in oats and wheat results from low dry matter per unit length of culm, which can be caused by a relatively low content of lignin or other carbohydrates. Welton (1928) also noticed that hypernutrition tended to induce a greater elongation of culms and tillering process, increasing shading, thus a higher risk of lodging. Salmon (1931) postulated that the breaking strength of the straw might be used as an index for resistance to lodging. In 1933 Clark and Wilson found a significant correlation between the diameter of culm and breaking strength in wheat, followed by studies of Brady (1934) revealing the thickness of the culm wall, number of vascular bundles, the width of lignified tissues, plant height, length of the internodes, and diameter of lower internodes closely associated with varietal differences in the lodging of oats. Mulder (1954) also pointed out the importance of strong lower internodes and their determinants, especially the occurrence of a sclerenchymatous ring in the outer layer of stem and the number of vascular bundles, as well as the lignification of the ground parenchyma, which influences culm greatest moment of force resistance. Additionally, the resistance to lodging has been associated with the weight of higher internodes of the stems plus leaves and heads in relation to the length of the culms, which determine the moment of force acting upon the lower internodes and roots (Mulder, 1954). Moreover, Mulder (1954) reported that rye plants, which were very liable to lodge, had longer lower internodes. Later Pinthus (1973) explained that the diameter of the basal internode and its wall thickness, primarily

the second internode, were determining flexural rigidity, an important parameter from the mechanical point of view. Kong *et al.* (2013) concluded that 99% of the variation in lodging resistance in wheat could be explained by the width of the mechanical tissue layer. Solid stemmed varieties of wheat have often been linked with greater lodging resistance. However, Ford *et al.* (1979) found no qualitative anatomical differences between solid and hollow stems since the pith of the solid stems was thin walled parenchyma, which was not expected to contribute significantly to the stem structural integrity. Atkins (1938) reported that in wheat varieties positive and significant, though small, correlations could be found for: lodging and length of lower internode, lodging and weight of grain per 100 heads. Atkins also found a small negative significant correlation between lodging and weight per 100 culms and weight per unit length of the culm.

As reported by Pinthus (1973) and Neenan and Spencer-Smith (1975), resistance to bending of basal internodes is also determined by Young's modulus and the outer diameter of the straw. Additionally, the shape of the head affects the magnitude of the lodging-inducing torque (Pinthus, 1973). Zuber *et al.* (1999) reported that 49.7 % of the variation in lodging could be explained by the variation in stem weight, and thicker and heavier stems (mg per cm) were indicative for better lodging resistance. Additionally, as much as 77.2 % of the variation in lodging resistance in wheat was based on stem weight per cm and the weight of the ear (Zuber *et al.*, 1999). Kong *et al.*, (2013) found out that especially the weight of lower internodes is highly correlated (R^2 = 0.986, P < 0.05) with lodging resistance in wheat. The thickness of sclerenchyma cell walls has also been positively correlated with lodging resistance in barley (Cenci *et al.*, 1984). Studies on Arabidopsis mutants have shown that decreased stem strength is caused by a deficiency in cellulose and lignin deposition in the secondary wall (Turner and Somerville, 1997; Jones *et al.*, 2001). Kong *et al* (2013) in studies on wheat cultivars proposed that cellulose and lignin play an essential role in lodging resistance, as they found significant correlations between the degree of lodging resistance and lignin (R^2 = 0.978, P < 0.01), as well as cellulose (R^2 = 0.944, P < 0.05) content. On the other hand, studies on two rye brittle stem lines ($bs_1bs_1Bs_2Bs_2$ and $Bs_1Bs_1bs_2bs_2$) and the control revealed statistically significant differences in the content of hemicellulose and a-cellulose, which were more abundant in the control genotype. In contrast, the differences in lignin content were less pronounced in those lines (Kubicka and Kubicki, 1988). Obtained data suggest that gene bs_1 causes disorders in the synthesis of cellulose and hemicellulose, whereas bs_2 gene affects cellulose and hemicellulose, as well as lignin content (Kubicka and Kubicki, 1988).

As lodging is a quantitative trait (Keller *et al.*, 1999), a number of genes with the crucial effect of the environment are controlling this complex trait, and several studies were conducted to identify Quantitative Trait Loci (QTL) for the lodging resistance in wheat, barley, and rye (Backes *et al.*, 1995; Hayes *et al.*, 1995; Larson *et al.*, 1996; Keller *at al.*, 1999; Börner *et al.*, 2002; Ma *et al.*, 2002; Milczarski, 2008). However, the most significant QTL were often associated with height differences, not stem nor anchorage strength. Studies on rye by Milczarski (2008) revealed 2 QTL for the length of the second internode (3RL, 5RL), and 3 QTL for the thickness of the second internode (2RL, 6RL, 7RS) and the genetic background of those traits was distinct. Milczarski (2008) also found 3 QTL for a so-called lodging coefficient in rye (2RS, 3RL, 5RL): a ratio between the thickness of the second internode and plant height. So far, less is known about the genetic control of the thickness of the stem wall, an important component of stem strength in cereals.

1.2.4 | Effects of lodging on yield

Lodging can reduce yield by reducing grain size, weight, number, and quality, resulting from rapid chlorosis, reduced carbon assimilation, reduced translocation of mineral nutrients and carbon for grain filling, or by reduced amount of crop that can be collected by the combine harvester (Mulder, 1954; Day and Dickson, 1958; Weibel and Pendleton, 1964; Pinthus, 1973; Fischer and Stapper, 1987; Berry *et al.*, 2004; Kelbert *et al.*, 2004). The greatest lodging-induced reductions in potential grain yield occur when plants are lodged at anthesis stage or early on in grain filling stage (Fischer and Stapper, 1987; Berry *et al.*, 2004; Kelbert *et al.*, 2004). In this case, lodging can reduce yields of wheat by up to 80% (Easson *et al.*, 1993). Smaller yield losses have been observed when the angle of lodging is less than 90° from the vertical, and artificially induced lodging at 45° caused 25 to 50% reduction of that at 90° (Pinthus, 1973; Berry *et al.*, 2004). Additionally, crops which lodge before anthesis often have smaller yield losses than crops that lodge soon after anthesis (specially early grain filling growth stage: GS75), associated with the upper internodes bending upwards to partially re-erect the plant, which is impossible after anthesis, since the plant has completed stem extension (Pinthus, 1973; Fischer and Stapper, 1987). Recovered lodging can contribute to the prevention of later lodging by its height reducing the effect and, in certain cases, by the development of adventitious roots at the lowest bent node (Pinthus, 1973). Lodging close to maturity cannot affect grain yield directly but may cause losses due to problematic harvesting (Pinthus, 1973). Additional reduction in grain size, number, and its quality results mostly from reduced carbohydrate assimilation, caused by shading of a large part of the shoots by plants, which are leaning or lying on top of them (Mulder, 1954; Pinthus, 1973).

Lodging is known to reduce the malting quality of barley and preharvest sprouting has also been found to occur more frequently in lodged crops (Day and Dickson, 1958; Pinthus, 1973; Fischer and Stapper, 1987). It is worth to mention that lodging also poses a potential health risk, since high humidity in lodged crops increases the likelihood of fungal infections, contaminating the grain with mycotoxins (Pinthus, 1973; Berry *et al.,* 2003; Berry *et al.,* 2004).

1.2.5 | Prevention of lodging risk

The lodging risk of wheat (almost always) and barley (usually) is reduced by delaying sowing (Berry *at al.,* 2004). The amount of lodging in wheat can be reduced as much as 30% by two weeks of delay of sowing, what reduces the number of extended internodes contributing to the shorter stems and smaller base bending moment (Berry *et al.,* 2004). More tillers resulting from early sowing contribute to a higher base bending moment, since the stems are weaker with narrower and thinner wall, due to a higher number of shoots competing for limited photo-assimilates during early stem extension, reducing the dry matter per unit length of the lower internodes (Berry *et al.,* 2000; Berry *et al.,* 2004). Reducing the plant density also causes a significant reduction of the lodging risk in wheat and barley (Kirby, 1967; Pinthus, 1973; Easson *et al.,* 1993; Webster and Jackson, 1993; Berry *et al.,* 2004). Noteworthy is the fact that early sowing and higher plant density also increases the prevalence of stem base diseases, which may increase lodging by weakening the stem (Bremner, 1969; Berry *et al.,* 2004).

Great strides were made during the 1950's and 1960's to reduce lodging risk by the introduction of dwarf and semi-dwarf varieties with shorter and stiffer straw. They not only reduced lodging risk but also gave greater yield by reduced stem growth rates during the development of the ear, resulting in more fertile florets and more grains per square meter, since they responded to higher amounts of fertilisers without causing an excessive risk to lodging (Pinthus, 1973; Fischer and Stapper, 1987; Berry et al., 2004; Kelbert *et al.,* 2004). In wheat, the *Reduced height (Rht)* alleles cause insensitivity to gibberellic acid (GA), suggesting their involvement in the GA signalling pathway, reducing the elongation of internode cells, as a consequence resulting in shorter plants, although in some mutants normal growth can be restored by exogenous application of GA, indicating the involvement of these genes in the biosynthetic pathway of GA (*Rht4-9*; Worland *et al.,* 1990; Gale and Youssefian, 1985; Berry *et al.,* 2000; Kowalski *et al.,* 2016). Initially, their use was motivated by the need for shorter and stiffer straw to reconcile higher levels of fertiliser without lodging (Kertesz *et al.,* 1991). However, in stress environments (like drought or typical Central and Eastern European conditions), wheat

lines with one or both alleles, *Rht1* and *Rht2*, are characterised by lower kernel weights than the control (Pinthus and Levy, 1983; Pinthus and Gale, 1990; Allan, 1986), partially compensated by an increase in grain number per ear and increase in tiller number per square meter (Kertesz *et al.,* 1991). On the other hand, *Rht3* causes negative effects on yield, volume weight, kernel weight, and tiller number in wheat (Allan, 1986; Balyan and Singh, 1994). In rye, several dwarfing genes were reported on all of the chromosomes (Table 1) and, likewise in wheat, there are two categories of dwarfing mutants based on their response to applied exogenously gibberellic acid: GA-sensitive (synthesis mutants) and GA-insensitive, with reduced response or complete insensitivity to applied GA (Börner and Melz, 1988; Börner, 1991; Börner *et al.,* 1996; Börner *et al.,* 1998; Schlegel, 2014). *Dw1* *(Dwarf1*, or *Ddw1 – Dominant dwarf1)*, a dominant dwarfing gene, initially named *Hl* (*Humilus*), was discovered in 1972 (Kobyljanski) in the spontaneous 'EM 1' mutant, and since then it has been broadly used to improve lodging resistance in population varieties in rye breeding programmes, especially in the Baltic countries (Melz, 1989; Börner *et al.,* 1996; Milach and Federizzi, 2001; Milczarski and Masojć, 2002; Tenhola-Roininen and Tanhuanpää, 2010). Another dominant dwarfing gene was discovered in 1984 (Smirnov and Sosnichina, 1984; reviewed by Börner *et al.,* 1996) in the accession 'K-10028'. The gene was further localised on the chromosome 7R by genetic and trisomic analysis (Melz, 1989). Recently *Ddw3*, a new dominant dwarfing gene localised on the long arm of chromosome 1R, was described (Stojałowski *et al.,* 2015), and similarly to previous dominant genes of rye, it is characterised by sensitivity to the exogenously applied GA (Table 1).

Besides the mentioned dominant dwarfing genes, 12 recessive dwarfing genes were discovered in rye so far (Sybenga and Prakken, 1963; Sturm and Müller, 1982; De Vries and Sybenga, 1984; Börner and Melz, 1988; Melz, 1989; Börner, 1991; Melz *et al.,* 1992; Devos *et al.,* 1993; Plaschke *et al.,* 1993; Plaschke *et al.,* 1995b; Korzun *et al.,* 1996; Schlegel *et al.,* 1998; Malyshev *et al.,* 2001; Voylokov and Priyatkina, 2004), among which both: GA-sensitivity and GA-insensitivity, can be observed (Table 1). Nevertheless, worth mentioning is the fact, that under certain agronomic conditions, even modern short cultivars lodge (Fischer and Stapper, 1987) and not always plant height reducing genes have positive pleiotropic effects on grain yield, as in the case of some wheat and rye dwarfing genes (Milach and Federizzi, 2001; Miedaner *et al.,* 2011). Moreover, in high-yielding semi-dwarf cultivars with higher kernel numbers yield can be more sensitive to post-anthesis lodging (Fischer and Stapper, 1987). Although it is well known that lodging results from low dry matter per unit length of culm (Welton, 1928), until the late 1980s breeders were increasing grain yield without altering total biomass at the expense of straw,

approaching the theoretical maximum for the proportion of total biomass that could be allocated to grain without weakening the supporting stem (Foulkes *et al.,* 2011). The scope for further reducing crop height appears to be limited, because of the incompatibility of more extreme dwarfing genes with high yields and problematic harvesting of shorter varieties, combined with the poor seedling establishment and low early vigour associated with the presence of GA-insensitive genes (Milach and Federizzi, 2001).

Table 1 Dwarfing genes in rye with their inheritance, localization, and sensitivity to GA.

Dwarfing gene	Inheritance	Chromosome	GA sensitivity	Reference
Ddw1 (syn. *Dw1*)	Dominant	5RL	Sensitive	Kobyljanski, 1972; Sturm and Engel, 1980; Börner and Melz, 1988; Melz *et al.,* 1992; Geiger and Miedaner, 1996; Börner *et al.,* 1996; Korzun *et al.,* 1996; Schlegel *et al.,* 1998; Börner *et al.,* 1999; Börner *et al.,* 2000; Milczarski and Masojć, 2002; Voylokov and Priyatkina, 2004
Ddw2 (syn. *Dw2*)	Dominant	7R	Sensitive	Kobyljanski, 1975; Melz, 1989; Melz *et al.,* 1992; Börner *et al.,* 1996; Schlegel *et al.,* 1998
Ddw3	Dominant	1RL	Sensitive	Stojałowski *et al.,* 2015
dw1 (syn. *d1*)	Recessive	7R	Sensitive	Sybenga and Prakken, 1963
dw2 (syn. *d2*)	Recessive	2R	Sensitive	De Vries and Sybenga, 1984; Melz, 1989; Melz *et al.,* 1992; Korzun et al., 1996; Schlegel *et al.,* 1998
dw3	Recessive	3R		De Vries and Sybenga, 1984; Melz, 1989; Melz *et al.,* 1992; Korzun et al., 1996; Schlegel *et al.,* 1998
dw4	Recessive	1R		Melz, 1989; Melz *et al.,* 1992; Korzun et al., 1996; Schlegel *et al.,* 1998
dw5	Recessive	4R		Melz, 1989; Melz *et al.,* 1992; Korzun *et al.,* 1996; Schlegel *et al.,* 1998
dw6	Recessive	5R	Insensitive	Melz, 1989; Börner, 1991; Melz *et al.,* 1992; Korzun *et al.,* 1996; Schlegel *et al.,* 1998
dw7	Recessive	6R		Melz, 1989; Korzun *et al.,* 1996; Schlegel *et al.,* 1998
dw8	Recessive	5RL		Devos *et al.,* 1993; Schlegel *et al.,* 1998
ct1	Recessive	7RL	Insensitive	De Vries and Sybenga, 1984; Melz, 1989; Börner, 1991; Melz *et al.,* 1992; Plaschke *et al.,* 1995b; Schlegel *et al.,* 1998
ct2	Recessive	5RL	Insensitive	Sturm and Müller, 1982; De Vries and Sybenga, 1984; Börner and Melz, 1988; Börner, 1991; Melz *et al.,* 1992; Plaschke *et al.,* 1993; Voylokov and Priyatkina, 2004
ct3	Recessive	7R		Malyshev *et al.,* 2001
np	Recessive	4RL	Sensitive	Malyshev *et al.,* 2001; Voylokov and Priyatkina, 2004

Further improvement in yields has been obtained by the use of plant growth regulators (PGRs), synthetic compounds, which are a cost-effective method of reducing the risk of lodging. PGRs act as: inhibitors of GA biosynthesis (like chlormequat chloride, mepiquat chloride, or trinexapac-ethyl), which reduce crop height by reducing cell elongation and decreasing the rate of cell division; or as ethylene releasing compounds, like ethephon (Rademacher, 2000; Berry *et al.,* 2003; Berry *et al.,* 2004). Chlormequat has been shown to be effective at reducing lodging in winter and spring wheat, oats, and rye, but less effective in barley (Berry *et al.,* 2000). Triadimenol, an inhibitor of ergosterol and GA biosynthesis, can also reduce the risk of lodging in wheat, increasing crown depth by shortening the sub-crown internode (Montfort *et al.,* 1996).

Although dwarfing genes and PGRs have been very effective tools for reducing lodging risk, they have not eradicated lodging (Fischer and Stapper, 1987; Berry *et al.*, 2004). Furthermore, farmers will not be able to rely on those tools since several studies have shown that yield is reduced when crops are shortened too much (Allan, 1986; Kertesz *et al.*, 1991; Balyan and Singh, 1994; Miralles and Slafer, 1995; Flintham *et al.*, 1997; Berry *et al.*, 2004). Analyses in wheat have revealed that the minimum crop height for optimum grain yield is 0.7 m and it was already approached for some cereals (Flintham *et al.*, 1997). Therefore, it seems unlikely that further improvement in lodging resistance can be made by continuing to shorten cereals. Great potential lies in increasing of the strength of the stem base and related to that stem flexural rigidity, as well as the identification of molecular genetic markers to understand the genetic control of these traits and to help plant breeders in selection.

1.3 | Plant cell walls

A cell wall (CW) is a complex and dynamic structural layer surrounding plant cells providing them protection against mechanical stress, rigidity, and elasticity to withstand internal osmotic pressure (Cosgrove, 2005). It also has a crucial role in plant growth, cell differentiation, intercellular communication, defence, and the circulation and distribution of water, minerals, and other nutrients (Cosgrove, 2005).

The composition of the CW of grasses is critical for uses as food, feed, and energy crops, as well as plant stability (Cosgrove, 2005; Vogel, 2008). The grass CW differs significantly from the dicotyledonous regarding major structural polysaccharides, linkages between those polysaccharides, the abundance and importance of pectins, proteins, and phenolic compounds. Yet the similarities are found in the network made of cellulose and lignin surrounded by a matrix of non-cellulosic polysaccharides (Vogel, 2008). The primary CW of higher plants can be divided into two types. Type I is found in dicots, noncommelinoid monocots (like aroids, alismatids, and lilioids), and gymnosperms, which consist of cellulose encased in a network of xyloglucan, pectin, and structural proteins. Type II is found only in the commelinoid monocots (like grasses, rushes, and gingers) and is composed of cellulose fibres encased in glucuronoarabinoxylans and (1,3;1,4)-β-D-glucans, high levels of hydroxycinnamates, and very low levels of pectin, glucomannans, xyloglucans, and structural proteins (Farrokhi *et al.*, 2006; Vogel, 2008).

1.3.1 | Composition of the cell wall of grasses

The plant CW is composed mainly of polysaccharides: cellulose and hemicelluloses, components of the primary and secondary CW (Carpita, 1996; Lerouxel *et al.*, 2006; Vogel, 2008). The primary CW is a robust framework of cellulose microfibrils intertwined with xyloglucans or glucuronoarabinoxylans, embedded in a gel of pectins rich in uronic acid, and cross-linked with hydroxyproline-rich glycoproteins (Carpita, 1996; Lerouxel *et al.*, 2006; Vogel, 2008). The primary CW of grasses is less abundant in structural proteins than dicots (Carpita, 1996). The secondary CW contains little proteins and pectins, however, is abundant in lignins (Lerouxel *et al.*, 2006). The CW of grasses is much more abundant in xylan and mixed-linked β-glucans than dicots (Carpita, 1996; Sindhu *et al.*, 2007). Significant quantities of hydroxycinnamates ferulic acid (up to 4%) and p-coumaric acid (up to 3%) are also present in the primary and secondary CW of grasses (Vogel, 2008). These hydroxycinnamates exist as unbound acids or are linked to various positions in lignin and ester- and ether-linked to the arabinosyl units of glucuronoarabinoxylans crosslinking their molecules (Vogel, 2008).

Cellulose has an essential economic value in the form of paper, textiles, wood products, polymers, animal feed, and biomass for energy uses (Cosgrove, 2014). The cellulose microfibril is composed of numerous (18-24) unbranched (1,4)-linked β-D-glucan chains, which form mechanically strong and highly resistant to enzymatic attack crystalline microfibril (Cosgrove, 2014). The physical properties of cellulose microfibrils are determined by their hydrophobic and hydrophilic surfaces responsible for binding of xyloglucan, xylan, and lignin with different affinities (Cosgrove, 2014).

Heteroxylans are abundant in the CW of grasses and can be classified into arabinoxylans and glucuronoarabinoxylans (Fincher, 2009). Arabinoxylans of grasses consist of (1,4)-β-D-xylan backbone, in which β-D-xylopyranosyl (Xyl*p*) units are substituted with single α-L-arabinofuranosyl (Ara*f*) units at *O*-3, and *O*-2 positions of the Xyl*p* units (Fincher, 2009). Arabinoxylans are widespread in the CW of all flowering plants, but in dicots, the polymer is of much lower abundance, and the α-L-arabinosyl units are attached mostly at the *O*-2 position of the xylosyl units (Carpita, 1996). Glucuronoarabinoxylans (GAX) consist of *t*-α-L-arabinofuranosyl units attached at the *O*-3 positions in (1,4)-β-D-xylan backbone and *t*-α-D-glucuronic acids attached to *O*-2 positions (Carpita, 1996; Vogel, 2008). In many grasses, the arabinosyl units of GAX are being hydrolysed after incorporation into the wall. Moreover, the xylosyl units are also substituted with acetyl groups at the *O*-2 and *O*-3 position (Carpita, 1996). A highly substituted GAX is associated with the maximum growth rate of coleoptiles (Carpita, 1996).

Noncellulosic (1,3;1,4)-β-D-glucans are unbranched, contain β-D-glucopyranosyl monomers polymerised through both (1,3)- and (1,4)-linkages in a ratio of about 1:2 to 1:3 (Carpita, 1996; Vogel, 2008; Fincher, 2009). (1,3;1,4)-β-D-glucans are found at certain stages in plant development, and they are relatively minor components of vegetative tissues of cereals and grasses (Carpita, 1996; Vogel, 2008; Fincher, 2009). Moreover, their concentration in vegetative cells is highly correlated with cell growth and peaks at the same time as cell expansion, showing their role in that process (Vogel, 2008; Fincher, 2009).

Small amounts of xyloglucans (XyGs), with a backbone similar to that of cellulose with xylose branches on 3 out of 4 glucose residues, can also be found in the grass CW, especially in meristematic cells, before the onset of enhanced β-D-glucan and GAX synthesis during elongation (Carpita, 1996). XyGs has been considered an essential structural component, which metabolism has a putative role in CW loosening and induction of growth by auxin and other hormones, thus in CW structure and its mechanics (Cosgrove, 2014). Another glucan represented in small amounts in the CW of grasses is glucomannan, found tightly bound to the microfibrils, especially in the barley and wheat endosperm CW and in maize coleoptiles (Carpita, 1996).

Two fundamental polymers of pectins are: polygalacturonic acid (PGA, a homopolymer of (1,4)-a-D-galactosyluronic acid), and rhamnogalacturonan I (RG I, a heteropolymer of repeating (1,2)-a-L-rhamnosyl-(1,4)a-D-galactosyluronic acid disaccharide units), which are found in grasses in smaller amounts than in dicots, and serve as mechanical tethers between cellulose microfibrils in parallel with xyloglucan as the CW expands (Jarvis, 1984; Carpita, 1996; Cosgrove, 2014).

The CW of grasses also contains arabinans, galactans, and highly branched arabinogalactans (AGs) attached to the *O*-4 of the rhamnosyl residues of RG (Carpita, 1989; Carpita, 1996). The arabinans are mostly 5-linked arabinofuranosyl units (Carpita, 1996). The galactans and two classes of AGs are the major side-chains (Carpita, 1996). Pectins are important determinants of CW porosity and form hydrated gels pushing cellulose microfibrils apart and easing their sideways slippage during cell growth, while also locking them in places when growth ceases (Cosgrove, 2005).

The nonlignified CWs of Poales are enriched with aromatic substances, like esters of hydroxycinnamates, ferulate, and *p*-coumarate (Rudall and Caddick, 1994; Carpita, 1996). Esterified and etherified hydroxycinnamates are cross-linking GAXs, being responsible for maintaining of complexes of polysaccharides and lignin (Scalbert *et al.*, 1985; Carpita, 1996). More complex interactions between polysaccharides and aromatic

substances involve ester-ether interactions (Iiyama *et al.,* 1990; Lam *et al.,* 1992; Iiyama *et al.,* 1994; Lam *et al.,* 1994; Carpita, 1996).

The secondary CW of grasses, which is deposited after cells cease enlargement, comprise at least 50% of the CW mass in both leaves and stems (Cosgrove, 2005; Vogel, 2008). Secondary CW is deposited inside the primary CW of xylem, fibres, and sclerenchymal cells (Vogel, 2008). The typical grass secondary CW is mostly composed of cellulose, GAX, and lignin (Vogel, 2008). The GAX found in the secondary CW has fewer side-chains than the GAX of primary CW, resulting in a stronger GAX-cellulose interaction (Vogel, 2008). Lignin comprises around 20% of the grass secondary CW and fills the pores between the polysaccharides (Vogel, 2008). The main components of grass lignin are syringyl (40–61%), guaiacyl (35–49%), and a small but a significant percentage (4–15%) of ρ-hydroxyphenyl units (Vogel, 2008). In some grasses during maturation, syringyl lignin increases in relative proportion to guaiacyl and *p*-hydroxyphenyl lignins (Carpita, 1996). Grass lignin also contains substantial amounts of r-coumaric acid and ferulic acid, residues attached to GAX, which may serve as nucleation sites for lignin formation (Carpita, 1996; Vogel, 2008).

CW proteins play a role: as structural proteins cross-linking the CW carbohydrates, enzymes, or as regulator proteins (Carpita, 1996, Vogel, 2008). The EXTC (extensin type gamma), previously called threonine-hydroxyproline-rich glycoproteins (THRGPs), homologs of dicots hydroxyproline-rich glycoproteins (HRGPs) – extensins, are abundant in periderm, protoxylem, metaxylem, and the longitudinal radial CW of the epidermis, stabilising intramolecular isodityrosine linkage (Stiefel et al., 1990; Hood *et al.,* 1991; Showalter, 1993; Kieliszewski and Lamport, 1994; Smallwood *et al.,* 1995; Carpita, 1996). They represent one of the main structural protein components of the CW and were shown to play critical roles in CW structure and function, as during development or defence response to wounding (Carpita and Gibeaut, 1993; Showalter, 1993; Sturaro *et al.,* 1998; Newman and Cooper, 2011). Extensins can also interact with negatively charged uronic acids of pectins, thus can be a part of CW pH and Ca^{+2} regulating system (Showalter, 1993). A large superfamily of nonenzymatic CW proteins, expansis, is playing a pivotal role in the activated by acidification CW loosening, disrupting non-covalent binding of CW polysaccharides to one another, and mediating acid-induced growth (Cosgrove, 2005). Glycine-rich proteins (GRPs) have a broad spectrum of cytosolic and CW functions, although many of them in grasses lack signal peptides indicating their cytosolic functions (Showalter, 1993; Vogel, 2008). In CWs GRPs play structural functions and are expressed in response to a variety of developmental and stress conditions (Showalter, 1993). Proline-rich proteins (PRPs) are another class of CW proteins involved in plant development

(Showalter, 1993). PRPs are insolubilized in the CW and insolubilization can occur rapidly in response to stress-mediated by the release of hydrogen peroxide catalysed by a CW peroxidase (Showalter, 1993). Arabinogalactan proteins (AGPs), a large heterogeneous family of hydroxyproline-rich glycoproteins, are also involved in many processes, such as cell division, programmed cell death, cell differentiation, cell expansion, and host/microbe interactions (Showalter, 1993; Marzec *et al.,* 2015). The glycan part of those glycoproteins consists of arabinose, galactose, rhamnose, fucose, glucuronic acid, and xylose, and the post-translational modification of the AGPs influences their function stronger than does their peptide sequence (Showalter, 1993; Marzec *et al.,* 2015). The grass CW is highly abundant in xyloglucan transglycosylases/hydrolases (XTHs), which can act not only as modulators of xyloglucan structure, but also as heterotrans-glycosylating enzymes covalently linking different classes of polysaccharides in the CW, influencing its strength, flexibility, and porosity (Cosgrove, 2005; Fincher, 2009). XTH gene expression is high in the regions of active CW formation, like elongation zones, and in the regions where CW deposition continues after cell enlargement has ceased, or where other forms of CW remodelling occur (Cosgrove, 2005). Besides described proteins in CWs are present also enzymes, such as esterases, peroxidases, phosphatases, mannosidases, glucanases, and several other enzymes, which function in the modification of CW polymers (Cassab and Varner, 1988; Showalter, 1993; Vogel, 2008).

1.3.2 | Biosynthesis of cell wall polysaccharides in grasses

The discovery of cellulose synthase A (coded by *CesA* gene; Pear *et al.,* 1996), the catalytic subunit of the cellulose synthase complex, was the first step to understand cellulose biosynthesis. Linear (1,4)-β-linked glucan chains of cellulose microfibril are synthesised in parallel by protein complexes embedded in the plasma membrane (Cosgrove, 2014). Concurrent expression of three different *CesA* genes is normally needed for cellulose synthesis, providing a simple mechanism for self-assembly of CESAs into a trimeric functional cellulose-synthesising complex, and then into hexameric rosettes (Cosgrove, 2014). The assembly requires CESA dimerisation, which is mediated by two zinc fingers in the N-terminal region of the CESA proteins (Cosgrove, 2005). The initial acceptors for the microfibril chain elongation are sterol-β-glucosides, which are common components of plant cell membranes (Cosgrove, 2005). The orientation of microfibrils is determined by CSI1, a protein that binds CESA to cortical microtubules (Cosgrove, 2014). The crystallisation of glucan can be a spontaneous process, or it is a guided process in which cellulose binding proteins, such as CHITINASE-LIKE1 described in *Arabidopsis* and BRITTLE CULM1 from rice, facilitate microfibril assembly (Cosgrove, 2014).

As it was mentioned before, the CWs of grasses are unique in plants world for the content of (1,3;1,4)-β-D-glucans (Carpita, 1996; Burton *et al.,* 2006; Vogel, 2008; Fincher, 2009). It has been indicated that *Csl* (*CELLULOSE SYNTHASE-LIKE*) genes, which products contain sequence motifs characteristic for β-glycosyltransferases but lack the N-terminal region containing the zinc-finger domain characteristic for CESA, are responsible for the biosynthesis of some noncellulosic CW polysaccharides, as xylan backbones in the Golgi Apparatus (Cosgrove, 2005; Vogel 2008; Fincher, 2009). The last intensive years of investigation based on comparative genomics in rice and barley revealed that the cellulose synthase-like *CslF* family of genes, unique to order Poales, is involved in the biosynthesis of (1,3;1,4)-β-D-glucans (Vogel, 2008; Fincher, 2009). Another *Csl* family of genes, *CslA*, was shown to encode β-mannan synthases which synthesise mannan and glucomannan in both, dicots and grasses (Cosgrove, 2005; Vogel, 2008). (1,3;1,4)-β-D-glucans like other noncellulosic polysaccharides of the CW are biosynthesised in the Golgi apparatus, and the newly synthesised polymers are transported to the plasma membrane in Golgi-derived vesicles, afterwards deposited into the extracellular space, and incorporated into the CW by association with newly synthesised cellulose microfibrils and pre-existing CW polymers to form a strong and extensible network (Cosgrove, 2005; Fincher, 2009). The integration of newly secreted matrix polysaccharides into the existing network might be mediated by endotransglycosylases, such as xyloglucan endo-transglycosylase (XET), which cuts the xyloglucan backbone and re-forms a glycosidic bond with the free end of another xyloglucan chain (Cosgrove, 2005). Some members of xyloglucan endotransglycosylase/hydrolase (XTH) family might target arabinoxylan and (1,3;1,4)-β-D-glucan in grass CW (Cosgrove, 2005).

A few genes controlling the biosynthesis of the secondary CW were identified in plants. *COBRA* gene and related *COBRA-LIKE* genes have been shown to be critical for the development of secondary CW in *Arabidopsis* (Vogel, 2008). The *cobra* mutant in Arabidopsis is defective in cellulose synthesis and microfibril orientation in roots (Roudier *et al.,* 2005). The *COBRA-LIKE* genes described in monocots: *BRITTLE CULM1* (*Bc1*) from rice and *Brittle stalk2* (*Bk2*) from maize, have been shown to be required for normal secondary CW development, and when mutated the stalks become brittle associated with reduced secondary CW development (Sindhu *et al.,* 2007; Vogel, 2008). This reduced development of secondary CW is caused by decreased cellulose content in the mature zones, while lignin deposition is enhanced, suggesting that these genes are required for normal cellulose deposition in the secondary CW (Sindhu *et al.,* 2007; Vogel, 2008). Lack of a proper cellulosic matrix in the secondary CW leads to an aberrant lignin polymerisation, resulting in the brittle phenotype, which is not an effect of loss of tensile strength but a loss

in flexibility (Sindhu *et al.*, 2007). Sindhu *et al.* (2007) suggested that extreme loss of flexibility exhibited in the mutant is caused by lack of proper formation of lignocellulosic interactions during a change in lignin architecture. It has been suggested that the glycosyl-phosphatidylinositol (GPI) anchored COBRA protein guides the cellulose synthase complex along microtubules to maintain proper cellulose microfibrils orientation (Vogel, 2008). Another protein necessary for the development of secondary CW is caffeic acid 3-O-methyltransferase (COMT), which catalyses the multi-step methylation reactions of hydroxylated monomeric lignin precursors, and occupies a key role in the lignin biosynthetic pathway (Ma and Xu, 2008). A TaCM protein discovered in wheat had shown a high degree of identity with COMT from other plants, particularly in SAM binding motif, and the residues responsible for catalytic and substrate specificity, and the highest catalysing efficiency was towards caffeoyl aldehyde and 5-hydroxyconiferaldehyde as substrates, suggesting a pathway leads to S lignin via aldehyde precursors (Ma and Xu, 2008). Moreover, the reduction in COMT activity resulted in a marginal decrease in lignin content, but a sharp reduction in the syringyl lignin (Ma and Xu, 2008).

2. Aims of study

To answer the question about the genetic background of 'Stabilstroh' ('Stable straw'), a lodging resistant genotype of rye, the following objectives were pursued: (1) providing anatomical and histological details about the differences between the lodging resistant and wildtype parental lines; (2) identification of easily measurable culm traits related to lodging resistance to simplify the selection process in breeding programs; (3) detection of QTL underlying anatomical and morphological traits determining lodging resistance and elucidate the genetic basis of the lodging resistance in rye; (4) and finally the development of molecular markers for marker-assisted selection (MAS).

In this project, the prerequisites were to determine anatomical and morphological traits describing the new lodging resistant genotype of rye. The purpose of this goal was to reduce selection time and financial effort of this process to significantly improve the straw mechanical stability of new rye varieties, which is of great importance for yield quality and quantity, especially in organic cultivation. Additionally, the characterisation of traits at the ultrastructural and physiological level will allow the identification of trait interactions and indirect selection criteria to accelerate breeding progress.

To characterise parental lines anatomically and histologically, and to identify traits related to lodging resistance, light (LM), scanning electron (SEM), and transmission electron microscopy (TEM) were used. Additionally, for a better understanding of lodging resistance of 'Stabilstroh' genotype, Inductively Coupled Plasma Mass Spectrometry (ICP-OES) was used to analyse the content of elements influencing physical properties of cell walls, or having direct or indirect control upon biosynthesis of primary or secondary cell wall components.

In order to detect QTL responsible for traits related to lodging resistance and develop PCR-based molecular markers, parental lines and 130 individuals of 304/1 F_2 population was genotyped with SSR and DArTseq markers. For the selection of SNPs associated with at least four traits, KASP primers were designed, which can be used for marker-assisted selection process in the development of new lodging resistant rye varieties to complement empirical breeding and hasten progress to increased rye production.

3. Material and methods

3.1 | Plant material

In the study two winter rye (*Secale cereale* L.) parental lines: 'ms 135' (original 'Stabilstroh') and 'R 1124' (wildtype), and 130 individuals of '304/1' F_2 mapping population were investigated. The 'ms 135' male sterility was based on so-called G-plasma ('Gülzower Plasma'; G-type male sterility), found in 1962 in Gülzow as a random mutation, and since then used in hybrid seed production. The 'ms 135', originally called 'Steifstroh' ('stiff straw') and afterwards 'Stabilstroh' ('stable straw') because of its remarkable phenotype, is a spontaneous mutant characterised by high lodging resistance combined with long culms with thick walls. The interesting phenotype of this line was used for the development of two rye hybrid cultivars: 'Hellvus' and 'Helltop, characterised by outstanding lodging resistance, brackling resistance, and high biomass production (Table 2).

The parental lines, as well as the mapping population, were vernalized eight weeks at the temperature of 4 ℃ in a growth chamber, subsequently hardened for 7 days to gradually acclimatise the plants under 12h/12h and ~14/~12 ℃, day/night and temperature conditions respectively. Afterwards, the plants were grown in a greenhouse under controlled conditions (14h/10h day/night, ~15-18/~12-15 °C day/night at the early growth stage, and 16h/8h day/night, 20-23/17-20 °C day/night from the late growth stage until the maturity stage) with humidity around 60% and light intensity of 20,000 lx. Plant material for phenotyping was collected in 2011 at the IPK-Gatersleben. Dry tillers of parental lines and 304/1 F_2 population were prepared for LM and scanning electron microscopy (SEM). Fresh material for light microscopy (LM) and transmission electron microscopy (TEM) was provided in 2013 and 2014 by Dieckmann Seeds GmbH, later Monsanto Saaten GmbH was investigated in LM and TEM. Leaves preserved in liquid nitrogen were used for the extraction of DNA from parental lines and 304/1 F_2 population.

TABLE 2 Comparison of winter rye cultivars (Beschreibende Sortenliste, 2009).
H - hybrid; P – population; S – synthetic; TGW – thousand grain weight.

Cultivar name	Year of registration	Type	Plant height	Susceptibility to:		Grain number/ear	TGW
				lodging	brackling		
Hellvus	*2007*	*H*	*7*	*1*	*3*	*6*	*8*
Festus	2004	H	3	1	4	6	4
Helltop	*2009*	*H*	*6*	*2*	*3*	*7*	*7*
Walet	2001	P	6	2	3	4	5
Brasetto	2009	H	4	3	3	6	5
Palazzo	2009	H	5	3	4	6	5
Dankowskie Diament	2007	P	5	3	3	4	5
Amilo	1992	P	6	4	4	4	4
Askari	2003	H	5	4	5	6	4
Cantor	2007	S	5	4	6	5	5
Dukato	2008	P	6	4	5	4	5
Evolo	2006	H	4	4	4	5	6
Guttino	2009	H	3	4	4	6	5
Minello	2008	H	4	4	4	6	4
Picasso	1999	H	4	4	4	5	5
Avanti	1997	H	5	5	5	5	5
Balistic	2006	H	3	5	3	4	7
Bellami	2008	H	4	5	3	5	5
Caroass	2002	S	6	5	5	5	4
Carotop	2002	S	5	5	5	5	4
Conduct	2006	P	7	5	5	4	5
Gonello	2009	H	3	5	5	6	5
Kapitän	2008	S	5	5	4	5	4
Marcelo	2007	P	6	5	5	4	5
Matador	2001	P	6	5	5	5	5
Nikita	1998	P	6	5	5	4	5
Rasant	2004	H	5	5	5	6	6
Recrut	2002	P	6	5	5	4	5
Visello	2006	H	4	5	4	5	5
Agronom	2005	H	5	6	6	5	5
Amato	2005	H	4	6	6	6	6
Boresto	2000	P	8	6	5	4	5
Fugato	2004	H	6	6	6	6	5
Placido	2007	H	4	6	4	5	5

3.2| Phenotyping

Plant height and weight of parental lines and 304/1 F_2 population were measured at the harvest time. Scanning electron microscopy (SEM) was chosen as a fast phenotyping approach to screen whole 304/1 F_2 population, enabling structural analysis of tillers. More sophisticated methods, demanding chemical fixation and time-consuming embedding of samples, were used to evaluate SEM obtained data by light (LM) and transmission electron microscopy (TEM). The content of elements was determined by inductively coupled plasma optical emission spectrometry (ICP-OES).

3.2.1| Scanning Electron Microscopy

Around 1 cm thick hand cross-sections of basal internodes of parental lines: 'ms 135' (6 individuals) and 'R 1124' (5 individuals), as well as '304/1' F_2 mapping population (130 individuals), were attached onto carbon coated aluminium specimen mounts. Afterwards, specimens were gold sputtered three times at 40 mA and 0.3 mbar pressure of argon, one minute each (giving a 45 nm layer of gold), in an Edwards Sputter Coater S150B (Edwards High Vacuum Inc., Crawley, West Sussex, UK), and examined in a field-emission scanning microscope, Hitachi S-4100 (Hisco Europe, Ratingen, Germany), at an acceleration voltage of 10 kV. Digital recordings at a magnification of 20-30, 130, and 1000 x of at least three cross-sections of internodes were analysed for each individual. Total numbers of cross-sections analysed in the SEM was 423 (33 of parental lines and 390 of the F_2 population).

3.2.2| Light Microscopy

Semi-thin sections of parental lines basal internodes embedded in Spurr's resin were analysed in a bright-field after staining with Azur II/methylene blue, standard histological staining (see chapter 2.2.2), as well as in UV light after staining with 0.01% aqueous solution basic fuchsin (see chapter 2.2.3). Additionally, 100 µm thick sections of fresh and dry tillers embedded in 8% agarose, prepared with the aid of a Leica VT1000S vibrating microtome, were used for phloroglucinol staining of lignins and analysed in a bright-field microscope (see chapter 2.2.4).

3.2.2.1| Microwave-assisted fixation, dehydration, and infiltration of rye basal internodes for LM

For comparative histological analysis, conventional and microwave-assisted fixation, substitution, and resin embedding were performed in a PELCO Bio Wave®34700-230 (Ted Pella, Inc., Redding CA, USA). Around 1 mm thick fragments of dry and fresh internodes were fixed in 2% glutaraldehyde (GA) and 2% formaldehyde (FA) in cacodylate buffer

(50 mM, pH 7.2) using the modified fixation method of chemical fixation combined with microwave irradiation (1 min at 150 W with 15 mm Hg of vacuum), followed by overnight incubation, as shown in Table 3. After fixation, the samples were washed once with cacodylate buffer (50 mM, pH 7.2) and twice with degassed ultrapure water. Afterwards, the probes were dehydrated through an ethanol series and treated twice with 100% propylene oxide (PO), which is a suitable solvent for Spurr's low viscosity resin. The advantage of microwave irradiation was also taken in washing and dehydration steps (45 seconds at 150 W), followed by 15 minutes of incubation. Next, the probes were infiltrated with a progressive series of Spurr in PO solutions by combining microwave irradiation (3 min at 250 W with 5 mm Hg of vacuum) with 3 hours of incubation.

TABLE 3 Protocol of microwave-assisted fixation, dehydration, and infiltration of basal internodes for LM.

Process	Chemical compound	Microwave irradiation	Time of irradiation	Vacuum
Fixation	2% GA + 2% FA in 50 mM cacodylate buffer (pH 7.2)	150 W	1 min.	**15 mm Hg**
		+ overnight incubation at RT		
Washing	1x 50 mM cacodylate buffer (pH 7.2)	150 W	45 s	-
	2x degassed ultrapure water	+ 15 min incubation at RT		
Dehydration	Ethanol series: 30%, 40%, 50%, 60%, 70%, 80%, 90% 2x 100% EtOH And 2x propylene oxide	150 W	45 s	-
		+ 15 min incubation at RT		
Infiltration	25% Spurr in PO 40% Spurr in PO	250 W	3 min	**5 mm Hg**
		+ 3 h incubation at RT		
	50% Spurr in PO	250 W	3 min	**5 mm Hg**
		+ overnight incubation at RT		
	60% Spurr in PO 70% Spurr in PO 80% Spurr in PO 90% Spurr in PO	250 W	3 min.	**5 mm Hg**
		+ 3 h incubation at RT		
	100% Spurr	250 W	3 min	**5 mm Hg**
		+ overnight incubation at RT		
	100% Spurr	250 W	3 min	**5 mm Hg**
		+ 3 h incubation at RT		

Eventually, samples were polymerised at 70°C for 24 hours in beem capsules size 00 (Plano GmbH, Wetzlar) in Spurr's resin. Hardened sample blocks were trimmed with a Leica EM TRIM (Leica, Vienna, Austria) equipped with a diamond miller (Leica, Vienna, Austria), and cut into 2 µm thick sections with the aid of a Reichert-Jung Ultracut S microtome (Leica, Vienna, Austria) equipped with a DiATOME histo diamond knife (size 6.0; DiATOME Ltd, Biel, Switzerland). Semi-thin sections were mounted on slides and used for histological examination.

3.2.2.2 | Azur II/methylene blue staining

2 µm thick cross-sections on poly-L-lysine coated glass slides (Poly-Prep Slides, Sigma-Aldrich, St. Louis, USA) were stained with standard histological staining, 1% Azur II / 1% methylene blue in 1% aqueous borax, for 2 minutes on a heating plate (Leica HI1220, Leica Biosystems Nussloch GmbH, Nussloch) set at 60°C, washed three times with ultrapure water (5 min each), dried on the heating plate, and cover-slipped with Entallan embedding medium (Merck, Darmstadt, Germany). The sections were analysed and recorded in a bright field in a Zeiss Axio Imager M2 light microscope equipped with an Axiocam (Carl Zeiss, Jena, Germany).

3.2.2.3 | Basic fuchsin staining

Basic fuchsin staining was performed for analysis using fluorescence microscopy, as it has an affinity for lignified, suberized or cutinised CW (Dharmawardhana *et al.*, 1992; Kraus *et al.*, 1998). 2 µm thick cross-sections on poly-L-lysine coated glass slides (Poly-Prep Slides, Sigma-Aldrich, St. Louis, USA) were stained with 0.01% aqueous solution of basic fuchsin for 5 minutes on a heating plate (Leica HI1220, Leica Biosystems Nussloch GmbH, Nussloch) set at 40°C, washed three times with ultrapure water (5 min each), dried on a heating plate, and cover-slipped with Entallan embedding medium (Merck, Darmstadt, Germany). The sections were analysed in a Zeiss Axio Imager M2 light microscope equipped with a filter set 20 (excitation: 546 nm, beamsplitter: 560 nm, emission: 575-640 nm) and recorded with an Axiocam (Carl Zeiss, Jena, Germany).

3.2.2.4 | Phloroglucinol/HCl staining

In order to visualize differences in lignin content, 100 µm sections of fresh and dry tillers, embedded in 8% agarose, prepared with the aid of a Leica VT1000S vibrating microtome (Leica Biosystems Richmond, Richmond, USA) were used for phloroglucinol/HCl staining (Wiesner test; in 1878 Wiesner reported the classic colour reaction of lignin with phloroglucinol; McCarthy and Islam, 1999). The sections were treated 30 minutes with 1 % (w/v) phloroglucinol in 10.1 M hydrochloric acid-ethanol (25/75; v/v) solution

in the darkness and afterwards were analysed and recorded in a bright-field in a Zeiss Axio Imager M2 light microscope equipped with an Axiocam (Carl Zeiss, Jena, Germany).

3.2.3 | Transmission Electron Microscopy

For ultrastructure analysis of the CWs, 70 nm thick sections of Spurr-embedded fresh and dry material were contrasted with uranyl acetate and lead citrate prior to examination in an FEI Tecnai G^2 Sphera TEM at 120 kV.

3.2.3.1 | Microwave-assisted fixation, dehydration, and infiltration of rye basal internodes for TEM

For a comparative ultrastructural analysis material was prepared similarly to the protocol for light microscopy. Namely, around 1 mm thick fragments of dry and fresh internodes were fixed in 2% glutaraldehyde (GA) and 2% formaldehyde (FA) in cacodylate buffer (50 mM, pH 7.2) using the modified fixation method of chemical fixation combined with microwave irradiation (1 min at 150 W with 15 mm Hg of vacuum), followed by overnight incubation, as shown in Table 4. After fixation, the samples were washed once with cacodylate buffer (50 mM, pH 7.2) and twice with degassed ultrapure water taking advantage of microwave irradiation (45 seconds at 150 W), followed by 15 minutes of incubation. Next, the material was post-fixed with 1% aqueous solution of osmium tetroxide in three steps: 2 minutes in 15 mm Hg of vacuum, 2 minutes of 80 W of microwave irradiation combined with 15 mm Hg of vacuum, and eventually another 2 minutes in 15 mm Hg of vacuum, followed by 1 hour of incubation at room temperature. Afterwards, samples were washed three times with degassed ultrapure water (combining 45 s at 150 W of microwave irradiation with 15 min of incubation). The next step was microwave-assisted (45 s at 150 W, followed by 15 minutes of incubation) dehydration of samples through an ethanol series and treatment with 100% PO, as shown in Table 4. Eventually, the samples were infiltrated with a progressive series of Spurr in PO solutions by combining microwave irradiation (3 min at 250 W with 5 mm Hg of vacuum) with 3 hours of incubation. Afterwards, they were polymerised at 70°C for 24 hours in beem capsules size 00 (Plano GmbH, Wetzlar) in Spurr's resin, and trimmed with a specimen trimming device (Leica EM TRIM, Leica, Vienna, Austria) equipped with a diamond miller (Leica, Vienna, Austria). Afterwards, samples were cut into approximately 70 nm thick sections with the aid of a Reichert-Jung Ultracut S (Leica, Vienna, Austria) equipped with a DiATOME ultra 45° diamond knife (DiATOME Ltd, Biel, Switzerland) and collected on 50 mesh hexagonal copper grids (Plano GmbH, Wetzlar, Germany) covered with Formvar polyvinyl formal (Sigma-Aldrich Chemie GmbH, Steinheim, Germany).

TABLE 4 Protocol of microwave-assisted fixation, dehydration, and infiltration of basal internodes for TEM.

Process	Chemical compound	Microwave irradiation	Time of irradiation	Vacuum
Fixation	2% GA + 2% FA in 50 mM cacodylate buffer (pH 7.2)	150 W	1 min	**15 mm Hg**
		+ overnight incubation at RT		
Washing	50 mM cacodylate buffer (pH 7.2)	150 W	45 s	-
	2x degassed ultrapure water	+ 15 min incubation at RT		
Post-fixation	1% osmium tetroxide	-	2 min	**15 mm Hg**
		80 W	2 min	**15 mm Hg**
		-	2 min	**15 mm Hg**
		+ 1 h incubation at RT		
Washing	3x degassed ultrapure water	150 W	45 s	-
		+ 15 min incubation at RT		
Dehydration	Ethanol series: 30%, 40%, 50%, 60%, 70%, 80%, 90% 2x 100% EtOH And 2x propylene oxide	150 W	45 s	-
		+ 15 min incubation at RT		
Infiltration	25% Spurr in PO 40% Spurr in PO	250 W	3 min	**5 mm Hg**
		+ 3 h incubation at RT		
	50% Spurr in PO	250 W	3 min	**5 mm Hg**
		+ overnight incubation at RT		
	60% Spurr in PO 70% Spurr in PO 80% Spurr in PO 90% Spurr in PO	250 W	3 min	**5 mm Hg**
		+ 3 h incubation at RT		
	100% Spurr	250 W	3 min	**5 mm Hg**
		+ overnight incubation at RT		
	100% Spurr	250 W	3 min	**5 mm Hg**
		+ 3 h incubation at RT		

3.2.3.2 | Contrasting of ultra-thin sections and TEM analysis

Ultra-thin sections on copper grids were contrasted in a QG-3100 Automated TEM Stainer (RMC Products by Boeckeler, Boeckeler Instruments Inc., Tucson, USA) with 2% aqueous solution of uranyl acetate (UA; see the preparation of solution in 2.3.3) and lead citrate (PbC; see the preparation of solution in 2.3.3) using a light staining program, as shown

in Table 5. Afterwards contrasted grids were analysed in an FEI Tecnai G^2 Sphera TEM (FEI Company, Eindhoven, the Netherlands) at 120 kV and recorded by an Olympus Veleta side mounted TEM CCD camera (Olympus Deutschland GmbH, Hamburg, Germany).

TABLE 5 Staining program of ultra-thin sections with uranyl acetate (UA) and lead citrate (PbC).

Step No.	Process		Time
1	Filling the chamber with degassed Millipore water		1 min
2	Wait state (the staining chamber and tubes soak) to wet the grids		10 min
3	Filling the chamber with UA		24 s
4	Staining with UA		10 min
5	Disposing of UA (washing with degassed water)		2 min
6	Wait state (the interim step before next command)		6 s
7	Filling the chamber with PbC		24 s
8	Staining with PbC		5 min
9	Disposing of PbC (washing with degassed water)		2 min
10	Wait state (the interim step before next command)		6 s
11	Filling the chamber with degassed Millipore water		1 min

3.2.3.3| Preparation of contrasting solutions

3.2.3.3.1| 2% Uranyl acetate
1. 4.0 g uranyl acetate was added to 200 ml of degassed water and stirred until dissolved;
2. A 0.2 μm pore filter was used to filter the solution;
3. Stored in a brown flask away from light.

3.2.3.3.2| Lead citrate (modified after Reynolds, 1963)
1. 2.66 g of lead nitrate and 3.52 g sodium citrate was added to a 125 Erlenmeyer flask;
2. 60 ml of degassed water was added and shook well;
3. The mixture was let stand for 10 minutes and shook gently about 5 times;
4. Approximately 11 ml of 1.0 M NaOH solution was added to the flask to bring the pH close to 12;
5. 1.0 M NaOH was added drop by drop until a pH of 12 was reached;
6. Filled up to 100 ml with degassed water.

3.2.4| Measurements of anatomical traits

The following traits: the diameter of the second basal internode, culm wall thickness, the thickness of sclerenchymal tissue, the ratio of the thickness of sclerenchyma to the diameter of the basal internode, the diameter of epidermal and sclerenchymal cells, the thickness of sclerenchymal and inner periclinal cell walls of the epidermis recorded in LM, SEM, and TEM were measured using Fiji open-source platform for biological-image analysis (Schindelin *et al.,* 2012).

3.2.5| Content of elements

25 mg of dry plant material ground in a Vibratory Disc Mill (RS 200, Retsch) was used for the evaluation of silicon content. The samples were prepared according to the method developed by Dr. Kai Eggert and Dr. Yudelsy Antonia Tandron Moya (Molecular Plant Nutrition Group, Leibniz Institute of Plant Genetics and Crop Plant Research in Gatersleben), which was adapted from the method described by Guntzer *et al.* (2010). The content of silicon in samples was evaluated by Inductively Coupled Plasma Mass Spectrometry (iCAP 6500 dual OES spectrometer, Thermo Fischer Scientific, Waltham, MA, USA) coupled to an ASX-520 Autosampler (ASXpress® plus system, CETAC) for sample introduction. Silicon content was determined by the measurement of the intensity of the light emitted at 251.6 nm wavelength, which was a relative intensity to the Yttrium signal at 371.0 nm wavelength.

40 mg of dry plant material ground a Vibratory Disc Mill (RS 200, Retsch) was weighted into PTFE digestion tubes and used for the evaluation of boron, calcium, copper, iron, potassium, magnesium, manganese, molybdenum, sodium, nickel, phosphorus, sulfur, and zinc content. Afterwards, samples were digested in nitric acid under pressure using a microwave digester (UltraCLAVE IV; MLS, Leutkirch, Germany). Elemental analysis was undertaken using inductively coupled plasma optical emission spectroscopy (iCAP 6500 dual OES spectrometer; Thermo Fischer Scientific, Waltham, MA, USA) coupled to an ASX-520 Autosampler (ASXpress® plus system, CETAC) for sample introduction. CertiPUR Yttrium ICP standard (Merck KGaA) was used as a standard for evaluation of elements, with the final ISTD concentration of 2 ppm in water acidified 0.2% with HNO_3.

3.2.6| Post-hoc analysis of phenotypic data

The collected data were analysed using GenStat Sixteenth Edition (VSN International Ltd.), a statistical package, at probability level $P \leq 0.05$. A Welch *t*-test was used to compare traits between parental lines and to find statistically significant differences. Person's moment coefficient of skewness and kurtosis was calculated using GenStat in order to

check the normality of data. The skewness of a random variable X (the third standardised moment γ_1) was calculated according to the equation:

$$\gamma_1 = \frac{E[(X - \mu)^3]}{(E[(X - \mu)^2])^{3/2}},$$

and kurtosis (fourth standardised moment γ_2) according to the equation:

$$\gamma_2 = \frac{E[(X - \mu)^4]}{(E[(X - \mu)^2])^2} - 3,$$

where μ is the mean and E is the expectation operator.

Pearson correlation coefficients (PCC) were calculated between all the traits analysed using GenStat to investigate the degree of linear dependence between the traits. Broad-sense heritability (H) was calculated to estimate how much variation in a phenotypic trait in a population was due to genetic variation among individuals in that population, according to Mahmud and Kramer (1951), as follows:

$$H = \frac{\sigma^2 F_2 - \sqrt{(\sigma^2 P_1 \times \sigma^2 P_2)}}{\sigma^2 F_2},$$

where $\sigma^2 F_2$, $\sigma^2 P_1$, and $\sigma^2 P_2$ are the variances of the F_2 population, female parent, and male parent respectively.

3.3 | Genotyping

Prior to the construction of a linkage map the two parental lines: 'ms 135' and 'R 1124' were screened for polymorphism with 269 single sequence repeat (SSR) primer pairs. The 304/1 F_2 population (129 individuals) was genotyped using polymorphic SSR markers, and afterwards using DArTseq platform because of low polymorphism between parental lines (only 45 SSRs could finally be used for mapping).

3.3.1 | Isolation of DNA

DNA was isolated from liquid nitrogen preserved leaves in of 'ms 135', 'R 1124', and 304/1 F_2 population, using a previously described method (Plaschke *et al.*, 1995a), as follows:
1. Leaf tissue was ground in liquid nitrogen chilled mortar;
2. The powder was transferred into liquid nitrogen chilled 50 ml propylene tube;
3. 25 ml of heated to 60 °C extraction buffer (see 3.2.1) was added to frozen plant powder;

4. Material with buffer was incubated 45 min at 60 °C, shaking every 10 minutes;

5. Chloroform : isoamyl alcohol (24:1) mixture was added to the top of the mixture up to 45 ml, and mixed vigorously until a good emulsion was formed;

6. The mixture was centrifuged for 25 minutes at 3000 rpm;

7. The upper phase was collected into a new 50 ml tube;

8. Steps 5-7 were repeated;

9. 2 volumes of chilled to -20 °C 95% ethanol were added and mixed to precipitate nucleic acids;

10. Nucleic acids were scooped out with a glass hook and transferred into 15 ml propylene tube containing 5 ml of chilled to -20 °C 70% ethanol, afterwards sedimented by 5 minutes of centrifugation at 3000 rpm and let air dry;

11. Nucleic acids were afterwards dissolved in 4 ml of TE buffer (see 3.2.3);

12. 20 µl of a 10 mg/ml stock solution of RNase was added, vortexed gently, and incubated at 60 °C for 1 hour;

13. 5 ml of chloroform : isoamyl alcohol (24:1) mixture was added, mixed;

14. Samples were centrifuged for 20 minutes at 3000 rpm, and the upper phase was transferred into a new 15 ml tube;

15. Steps 13-15 were repeated;

16. 0.1 volume (around 400 µl) of 3M sodium acetate (pH 5.2; see 3.2.4) and 2 volumes (8 ml) of chilled to -20 °C 95% ethanol was added and gently mixed to precipitate DNA;

17. Samples were centrifuged for 15 minutes at 3000 rpm;

18. Afterwards, the pellet was washed with chilled to -20 °C 70% ethanol (5 ml);

19. DNA was pelleted by centrifugation (5-10 minutes at 3000 rpm), let air dry;

20. 0.5 - 1 ml of TE buffer was added and incubated for 1 hour at 60 °C, occasionally vortexed until dissolved;

21. The quality of DNA was checked on 1.5% agarose gel after electrophoresis at 108 V using 2 µl of extracted DNA per well and 5 µl of a GeneRuler 1kb Plus DNA Ladder (Thermo Fisher Scientific, Waltham, MA, USA) as a molecular-weight size marker.

3.3.2 | Preparation of buffers for the isolation of DNA

3.3.2.1 | DNA extraction buffer solution:

100 mM Tris-HCl pH 8.0

500 mM NaCl

50 mM EDTA

1.25% SDS

3.8 g/l sodium bisulfate

3.3.2.2 | Tris-HCl pH 8.0 solution (1L):

     121.1 g Tris dissolved in 800 ml H_2O

     42 ml of concentrated HCl

3.3.2.3 | TE buffer (pH 7.5 solution):

     10 mM Tris-Cl, pH 7.5

     1 mM EDTA

3.3.2.4 | 3 M sodium acetate solution (1L):

     408.1 g of sodium acetate dihydrate dissolved in 800 ml H_2O

     pH adjusted with glacial acetic acid to 5.2, and filled up to 1 L with H_2O

3.3.3 | SSR markers

269 Single Sequence Repeats (SSRs, microsatellites: 68 WMS, 109 RMS, 36 REMS, and 56 SCM markers; Röder *et al.,* 1998; Saal and Wricke, 1999; Korzun *et al.,* 2001; Hackauf and Wehling, 2002; Chebotar *et al.,* 2003; Khlestkina *et al.,* 2004) were amplified in a volume of 25 µl containing: 50-100 ng of template DNA, 250 nM of each primer (left primers were labelled with Cy5), 200 µM of each deoxynucleotide, PCR buffer (10 mM of Tris-HCl, 50 mM of KCl, 1.5 mM of $MgCl_2$, and 0.01% of gelatin to stabilise *Taq* DNA polymerase), and 1 U of *Taq* DNA polymerase. 96-well thermal cyclers (Applied Biosystems, Thermo Fisher Scientific Inc.) were used to amplify SSRs with following PCR program: 3 minutes of initial denaturation at 94ºC, followed by 45 cycles of 1 minute of denaturation at 94ºC, 1 minute of annealing at 50, 55, or 60 ºC, depending on the primer set, 2 minutes of elongation at 72ºC, and 10 minutes of the final extension at 72ºC. Products were analysed for length polymorphism on 6% polyacrylamide gel (SequaGel, Biozym, National Diagnostics USA) conducted in 1 × TBE buffer (90 mM Tris-borate, pH 8.3, and 2 mM EDTA) by automated laser fluorescence ALF Express DNA sequencer (Amersham Biosciences Europe GmbH, Freiburg, Germany) at 600 V of voltage, 50 mA of current, 50 W of power, and a sampling interval of 2 s, using a short gel cassette. An external standard with four fragments of different size (73, 122, 196, and 231 bp, also 304 bp if the size of the product was greater than 231 bp or similar to that size) was loaded in the first lane. Internal standards of choice, depending on the size of the product, were loaded in each lane with the products. Fragment sizes were calculated using the ALFwin Fragment Analyzer software package (Version 1.02; Pharmacia, Tokyo, Japan) by comparison with the internal and external size standards.

3.3.4 | DArTseq

A high-density DArTseq (Diversity Arrays Technology) platform, developed by Diversity Arrays Technology Pty Ltd. (Canberra, Australia) for high-throughput genotyping based on sequencing results generated by NGS technologies, was chosen as a fast and cost-effective genotyping technology profiling the whole genome in a single assay on an automated platform (Jaccoud *et al.,* 2001), recently developed for rye with high efficacy corresponding predominantly to active genes (Bolibok-Brągoszewska *et al.,* 2009; Milczarski *et al.,* 2011; Bolibok-Brągoszewska *et al.,* 2014). 20 µL at 50-100 ng/µL of extracted genomic DNA per each sample of parental line and 130 individuals of 304/1 F_2 population line were used for genotyping using Rye GBS 1.0 platform developed by the Diversity Arrays Technology Pty Ltd, as previously described (Bolibok-Brągoszewska *et al.,* 2009). DArTseq as a combination of complexity reduction methods developed initially for a hybridisation-based DArT microarray and sequencing of resulting representations on next-generation sequencing platforms provided two types of markers: (1) dominant SilicoDArTs (scored for presence or absence of a given sequence variant, analogous to microarray DArTs), extracted *in silico* from sequences obtained from genomic representations, and (2) co-dominant SNPs in fragments present in the representation.

3.4 | Construction of a genetic map

The genetic map was constructed in JoinMap 4.1 (Kyazma B.V.) basing on the segregating markers (checked with χ^2-test, P < 0.05) with the lowest number of missing data (less than 10%). Markers of unknown parental origin and not segregating were removed from the dataset. LOD > 12 was used to separate 7 linkage groups of markers. The order of markers was determined in JoinMap 4.1 by maximum likelihood mapping, and afterwards, the distances between markers were determined by regression mapping with Kosambi function (Kosambi, 1943). Afterwards, the groups were assigned to chromosomes using GenomeZipper (Martis *et al.*, 2013). Graphical genotypes were inspected visually to verify the order of the markers; singletons data points were recorded as missing data in the dataset and calculations were repeated.

3.5 | QTL analysis

Phenotypic data for 129 individuals of 304/1 F_2 population and genotypic/map data based on 1,041 SNP and SSR markers were used for QTL analysis in GenStat Sixteenth Edition (VSN International Ltd, Hemel Hempstead, Herfordshire, UK). To confirm the significance level of 3.0 LOD threshold a permutation test with 10,000 interations for each trait was performed using QGene 4.3.10 (R.Joehanes and J.C.Nelson, Department of Plant Pathology, Kansas State University; Nelson, 1997; Joehanes and Nelson, 2008). Available in QGene single-marker regression function was also used for initial analysis of QTL. Genome-wide scans (Simple and Composite Interval Mapping) for QTL effects were performed in GenStat. The initial genome-wide scan was performed by Simple Interval Mapping (SIM) to obtain candidate QTL positions. Genome-wide scan for QTL effects was performed by Composite Interval Mapping (CIM) with cofactors, which were potential QTL positions set as the candidate QTL detected at the previous scan. 'Select Final Model' dialog was used to select and fit the final QTL model from a list of candidate QTL to estimate QTL effects for all QTL retained in the selected model. QSESTIMATE command was used to estimate QTL effects, which fit the following model (Boer *et al.,* 2014):

$$y_i = \mu + \Sigma_{l \in L} \left(x_{il}^{add} \, \alpha_l^{add} + x_{il}^{dom} \, \alpha_l^{dom} \right) + G_i$$

where y_i is the trait value of genotype i, x_{il}^{add} are the additive genetic predictors of genotype i for locus l, and α_l^{add} are the associated effects, x_{il}^{dom} are the dominance genetic predictors, and α_l^{dom} are the associated effects, G_i is the residual unexplained genetic and environmental variation, which is assumed to follow a normal distribution with mean 0 and variance σ^2. Genetic predictors are genotypic covariables that reflect the genotypic composition of a genotype at a specific chromosome location (Lynch and Walsh, 1998).

3.6 | Development of KASP markers

From the SNP markers, which were segregating, and each was associated with at least four traits, 6 were chosen to develop KASP markers for marker-assisted selection (MAS). Four of the SNPs (two on the chromosome 1R and two on 7R) were associated with plant height. Three of the selected SNPs were linked to the thickness of the culm wall (on 4R and 7R). Two of the markers located on 1R were associated with the thickness of sclerenchymal and inner periclinal CW of the epidermis, and the content of zinc.

Two of the markers on 7R were linked to the thickness of sclerenchyma, the content of molybdenum and copper. One SNP located on 3R was associated with the number of epidermal invaginations, the length of the second basal internode, dry weight of culms, and the number of tillers. And finally, one SNP on the chromosome 4R was linked to the diameter of the sclerenchymal and epidermal cell, as well as sulfur content.

The flanking sequences (Table 6) for the development of KAPS primers were kindly provided by Doctor Eva Bauer (Technische Universität München) since the sequences provided with DArT markers were only around 50 to 60 base pairs long. For each KASP marker, two allele-specific forward primers and one common reverse primer were designed. Approximately 1.5 µL of 20 ng/µL of DNA was used in a single PCR reaction, which was performed in a total volume of 10 µL containing 5 µL of 2x KASP reaction mix and 0.014 µL of assay mix of primers and thermal cycling conditions shown in Table 7.

After completion of the PCR reaction, the SNP allele-specific detection was based on the homogenous fluorescence assay (FRET). Each forward primer incorporated one distinct fluorescence dye (6-carboxyfluorescein, with maximum absorbance at 495 nm light wavelength and maximum emission at 518 nm, or hexafluorofluoresceine, with maximum absorbance at 535 nm and maximum emission at 556 nm). The detection of fluorescence was performed using an Omega Fluorostar scanner (BMG LABTECH GmbH, Offenburg, Germany), and analysed using the SNPviewer 2 Version 4.0 software (LGC Genomics, UK).

TABLE 6 Sequences used for the development of KASP markers. The sequences provided with DArT markers highlighted with yellow colour.

SNP ID	Sequence
5218584	CGCGCTCCGACATGGACATGGGCTTCGCCGGCCCCACCACCTGCCCGCCGCCGCCGCCGTCCCCGCCTTCAG[T/C]AAGCGTCCCCTGCTGCATGATTGACGGCTGCAGGAGCTCATGGTTGTTGCAGCCGCCGTCGCCGGCGCCACCAC
3349542	CTTGTCGAGCCACCGGTATGTGAATGTGTTCGTGTGTGAGGGAGGCACGATGTTGATCTGGAGGGTGTCAAAGCATCATGGCCAAACCTCACGACCGTAAGTACAATGAGCTAGAATGTGAT[T/C]AATGTTGTCCTTGTCATGTAAGCATGTGAAGCAAGCAAAAGGCACATCCTGCAGATCGTGCCTAGCACGTCTGTCAGAGGTCCATCGTCGATATTG
5224120	CTGTAAATACATAACGATTTAATGGGTGCTGAACATACAAATCCCCATCCCTCCTTCGTGAACTCCTGACCGACTATTCTGAAGTTGCAGTGGGTTGACAGGAAGATCTCAACACATGGCATCTCGTCAACAACTGCAGCAACACC[G/A]CCGTCTTTCGGCCCACGATTAAGGGCATTGGCGTACTCCTCAACAGTGCTCAGTGGTACTAACCGGGATTCAGGT
3596125	GCCGGTTGCCTAAATTTCCAGCGCATGCATATGGCCACGTATGGTAGCCCGACCTGGTCAAACTAGATAAGGGAGAGCCCGAGTCACTTCGATCCCAAATCCA[T/C]AGCGGAGACCCCAGGGCCAGCCGCATCACCGACTGCAGGAAGAGCTCTAGGCGTGCTCGTCCTCGTCGGAAAAGCCCCTAGGAATGAGTGTGTAGGGTGTGATGCCGTTCGCGT
3353579	GAGCAGGCGCCGGTGACGGCGACGGGGCTGTTCTGCCGGCCGCTGAAGACGCTGGACCTCTTCCCCGGCGCGATCAAGGAGGAGCAGCGCGACGTCGCCTAGC[C/T]ACCTCCAACCTATAGCTAGCTGCAGCAGCAGTCGTCGTCGTCGTCGTAGTACGTAGAGCAGTCCGTACGTTACGCGCGCCGCGCGTTGTACGTACGCAGGTAGAGCAGCAGCAG
100074162	CTCCACCTCGAGCGAGCAAACGACAGCCAGCGGAAGCAAGAGC[G/A]CCCAGCAGGCCTAGGTGCGCCGCCCAAGCTCTTCTTCACGACGGCGCCGAGCCGCCTGCGCGCGTGGCAACACGCTCCTCCGCCGGTGCTGCGTGAGCTGA

TABLE 7 Thermal cycle conditions for KASP reactions.

Step	Process	Temperature	Time	No. of cycles per step
1	Activation	94 °C	15 min	1
2	Denaturation	94 °C	20 s	10
	Annealing/elongation	61 – 55 °C	60 s (drop 0.6 °C per cycle)	
3	Denaturation	94 °C	20 s	26
	Annealing/elongation	55 °C	60 s	

4. RESULTS

4.1 | Identification of the traits responsible for lodging resistance

Morphological and structural analysis of the lodging resistant line and wildtype line in Light (LM), Scanning Electron (SEM), and Transmission Electron Microscope (TEM) revealed statistically significant differences (tested with Welch's t-test, p < 0.05) in: the plant height, the number of tillers per plant, dry weight of culms and of a single culm, the diameter of the second internode, the number of epidermal invaginations stabilizing the tiller, the thickness of culm wall, the thickness of sclerenchymal tissue, the ratio of sclerenchyma to the diameter of the second internode, the number of vascular bundles present in the sclerenchymal layer, and the thickness of sclerenchymal cell walls and inner periclinal cell walls of the epidermis. Additionally, the analysis of elements by Inductively Coupled Plasma Optical Emission Spectrometry (ICP-OES) revealed significant differences in the content of calcium, copper, magnesium, manganese, potassium, sulfur, zinc, and silicon.

4.1.1 | External morphology

The mean plant height (PH) was 110.7 cm (± 6.919 SD) for 'ms 135', the lodging resistant parental line, and 95 cm (± 15.22 SD) for 'R 1124', the wildtype parental line (Fig.6A, Table 8). The differences in PH between two parental lines were statistically significant according toWelch's t-test (p < 0.05). This phenotypic trait was used for screening of 130 individuals of segregating F_2 population. The minimum value for PH in '304/1' F_2 population was 85 cm, and the maximum was 139 cm (Fig.6B, Suppl. Fig.45A, Table 8). The distribution of the trait was normal (Suppl. Fig.45B) with a skewness of -0.323 and kurtosis of 0.441.

On the other hand, the length of the second basal internode (LBI) did not differ (t-test, p > 0.5) between two parental lines. *Id est:* in lodging resistant line it varied between 9.8 and 19.5 cm, with a mean value of 14.72 cm (± 2,899 SD). In the case of 'R 1124' line, the LBI varied between 12.6 and 18.7 cm, with a mean of 15.58 cm (± 2,439 SD; Fig.7A, Table 8). In 304/1 population the LBI varied between 12 and 19.4 cm (mean ± SD was equal to 16.85 ± 1.861 cm; Fig.7B, Suppl. Fig.45C, Table 8) and the distribution of this trait in 304/1 population was characterised by skewness of -0.805 and kurtosis -0.204 (Suppl. Fig.45D).

TABLE 8 External morphology of parental lines and 304/1 F_2 population: heritability (H), mean value (μ), median (Q_2), range ($[X_{min}, X_{max}]$), lower quartile (Q_1), upper quartile (Q_3), and standard deviation (SD).

	Trait	H	P-value	Population	μ	Q_2	$[Xmin, Xmax]$	Q_1	Q_3	SD
External morphology	Plant height [cm]	0.8379	0.0491	'ms 135'	110.7	112	[102, 118]	103	117	6.919
				'R 1124'	95	103	[70, 106]	85.75	105.2	15.22
				304/1	114.4	115	[85, 139]	108.5	121	9.988
	Length of the basal internode [cm]	0.2781	0.5397	'ms 135'	14.72	14.7	[9.8, 19.5]	13.2	17.4	2.899
				'R 1124'	15.58	16.2	[12.6, 18.7]	13.42	17.2	2.439
				304/1	16.85	17.3	[12, 19.4]	15.7	18.42	1.861
	No. of tillers	0.9751	0.0002	'ms 135'	16	16.5	[10, 21]	13	19	4.099
				'R 1124'	3	2	[1, 7]	1.75	4	2.345
				304/1	8.318	8	[2, 20]	6	10.25	3.423
	Culms dry weight [g]	0.9630	0.0007	'ms 135'	13.68	13.1	[6.6, 21.1]	11.1	17.1	4.984
				'R 1124'	1.72	1.2	[0.2, 4.4]	0.575	2.675	1.654
				304/1	15.35	14.7	[4.9, 30.5]	10.7	19	5.761
	Mean dry weight of culm [g]	0.8496	0.0415	'ms 135'	0.84	0.834	[0.66, 1.111]	0.728	0.873	0.155
				'R 1124'	0.546	0.629	[0.1, 0.7]	0.475	0.7	0.253
				304/1	1.944	1.893	[0.707, 3.775]	1.62	2.229	0.534
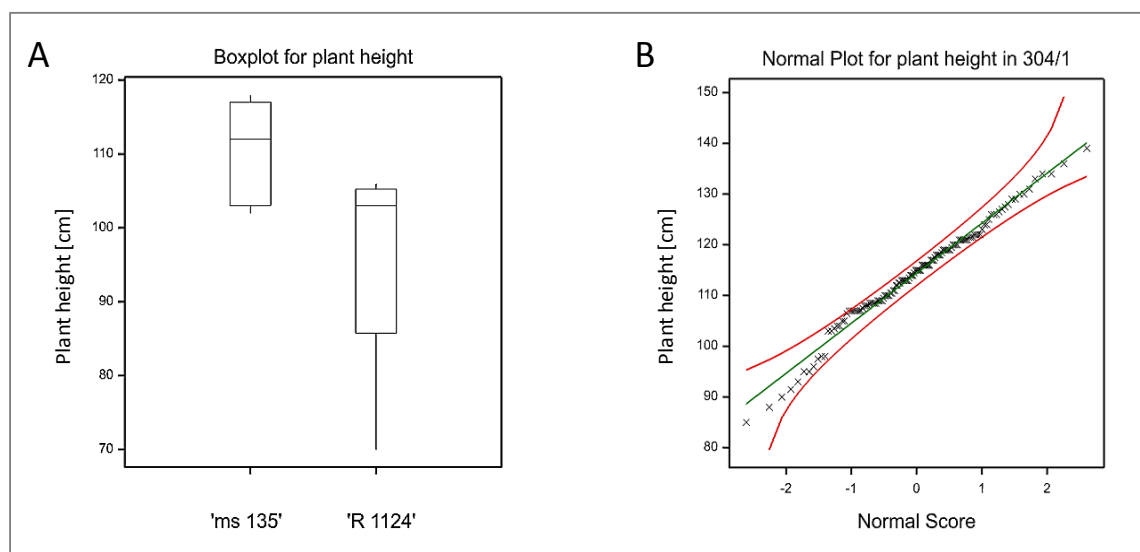
FIGURE 6 Boxplot showing median values for plant height, with whiskers indicating variability outside the upper and lower quartiles in two parental lines ('ms 135' and 'R 1124') (**A**). A Quantile-Quantile plot with 95% simultaneous confidence bands and a 1-1 reference line plotting observed data for 304/1 F_2 population against their expected quantiles for plant height (**B**).
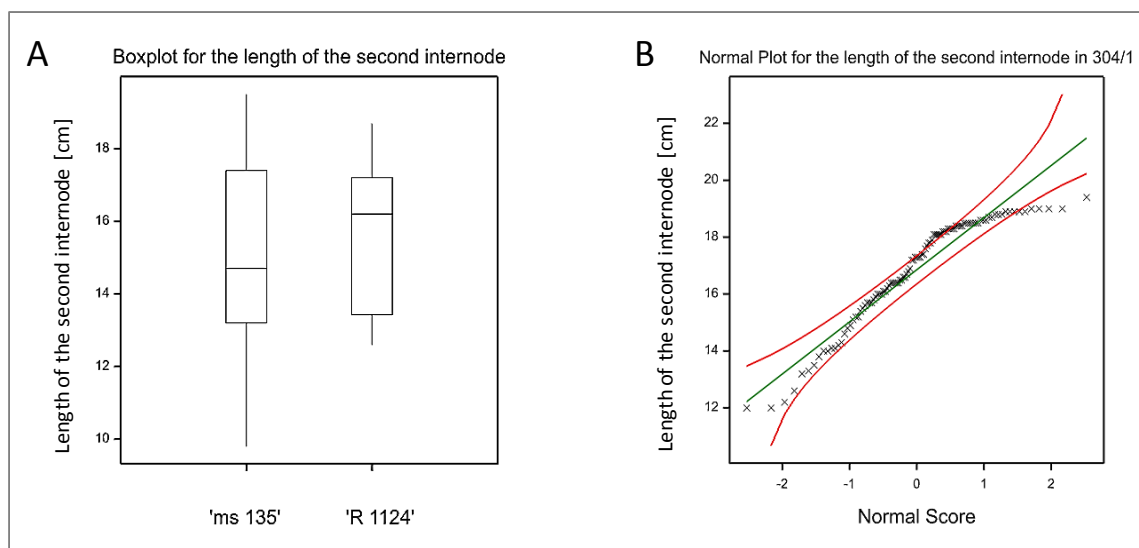
FIGURE 7 Boxplot showing median values for the length of the second internode, with whiskers indicating variability outside the upper and lower quartiles in two parental lines ('ms 135' and 'R 1124') (**A**). A Quantile-Quantile plot with 95% simultaneous confidence bands and a 1-1 reference line plotting observed data for 304/1 F_2 population against their expected quantiles for the length of the second basal internode (**B**).

The number of tillers (NoT) in the lodging resistant line varied between 10 and 21, with the mean value of 16 tillers per plant (± 4.099 SD; Fig.8A, Table 8). In the case of the wildtype, NoT was lower in comparison to 'ms 135' line, with a mean of 3 (± 2.345 SD), and these differences between parental lines were statistically significant (*t*-test, p < 0.0005). The mean value for this trait in 304/1 F_2 population was 8.318 (± 3.423 SD; Fig.8B, Suppl. Fig.45E, Table 8). The distribution of this trait was normal (Suppl. Fig.45F) and characterised by skewness of 0.734 and kurtosis of 0.315.
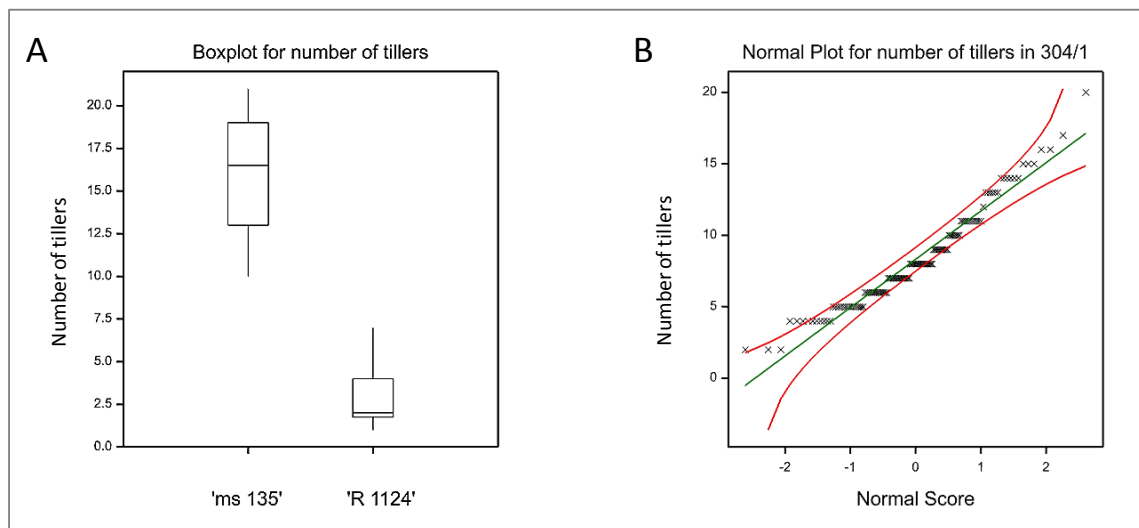
FIGURE 8 Boxplot showing median values for the number of tillers, with whiskers indicating variability outside the upper and lower quartiles in two parental lines ('ms 135' and 'R 1124') (**A**). A Quantile-Quantile plot with 95% simultaneous confidence bands and a 1-1 reference line plotting observed data for 304/1 F_2 population against their expected quantiles (**B**).

The dry weight of culms (DWC) in 'ms 135' line ranged between 6.6 and 21.1 g (mean ± SD = 13.68 ± 4,984 g) and was significantly (*t*-test, p < 0.001) higher than in the other parental line, where mean value was only 1.72 g (Fig.9A, Table 8). In 304/1 F$_2$ population, DWC varied between 4.9 and 30.5 g, with a mean of 15.35 g (± 5.761 SD; Fig.9B, Suppl. Fig.46A, Table 8), and the distribution (Suppl. Fig.46B) of this trait in population was described by skewness of 0.501 and kurtosis of -0.421.
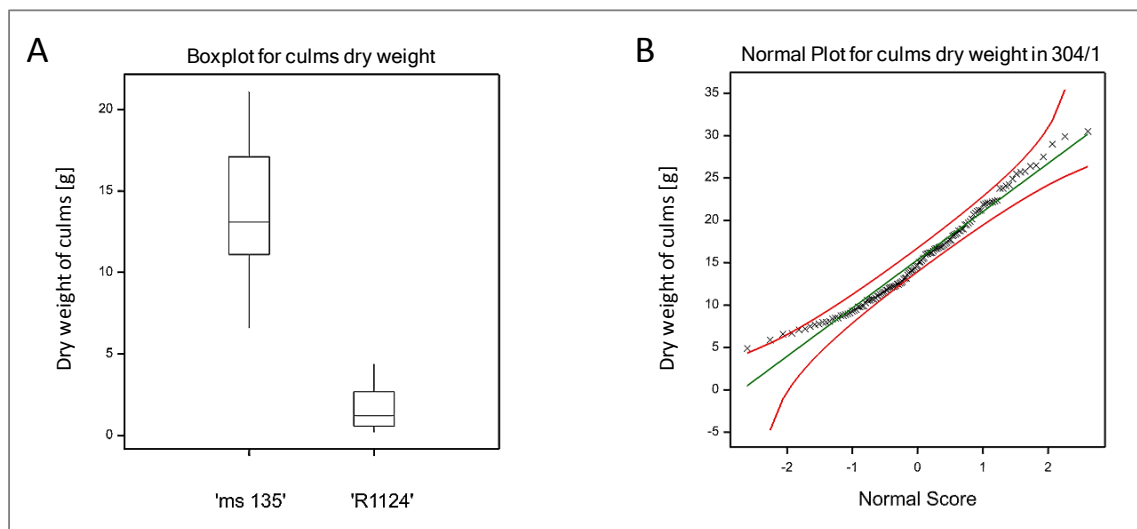
FIGURE 9 Boxplot showing median values for culms dry weight, with whiskers indicating variability outside the upper and lower quartiles in two parental lines ('ms 135' and 'R 1124') (**A**). A Quantile-Quantile plot with 95% simultaneous confidence bands and a 1-1 reference line plotting observed data for 304/1 F$_2$ population against their expected quantiles (**B**).

Similarly, also in the case of the dry weight of a single culm (DWS) statistically significant differences (*t*-test, p < 0.05) were found in two parental lines. Namely, mean dry weight of the wildtype culm was significantly smaller (ranged between 0.1 and 0.7 g with a mean of 0.546 g) in comparison to the lodging resistant line (minimum= 0.66 g, maximum = 1.111 g, mean = 0.84 g; Fig.10A, Table 8). In 304/1 F$_2$ population DWS varied between 0.707 and 3.775 g, with a mean of 1.944 g (± 0.534 SD; Fig.10B, Suppl. Fig.46C, Table 8). The distribution of this trait in 304/1 F$_2$ population was normal and characterised by skewness of 0.561 and kurtosis of 1.069 (Suppl. Fig.46D).
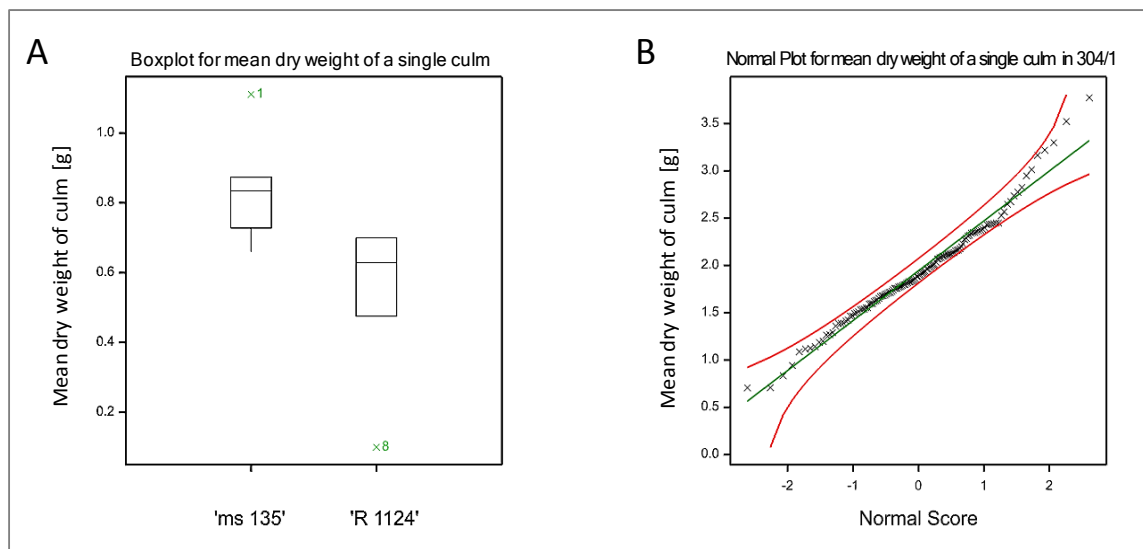
FIGURE 10 Boxplot showing median values for the mean dry weight of a single culm, with whiskers indicating variability outside the upper and lower quartiles in two parental lines ('ms 135' and 'R 1124') (**A**). A Quantile-Quantile plot with 95% simultaneous confidence bands and a 1-1 reference line plotting observed data for 304/1 F_2 population against their expected quantiles (**B**).

4.1.2 | Anatomy of tillers

The analysis of all tillers from parental lines (5 individuals from 'R 1124' and 6 from 'ms 135' line) and 130 individuals from F_2 population in SEM revealed typical for rye and grasses anatomy of internodes (Fig.11A-B). Particularly, internodes were covered with a single layer of the epidermis, underneath which 5-6 layers of sclerenchymal cells could be distinguished with a number of outer vascular bundles. Under sclerenchyma a few layers

FIGURE 11 Scanning Electron microphotograph showing typical for rye and all of analysed tillers anatomy (**A**) with a diagram of internode anatomy (**B**); bar = 200 µm.

of parenchymal cells were present with a number of inner vascular bundles. The detailed analysis of the anatomical features in two parental lines using a Fiji image processing package (Schindelin *et al.,* 2012) revealed that the differences between parental lines in the diameter of basal internodes (DBI; Fig.12A-C, Table 9) were statistically significant (t-test, p < 0.0005).

TABLE 9 Anatomy of the second basal internode in parental lines and 304/1 F_2 population: heritability (H), mean value (μ), median (Q_2), range ([X_{min},X_{max}]), lower quartile (Q_1), upper quartile (Q_3), and standard deviation (SD).

	Trait	H	P-value	Population	μ	Q_2	[X_{min},X_{max}]	Q_1	Q_3	SD
Anatomy of the basal internode	Diameter of the basal internode [µm]	0.9435	0.0002	'ms 135'	3638	3673	[2687, 4685]	3272	4002	516
				'R 1124'	4381	4339	[3451, 5617]	3833	4840	616.1
				304/1	4266	4244	[3038, 5630]	3950	4562	436.8
	No. of epidermal invaginations	0.9330	0.0008	'ms 135'	5.81	4	[1, 15]	3	8	3.995
				'R 1124'	1.182	2	[0, 3]	0	2	1.168
				304/1	4.879	2.583	[0, 31]	0.333	5.333	6.813
	Thickness of stalk tissues [µm]	0.9732	< 0.0001	'ms 135'	341.8	323.9	[226.3, 503]	298.1	395.3	61.49
				'R 1124'	389.7	388.8	[240.6, 512.4]	344.4	433.3	55.05
				304/1	466.5	469.9	[279.9, 643.5]	424.3	514.7	64.54
	Thickness of sclerenchymal tissue [µm]	0.9967	< 0.0001	'ms 135'	70.83	67.85	[48.5, 113.7]	61	80.8	13.06
				'R 1124'	49.59	48.6	[28.5, 78.9]	41.7	55.77	10.21
				304/1	72.19	72.03	[46.15, 101.7]	64.87	79.13	10.82
	Sclerenchyma ratio	0.9987	< 0.0001	'ms 135'	0.0198	0.0189	[0.0141, 0.0297]	0.0173	0.0218	0.00352
				'R 1124'	0.0112	0.0109	[0.0062, 0.0184]	0.00945	0.0125	0.00231
				304/1	0.017	0.0167	[0.0109, 0.0237]	0.0151	0.0184	0.00269
	No. of inner vascular bundles	0.5013	0.3234	'ms 135'	31.91	32	[27, 39]	30	33	2.968
				'R 1124'	31	31	[29, 33]	30	32	1.414
				304/1	34.71	35	[24, 41]	32.67	37	3.208
	No. of outer vascular bundles	0.9904	< 0.0001	'ms 135'	27.43	27	[24, 31]	25.25	29	2.128
				'R 1124'	18.83	18	[15, 24]	16.5	21.5	2.823
				304/1	25.22	25	[13, 33]	23	27.67	3.938
	Diameter of epidermal cell [µm]	0.7691	0.0684	'ms 135'	12.33	12.05	[8.819, 16.97]	10.68	13.74	2.092
				'R 1124'	12.63	12.81	[8.081, 17.22]	10.95	14.33	2.286
				304/1	13.83	13.44	[9.958, 22.01]	12.53	14.54	2.232
	Diameter of sclerenchymal cell [µm]	0.6298	0.1928	'ms 135'	13.21	12.9	[9.053, 20.1]	11.06	15.08	2.606
				'R 1124'	13.55	13.34	[8.629, 20.71]	11.24	15.58	2.929
				304/1	15.96	15.6	[9.302, 23.74]	14.53	17.12	2.411
	Thickness of sclerenchymal CW [µm]	0.9983	< 0.0001	'ms 135'	1.534	1.497	[0.63, 2.961]	1.256	1.748	0.42
				'R 1124'	0.77	0.732	[0.239, 1.762]	0.563	0.96	0.283
				304/1	1.212	1.211	[0.604, 1.997]	0.975	1.408	0.289
	Thickness of inner periclinal CW of epidermis [µm]	0.9975	< 0.0001	'ms 135'	0.873	0.833	[0.304, 1.656]	0.668	1.079	0.259
				'R 1124'	0.502	0.481	[0.178, 1.079]	0.39	0.593	0.162
				304/1	0.713	0.692	[0.396,1.153]	0.603	0.827	0.166
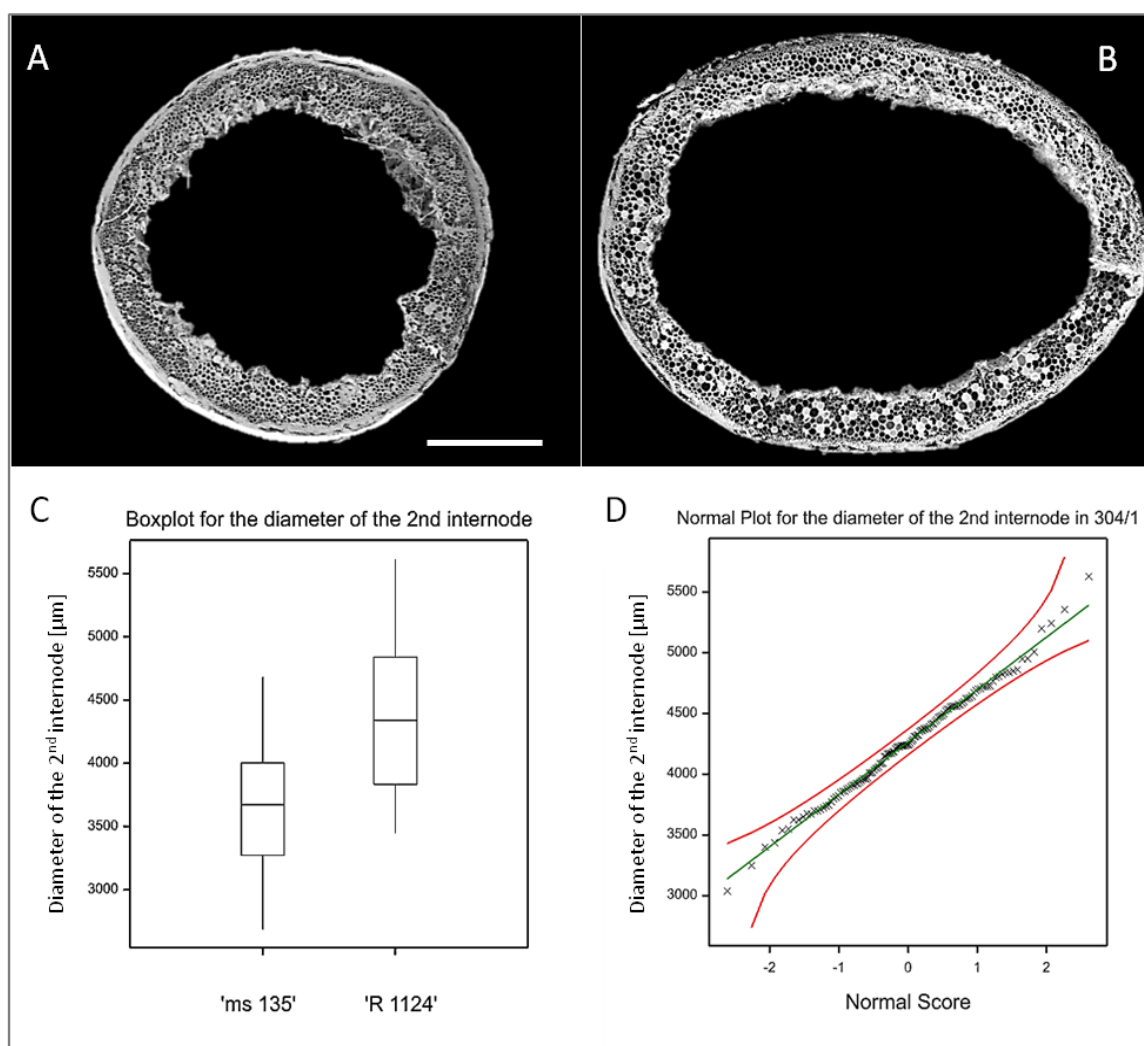
FIGURE 12 Examples of cross sections of tillers observed in SEM showing the differences in internode diameter of 'ms135' (**A**) and 'R 1124' line (**B**); bar = 1 mm. Boxplot showing median values for the diameter of basal internodes with whiskers indicating variability outside the upper and lower quartiles in two parental lines ('ms 135' and 'R 1124') (**C**). A Quantile-Quantile plot with 95% simultaneous confidence bands and a 1-1 reference line plotting observed data for 304/1 F_2 population against their expected quantiles (**D**).

Namely, 'R 1124' line was characterised by a greater DBI (mean ± SD = 4381 ± 616.1 µm) in comparison to the lodging resistant line (mean ± SD = 3638 ± 516 µm). In 304/1 F_2 population, the DBI varied between 3037.5 and 5630 µm, with a mean value of 4266 µm (±436,8 SD; Fig.12D, Suppl. Fig.46E, Table 9), and the distribution of the trait was normal and characterised by skewness of 0.1 and kurtosis of 0.27 (Suppl. Fig.46F).

Statistically significant differences were also found in the number of epidermal invaginations (EpI; *t*-test, p < 0.001).The lodging resistant parental line in comparison to the wildtype (mean value = 1.182) was characterised by a significantly higher number (mean = 5.81) of these important from the mechanical point of view invaginations (Fig.13A-F, Table 9), which can stabilise a tiller. In 304/1 F_2 population, the EpI ranged between 0 and

31, with a mean value of 4.879 (Fig.13G, Suppl. Fig.47A, Table 9). The distribution of this trait was skewed, and data was clearly not normally distributed (skewness = 2.053, kurtosis = 3.739; Suppl. Fig.47B).
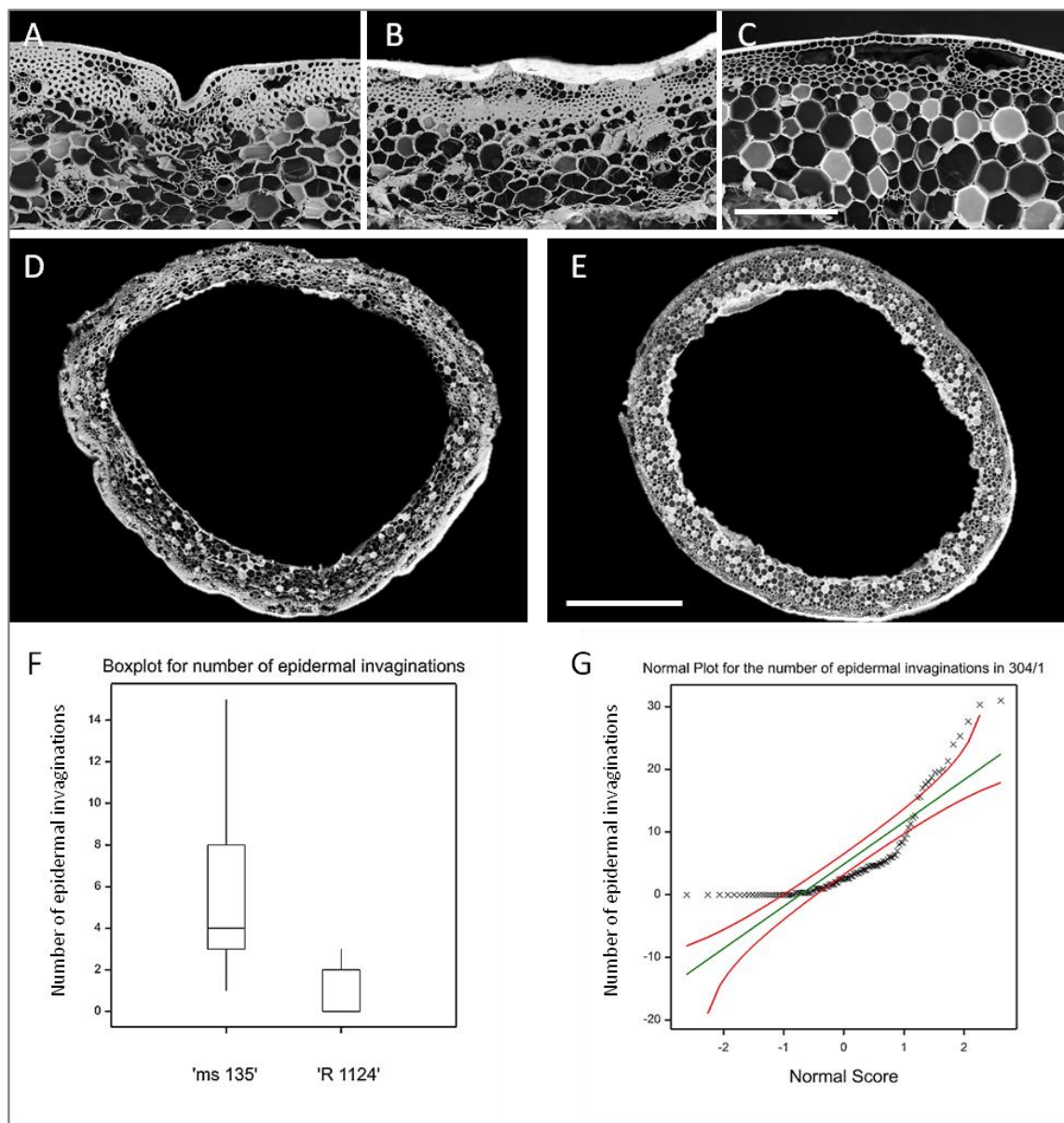
FIGURE 13 The surface of 'ms 135' internode of with a number of pronounced epidermal invaginations (**A**) or/and wavy surface (**B**) in contrast to the smooth surface of 'R 1124' line (**C**; bar = 200 μm). Cross sections of internodes observed in SEM showing the differences in the number of epidermal invaginations in 'ms135' (**D**) and 'R 1124' line (**E**); bar = 1 mm. A boxplot showing median values for the trait, with whiskers indicating variability outside the upper and lower quartiles in two parental lines (**F**). A Quantile-Quantile plot with 95% simultaneous confidence bands and a 1-1 reference line plotting observed data for 304/1 F_2 population against their expected quantiles (**G**).
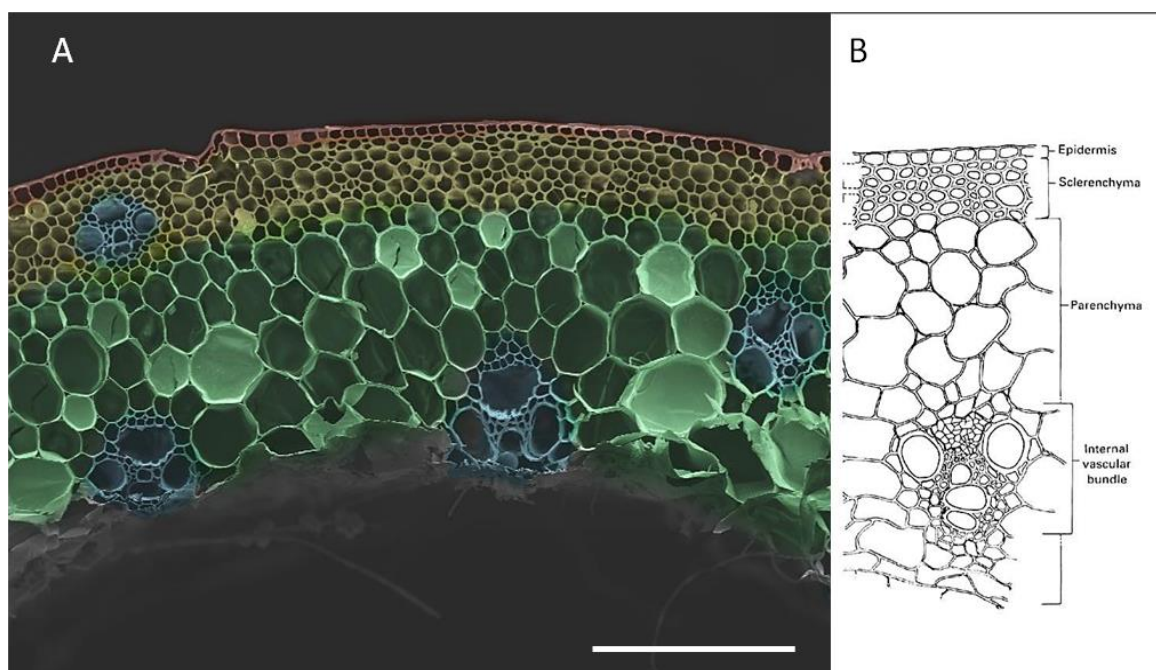
The analysis of the culm wall thickness (CWT) of the second basal internode revealed that the differences between the parental lines were also statistically significant (*t*-test, p < 0.0001). The mean value was 341.8 µm (± 61.49 SD) for 'ms 135' line, and 389.7 µm (± 55.05 SD) for 'R 1134' line (Fig.14A-C, Table 9). In 304/1 F_2 population, the thickness of stalk tissues varied between 279.9 and 643.5 µm with a mean value of 466.5 µm (± 64.54 SD; Fig.14D, Suppl. Fig.47C, Table 9) and the distribution of the trait was normal and characterised by skewness of -0,234 and kurtosis of -0,0286 (Suppl. Fig.47D).
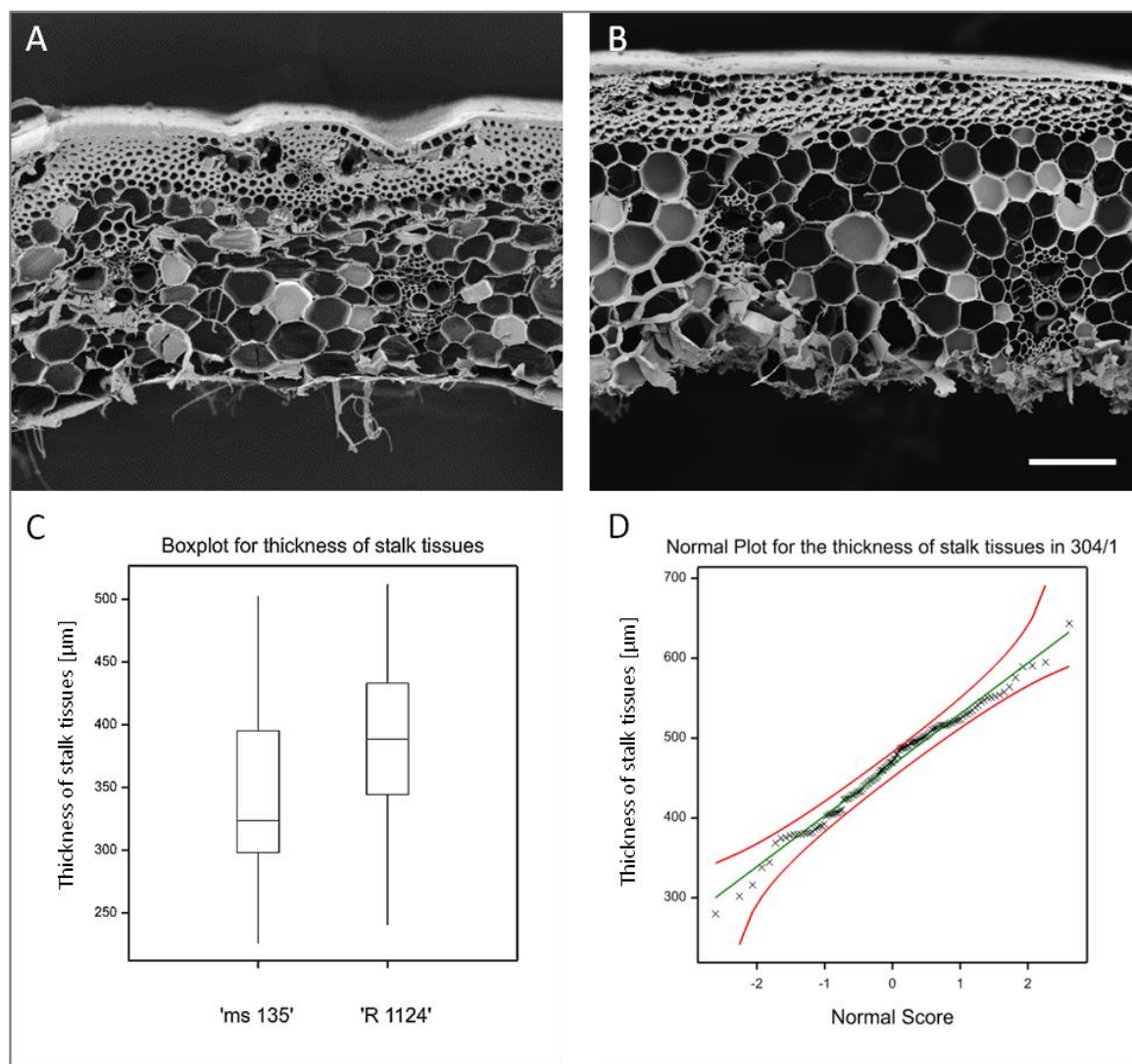
FIGURE 14 Examples of cross sections of tillers observed in SEM showing the culm wall thickness in 'ms 135' (**A**) and 'R 1124' line (**B**); bar = 100 µm. Boxplot showing median values for the trait, with whiskers indicating variability outside the upper and lower quartiles in two parental lines ('ms 135' and 'R 1124') (**C**). A Quantile-Quantile plot with 95% simultaneous confidence bands and a 1-1 reference line plotting observed data for 304/1 F_2 population against their expected quantiles (**D**).

The thickness of sclerenchymal tissue layer (ScL) was also significantly different between parental lines (*t*-test, p < 0.0001). Namely, the lodging resistant parental line was

characterised by thicker ScL in comparison to 'R 1124', and the mean value in the case of 'ms 135' was 70.8 µm (± 13.06 SD), whereas for the wildtype it was only 49.59 µm (± 10.21 SD; Fig.15C, Table 9). The thickness of ScL in 304/1 population ranged between 46.15 and 101.7 µm with the mean value similar to the one obtained for the lodging resistant line and was equal to 72.19 µm (± 10.82 SD; Fig.15D, Suppl. Fig.47E, Table 9). The distribution of the trait was normal and characterised by skewness of 0.206 and kurtosis of -0.204 (Suppl. Fig.47F).
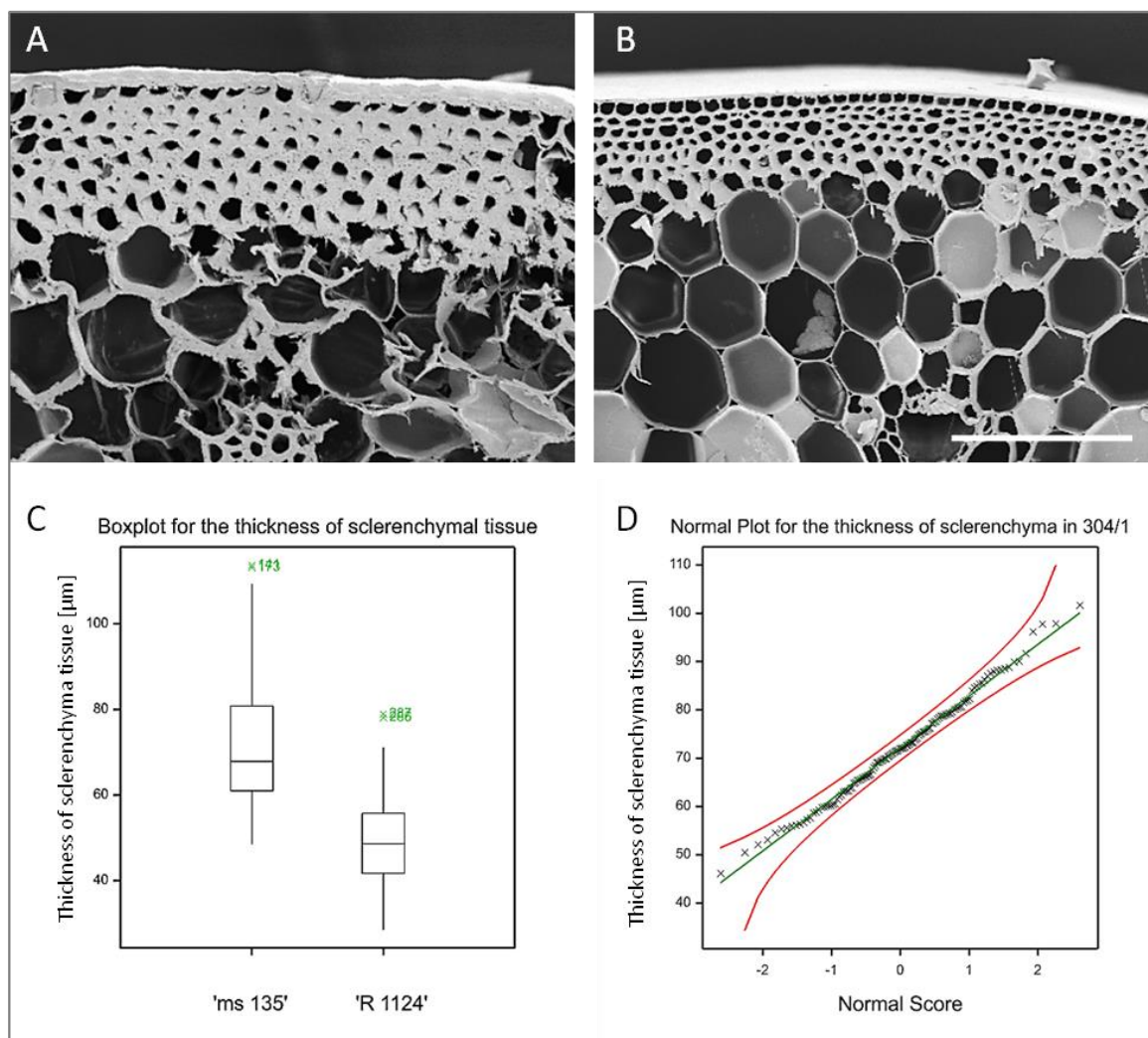
FIGURE 15 Examples of cross sections of tillers observed in SEM showing the thickness of the sclerenchymal layer in 'ms 135' (**A**) and 'R 1124' line (**B**); bar = 100 µm. Boxplot showing median values for the thickness of sclerenchyma with whiskers indicating variability outside the upper and lower quartiles in two parental lines ('ms 135' and 'R 1124') (**C**). A Quantile-Quantile plot with 95% simultaneous confidence bands and a 1-1 reference line plotting observed data for 304/1 F_2 population against their expected quantiles (**D**).

The lodging resistant line ('ms 135') was also characterised by a higher ratio of sclerenchyma to the diameter of the internode (ScR) in comparison to the wildtype ('R 1124') line and the average value of this ratio was equal to 0.0198 (± 0.00352 SD) in

'ms 135' line, and to 0.0112 (± 0.00231 SD) in 'R 1124' parental line (Fig.16A-E; Table 9). The observed differences were statistically significant (*t*-test, p < 0.0001). In 304/1 F$_2$ population, ScR ranged between 0.0109 and 0.0237 with an average value of 0.017 (Fig.16F, Suppl. Fig.48A, Table 9) and the distribution of the trait was normal with skewness of 0.379 and kurtosis of -0.128 (Suppl. Fig.48B).
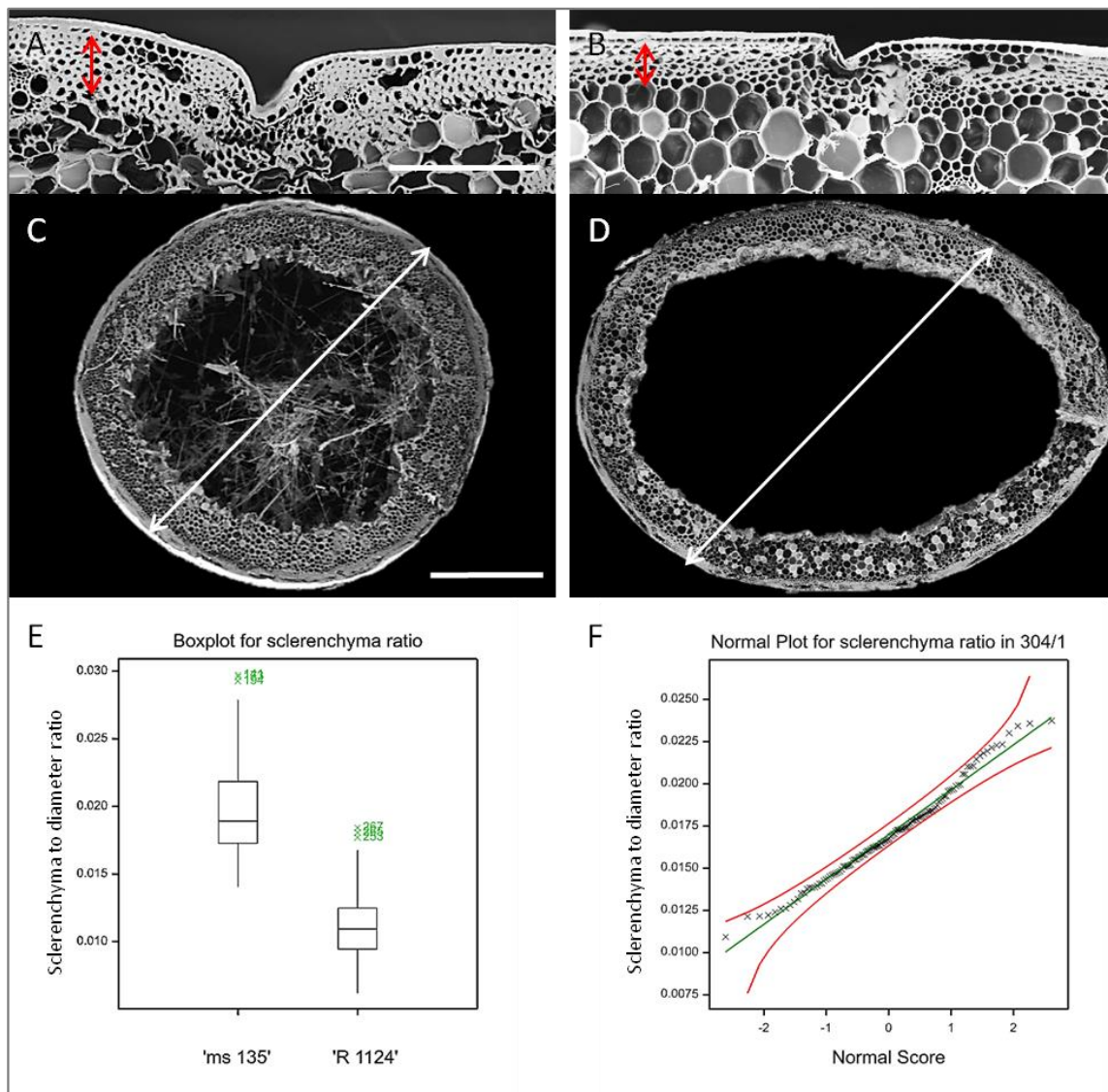
FIGURE 16 Sclerenchyma ratio (ratio between thickness of sclerenchyma, indicated with a red arrow, to the diameter of internode, indicated with a white arrow) in 'ms135' (**A,C**) and 'R 1124' line (**B,D**); bar in A and B = 200 μm; bar in C and D = 1 mm. Boxplot showing median values for sclerenchyma ratio with whiskers indicating variability outside the upper and lower quartiles in two parental lines ('ms 135' and 'R 1124'; **E**). A Quantile-Quantile plot with 95% simultaneous confidence bands and a 1-1 reference line plotting observed data for 304/1 F$_2$ population against their expected quantiles (**F**).

On the other hand, no statistically significant differences (*t*-test, p > 0.1) were found in the number of inner vascular bundles (IVB) located in the parenchymal layer

(Fig.17A-C, Table 9). They varied between 27 and 39 in 'ms 135' line, with a mean value of 31.91 (± 2.968 SD) inner vascular bundles per internode. In the case of the other parental line the number of IVB was similar and ranged from 29 to 33 (mean ± SD = 31 ± 1.414; Fig.17C, Suppl. Fig.48C, Table 9). In 304/1 F_2 segregating population this trait was normally distributed (skewness of -0.497, kurtosis of 0.229) and ranged between 24 to 41, with a mean value of 34.71 IVB per internode (± 3.208; Suppl. Fig.48D, Table 9).
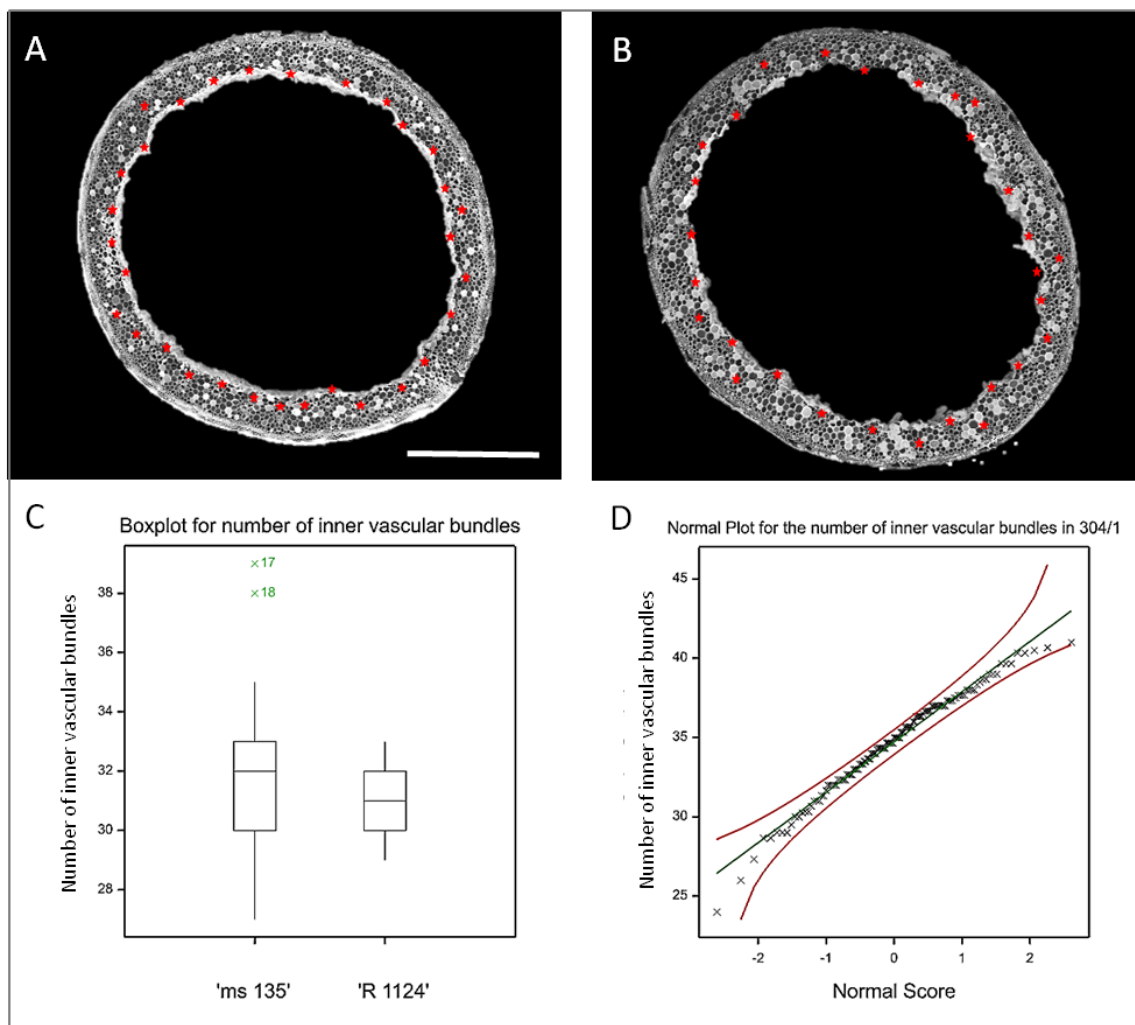
FIGURE 17 Cross sections of tillers observed in SEM: inner vascular bundles (red asterisks) in 'ms135' (**A**) and 'R 1124' line (**B**); bar = 1 mm. Boxplot showing median values with whiskers indicating variability outside the upper and lower quartiles for the number of inner vascular bundles in 'ms135' and 'R 1124' line (**C**). A Quantile-Quantile plot with 95% simultaneous confidence bands and a 1-1 reference line plotting observed data for 304/1 F_2 population against their expected quantiles (**D**).

However, outer vascular bundles (OVB) were significantly (*t*-test, p < 0.0001) more abundant in the lodging resistant line, compared to 'R1124' (Fig.18A-E, Table 9). Their number varied between 24 and 31 in 'ms 135', and between 15 and 24 in 'R 1124' line, with the mean value of 27.43 (± 2.128 SD) and 18.83 (± 2.823 SD) vascular bundles

per internode, respectively. In 304/1 F_2 population, the number of outer vascular bundles varied between 13 and 33, with the mean value of 25.22 bundles per internode (Fig.18F, Suppl. Fig.48E, Table 9). The distribution of the trait in 304/1 F_2 population was normal (characterised by skewness of -0,357 and kurtosis of 0,128; Suppl. Fig.48F).
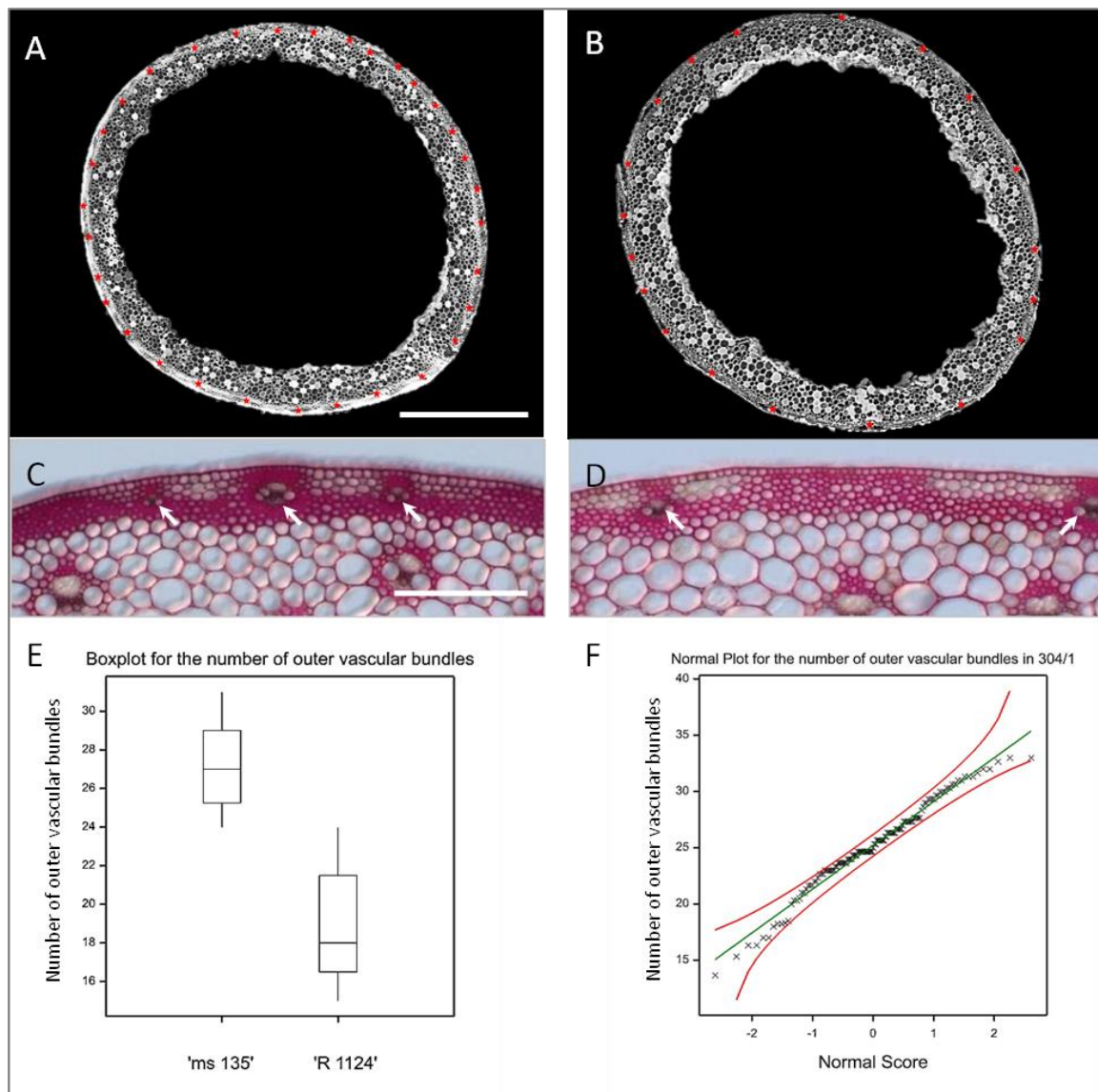
FIGURE 18 Cross sections of internodes observed in SEM showing the number of outer vascular bundles in 'ms135' (**A**) and 'R 1124' line (**B**; red asterisks indicate outer vascular bundles; bar = 1 mm). Differences in the distribution of outer vascular bundles between 'ms135' (**C**) and 'R 1124' line (**D**; white arrows indicate outer vascular bundle; bar = 100 μm). Boxplot showing median values for the number of outer vascular bundles with whiskers indicating variability outside the upper and lower quartiles in two parental lines ('ms 135' and 'R 1124'; **E**). A Quantile-Quantile plot with 95% simultaneous confidence bands and a 1-1 reference line plotting observed data for 304/1 F_2 population against their expected quantiles (**F**).

No statistically significant differences were found in the diameter of epidermal cells (DEC) and the diameter of sclerenchymal cells (DSC; *t*-test, p > 0.05 and p > 0.1

respectively; Fig.19A-D, Table 9). The DEC varied between 8.819 and 16.97 µm in 'ms 135' line (with a mean value of 12.33 µm ± 2.092 SD) and between 8.081 and 17.22 µm in 'R 1124' line (mean value of 12.63 µm ± 2.286 SD; Fig.20A, Table 9). In 304/1 F_2 population, DEC varied between 9.958 and 22.01 µm, with a mean value of 13.83 µm (± 2.232; Fig.20B, Suppl. Fig.49A, Table 9), and the distribution of this trait was skewed and characterised by skewness of 1.361 and kurtosis of 2.53 (Suppl. Fig.49B). In the case of the DSC, the differences were even less pronounced and mean ± SD for 'ms 135' and 'R 1124' parental lines was equal to 13.21 ± 2.606 µm and 13.55 ± 2.929 µm (Fig.21A, Table 9), respectively. In 304/1 F_2 population it varied between 9.302 and 23.74 µm, with mean value of 15.96 µ (± 2.411; Fig.21B, Suppl. Fig.49C, Table 9), and the distribution of this trait was less skewed in comparison to the previous trait (skewness of 0.807, kurtosis of 1.318; Suppl. Fig.49D).
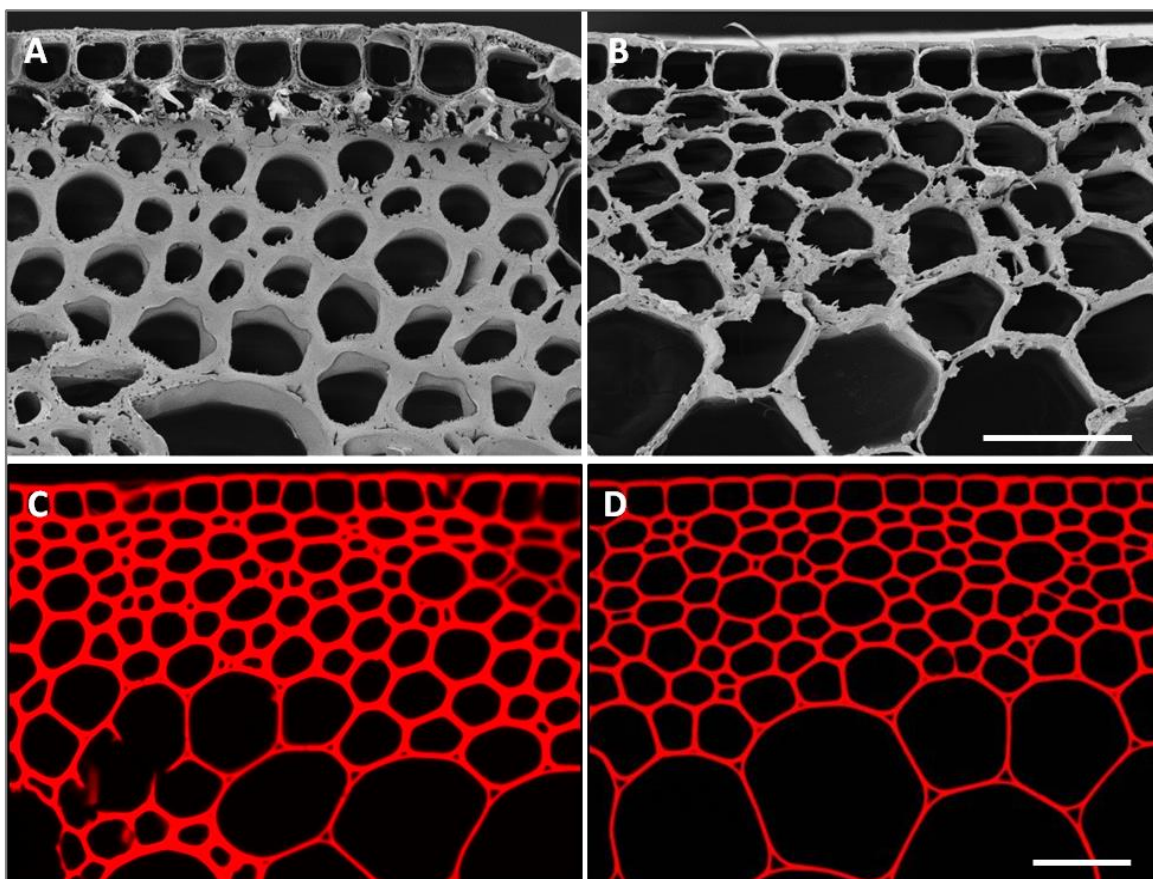
FIGURE 19 Examples of cross sections of the second basal internode observed in SEM showing no differences in the diameter of epidermal and sclerenchymal cells in 'ms135' (**A**) and 'R 1124' line (**B**). Internodes of 'ms 135' (**C**) and 'R 1124' (**D**) in LM after staining with basic fuchsin solution; bar = 30 µm.
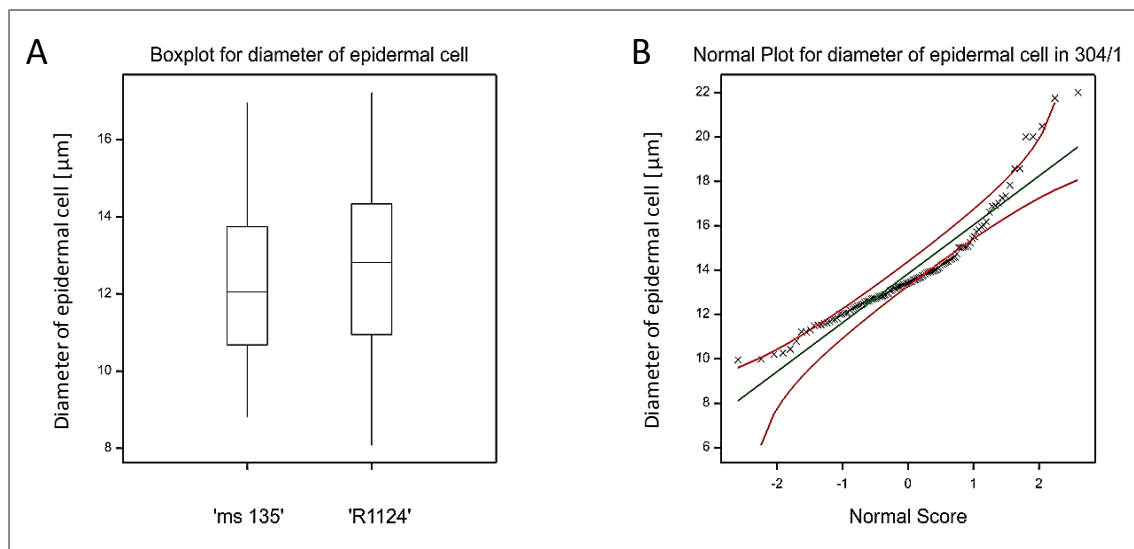
FIGURE 20 Boxplot showing median values for the diameter of the epidermal cell with whiskers indicating variability outside the upper and lower quartiles in two parental lines ('ms 135' and 'R 1124') (**A**). A Quantile-Quantile plot with 95% simultaneous confidence bands and a 1-1 reference line plotting observed data for 304/1 F_2 population against their expected quantiles (**B**).
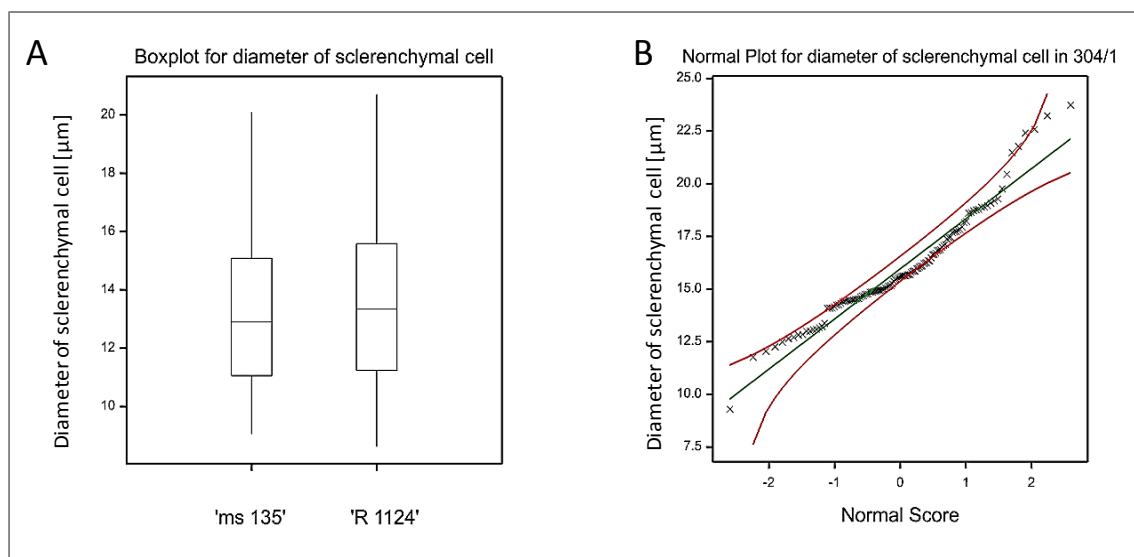
FIGURE 21 Boxplot showing median values for the diameter of the sclerenchymal cell with whiskers indicating variability outside the upper and lower quartiles in two parental lines ('ms 135' and 'R 1124') (**A**). A Quantile-Quantile plot with 95% simultaneous confidence bands and a 1-1 reference line plotting observed data for 304/1 F_2 population against their expected quantiles (**B**).

Clear differences (*t*-test, p < 0.0001) between two parental lines were observed in the thickness of sclerenchymal cell wall (SCW; Fig.22A-F, Fig.23A, Table 9). The lodging resistant line was characterised by almost twice thicker cell walls in comparison to the wildtype, with the mean value of 1.534 µm (± 0.42 SD) and 0.77 µm (± 0.283 SD) respectively. In 304/1 F_2 population, the thickness of SCW varied between 0.604 and 1.997 µm, with a mean value of 1.212 µm (± 0.289 SD; Fig.23B, Suppl. Fig.49E, Table 9). The

distribution of this trait was normal and characterised by skewness of 0.239 and kurtosis of -0.305 (Suppl. Fig.49F).
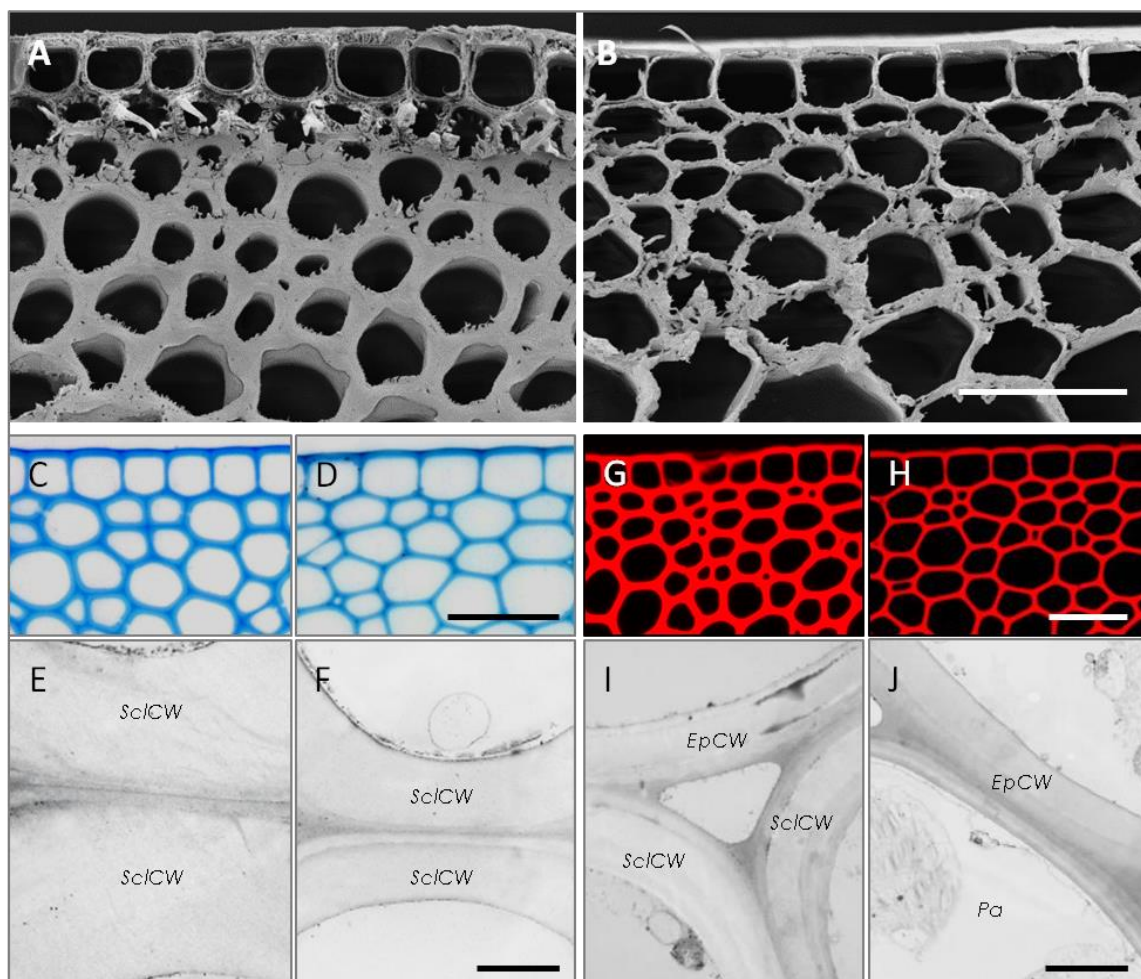
FIGURE 22 Examples of cross sections of the basal internodes observed in SEM showing clear differences in the thickness of cell walls between 'ms135' (**A**) and 'R 1124' line (**B**); bar = 30 μm. Sclerenchymal cell wall of 'ms 135' (**C, E**) and 'R 1124' (**D, F**) in LM (**C, D;** bar = 15 μm) and TEM (**E, F;** bar = 1 μm). The inner periclinal cell wall of the epidermis in 'ms 135' (**G, I**) and 'R 1124' (**H, J**) in LM (**G, H;** bar = 30 μm) and TEM (**I, J;** bar = 1 μm). *SclCW – sclerenchymal cell wall, EpCW – inner periclinal cell wall of the epidermis, Pa – parenchymal cell*.

Additionally, statistical differences (*t*-test, p < 0.0001) were also found in the thickness of inner periclinal cell wall of the epidermis (ECW; Fig.22A-B, Fig.22G-J, Fig.24A, Table 9), which were also thicker in the lodging resistant line (mean ± SD = 0.873 ± 0.259 μm) in comparison to 'R 1124' (mean ± SD = 0.502 ± 0.162 μm). In 304/1 F_2 population, the thickness of these cell walls varied between 0.396 and 1.153 μm, with the mean value of 0.713 μm (± 0.166 SD; Fig.24B, Suppl. Fig.50A, Table 9). The distribution of this trait was normal and characterised by skewness of 0.392 and kurtosis of -0.338 (Suppl. Fig.50B).
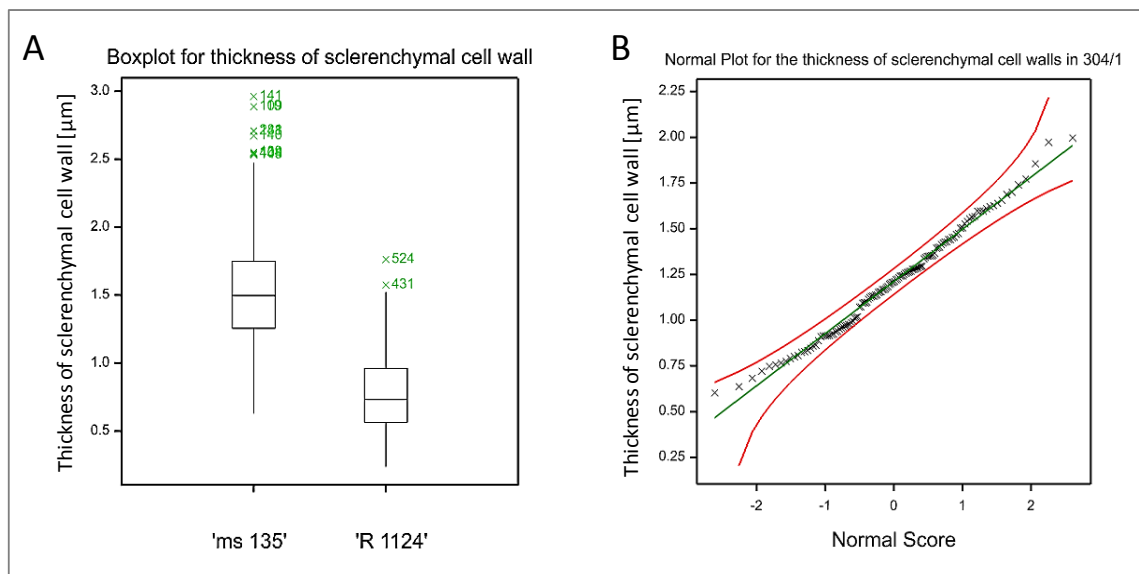
FIGURE 23 Boxplots showing median values for the thickness of sclerenchymal cell wall with whiskers indicating variability outside the upper and lower quartiles in two parental lines ('ms 135' and 'R 1124'; **A**). A Quantile-Quantile plot with 95% simultaneous confidence bands and a 1-1 reference line plotting observed data for 304/1 F_2 population against their expected quantiles (**B**).
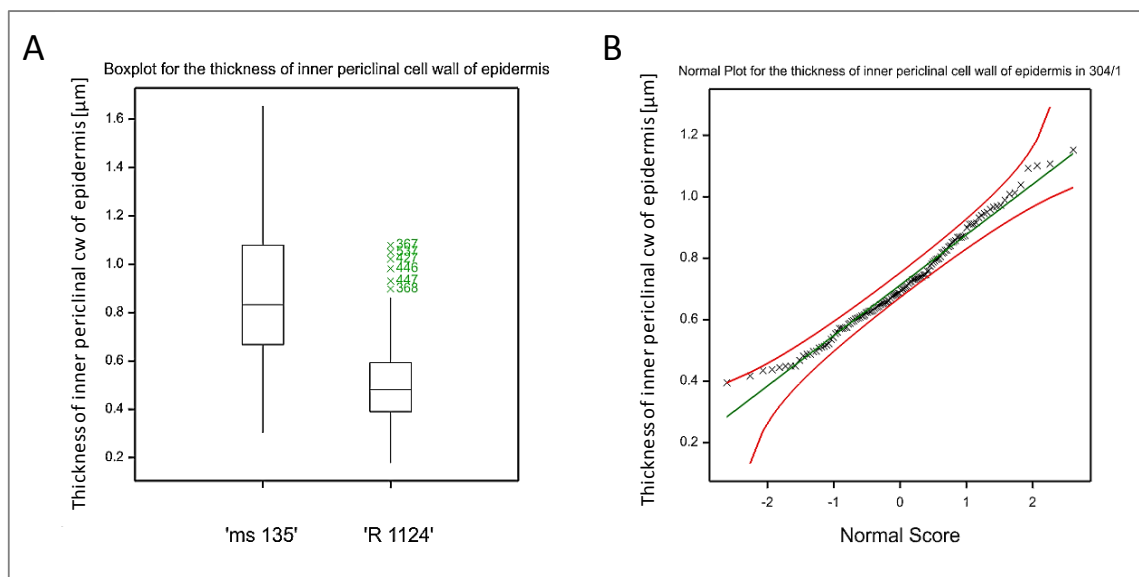
FIGURE 24 Boxplots showing median values for the thickness of inner periclinal cell wall of epidermis with whiskers indicating variability outside the upper and lower quartiles in two parental lines ('ms 135' and 'R 1124' **A**). A Quantile-Quantile plot with 95% simultaneous confidence bands and a 1-1 reference line plotting observed data for 304/1 F_2 population against their expected quantiles (**B**).

4.1.3 | Content of elements

The content of boron, calcium, copper, iron, magnesium, manganese, molybdenum, nickel, phosphorus, potassium, sodium, sulfur, zinc, and silicon was measured using Inductively Coupled Plasma Optical Emission Spectrometry (ICP-OES), which revealed that two parental lines did not exhibit significantly different content in dry weight of basal internodes for: boron (*t*-test, p > 0.3), iron (*t*-test, p > 0.6), molybdenum (*t*-test, p > 0.05), nickel (*t*-test, p > 0.4), phosphorus (*t*-test, p > 0.05), and sodium (*t*-test, p > 0.8; Table 10).

TABLE 10 Analysis of the content of elements in parental lines and 394/1 F_2 population: mean value (μ), median (Q_2), range ([X_{min},X_{max}]), lower quartile (Q_1), upper quartile (Q_3), and standard deviation (SD).

	Trait	H	P-value	Population	μ	Q_2	[X_{min},X_{max}]	Q_1	Q_3	SD
Analysis of the content of elements	B [µg/g]	0.4889	0.3404	'ms 135'	13.15	12.65	[5.025, 23.42]	10.43	16.31	5.301
				'R 1124'	16.15	13.88	[7.8, 34.32]	10.83	16.74	8.259
				304/1	7.806	6.506	[2.138, 24.41]	4.274	9.416	4.641
	Fe [µg/g]	0.1692	0.6625	'ms 135'	88.08	81.75	[62.28, 137,8]	64.89	100	28.16
				'R 1124'	81.55	81.6	[58.24, 106,3]	72.5	89.85	17.18
				304/1	58.29	52.08	[23.91, 148.1]	39.86	71.32	24.45
	Mo [µg/g]	0.8108	0.0628	'ms 135'	1.03	1.26	[0.443, 1.507]	0.536	1.466	0.496
				'R 1124'	2.513	1.643	[0.863, 5.003]	1.275	4.651	1.83
				304/1	3.195	2.942	[0.359, 9.489]	1.627	4.293	2.068
	Ni [µg/g]	0.3484	0.4814	'ms 135'	2.805	2.572	[1.538, 4.605]	2.016	3.36	1.041
				'R 1124'	2.666	2.448	[1.988, 3.638]	2.167	3.308	0.67
				304/1	1.493	1.249	[0.417, 3.900]	0.930	1.781	0.775
	P [µg/g]	0.7931	0.0859	'ms 135'	2493	2446	[2036, 2864]	2308	2755	319.4
				'R 1124'	3953	4331	[2076, 6060]	2429	5078	1637
				304/1	2748	2539	[879.3, 6403]	1909	3562	1250
	Na [µg/g]	0.0547	0.8148	'ms 135'	3142	3136	[2116, 4572]	2122	3770	955.8
				'R 1124'	2923	2149	[1148, 6525]	1648	3920	2014
				304/1	4232	3854	[801.3, 9627]	2282	5836	2250
	Ca [µg/g]	0.9775	< 0.0001	'ms 135'	4835	4365	[1365, 8708]	2918	7296	2460
				'R 1124'	14686	12368	[11167, 24772]	12158	17415	4245
				304/1	6335	3617	[919.4, 24568]	1994	9240	6002
	Cu [µg/g]	0.9175	0.0026	'ms 135'	4.554	4.924	[1.92, 7.8]	2.175	6.173	2.29
				'R 1124'	8.211	7.748	[2.58, 14.45]	5.82	9.713	3.406
				304/1	5.553	4.768	[2.02, 14.18]	3.76	6.897	2.528
	K [µg/g]	0.8525	0.0296	'ms 135'	56521	52575	[34106, 86250]	45390	66881	17694
				'R 1124'	75388	76238	[50130, 92175]	66788	87375	14180
				304/1	58210	58057	[14492, 98035]	47865	66973	15978
	Mg [µg/g]	0.9302	0.0026	'ms 135'	1986	1740	[1550, 3124]	1611	2180	557.7
				'R 1124'	3699	3842	[1546, 4993]	3163	4686	1132
				304/1	2829	2458	[719.7, 7597]	1322	3842	1764
	Mn [µg/g]	0.9407	0.0022	'ms 135'	15.43	13.69	[8.685, 21.23]	11.68	19.91	4.913
				'R 1124'	39.19	34.43	[27.17, 67.58]	28.68	42.88	14.97
				304/1	12.13	7.832	[3.177, 79.64]	5.646	12.52	12.96
	S [µg/g]	0.9460	0.0005	'ms 135'	3805	3708	[3223, 4513]	3574	4102	448
				'R 1124'	8294	8069	[6058, 11752]	6622	9195	2117
				304/1	5135	4540	[1568, 12141]	3176	6655	2668
	Zn [µg/g]	0.9649	0.0003	'ms 135'	116.8	104.5	[72.47, 160.7]	99.88	142.7	30.62
				'R 1124'	46.07	46.88	[24.68, 60.45]	40.58	56.97	12.95
				304/1	94.06	86	[34.86, 246.7]	62.35	111.4	44.4
	Si [µg/g]	0.8936	0.0079	'ms 135'	6960	7238	[3866, 9639]	5489	8409	1805
				'R 1124'	4903	3848	[3090, 7566]	3532	6953	1803
				304/1	5419	5387	[3989, 8443]	4795	5783	797

Namely, mean ± SD for boron content (BC) was equal to 16.15 ± 8.259 µg/g in 'R 1124' line, and 13.15 ± 5.301 µg/g in 'ms 135' (Fig.25A, Table 10). In 304/1 F_2 population mean value of BC was much lower in comparison to two parental lines and equal to 7.806 µg/g (± 4.641 SD; Fig.25B, Suppl. Fig.50C, Table 10), and the distribution of this trait in the population was skewed and characterised by skewness of 1.414 and kurtosis of 1.629 (Suppl. Fig.50D).

In the case of iron content (FeC), parental lines expressed higher variability within their groups, and differences between parental lines were even less pronounced than in case of boron, with means of 88.08 µg/g (± 28.16 SD) in the lodging resistant line, and 81.55 µg/g (± 17.18 SD; Fig.26A, Table 10) in the wildtype. The content of this element in 304/1 F_2 population varied between 23.91 and 148.1 µg/g, with a mean value of 58.29 µg/g (± 24.45 SD; Fig.26B, Suppl. Fig.50E, Table 10), and the distribution of this trait was also skewed (skewness of 1.451, kurtosis of 2.219; Suppl. Fig.50F).

There were also no statistical differences between parental lines in the content of molybdenum (MoC), which mean value was 1.03 µg/g (± 0.496 SD) in 'ms 135', 2.513 µg/g (± 1.83 SD; Fig.27A) in 'R 1124', and 3.195 µg/g (± 2.068 SD; Fig.27B, Suppl. Fig.51A, Table 10) in 304/1 F_2 population. The distribution of that trait in this population was, as well as in the case of previous elements, skewed and characterised by skewness of 0.965 and kurtosis of 0.438 (Suppl. Fig.51B).

In the case of the content of nickel (NiC) the lodging resistant line was characterised by a mean value of 2.805 µg/g (± 1.041 SD), whereas the mean value for the wildtype was comparable and equal to 2.666 µg/g (± 0.67 SD; Fig.28A, Table 10). In 304/1 F_2 population the content of this element varied between 0.417 and 3.9 µg/g, with mean value of 1.493 µg/g (± 0.775 SD; Fig.28B, Suppl. Fig.51C, Table 10), and the distribution of this trait was characterised by skewness of 1.119 and kurtosis of 0.504 (Suppl. Fig.51D).

Another element, which content between two parental lines was not significantly different, was phosphorus (PC). The mean content of this element was 2493 µg/g (± 319.4 SD) in 'ms 135', 3953 µg/g (± 1637 µg/g SD; Fig.29A, Table 10) in 'R 1124', and 2748 µg/g (± 1250 SD; Fig.29B, Suppl. Fig.51E, Table 10) in 304/1 F_2 population. The distribution of PC in this population was characterised by skewness of 0.678 and kurtosis of 0.0996 (Suppl. Fig.51F).

Finally, the last element with no significant differences between parental lines was sodium (NaC), which mean content in 'ms 135' was 3142 µg/g (± 955.8 SD) and 2923 µg/g (± 2014 SD; Fig.30A, Table 10) in 'R 1124' line. In 304/1 F_2 population it varied between 801.3 and 9627 µg/g, with mean value of 4232 µg/g (± 2250 SD; Fig.30B, Suppl. Fig.52A,

Table 10), and the distribution of NaC in this population was characterised by skewness of 0.498 and kurtosis of -0.601 (Suppl. Fig.52B).
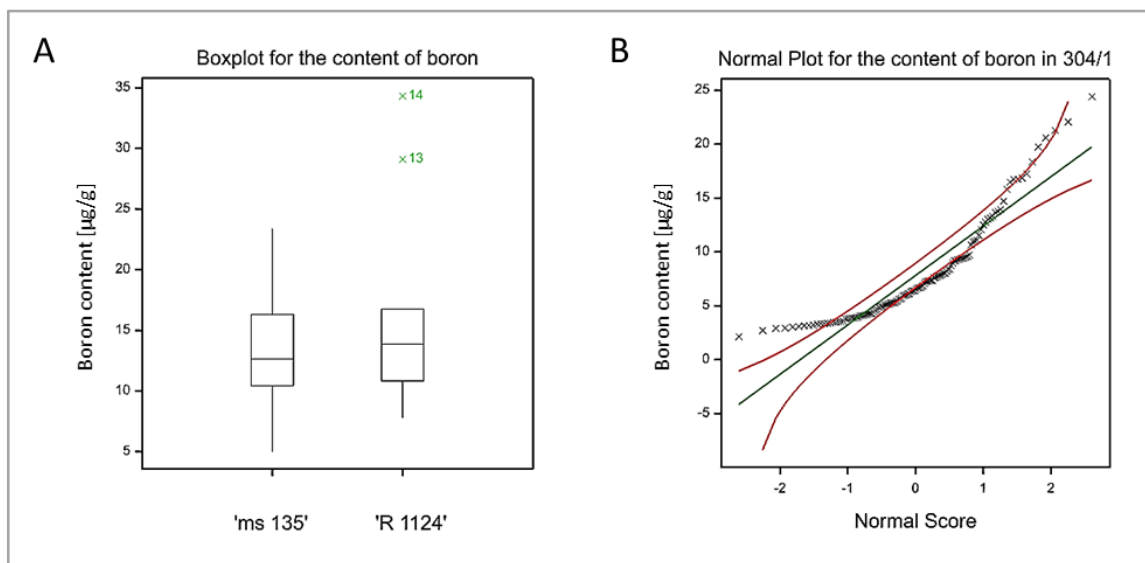

FIGURE 25 Boxplot showing median values for the content of boron in dry weight with whiskers indicating variability outside the upper and lower quartiles in two parental lines ('ms 135' and 'R 1124' **A**). A Quantile-Quantile plot with 95% simultaneous confidence bands and a 1-1 reference line plotting observed data for 304/1 F_2 population against their expected quantiles (**B**).
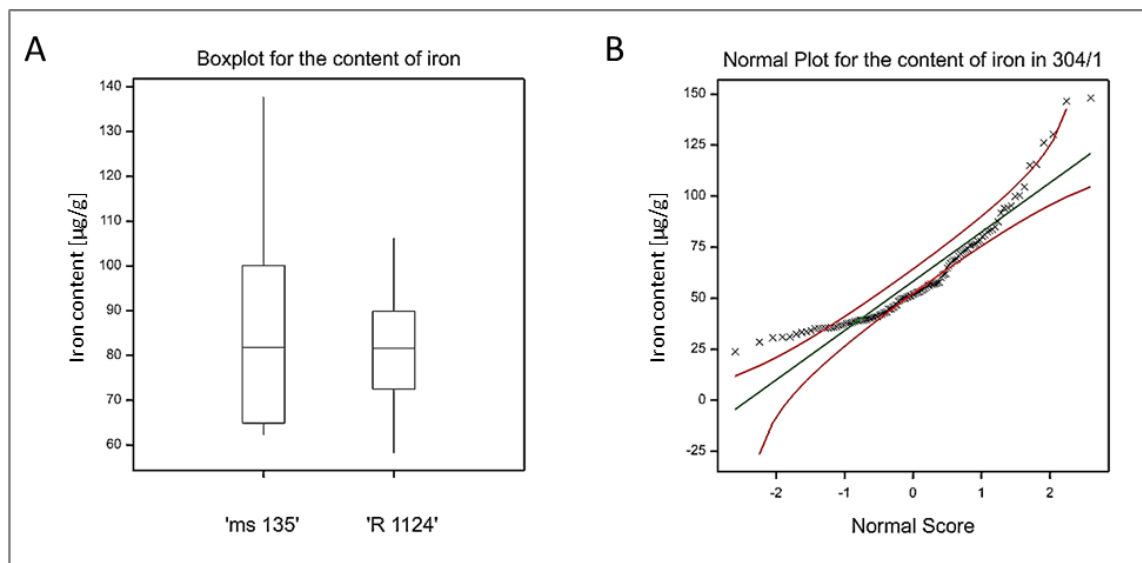
FIGURE 26 Boxplot showing median values for the content of iron in dry weight with whiskers indicating variability outside the upper and lower quartiles in two parental lines ('ms 135' and 'R 1124' **A**). A Quantile-Quantile plot with 95% simultaneous confidence bands and a 1-1 reference line plotting observed data for 304/1 F_2 population against their expected quantiles (**B**).
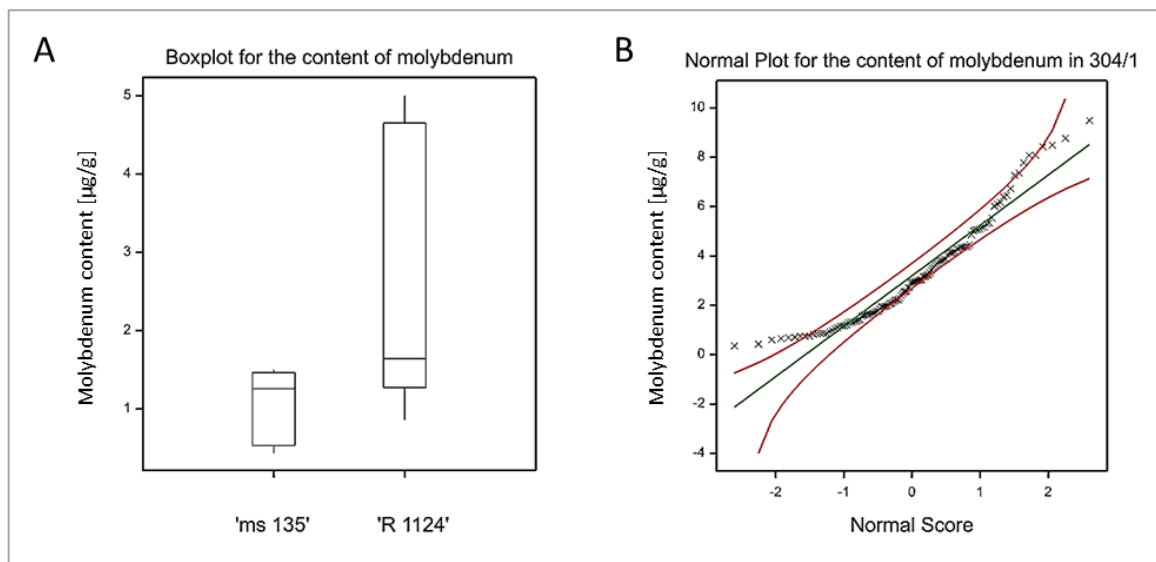
FIGURE 27 Boxplot showing median values for the content of molybdenum in dry weight with whiskers indicating variability outside the upper and lower quartiles in two parental lines ('ms 135' and 'R 1124' **A**). A Quantile-Quantile plot with 95% simultaneous confidence bands and a 1-1 reference line plotting observed data for 304/1 F_2 population against their expected quantiles (**B**).

FIGURE 28 Boxplot showing median values for the content of nickel in dry weight with whiskers indicating variability outside the upper and lower quartiles in two parental lines ('ms 135' and 'R 1124' **A**). A Quantile-Quantile plot with 95% simultaneous confidence bands and a 1-1 reference line plotting observed data for 304/1 F_2 population against their expected quantiles (**B**).
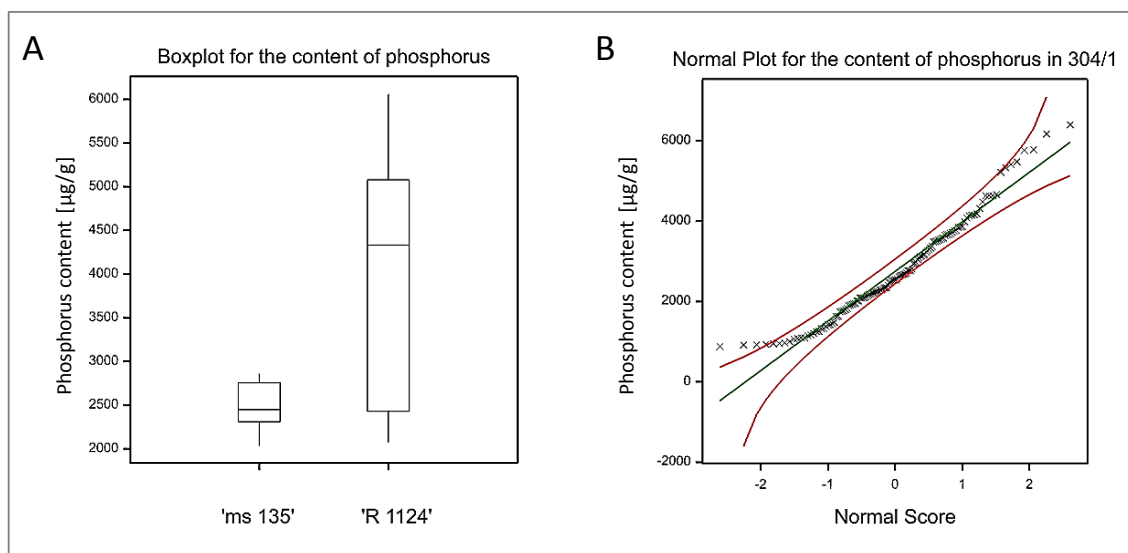
FIGURE 29 Boxplot showing median values for the content of phosphorus in dry weight with whiskers indicating variability outside the upper and lower quartiles in two parental lines ('ms 135' and 'R 1124' **A**). A Quantile-Quantile plot with 95% simultaneous confidence bands and a 1-1 reference line plotting observed data for 304/1 F_2 population against their expected quantiles (**B**).
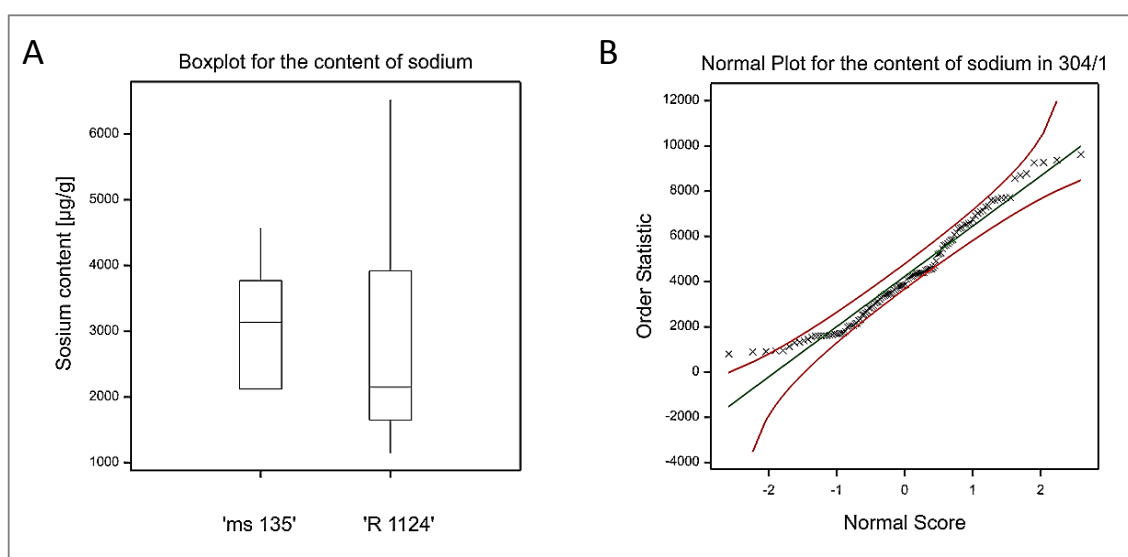
FIGURE 30 Boxplot showing median values for the content of sodium in dry weight with whiskers indicating variability outside the upper and lower quartiles in two parental lines ('ms 135' and 'R 1124' **A**). A Quantile-Quantile plot with 95% simultaneous confidence bands and a 1-1 reference line plotting observed data for 304/1 F_2 population against their expected quantiles (**B**).

In the case of calcium content (CaC) the 'ms 135' parental line was characterized by a significantly (*t*-test, $p < 0.0001$) lower content (mean ± SD = 4835 ± 2460 SD µg/g) in comparison to the wildtype (mean ± SD = 14686 ± 4245 µg/g; Fig.31A, Table 10). In 304/1 F_2 population CaC ranged from 919.4 to 24568 µg/g with a mean of 6335 µg/g (± 6002 SD; Fig.31B, Suppl. Fig.52C, Table 10), and the distribution of this trait was clearly skewed and characterised by skewness of 1.411 and kurtosis of 1.034 (Suppl. Fig.52D).

The content of copper (CuC) was also significantly (*t*-test, p < 0.005) lower in lodging resistant line in comparison to 'R 1124', where mean values were equal to 4.554 µg/g (± 2.29 SD) and 8.211 µg/g (± 3.406 SD; Fig.32A, Table 10), respectively. In 304/1 F$_2$ population, the CuC ranged between 2.02 and 14.18 µg/g, with a mean of 5.553 µg/g (± 2.528 SD; Fig.32B, Suppl. Fig.52E, Table 10). The distribution of this trait in 304/1 F$_2$ population was characterised by skewness of 1.238 and kurtosis of 1.264 (Suppl. Fig.52F).

Significant differences between two parental lines (*t*-test, p < 0.05) were also found in the content of potassium (KC), which mean value was equal to 56521 µg/g (± 17694 SD) in 'ms 135' line and 75388 µg/g (± 14180 SD; Fig.33A, Table 10) in 'R 1124' parental line. In 304/1 F$_2$ population, the KC varied between 14492 and 98035 µg/g, with a mean of 58210 µg/g (± 15978 SD; Fig.33B, Suppl. Fig.53A, Table 10). The distribution of this trait in 304/1 F$_2$ population was normal and characterised by skewness of 0.0724 and kurtosis of 0.0912 (Suppl. Fig.53B).
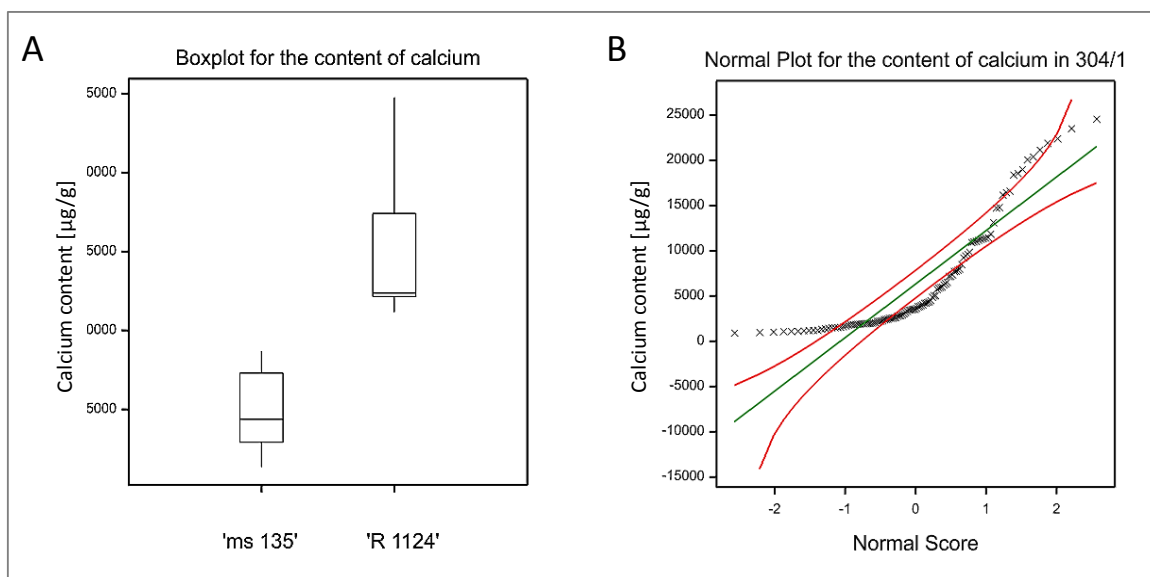
FIGURE 31 Boxplot showing median values for the content of calcium in dry weight with whiskers indicating variability outside the upper and lower quartiles in two parental lines ('ms 135' and 'R 1124' **A**). A Quantile-Quantile plot with 95% simultaneous confidence bands and a 1-1 reference line plotting observed data for 304/1 F$_2$ population against their expected quantiles (**B**).
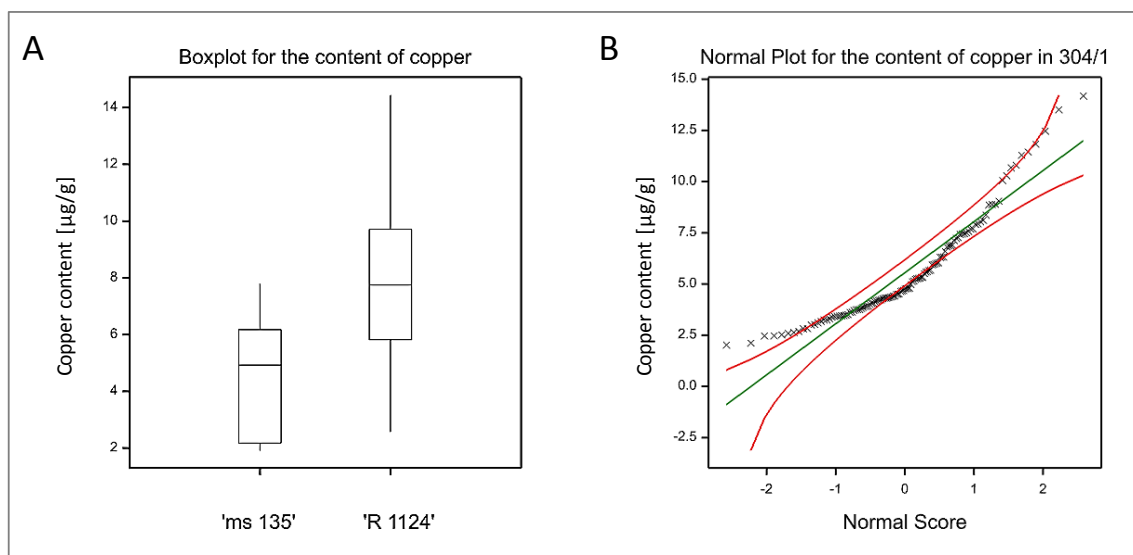
FIGURE 32 Boxplot showing median values for the content of copper in dry weight with whiskers indicating variability outside the upper and lower quartiles in two parental lines ('ms 135' and 'R 1124' **A**). A Quantile-Quantile plot with 95% simultaneous confidence bands and a 1-1 reference line plotting observed data for 304/1 F_2 population against their expected quantiles (**B**).
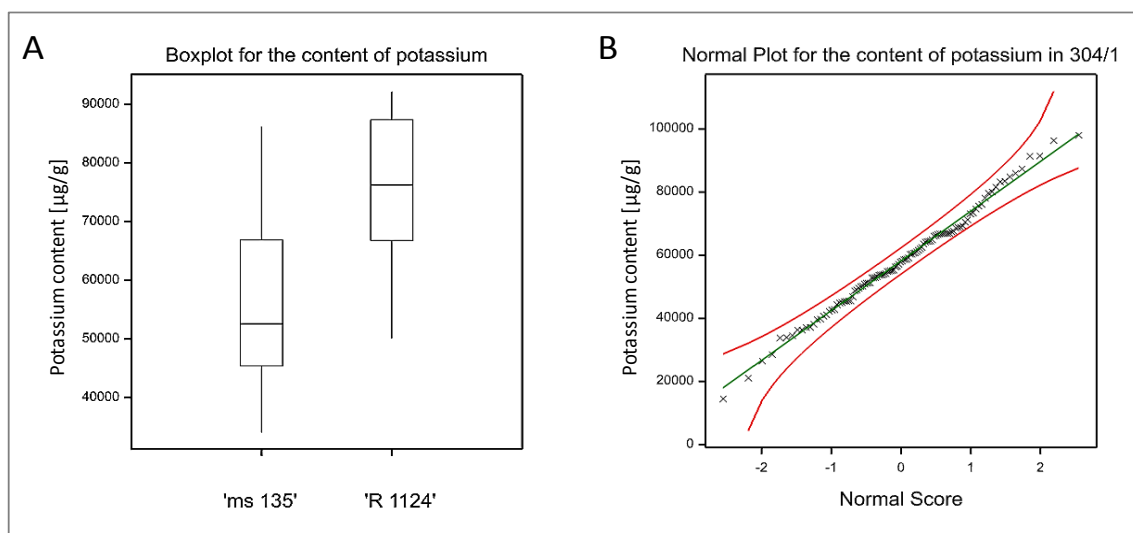
FIGURE 33 Boxplot showing median values for the content of potassium in dry weight with whiskers indicating variability outside the upper and lower quartiles in two parental lines ('ms 135' and 'R 1124' **A**). A Quantile-Quantile plot with 95% simultaneous confidence bands and a 1-1 reference line plotting observed data for 304/1 F_2 population against their expected quantiles (**B**).

The content of magnesium (MgC) was also significantly (*t*-test, p < 0.005) lower in 'ms 135' parental line (mean ± SD = 1986 ± 557.7 µg/g) in comparison to the wildtype (mean ± SD = 3699 ± 1132 µg/g; Fig.34A, Table 10). In 304/1 F_2 population, the MgC varied between 719.7 and 7597 µg/g, with a mean of 2829 µg/g (Fig.34B, Suppl. Fig.53C, Table 10). Similarly to calcium and copper, the distribution of this trait was skewed (skewness = 0.915, kurtosis = 0.0278; Suppl. Fig.53D).

In the case of manganese, its content (MnC) was also significantly higher (*t*-test, p < 0.005) in the wildtype in comparison to the lodging resistant line (Fig.35A, Table 10). Namely, mean MnC in 'R 1124' was 39.19 µg/g (± 14.97 SD), whereas only 15.43 µg/g (± 4.913 SD) in 'ms 135'. In the 304/1 population, the MnC varied between 3.177 and 79.64 µg/g, with a mean value of 12.13 µg/g (Fig.35B, Suppl. Fig.53E, Table 10). The distribution of this trait was skewed and characterised by skewness of 3.241 and kurtosis of 11.67 (Suppl. Fig.53F).
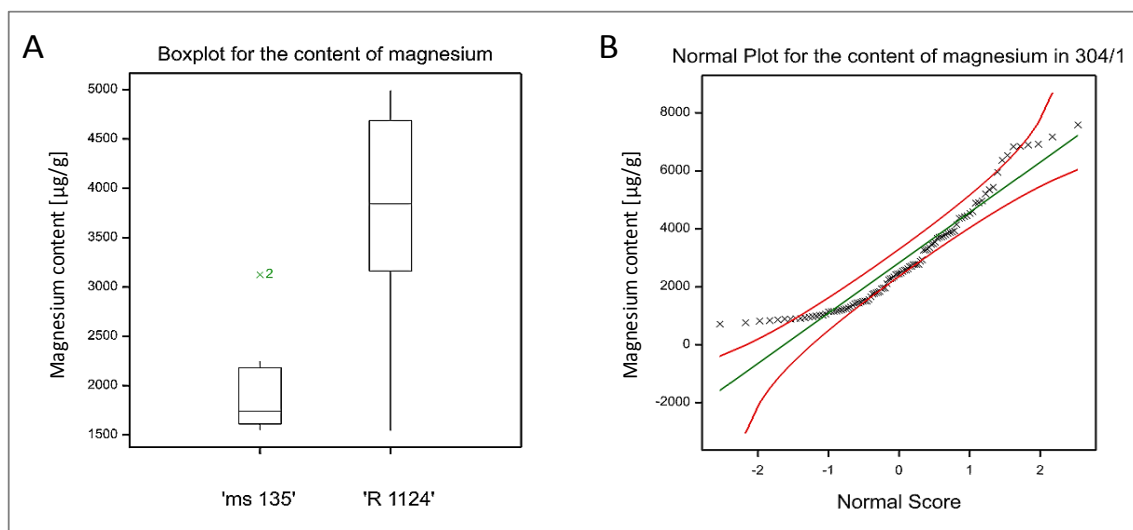
FIGURE 34 Boxplot showing median values for the content of magnesium in dry weight with whiskers indicating variability outside the upper and lower quartiles in two parental lines ('ms 135' and 'R 1124' **A**). A Quantile-Quantile plot with 95% simultaneous confidence bands and a 1-1 reference line plotting observed data for 304/1 F_2 population against their expected quantiles (**B**).
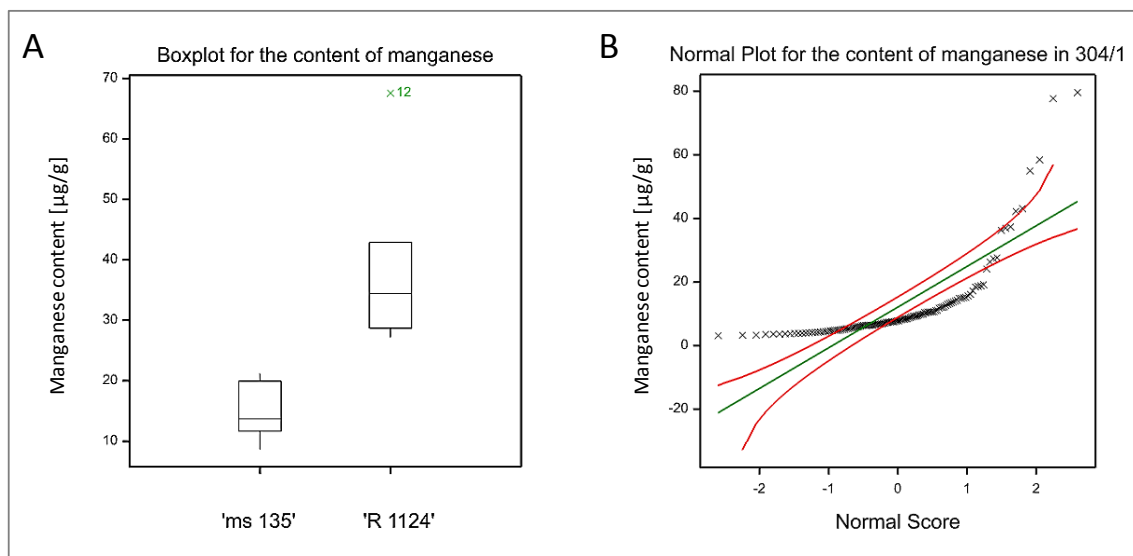
FIGURE 35 Boxplot showing median values for the content of manganese in dry weight with whiskers indicating variability outside the upper and lower quartiles in two parental lines ('ms 135' and 'R 1124' **A**). A Quantile-Quantile plot with 95% simultaneous confidence bands and a 1-1 reference line plotting observed data for 304/1 F_2 population against their expected quantiles (**B**).

In the case of sulfur (SC), its content in dry weight was also significantly higher (*t*-test, p < 0.005) in the wildtype, in comparison to the lodging resistant line (Fig.36A, Table 10). The mean value of SC in 'ms 135' was equal to 3805 µg/g (± 448 SD), and to 8294 µg/g (± 2117 SD) in the wildtype. In 304/1 F_2 population, SC varied between 1568 and 12141 µg/g, with a mean of 5135 µg/g (± 2668 SD; Fig.36B, Suppl. Fig.54A. Table 10), and the distribution was skewed and characterised by skewness of 0.862 and kurtosis of -0.0158 (Suppl. Fig.54B).

In contrast to previous elements, zinc content (ZnC) was significantly higher (*t*-test, p < 0.0005) in the lodging resistant line compared to 'R 1124' (Fig.37A, Table 10). Mean values for this trait were equal to 116.8 µg/g (± 30.62 SD) in 'ms 135', and to 46.07 µg/g (± 12.95 SD) in 'R 1124' parental line. In 304/1 F_2 population, ZnC varied between 34.86 and 246.7 µg/g, with a mean value of 94.06 µg/g (± 44.4 SD; Fig.37B, Suppl. Fig.54C, Table 10). The distribution of this trait in 304/1 F_2 population was not normal and characterised by skewness of 1.161 and kurtosis of 1.18 (Suppl. Fig.54D).
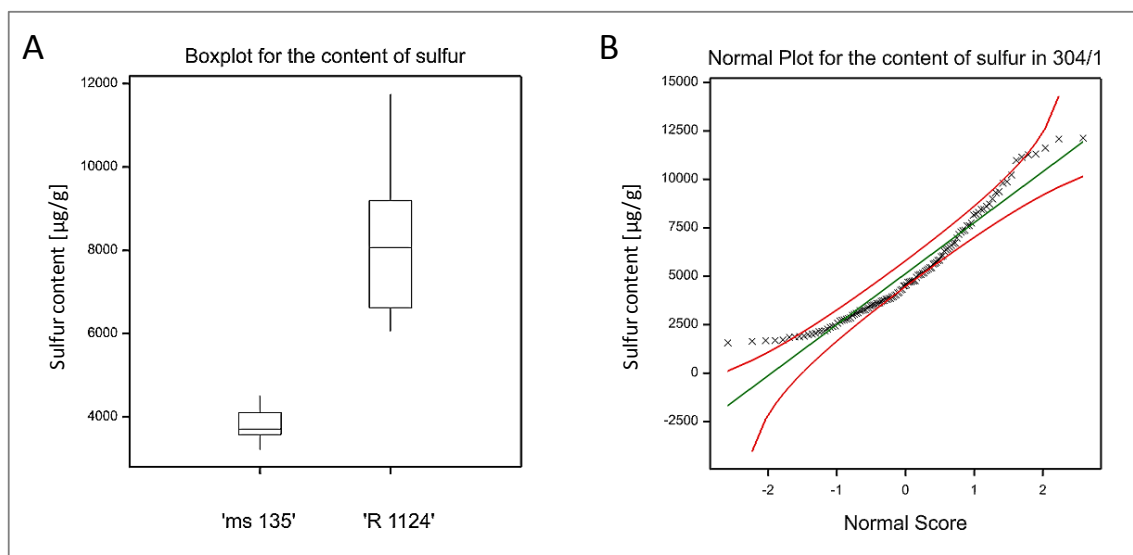
FIGURE 36 Boxplot showing median values for the content of sulfur in dry weight with whiskers indicating variability outside the upper and lower quartiles in two parental lines ('ms 135' and 'R 1124' **A**). A Quantile-Quantile plot with 95% simultaneous confidence bands and a 1-1 reference line plotting observed data for 304/1 F_2 population against their expected quantiles (**B**).

The content of the most interesting element from the mechanical point of view, silicon (SiC), since its known properties to enhance resistance of plants to various biotic and abiotic stresses including lodging (Ma and Yamaji, 2006), was significantly (*t*-test, p < 0.01) higher in the lodging resistant line (mean ± SD = 6960 ± 1805 µg/g), in comparison to the wildtype (mean ± SD = 4903 ± 1803 µg/g; Fig.38A, Table 10). The content of this element in 304/1 F_2 population varied between 3989 and 8443 µg/g, with mean equal to

5419 µg/g (± 797 SD; Fig.38B, Suppl. Fig.54E, Table 10), and the distribution of this trait was slightly skewed, characterized by skewness of 0.761 and kurtosis of 0.712 (Suppl. Fig.54F).
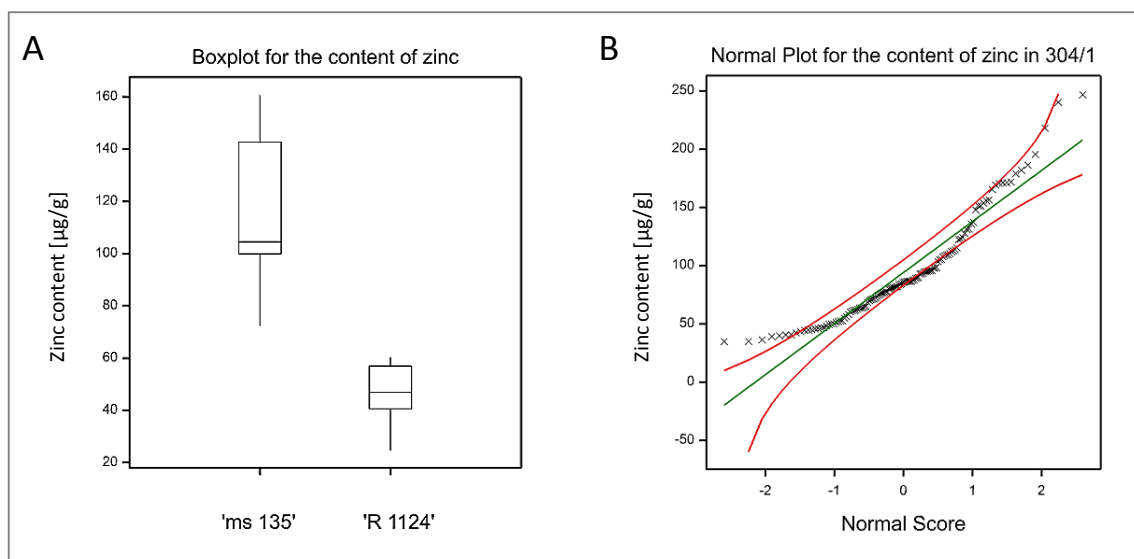
FIGURE 37 Boxplot showing median values for the content of zinc in dry weight with whiskers indicating variability outside the upper and lower quartiles in two parental lines ('ms 135' and 'R 1124' **A**). A Quantile-Quantile plot with 95% simultaneous confidence bands and a 1-1 reference line plotting observed data for 304/1 F_2 population against their expected quantiles (**B**).
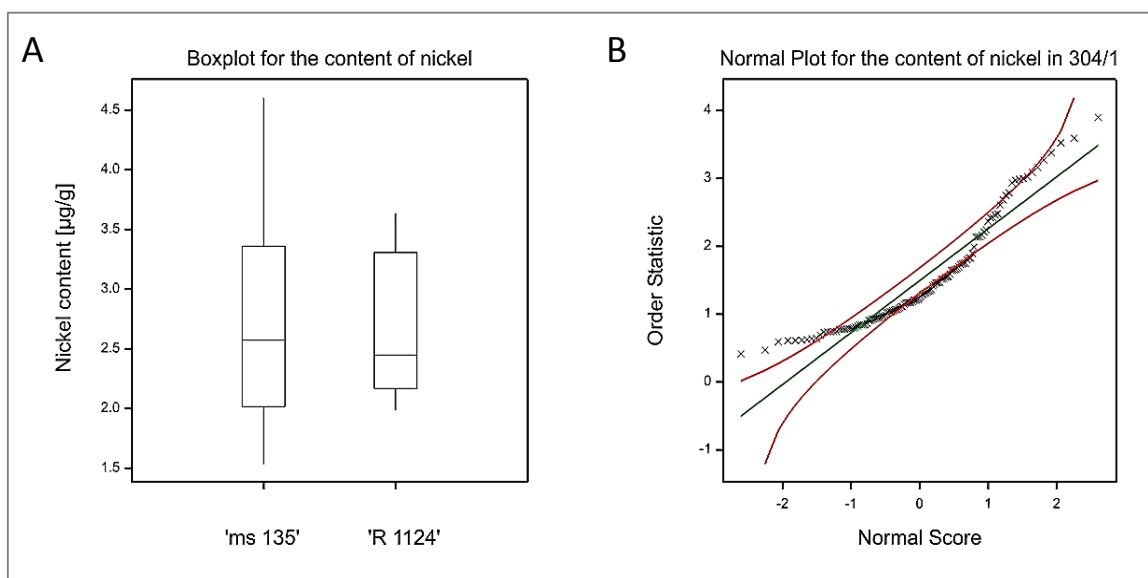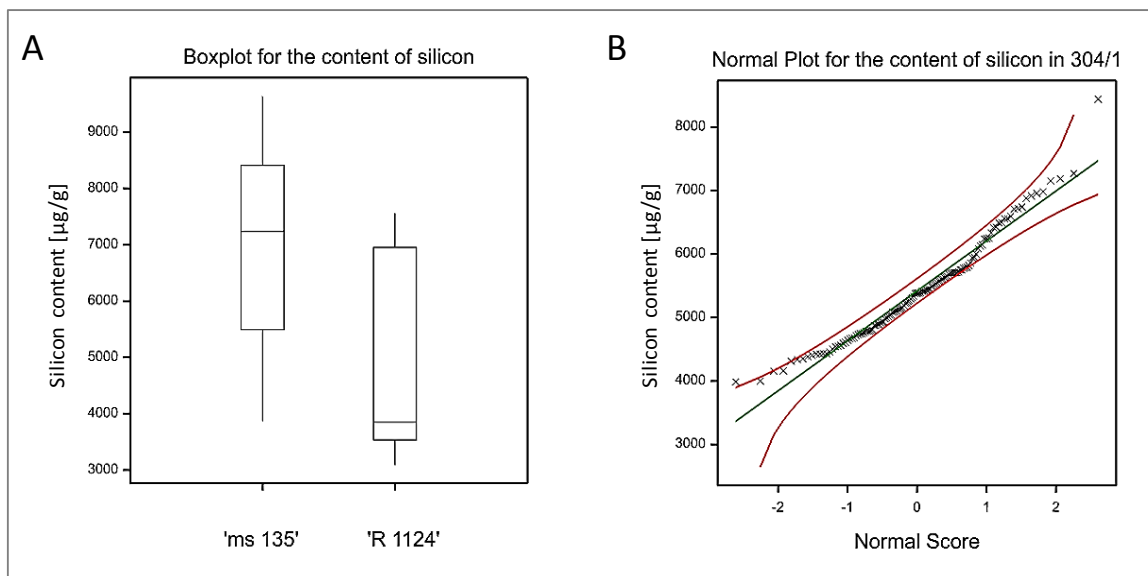

FIGURE 38 Boxplots showing median values for the content of silicon in dry weight with whiskers indicating variability outside the upper and lower quartiles in two parental lines ('ms 135' and 'R 1124' **A**). A Quantile-Quantile plot with 95% simultaneous confidence bands and a 1-1 reference line plotting observed data for 304/1 F_2 population against their expected quantiles (**B**).

4.2| Post-hoc analysis of phenotypic data

Phenotyping of 130 individuals of F_2 population revealed 143 significant correlations between traits (Fig.39). Thirty three of them were very strong to moderate. Namely, there were: two very strong positive correlations (0.8 < PCC < 1.0; Suppl. Fig.55), seven strong positive correlations (0.6 < PCC < 0.79; Suppl. Fig.56), twenty moderate positive correlations (0.4 < PCC < 0.59; Suppl. Fig.57-59), and four moderate negative correlations (-0.59 < PCC < -0.4). Additionally, fifty one weak (0.2 < PCC < 0.39) positive correlations and fifty nine weak (-0.39 < PCC < -0.2) negative correlations were found between traits analysed (Fig.39).

A very strong significant positive correlation, with PCC of 0.852 (p < 0.0001), was found in 304/1 F_2 population between CaC and MgC in basal internodes of tillers (Suppl. Fig.55A). Another very strong significant correlation (PCC = 0.801, p < 0.0001) was found between ScL and ScR (Suppl. Fig.55B).

Significant strong positive correlations were found between: MgC and SC (PCC = 0.788, p < 0.0001; Suppl. Fig.56A), DWC and the NoT (PCC = 0.771, p < 0.0001; Suppl. Fig.56B), CaC and SC (PPC = 0.743, p < 0.0001; Suppl. Fig.56C), DSC and DEC (PCC = 0.738, p < 0.0001; Suppl. Fig.56D), BC and MnC (PCC = 0.685, p < 0.0001; Suppl. Fig.56E), BC and CaC (PCC = 0.667, p < 0.0001; Suppl. Fig.56F), and between the CaC and NiC (PCC = 0.616, p < 0.0001; Suppl. Fig.56G).

Significant moderate positive correlations in 304/1 population were found between: NaC and SC (PCC = 0.579, p < 0.0001; Suppl. Fig.57A), BC and MgC (PCC = 0.573, p < 0.0001; Suppl. Fig.57B), MnC and CaC (PCC = 0.56, p < 0.0001; Suppl. Fig.57C), BC and SC (PCC = 0.537, p < 0.0001; Suppl. Fig.57D), MnC and PC (PCC = 0.532, p < 0.0001; Suppl. Fig.57E), CuC and KC (PCC = 0.522, p < 0.0001; Suppl. Fig.57F), MgC and NaC (PCC = 0.522, p < 0.0001; Suppl. Fig.57G), DWC and DBI (PCC = 0.514, p < 0.0001; Suppl. Fig.57H), NiC and MgC (PCC = 0.513, p < 0.0001; Suppl. Fig.58A), BC and NiC (0.51, p < 0.0001; Suppl. Fig.58B), BC and PC (PCC = 0.508, p < 0.0001; Suppl. Fig.58C), NiC and SC (PCC = 0.457, p < 0.0001; Suppl. Fig.58D), CWT and ScL (PCC = 0.436, p < 0.0001; Suppl. Fig.58E), DBI and the CWT (PCC = 0.43, p < 0.0001; Suppl. Fig.58F), CaC and NaC (PCC = 0.422; p < 0.0001; Suppl. Fig.58G), PH and CWT (PCC = 0.417, p < 0.0001; Suppl. Fig.58H), PH and SCW (PCC = 0.41, p < 0.0001; Suppl. Fig.59A), CuC and PC (PCC = 0.405, p < 0.0001; Suppl. Fig.59B), FeC and PC (PCC = 0.403, p < 0.0001; Suppl. Fig.59C), and between SCW and ECW (PCC = 0.403, p < 0.0001; Suppl. Fig.59D).

	1	2	3	4	5	6	7	8	9	10	11	12	13	14	15	16	17	18	19	20	21	22	23	24	25	26	27	28	29
2	0,277																												
3	0,076	-0,228																											
4	0,286	-0,103	0,771																										
5	0,192	0,122	-0,473	0,112																									
6	0,192	0,113	0,236	0,514	0,321																								
7	-0,122	0,104	0,072	0,069	-0,023	0,012																							
8	0,417	0,016	0,086	0,270	0,222	0,430	-0,369																						
9	0,240	0,007	0,064	0,222	0,163	0,230	-0,180	0,436																					
10	0,130	-0,087	-0,062	-0,073	-0,032	-0,381	-0,187	0,143	0,801																				
11	0,311	0,029	0,194	0,318	0,101	0,272	-0,252	0,284	0,093	-0,060																			
12	0,284	-0,003	0,111	0,384	0,329	0,190	-0,043	0,186	0,056	-0,042	0,364																		
13	-0,057	-0,098	0,015	0,029	0,069	0,088	-0,035	0,209	0,150	0,028	-0,126	-0,250																	
14	0,140	0,087	0,059	0,186	0,207	0,227	-0,041	0,258	0,258	0,057	0,018	-0,018	0,738																
15	0,410	0,065	-0,070	0,051	0,194	0,075	0,004	0,264	0,147	0,093	0,065	0,032	0,358	0,389															
16	0,243	-0,079	0,027	0,045	0,038	0,017	-0,010	0,143	0,088	0,085	-0,077	0,012	0,194	0,142	0,403														
17	-0,307	0,018	-0,248	-0,407	-0,144	-0,350	-0,185	-0,276	-0,159	0,065	-0,112	-0,073	-0,152	-0,203	-0,278	-0,170													
18	-0,314	-0,088	-0,207	-0,382	-0,145	-0,167	-0,002	-0,237	0,023	0,137	-0,246	-0,312	-0,063	-0,244	-0,128	0,025	0,370												
19	-0,156	0,028	-0,105	-0,141	-0,042	0,249	0,082	-0,084	0,166	0,002	-0,158	-0,332	0,064	0,131	-0,037	-0,073	-0,170	0,245											
20	-0,038	0,050	-0,164	-0,236	-0,029	-0,199	-0,162	-0,156	-0,133	0,006	0,011	0,031	-0,186	-0,251	-0,030	-0,018	0,510	0,389	-0,109										
21	-0,278	0,020	-0,230	-0,300	0,012	-0,165	0,020	-0,258	-0,087	0,021	-0,093	-0,148	-0,118	-0,028	-0,125	-0,123	0,508	0,403	0,194	0,096									
22	0,046	-0,122	0,085	0,201	0,078	-0,026	-0,214	0,103	-0,060	-0,055	0,293	0,275	0,058	0,075	0,068	0,069	0,170	-0,224	-0,282	0,291	-0,057								
23	-0,030	0,041	-0,188	-0,168	0,045	-0,295	-0,221	-0,110	0,003	0,183	0,009	0,256	-0,180	-0,151	-0,205	-0,174	0,667	0,054	-0,361	0,616	0,224	0,422							
24	-0,515	-0,136	-0,283	-0,422	-0,038	-0,093	-0,055	-0,188	-0,054	-0,007	-0,206	-0,241	-0,092	-0,162	-0,269	-0,229	0,309	0,260	0,227	-0,089	0,405	-0,252	0,035						
25	-0,390	0,109	-0,154	-0,333	-0,140	-0,088	0,022	-0,228	-0,083	-0,064	-0,170	-0,303	0,158	-0,069	-0,124	-0,121	0,147	0,226	0,263	-0,084	0,200	-0,144	-0,117	0,522					
26	-0,158	-0,155	-0,199	-0,161	0,081	-0,260	-0,247	-0,164	-0,133	0,037	0,127	0,129	-0,187	-0,203	-0,155	-0,135	0,573	0,020	-0,338	0,513	0,193	0,522	0,852	0,026	-0,116				
27	-0,226	-0,037	-0,209	-0,235	0,077	-0,170	-0,104	-0,119	-0,046	0,067	-0,034	0,119	-0,218	-0,201	-0,258	-0,129	0,685	0,239	-0,247	0,317	0,532	0,095	0,560	0,389	0,094	0,370			
28	-0,078	0,012	-0,119	-0,075	0,068	-0,121	-0,255	-0,128	-0,111	-0,024	0,149	0,168	-0,157	-0,237	-0,032	-0,078	0,537	0,000	-0,125	0,457	0,210	0,579	0,743	-0,005	0,076	0,788	0,366		
29	-0,228	-0,134	0,020	-0,077	-0,047	-0,091	0,087	-0,052	-0,048	0,017	-0,186	-0,223	0,075	0,031	-0,117	0,034	0,057	0,394	0,118	-0,139	0,396	-0,134	-0,150	0,305	0,165	-0,097	0,106	-0,125	
30	-0,078	0,061	-0,147	-0,246	-0,045	-0,241	-0,080	-0,082	-0,114	0,022	0,044	0,064	0,025	0,012	0,028	0,033	0,160	-0,038	-0,191	0,079	0,081	-0,015	0,136	0,134	0,123	0,015	0,217	-0,049	-0,092

1 - Plant height
2 - Length of the 2nd internode
3 - Number of tillers
4 - Culms dry weight
5 - Mean dry weight of a culm
6 - Diameter of the internode
7 - Number of epidermal invaginations
8 - Thickness of stalk tissues
9 - Thickness of sclerenchyma
10 - Sclerenchyma ratio
11 - Number of inner vascular bundles
12 - Number of outer vascular bundles
13 - Diameter of epidermal cell
14 - Diameter of sclerenchymal cell
15 - Thickness of sclerenchymal cell wall
16 - Thickness of inner periclinal cell wall of epidermis
17 - B content
18 - Fe content
19 - Mo content
20 - Ni content
21 - P content
22 - Na content
23 - Ca content
24 - Cu content
25 - K content
26 - Mg content
27 - Mn content
28 - S content
29 - Zn content
30 - Si content

FIGURE 39 Correlations between traits in 304/1 F_2 population. Significant correlations with $p < 0.05$ are indicated with the bold black font.

Four significant moderate negative correlations were found between: PH and CuC (PCC = -0.515, $p < 0.0001$; Suppl. Fig.60A), DWS and NoT (PCC = -0.473, $p < 0.0001$; Suppl. Fig.60B), DWC and CuC (PCC = -0.422, $p < 0.0001$; Suppl. Fig.60C), and between DWC and BC (PCC = -0.407, $p < 0.0001$; Suppl. Fig.60D).

Weak significant positive correlations were found between: PC and ZnC (PCC = 0.396, $p < 0.0001$), FeC and ZnC (PCC = 0.394, $p < 0.0001$), FeC and NiC (PCC = 0.389, $p < 0.0001$), MnC and CuC (PCC = 0.389, $p < 0.0001$), DSC and SCW (PCC = 0.389, $p < 0.0001$), DWC and OVB (PCC = 0.384, $p < 0.0001$), FeC and BC

(PCC = 0.37, p < 0.0001), MnC and MgC (PCC = 0.37, p < 0.0001), MnC and SC (PCC = 0.366, p < 0.0001), OVB and IVB (PCC = 0.364, p < 0.0001), SCW and the DEC (PCC = 0.358, p < 0.0005), OVB and DWS (PCC = 0.329, p < 0.0005), DBI and DWS (PCC = 0.321, p < 0.0005), DWC and IVB (PCC = 0.318, p < 0.0005), MnC and NiC (PCC = 0.317, p < 0.0005), PH and the IVB (PCC = 0.311, p < 0.0005), BC and CuC (PCC = 0.309, p < 0.005), CuC and ZnC (PCC = 0.305, p < 0.005), NaC and IVB (PCC = 0.293, p < 0.005), NaC and NiC (PCC = 0.291, p < 0.005), DWC and PH (PCC = 0.286, p < 0.005), PH and OVB (PCC = 0.284, p < 0.005), CWT and the IVB (PCC = 0.284, p < 0.005), PH and LBI (PCC = 0.277, p < 0.005), OVB and the NaC (PCC = 0.275, p < 0.005), DBI and IVB (PCC = 0.272, p < 0.005), DWC and the CWT (PCC = 0.27, p < 0.005), CWT and the ECW (PCC = 0.264, p < 0.005), MoC and KC (PCC = 0.263, p < 0.005), FeC and CuC (PCC = 0.26, p < 0.005), DSC and ScL (PCC = 0.258, p < 0.005), CWT and the DSC (PCC = 0.258, p < 0.005), OVB and CaC (PCC = 0.256, p < 0.005), DBI and MoC (PCC = 0.249, p < 0.01), FeC and MoC (PCC = 0.245, p < 0.01), PH and the ECW (PCC = 0.243, p < 0.01), PH and ScL (PCC = 0.24, p < 0.01), FeC and MnC (PCC = 0.239, p < 0.01), DBI and NoT (PCC = 0.236, p < 0.05), DBI and ScL (PCC = 0.23, p < 0.05), CuC and MoC (PCC = 0.227, p < 0.05), DBI and the DSC (PCC = 0.227, p < 0.05), FeC and KC (PCC = 0.226, p < 0.05), CaC and PC (PCC = 0.224, p < 0.05), CWT and DWS (PCC = 0.222, p < 0.05), DWC and ScL (PCC = 0.222, p < 0.05), MnC and SiC (PCC = 0.217, p < 0.05), PC and SC (PCC = 0.21, p < 0.05), CWT and DEC (PCC = 0.209, p < 0.05), DSC and DWS (PCC = 0.207, p < 0.05), and between DWC and NaC (PCC = 0.201, p < 0.05).

Weak significant negative correlations were found between: PH and KC (PCC = -0.39, p < 0.0001), DWC and the FeC (PCC = -0.382, p < 0.0001), DBI and ScR (PCC = -0.381, p < 0.0001), CWT and Epl (PCC = -0.369, p < 0.0001), CaC and MoC (PCC = -0.361, p < 0.0001), BC and the DBI (PCC = -0.35, p < 0.0005), DWC and the KC (PCC = -0.333, p < 0.0005), OVB and MoC (PCC = -0.332, p < 0.0005), FeC and PH (PCC = -0.314, p < 0.0005), FeC and OVB (PCC = -0.312, p < 0.0005), PH and the BC (PCC = -0.307, p < 0.005), OVB and KC (PCC = -0.303, p < 0.005), DWC and PC (PCC = -0.3, p < 0.005), DBI and the CaC (PCC = -0.295, p < 0.005), CuC and the NoT (PCC = -0.283, p < 0.005), NaC and MoC (PCC = -0.282, p < 0.005), PH and PC (PCC = -0.278, p < 0.005), BC and the SCW (PCC = -0.278, p < 0.005), BC and the CWT (PCC = -0.276, p < 0.005), CuC and the SCW (PCC = -0.269, p < 0.005), DBI and MgC (PCC = -0.26, p < 0.005), CWT and PC (PCC = -0.258, p < 0.005), MnC and SCW (PCC = -0.258, p < 0.005), SC and the Epl (PCC = -0.255, p < 0.005), IVB and Epl (PCC = -0.252, p < 0.005), CuC and NaC (PCC = -0.252, p < 0.005), DSC and NiC

(PCC = -0.251, p < 0.005), OVB and DEC (PCC = -0.25, p < 0.01), BC and the NoT (PCC = -0.248, p < 0.01), MnC and MoC (PCC = -0.247, p < 0.01), MgC and Epl (PCC = -0.247, p < 0.01), FeC and IVB (PCC = -0.246, p < 0.01), DWC and the SiC (PCC = -0.246, p < 0.01), FeC and DSC (PCC = -0.244, p < 0.01), DBl and SiC (PCC = -0.241, p < 0.01), CuC and OVB (PCC = -0.241, p < 0.01), MgC and MoC (PCC = -0.338, p < 0.01), FeC and CWT (PCC = -0.237, p < 0.05), DSC and the SC (PCC = -0.237, p < 0.05), DWC and the NiC (PCC = -0.236, p < 0.05), DWC and MnC (PCC = -0.235, p < 0.05), PC and NoT (PCC = -0.23, p < 0.05), CuC and ECW (PCC = -0.229, p < 0.05), NoT and LBI (PCC = -0.228, p < 0.05), PH and ZnC (PCC = -0.228, p < 0.05), CWT and KC (PCC = -0.228, p < 0.05), MnC and PH (PCC = -0.226, p < 0.05), FeC and NaC (PCC = -0.224, p < 0.05), OVB and ZnC (PCC = -0.223, p < 0.05), CaC and Epl (PCC = -0.221, p < 0.05), MnC and the DEC (PCC = -0.218, p < 0.05), NaC and Epl (PCC = -0.214, p < 0.05), MnC and NoT (PCC = -0.209, p < 0.05), FeC and the NoT (PCC = -0.207, p < 0.05), CuC and IVB (PCC = -0.206, p < 0.05), CaC and SCW (PCC = -0.205, p < 0.05), DSC and MgC (PCC = -0.203, p < 0.05), BC and the DSC (PCC = -0.203, p < 0.05), MnC and DSC (PCC = -0.201, p < 0.05).

4.3| Genotyping

The first analyses, based on SRR markers, uncovered low polymorphism between two parental lines. Amplification of 269 SSR markers in parental lines and 304/1 F_2 population revealed that the number of polymorphic and segregating markers was not sufficient (in total 45 polymorphic and segregating markers; Table 11) for the efficient QTL mapping and significantly different from the expected Mendelian ratio (1:2:1 for codominant markers and 1:3 for dominant markers; χ^2 test with p > 0.05) distorted segregations, were observed for 83.27% of analysed markers. Low polymorphism forced the change of the genotyping strategy. DArTseq markers were chosen, as a fast and relatively cheap genotyping platform (Jaccoud *et al.*, 2001; Bolibok-Brągoszewska *et al.*, 2009; Milczarski *et al.*, 2011). In this case, the percentage of polymorphic and segregating markers in 304/1 F_2 population was higher (between 25.27 and 27.26 %; Table 12) and the total number of markers, which could be used for the construction of the genetic map was 8,135 (45 SSRs, 6,254 DArTs, and 1,836 SNPs).

TABLE 11 Number of markers checked and percentage of polymorphic and segregating markers in 304/1 F_2 population investigated with WMS, RMS, REMS, and SCM markers.

	Number of markers checked	Polymorphic and segregating	% of polymorphic and segregating markers
WMS Wheat MicroSatellites	68	14	20.59%
RMS Rye MicroSatellites	109	18	16.51%
REMS Rye Expressed Microsatellites	36	6	16.67%
SCM Secale cereale Microsatellites	56	7	12.5%
Total	269	45	16.73%

TABLE 12 Number of markers checked and percentage of polymorphic and segregating markers in 304/1 F_2 population investigated with DArTseq.

	Number of markers checked	Polymorphic and segregating	% of polymorphic and segregating markers
DArTs	22944	6254	27.26%
SNPs	7265	1836	25.27%
Total	30209	8090	26.78%

4.4 | Construction of the genetic map

The linkage maps were constructed basing on 129 individuals of 304/1 F_2 population and the most informative 1,041 SNP and co-dominant SSR markers, which were used to determinate seven genetic linkage groups covering 783.8 cM, with the average distance between two markers of 0.75 cM (Table 13; Fig.40). The order of markers was determined in JoinMap 4.1 by maximum likelihood mapping. Afterwards regression mapping with Kosambi function was used to determine distances between markers, and the groups were assigned to chromosomes using GenomeZipper (Martis *et al.*, 2013).

The number of markers per chromosome varied between 110 markers for chromosome 4R and 191 markers for chromosome 2R (Table 13, Fig.40). The longest map was constructed for chromosome 3R, with the length of 124.9 cM, followed by 2R, 4R, and 1R with the length of 119.2, 115.4, and 113.7 cM, respectively (Table 13, Fig.40).

The shortest maps were developed for 5R, 6R, and 7R, with the length of 107.6, 106.6, and 96.43 cM, respectively (Table 13, Fig.40). The most saturated chromosome was 7R with the average distance between two markers of 0.53 cM, and the median distance between two markers of 0.1 cM. The least saturated chromosome was 4R with only 1.05 cM of the average distance between two markers and 0.4 cM of median distance between two markers, followed by 1R with 0.94 cM and 0.8 cM respectively. The average distance between two markers in the other linkage maps varied between 0.62 and 0.73 cM (0.62 cM for 2R, 0.65 cM for 3R and 5R, and 0.73 cM for 6R). The markers were not evenly distributed and there were 5 gaps, where the distance between adjacent markers was bigger than 10 cM (one on chromosome 2R, two on chromosome 3R, and two on chromosome 4R; Table 13, Fig.40).

TABLE 13 Seven linkage groups with the numbers of markers per chromosome, its length, median distance between markers, 95% percentile of distances, and the number of gaps bigger than 10 cM.

Chromosome	No. of markers	Length [cM]	Median distance between markers [cM]	95% percentile of distances [cM]	No. gaps > 10 cM
1R	121	113.7	0.8	2.3	0
2R	191	119.2	0.2	2.1	1
3R	124	124.9	0.2	5.8	2
4R	110	115.4	0.4	4.7	2
5R	165	107.6	0.4	1.4	0
6R	147	106.6	0.5	1.9	0
7R	183	96.4	0.1	2.0	0
Genome	1041	783.8	0.4	2.6	5
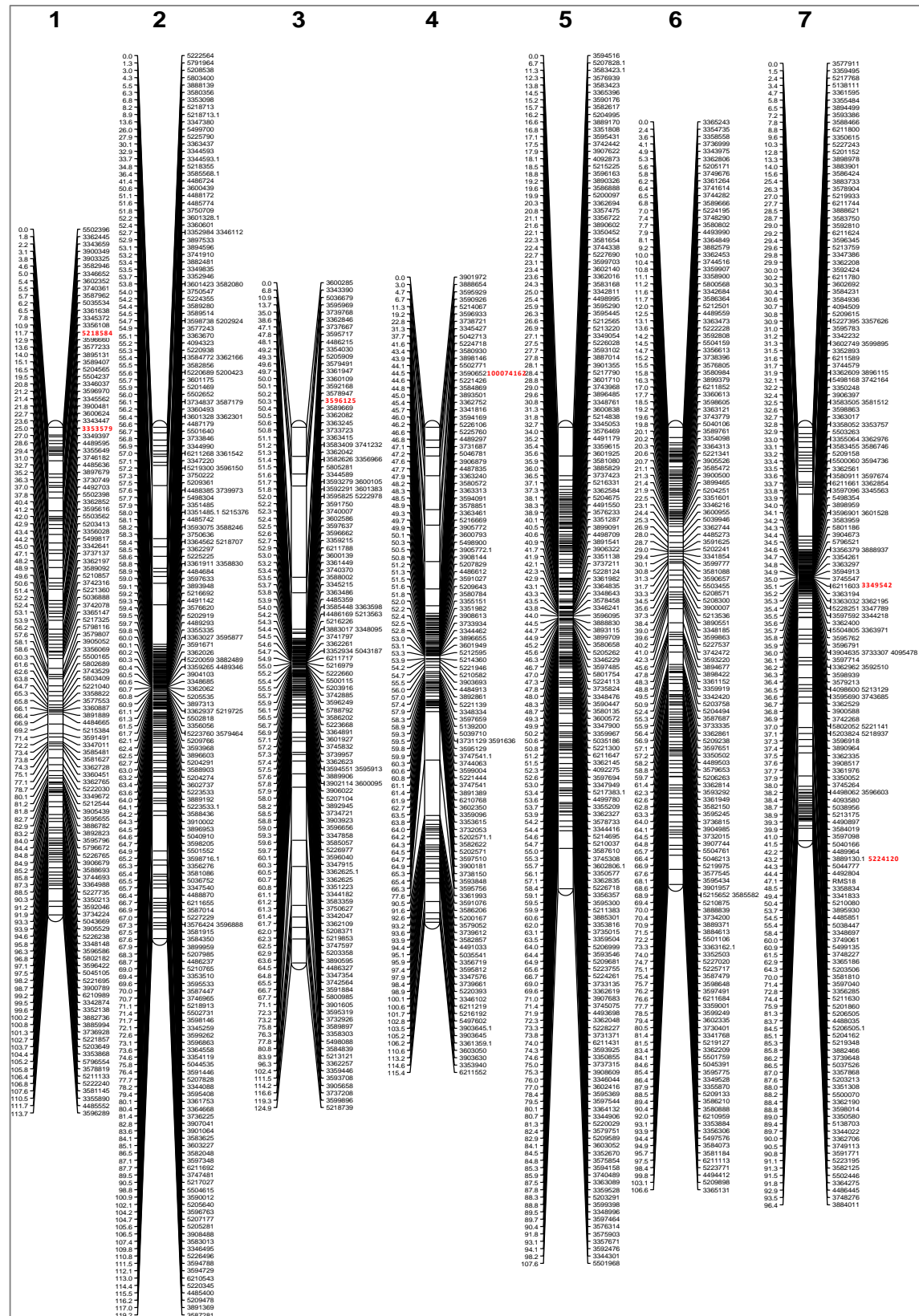
FIGURE 40 Seven linkage groups corresponding to rye chromosomes constructed in JoinMap basing on 1,041 SNP and SSR markers. SNPs used for the development of KASP markers marked with red font.

4.5| QTL mapping

Quantitative Trait Locus analysis was conducted in GenStat software using an initial genome-wide scan by simple interval mapping (SIM) to obtain candidate QTL positions. Simple (used as cofactors) and Composite Interval Mapping (CIM: scan with cofactors) for single environment trials were used to establish the final QTL model for the traits (for the overview of all the QTL found in the 304/1 F_2 population see Fig.41 and Table 14).

TABLE 14 Summary of all the QTL found in 304/1 F_2 population.

Trait	IDLocus	Chr.	Position [cM]	LOD	Lower and upper bounds [cM]	% Expl. Var.	Add. effect	High value allele	Dom. effect	Dom. allele
PH	3577233	1R	13.55	4.246	0 - 59.724	14.076	5.150	'ms 135'	1.811	'ms 135'
	3586746	7R	33.14	5.688	7.774 – 58.442	16.522	5.649	'ms 135'	1.486	'ms 135'
LBl	3901605	3R	71.06	3.02	0 – 124.88	9.133	0.744	'R 1124'	0.565	'R 1124'
NoT	3344182	3R	61.11	9.502	49.413 – 72.807	31.886	2.617	'ms 135'	0.840	'R 1124'
DWC	3906022	3R	57.93	9.551	45.342 – 70.518	30.118	4.513	'ms 135'	1.078	'R 1124'
Epl	3356966	3R	51.40	3.108	0 – 124.880	10.707	2.201	'ms 135'	2.190	'R 1124'
CWT	3580572	4R	48.17	3.001	0 – 115.400	10.351	29.366	'ms 135'	0.726	'ms 135'
	5044777	7R	44.27	4.072	0 – 74.334	14.892	35.198	'ms 135'	3.994	'ms 135'
ScL	3597040	7R	71.42	3.365	0 – 96.430	1.618	1.818	'ms 135'	7.008	'ms 135'
IVB	6211655	2R	66.69	3.369	0 – 119.160	10.423	1.465	'ms 135'	0.515	'ms 135'
DEC	3590926	4R	6.68	3.010	0 – 115.400	9.686	0.983	'ms 135'	0.150	'R 1124'
DSC	5212595	4R	53.32	3.641	0 – 115.400	1.682	0.442	'ms 135'	1.533	'R 1124'
SCW	4485636	1R	32.70	3.738	0 – 113.700	10.738	0.134	'ms 135'	0.035	'R 1124'
ECW	3362445	1R	1.75	5.333	0 – 113.700	3.412	0.041	'ms 135'	0.124	'R 1124'
	3590447	5R	48.25	3.737	0 – 107.590	7.690	0.063	'ms 135'	0.066	'ms 135'
MoC	3898978	7R	13.27	4.754	0 - 69.793	13.301	1.265	'R 1124'	0.817	'ms 135'
NiC	3355335	2R	59.84	3.050	0 – 119.160	0.010	0.011	'ms 135'	0.490	'R 1124'
CuC	5201152	7R	12.80	5.962	0 – 56.194	14.464	1.305	'R 1124'	1.272	'ms 135'
SC	3363240	4R	47.87	3.160	0 – 115.400	0.723	390.102	'R 1124'	1648.748	'R 1124'
	3575854	5R	84.79	3.000	0 – 107.590	0.627	303.571	'R 1124'	1577.704	'R 1124'
ZnC	3362852	1R	40.39	3.037	0 – 113.700	8.270	17.566	'ms 135'	20.072	'ms 135'
	3344593.1	2R	33.69	3.292	0 – 119.160	2.780	10.095	'R 1124'	27.204	'ms 135'
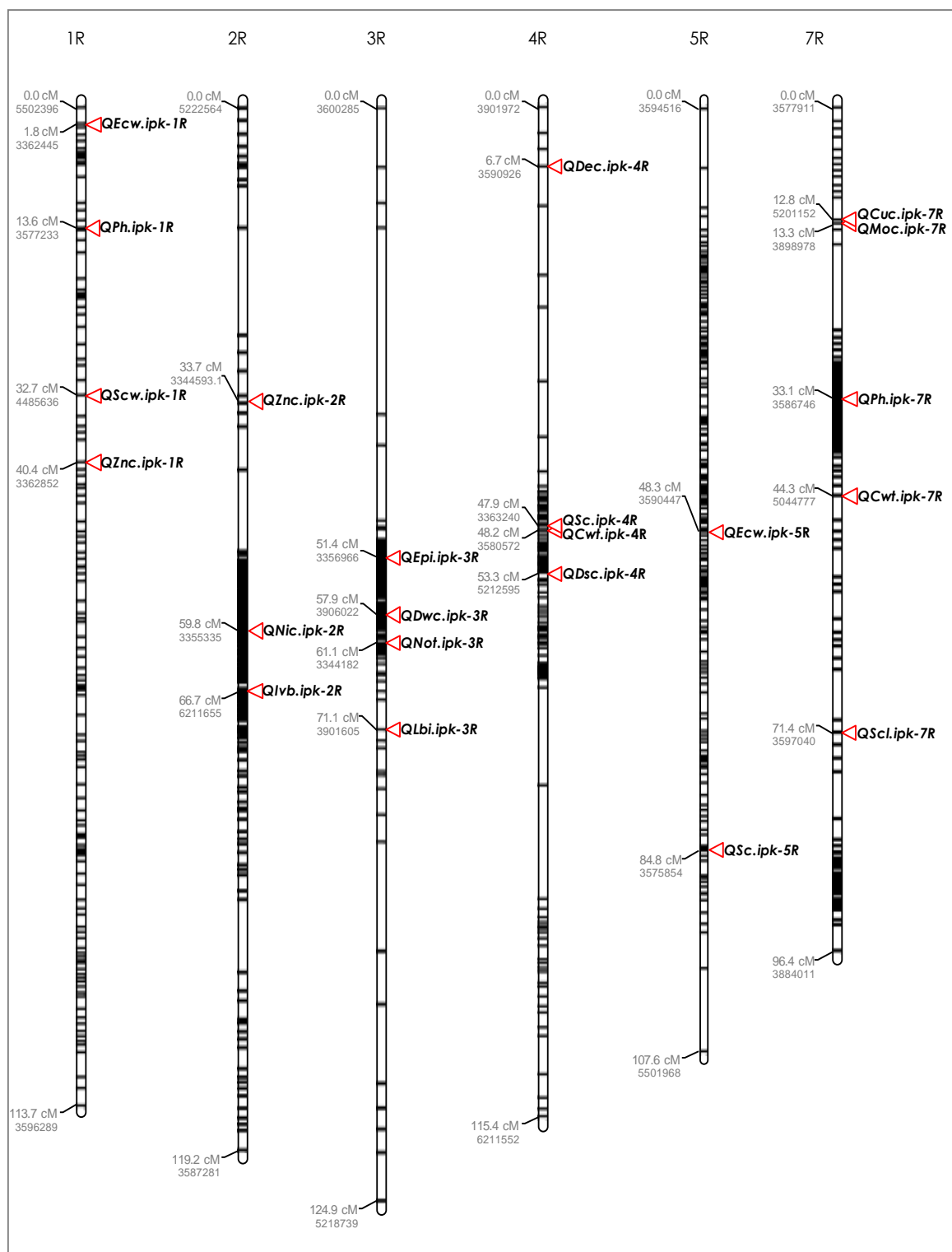
FIGURE 41 All the QTL associated with traits influencing lodging resistance found in 304/1 F$_2$ population. The arrowheads show the position of maximum LOD score. *Cuc – Cu content; Cwt – culm wall thickness; Dec – diameter of epidermal cell; Dsc – diameter of sclerenchymal cell; Dwc – dry weight of culms; Ecw – thickness of inner periclinal CW of epidermis; Epi – number of epidermal invaginations; Ivb – number of inner vascular bundles; Lbi – length of the second basal internode; Moc- Mo content; Nic – Ni content; Not – Number of tillers; Ph – plant height; Sc – S content; Scl – thickness of sclerenchyma; Scw – thickness of sclerenchymal CW; Znc – Zn content.*

QTL for the traits analysed were detected on all chromosomes, except chromosome 6R (Fig. 41, Table 13). The highest number of QTL was detected on chromosome 7R, where 5 QTL were detected responsible for: Scl, CWT, MoC, CuC, and PH. Equally same number of 4 QTL was found on 1R, 3R, and 4R. The least number of detectable QTL was obtained for 2R (3 QTL) and 5R (2 QTL; Fig. 41, Table 14).

For traits: mean dry weight of a single culm, the diameter of the second basal internode, the ratio between the thickness of sclerenchyma and diameter of internode, the number of outer vascular bundles, boron, iron, phosphorus, sodium, calcium, potassium, magnesium, manganese, and silicon content (Suppl. Fig.61-62), no QTL was detected since the LOD score was lower than a threshold (LOD = 3.0).

For plant height, SIM scan revealed 146 markers (145 SNPs, and 1 SSR) on chromosome 1R (5 SNPs at 10.9 – 14 cM) and 7R (141 markers at 1.5 – 50.4 cM), associated with this trait (LOD > 3.0; Suppl. Fig.63A), and 2 candidate QTL had been selected at following positions: on 1R at the position of 13.55 cM and on 7R at position of 33.14 cM. CIM scan reduced the number of markers associated with plant height to 135 markers: 6 SNPs on 1R (10.9 – 15.1 cM) and 129 SNPs on 7R (1.5 – 38.9 cM; Fig.42A). Eventually, the final model (Suppl. Fig.63C) consisted of two QTL: located on chromosome 1R (at the position of 13.55 cM, LOD = 4.246; additive effect: 5.15, dominance effect: 1.811), explaining 14.076% of the phenotypic variance, and 7R (at the position of 33.14 cM, LOD = 5.688; additive effect: 5.649, dominance effect: 1.486), explaining 16.522% of the phenotypic variance (Fig.41, Table 14).

On the other hand, SIM mapping revealed only one SNP on chromosome 3R at the position of 71.06 cM associated with the length of the second basal internode (LOD > 3.0; Suppl. Fig.63B), which did not overlap with any of the QTL detected for PH. This marker was selected after CIM mapping (Fig.42B) as a putative QTL (LOD = 3.02; additive effect: 0.744, dominance effect: 0.565, Suppl. Fig.63D) for this trait, explaining 9.133% of the phenotypic variance (Fig.36, Table 14).

110 SNP markers located on chromosome 3R (47.1 – 83.9 cM) associated with the number of tillers (LOD > 3.0) were revealed by SIM mapping (Suppl. Fig.63E), from which one candidate QTL at the position of 61.11 cM was chosen, and same results were obtained for CIM mapping (Fig.42C). One SNP marker associated with the number of tillers was selected for the final model of QTL (Suppl. Fig.63G) on chromosome 3R at the position of 61.11 cM (LOD = 9.502; additive effect: 2.617, dominance effect = 0.84), explaining 31.886% of the phenotypic variance (Fig.41, Table 14).

For culms dry weight, SIM scan revealed 109 SNP markers on chromosome 3R (38.5 – 76.2 cM) associated with this trait (LOD > 3.0; Suppl. Fig.63F), overlapping with

the QTL found for the number of tillers. One candidate QTL had been selected at the position of 57.93 cM, and the same results were obtained for CIM mapping (Fig.42D). The final model of one QTL (Suppl. Fig.63H) was located on chromosome 3R at the position of 57.93 cM (LOD = 9.551; additive effect: 4.513, dominance effect: 1.078), explaining 30.118% of the phenotypic variance (Fig.41, Table 14).

Only 4 SNPs on chromosome 3R, associated with the number of epidermal invaginations (LOD > 3.0), were revealed by SIM mapping (Suppl. Fig.64A) and one candidate QTL at the position of 51.4 cM was selected. Composite Interval Mapping gave same results as the first scan (Fig.42E) and the final QTL model (Suppl. Fig.64C) was located on 3R chromosome at the position of 51.4 cM (LOD = 3.108; additive effect: 2.201, dominance effect: 2.19) and explained 10.707% of the phenotypic variance (Fig.41, Table 14).

SIM scan revealed 42 SNP markers: 36 markers on 4R (19.2 – 53.1 cM) and 6 markers on 7R (41.0 – 44.5 cM), associated with culm wall thickness (LOD > 3.0; Suppl. Fig. 64B), from which two candidate QTL: on 4R at the position of 45.4 cM and 7R at the position of 44.27 cM, were chosen. CIM mapping reduced the number of markers associated with the trait to 18: 15 markers on 4R (at positions of 41.6 – 48.5 cM) and 3 markers on 7R (at positions of 43.2 – 44.5 cM; Fig.42F). 2 markers were selected for the final model of QTL responsible for the thickness of culm wall (Suppl. Fig.64D): on 4R at the position of 48.17 cM (LOD = 3.001; additive effect: 29.366, dominance effect: 0.726), explaining 10.351% of the phenotypic variance, and on 7R at the position of 44.27 cM (LOD = 4.072; additive effect: 35.198, dominance effect: 3.994), explaining 14.892% of the phenotypic variance (Fig.41, Table 14).

For the thickness of sclerenchymal tissue, SIM scan revealed 4 SNPs on chromosome 7R at positions of 71.4 – 74.4 cM associated with this trait (LOD > 3.0; Suppl. Fig.64E), CIM mapping gave same results as SIM scan (Fig.42G), and the final model of one QTL (Suppl. Fig.64G) was located on chromosome 7R at the position of 71.42 cM (LOD = 3.365; additive effect: 1.818, dominance effect: 7.008), explaining only 1.618% of the phenotypic variance (Fig.41, Table 14).

28 SNP markers located on 2R at positions of 63.2 – 74.4 cM were associated with the number of inner vascular bundles in the second basal internode, with the highest LOD score for the marker at the position of 66.69 cM, as it was revealed by SIM scan (LOD > 3.0; Suppl. Fig.64F). Same results were obtained with CIM scan (Fig.42H), what enabled to choose a putative QTL for this trait (Suppl. Fig.64H) on chromosome 2R at the position of 66.69 cM (LOD = 3.369; additive effect: 1.465, dominance effect: 0.515), explaining 10.423% of the phenotypic variance (Fig.41, Table 14).
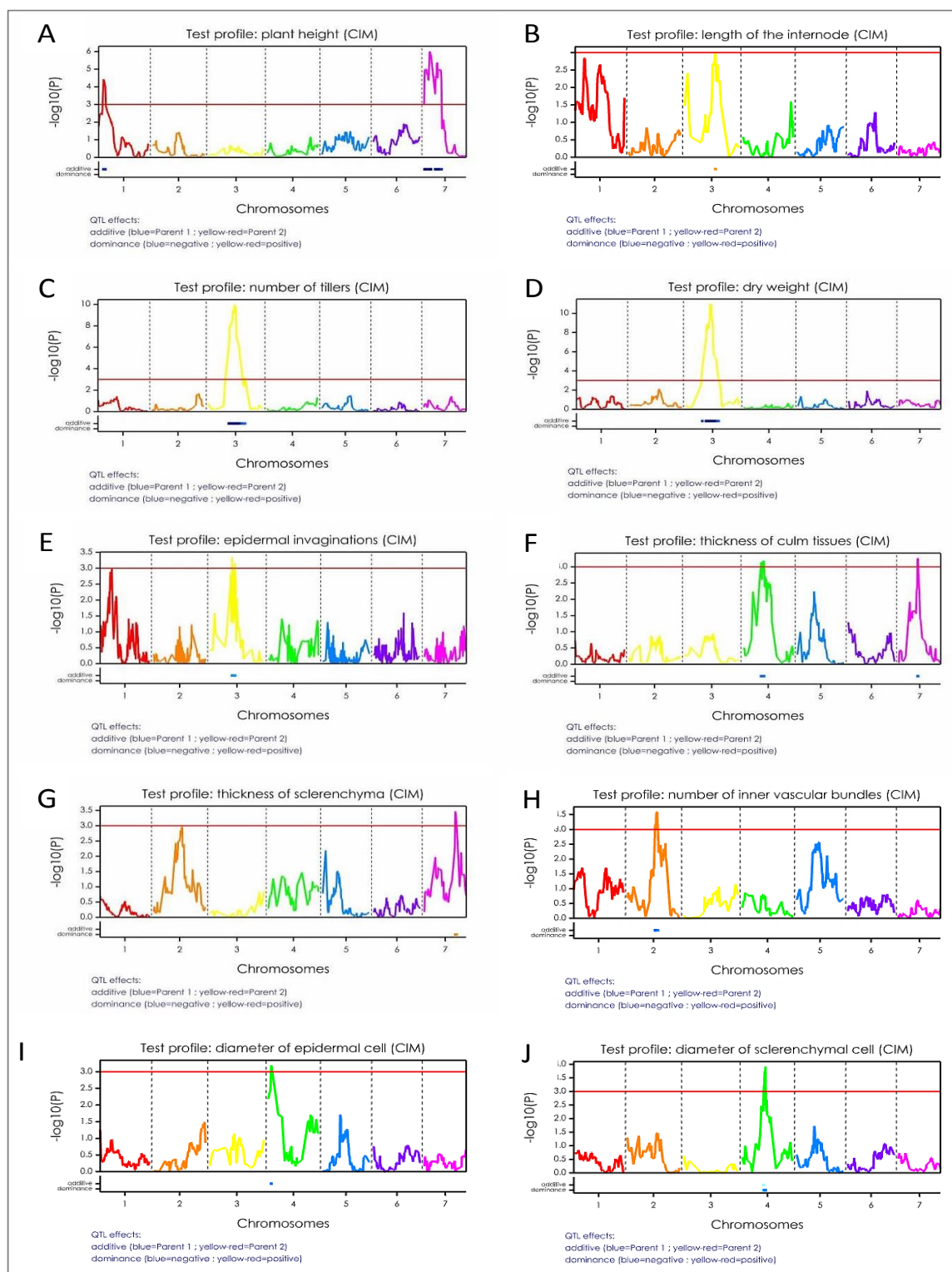
FIGURE 42 Genome-wide Composite Interval Mapping showing the association of mapped markers with: plant height (**A**), the length of the second basal internode (**B**), the no. of tillers (**C**), dry weight of culms (**D**), the no. of epidermal invaginations (**E**), culm wall thickness (**F**), the thickness of the sclerenchymal layer (**G**), the no. of inner vascular bundles (**H**), and the diameter of epidermal (**I**) and sclerenchymal cell (**J**).

SIM mapping revealed only one SNP associated with the diameter of the epidermal cell, located at the position of 6.68 cM on chromosome 4R (LOD > 3.0; Suppl. Fig.65A). Similar results were obtained with CIM scanning (Fig.42I), and the final model of one putative QTL for this trait (Suppl. Fig.65C) was established on chromosome 4R at the position of 6.68 cM (LOD = 3.01; additive effect: 0.983, dominance effect: 0.15), explaining 9.686% of the phenotypic variance (Fig.41, Table 14).

For the diameter of the sclerenchymal cell, the SIM scan revealed 20 SNPs associated with this trait (Suppl. Fig.65B), also located on 4R at positions of 49.3 – 53.32 cM, and the marker with the highest LOD score was chosen as a candidate QTL (at the position of 53.32 cM). CIM scan revealed similar results (Fig.42J) to the previous one, and the final model of QTL (Suppl. Fig.65D) was established on chromosome 4R at the position of 53.32 cM (LOD = 3.641; additive effect: 0.442, dominance effect: 1.533), explaining only 1.682% of the phenotypic variance (Fig.41, Table 14).

For the thickness of sclerenchymal cell wall, SIM scan revealed 6 SNPs associated with the trait (LOD > 3.0; Suppl. Fig.65E): 1 located on chromosome 1R (at the position of 13.6 cM), and 5 on 7R (at 43.1 - 44.0 cM). Nevertheless, CIM scan (Fig.43A) revealed only 2 SNPs on chromosome 1 R (31.0 – 32.7 cM) associated with the thickness of the sclerenchymal cell wall, and the final QTL model (Suppl. Fig.65G) was established on chromosome 1R at the position of 32.7 cM (LOD = 3.738; additive effect: 0.134, dominance effect: 0.035), explaining 10.738% of phenotypic variance (Fig.41, Table 14).

SIM scan revealed only one SNP at the position of 1.75 cM on chromosome 1R associated with the thickness of inner periclinal cell wall of the epidermis (LOD > 3.0; Suppl. Fig.65F). Nevertheless, Composite Interval Mapping (Fig.43B) increased the number of markers associated with this trait to 8 SNPs: 1 on chromosome 1R at the position of 1.75 cM and 7 on 5R (34.0 – 48.7 cM). The final model of QTL for this trait (Suppl. Fig.65H) was established on chromosome 1R at the position of 1.75 cM (LOD = 5.333; additive effect: 0.041, dominance effect: 0.124) and on chromosome 5R at the position of 48.25 cM (LOD = 3.737; additive effect: 0.063, dominance effect: 0.066), altogether explaining 11.102% of phenotypic variance (Fig.41, Table 14).

SIM scan allowed to find an association between the content of molybdenum and 7 SNPs located at 6.9 cM long region (8.8 – 15.7 cM) on chromosome 7R (Suppl. Fig.66A). The marker at the position of 13.27 cM was characterised by the highest LOD score and chosen as a candidate QTL for this trait. Similar results were obtained by CIM scanning (Fig.43C) and the final QTL model (Suppl. Fig.66C) was established on 7R at the position of 13.27 cM (LOD = 4.754; additive effect: 1.265, dominance effect: 0.817), which explained 13.301% of the phenotypic variance (Fig.41, Table 14).

14 SNPs located on chromosome 2R at positions of 59.8 – 60.9 cM were revealed by SIM scan to be associated with the content of nickel (Suppl. Fig.66B), and a SNP at the position of 59.84 cM was chosen as a candidate QTL for this trait. CIM scan gave same results as those obtained with SIM (Fig.43D), and QTL for the content of nickel in the basal internode (Suppl. Fig.66D) was established on 2R at the position of 59.84 cM (LOD = 3.05; additive effect: 0.011, dominance effect: 0.49), explaining only 0.01% of phenotypic variation (Fig.41, Table 14).

Another QTL, which could be detected, was associated with the content of copper in the basal internodes. SIM scan revealed 23 markers on chromosome 7R (16.9 – 74.7 cM), which were associated with this trait (Suppl. Fig.66E). CIM scan reduced the size of the region associated with that trait to 1.5 – 37.6 cM (90 SNPs on 7R chromosome; Fig.43E). The final QTL model for copper content (Suppl. Fig.66G) was established on 7R at the position of 12.80 cM (LOD = 5.962; additive effect: 1.305, dominance effect: 1.272), which explained 14.464% of the phenotypic variance (Fig.41, Table 14).

For the content of sulfur, SIM mapping revealed 3 SNPs associated with this trait, located on chromosome 4R at the position of 44.5 – 47.9 cM (LOD = 3.37; Suppl. Fig.66F), and CIM mapping revealed additional one SNP on 5R at the position of 84.79 cM (Fig.43F). The final QTL model for the content of sulfur (Suppl. Fig.66H) included one located on chromosome 4R at the position of 47.87 cM (LOD = 3.16; additive effect: 390.102, dominance effect: 1648.748) and one on 5R at the position of 84.79 cM (LOD = 3.0; additive effect: 303.571, dominance effect: 1577.704), and altogether explained only 1.35% of phenotypic variance (Fig.41, Table 14).

SIM mapping revealed only 3 SNP markers on chromosome 2R (30.1 – 33.7 cM) associated with the content of zinc (LOD > 3.0; Suppl. Fig.67A), from which one candidate QTL at the position of 33.69 cM was chosen. Nevertheless, CIM mapping revealed an additional marker associated with the trait on the 1R chromosome at the position of 40.39 cM (Fig.43G). These two markers were selected for the final model of QTL associated with the content of zinc (Suppl. Fig.67B): on chromosome 1R at the position of 40.39 cM (LOD = 3.037; additive effect: 17.566, dominance effect: 20.072), explaining 8.27% of the phenotypic variance, and on chromosome 2R at the position of 33.69 cM (LOD = 3.292; additive effect: 10.095, dominance effect: 27.204), explaining only 2.78% of the phenotypic variance (Fig.41, Table 14).
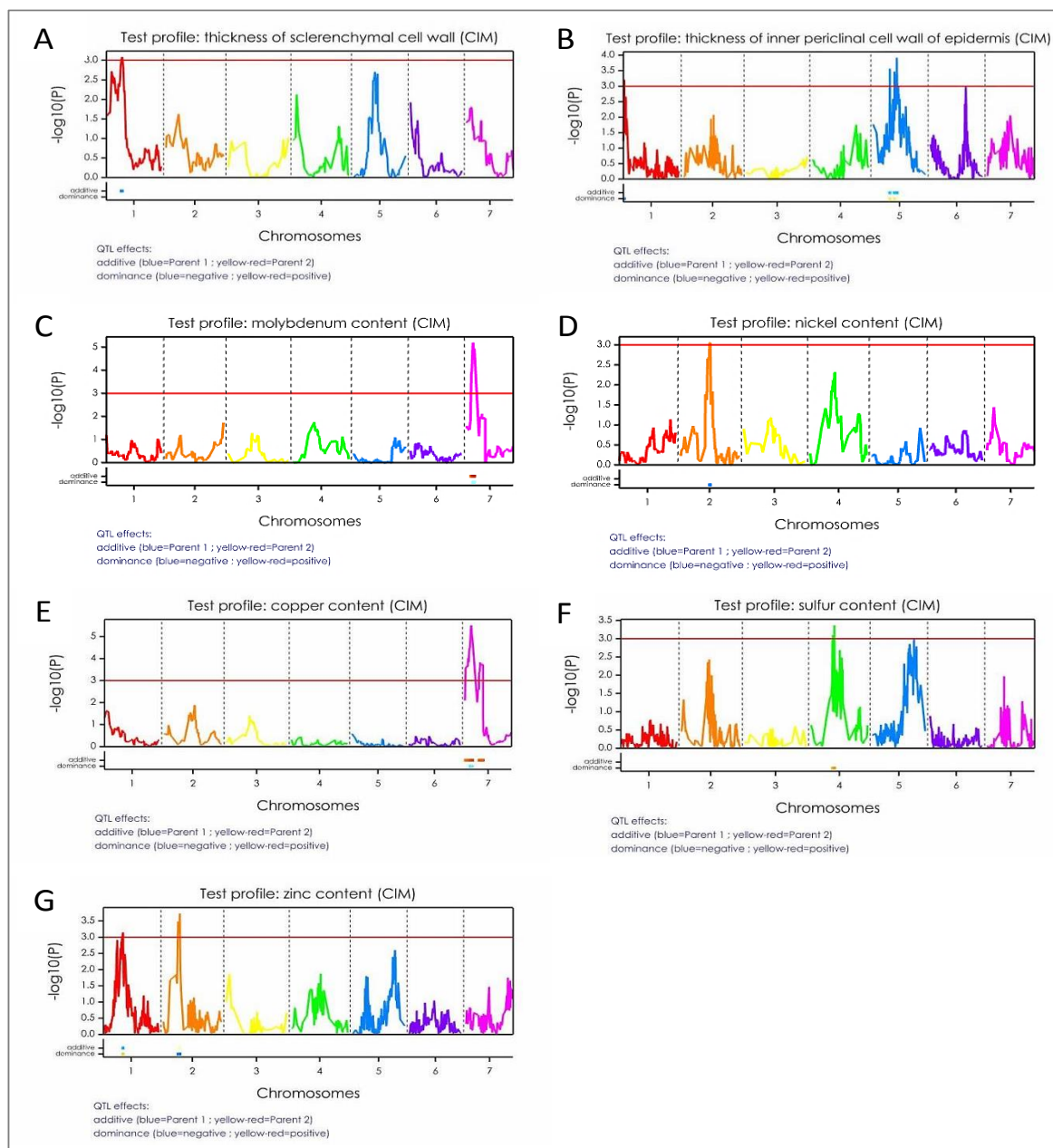
FIGURE 43 Genome-wide Composite Interval Mapping showing the association of mapped markers with: the thickness of sclerenchymal cell wall (**A**), the thickness of inner periclinal cell wall of epidermis (**B**), the content of molybdenum (**C**), the content of nickel (**D**), the content of copper (**E**), the content of sulfur (**F**), and the content of zinc (**G**).

4.5 | Development and validation of KASP markers

For 2 SNPs: 3596125 linked to the number of epidermal invaginations, the length of the second basal internode, dry weight of culms, and the number of tillers (chromosome 3R at 50.3 cM), and for 100074162 associated with culm wall thickness, the diameter

of epidermal and sclerenchymal cell, and the content of sulfur (chromosome 4R at 44.5 cM), the development of KASP markers was not successful (Fig.44C-D, Table 15). In the case of these two markers amplification failed or the fluorescence after the PCR reaction was not unequivocal to determine the allele.

For the SNP 5218584, located on the chromosome 1R at the position of 11.7 cM and associated with: the thickness of sclerenchymal cell wall and inner periclinal cell wall of the epidermis, the content of zinc, and plant height, the results were satisfactory and genotyping, except one line ('ms135'), was consistent with the data obtained by DArTseq (Fig.44A, Table 15).

KASP primers developed for the SNP 3353579, located on the chromosome 1R at 25 cM and linked to: the thickness of sclerenchymal cell wall and inner periclinal cell wall of the epidermis, the content of zinc, as well as plant height, enabled proper amplification, except one individual of 304/1 F_2 population (304/1-100; Fig.44B). The products accurately confirmed the genotypic data obtained by DArTseq (Table 15).

In the case of the SNP 3349542, located on the chromosome 7R at the position of 35.1 cM, associated with: the thickness of sclerenchymal layer and culm wall, the content of molybdenum and copper, as well as plant height, the results of the reaction were less consistent with the data obtained by DArTseq, with missing data for one individual of 304/1 F_2 population (304/1-13) and unlike allele for wildtype parental line (Fig.44E, Table 15).

TABLE 15 Genotyping by DArTseq and KASPs on parental lines and 14 individuals from 304/1 F_2 population.

ID SNP	Marker type	Line/ind.															
		ms135	R1124	304/1-1	304/1-2	304/1-13	304/1-18	304/1-21	304/1-22	304/1-25	304/1-28	304/1-37	304/1-38	304/1-47	304/1-48	304/1-68	304/1-100
5218584	DArT	0	1	0	0	1	2	0	2	2	2	0	1	1	2	2	2
	KASP	Y	C	T	T	C	Y	T	Y	Y	Y	T	C	C	Y	Y	Y
3353579	DArT	0	1	0	2	1	2	0	0	2	2	2	1	1	2	0	2
	KASP	T	C	T	Y	C	Y	T	T	Y	Y	Y	C	C	Y	T	-
3596125	DArT	1	0	2	1	1	2	0	2	0	2	2	2	0	2	1	0
	KASP	Y	Y	Y	Y	Y	Y	Y	Y	Y	Y	Y	Y	Y	Y	-	Y
100074162	DArT	1	0	2	2	2	0	1	2	2	2	1	0	2	2	1	0
	KASP	-	-	-	-	-	-	-	-	-	-	-	-	-	-	-	-
3349542	DArT	1	0	0	2	1	2	1	2	2	2	2	0	0	2	2	1
	KASP	C	Y	T	Y	-	Y	C	Y	Y	Y	Y	T	T	Y	Y	C
5224120	DArT	0	1	1	2	0	2	0	2	2	2	0	1	1	2	0	0
	KASP	G	A	A	R	G	R	G	R	R	R	R	A	A	R	G	G

FIGURE 44 KASP assays for: 5215854 (**A**), 3353579 (**B**), 3596125 (**C**), 100074162 (**D**), 3349542 (**E**), and 5224120 (**F**).

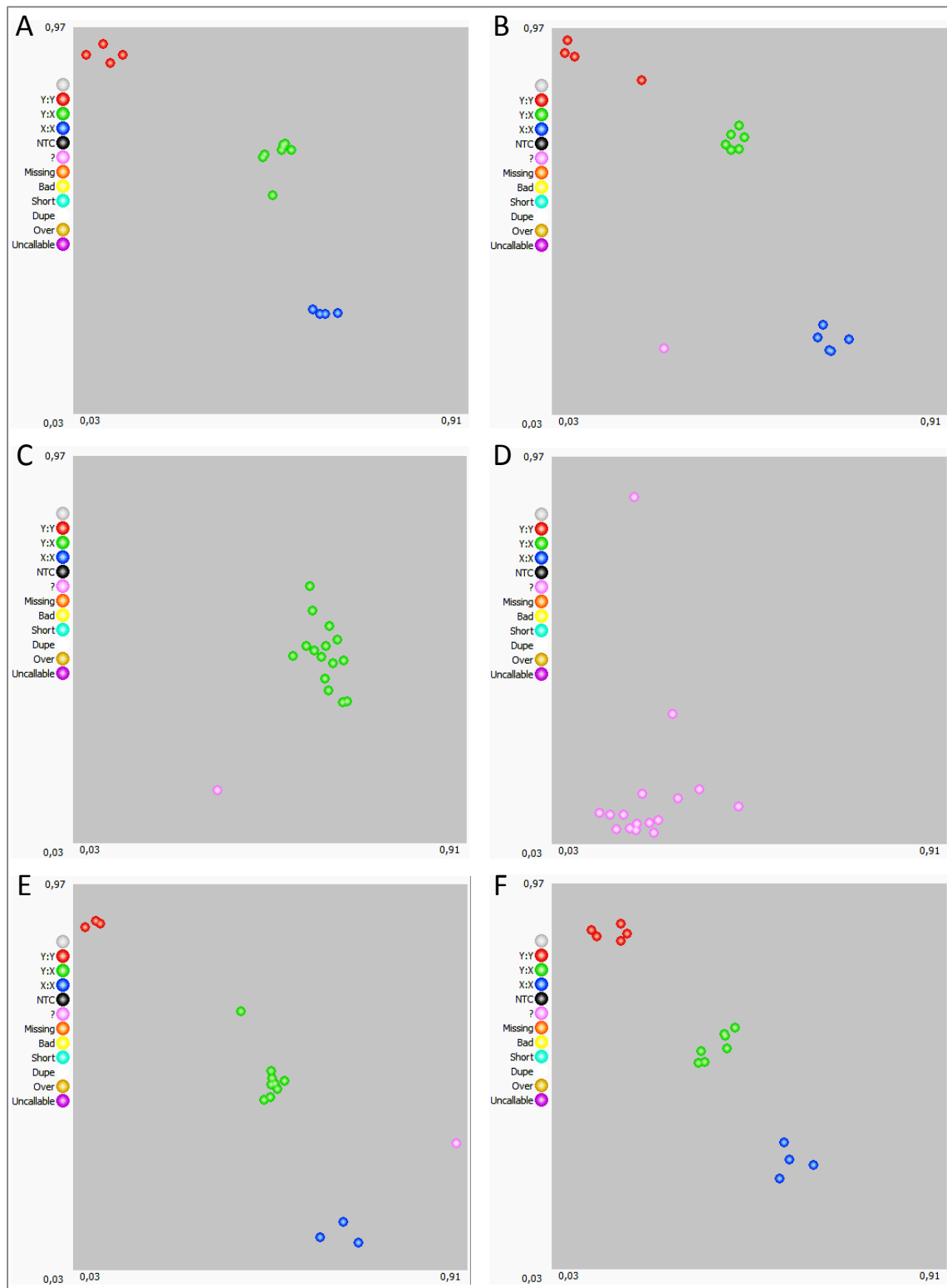Finally, near perfect match between genotypic data by DArTseq and KASP was obtained for the SNP 5224120, located on the chromosome 7R at the position of 43.2 cM, associated with: the thickness of the sclerenchymal layer and culm wall, the content of molybdenum and copper, and plant height, with only one unlike allele for the individual 304/1-37 (Fig.44F, Table 15).

5. Discussion

5.1 | Phenotypic traits determining lodging resistance

In this thesis, both parents and the 304/1 segregating F_2 population of the lodging resistant 'ms 135' rye line crossed with the lodging, but high yielding 'R 1124' line were phenotyped for morphological and anatomical traits. Additionally, the elemental analysis was performed on the basal internodes. The parental lines differed in morphology manifesting in plant height, the number of tillers per plant, the dry weight of culms and a single culm, and the diameter of the second internode. In order to reveal the anatomic characteristic of outstanding plant stability of 'ms 135' line, Scanning Electron (SEM), Transmission Electron (TEM), and Light Microscopy (LM) techniques were used in these studies. The results confirmed the morphological and anatomical importance of: the number of epidermal invaginations, the thickness of sclerenchymal tissue and sclerenchyma to diameter ratio, the number of vascular bundles, especially outer vascular bundles, the thickness of the sclerenchymal cell wall (CW) and inner periclinal CW of the epidermis, in mechanical stability of tillers. Moreover, the studies using Inductively Coupled Plasma Optical Emission Spectrometry confirmed the role of zinc and silicon in a complex trait of lodging resistance.

5.1.1 | External morphology and lodging resistance

The analysis of plant morphology revealed that the lodging resistant line, 'ms 135', is taller than the wildtype, 'R 1124'. It is well documented for *Triticum aestivum* that plant height correlates negatively with the basal internode breaking strength, suggesting semi-dwarf phenotype best contributing to lodging resistance in bread wheat (Atkins, 1938; Crook and Ennos, 1994; Pinthus, 1967; Sarker *et al.,* 2007). Short varieties also show better lodging resistance in barley (Murthy and Rao, 1980) and rye (Oehme, 1989). In most of the studies, lodging was so strongly correlated with plant height, that other morphological parameters influencing this phenomenon were hard to identify. Lodging is usually attributed to the increase in plant height most of the times. However, this is not always applicable, as in the case of wheat semi-dwarf varieties 'Baviacora' and 'Pastor' (Tripathi *et al.,* 2003). 'Baviacora' is a lodging tolerant variety (103 cm plant height) and on the contrary, 'Pastor' with similar height (101 cm), is prone to lodging, indicating that some of the genotypes are

lodging resistant, and some are susceptible, despite they both are semi-dwarf wheats (Tripathi *et al.*, 2003). Moreover, studies on ten rice cultivars and two near-isogenic lines revealed that plant height did not correlate with lodging resistance, measured in terms of pushing resistance, but instead is correlated with the diameter of basal internodes (Kashiwagi *et al.*, 2008). Short varieties and cultivars were favoured for many years, beginning with the 'Green Revolution', during which the *Rht* dwarfing alleles (*Rht-B1b* and *Rht-D1b*) were introduced into hexaploid bread wheat, making selecting for short varieties and cultivars easy. The *Rht* genes caused the reduced response to the gibberellic acid (GA; Gale and Youssefian, 1985; Keyes *et al.*, 1990), and biosynthesis and signal transduction pathway of auxin and GA was shown as a key to control plant stature and growth (Keyes *et al.*, 1990; Peng *et al.*, 1999; Monna *et al.*, 2002; Sasaki *et al.*, 2002; Spielmeyer *et al.*, 2002). Conversely, GA-overproduction or plant hypersensitivity to that hormone causes taller plant height and increases total biomass production, although it may decrease lodging resistance (Okuno *et al.*, 2014). Nevertheless, very short varieties can favour the epidemic spread of fungal diseases, thus increasing request for fungicide use (Keller *et al.*, 1999), which is not in line with ecological agriculture. Furthermore, cereal crops have recently been used as alternative energy sources, and therefore creating a lodging resistant variety with noteworthy height is of importance. Regarding biomass production, dwarfism is considered an unfavourable trait. The lodging resistant line used in this study is characterised by greater plant height than the wildtype, which opens possibilities to breed for a lodging resistant variety with a tall posture.

Brady (1934), Mulder (1954), and Verma *at al.* (2005) reported in oats, rye, and wheat the influence of the length of the basal internode on lodging resistance, comparable to the influence of plant height. The long and weak lower internodes have little resistance to bending, and therefore this trait was considered an important factor in causing a tendency to the lodging of the crop. In contrast to Verma's results, the 'ms 135' lodging resistant line, exhibited no significant differences in the length of the second basal internode compared to the wildtype, resulting in being less crucial for lodging resistance in this genotype. Nevertheless, this trait positively correlated in 304/1 F_2 population with plant height, but negatively with the number of tillers, indicating shading of the basal internodes not successful enough to significantly contribute to weak and long lower internodes.

The already mentioned wheat variety 'Baviacora' was recorded for lower lodging due to a low number of tillers per m^2 (413), compared to other semi-dwarf variety 'Pastor', which was characterised by a higher number of tillers per m^2 (482) and higher lodging risk (Tripathi *et al.*, 2003). It is also known in barley, that excessive tillering, when nitrogen was

available early in the growing season, results in smaller tiller survival rates and infertile tillers compete with the fertile tillers for light, water, and nutrients (Wych *et al.,* 1988; Baethgen *et al.,* 1995). The resulting thick canopies in wheat, barley, and oats favour the occurrence of lodging and foliar diseases (Pinthus, 1973). On the other hand, studies on ten rice cultivars and two near-isogenic lines shown no significant correlation between tiller number and lodging resistance, measured as pushing resistance (Kashiwagi *et al.,* 2008). Likewise, the analysed lodging resistant line 'ms 135' was characterised by a significantly higher number of tillers (16 ± 4.009), in comparison to the wildtype (3 ± 2.345), suggesting this trait of less importance for lodging resistance of 'ms 135'.

It is known for wheat and oats that the basal internode breaking strength is positively correlated with main shoot weight and stem weight per cm (Brady, 1934; Zuber *et al.,* 1999; Wang *et al.,* 2006; Sarker *et al.,* 2007; Kong *et al.,* 2013). Heavy basal internodes of sorghum could stand external force better than light stems (Esechie *et al.,* 1976). Mulder (1954) concluded that the tendency of a crop to lodging depends on the weight of higher internodes of the stems with leaves and heads in relation to the length of the culms, and the weight of lower internodes positively correlates with breaking strength of the straw. Similar results were obtained in the study on ten rice cultivars and two near-isogenic lines containing stem diameter QTL, where the weight of lower stem positively correlated with pushing resistance of the whole plant (Kashiwagi et al., 2008). In contrast, in barley and wheat, the main source of aboveground biomass production was associated with the number of tillers (Baethgen and Alley, 1989; Baethgen *et al.,* 1995), which can favour the occurrence of lodging. Additionally, Crook and Ennos (1994) reported that lodging resistance was associated with short and light stems in winter wheat. The explanation of this phenomenon can be that wind and gravity put more force to heavier stems and make heavy stems more susceptible to lodging. Thus it can be speculated that the heavy stems could counter the force of gravity. On the other hand, barley plants with low tiller densities produce heavier tillers, less prone to lodging (Baethgen et al., 1995). In this study, the lodging resistant line was not only characterised by higher dry weight of the culms but also higher mean dry weight of a single culm. Since the dry weight of culms correlated with the diameter of the internode, the number of vascular bundles, and thickness of stalk tissues and sclerenchymal layer, thus making aerial parts of the plant more stable, it confirms the importance of that factor for lodging resistance.

5.1.2 | Anatomy of tillers and lodging resistance

Lodging resistance was shown to be positively correlated with the diameter of two basal internodes in oats, common wheat, spelt, and rice (Brady, 1934; Atkins, 1938; Mulder, 1954;

Kelbert *et al.,* 2004; Wang *et al.,* 2006; Kashiwagi *et al.,* 2008; Packa *et al.,* 2015). In plants with comparable height, this trait can be crucial, as it was presented for two semi-dwarf varieties of wheat: 'Baviacora' - a tolerant variety with a greater diameter of three basal internodes, and 'Pastor' - lodging prone variety, with a lesser diameter of internodes (Tripathi *et al.,* 2003). In a segregating wheat x spelt population, Keller *et al.* (1999) found two QTL for lodging resistance corresponding with QTL for culm diameter. Moreover, a study on ten rice cultivars and two near-isogenic lines containing a single stem diameter QTL (*sdm8*; NIL114) and 4 stem diameter QTL (*sdm1, sdm7, sdm8, sdm12*; NIL28) revealed that larger stem diameter of those plants was correlating with a greater weight of lower stem and culm thickness, as well as greater stiffness of basal internodes (Kashiwagi *et al.,* 2008). Interestingly, in this study, the lodging resistant line was characterised by a smaller diameter of the second basal internode, compared to the wildtype, suggesting this trait less requisite for lodging resistance in the line 'ms 135'.

It is known that in *Triticum aestivum* and oats the basal internode breaking strength is positively correlated with its wall thickness and the width of mechanical tissue (Brady, 1934; Mulder, 1954; Tripathi *et al.,* 2003; Wang *et al.,* 2006; Sarker *et al.,* 2007; Kong *et al.,* 2013). Likewise, in studies on rice, thicker culm walls of basal internodes were associated with improved lodging resistance in two near-isogenic lines containing stem diameter QTL, indicating culm wall thickness QTL to be located close to stalk diameter QTL (Kashiwagi *et al.,* 2008). In contrast, the lodging resistant line used in this study was characterised by a smaller thickness of culm wall, in comparison to the wildtype, making this genotype quite extraordinary. On the other hand, the greater width of the sclerenchymal layer in lodging resistant line was supporting analyses done by Sarker *et al.* (2007), Kong *et al.* (2013), and studies on the *brittle stem* mutant in rye (Kubicka and Kubicki, 1981), confirming the importance of the thickness of the sclerenchymal layer for lodging resistance.

The number of vascular bundles is not only an essential factor for plant stability, but also for determining yield by controlling of assimilates partitioning to the developing spike. The correlations between lodging resistance and the number and size of vascular bundles in the transverse section have been investigated numerously in wheat, triticale, oats, and rye (Brady, 1934; Mulder, 1954; Khanna, 1991; Żebrowski, 1992; Zuber *et al.,* 1999; Wang *et al.,* 2006; Packa *et al.,* 2015). It is also worth to mention that in vascular tissues of leaf blades, leaf sheaths, and stems occurs silicification, which enhances the strength and rigidity of cell walls, thus enhances lodging resistance (Ma and Yamaji, 2006). Moreover, the outer periphery of the stalk of *brittle stalk2* (*bk2*) recessive mutant in maize, characterised by the brittleness of its all aerial organs, as well as inner part of the basal internode of *brittle stem* (*bs*) mutant in rye, had fewer vascular bundles in comparison

to the wildtype (Kubicka and Kubicki, 1981; Sindhu *et al.*, 2007), which supports findings of this project about their importance in mechanical stability of 'ms 135', the lodging resistant line.

The evidence in the literature of the influence of epidermal and sclerenchymal cells diameter on lodging resistance is meagre. Nevertheless, from cytomechanical studies on *Mesembryanthemum crystallinum,* using a tissue-cell pressure probe technique, it is known that cell geometry and dimensions decide about CW mechanical properties since CW elasticity depends on plant cell turgor and cell volume (Steudle and Zimmermann, 1977). In the mentioned study authors found a positive correlation between elastic modulus and cell diameter, and in the range of low volumes, there was a linear relationship between volume and elastic modulus (Steudle and Zimmermann, 1977). Cells with a larger diameter exhibit larger tension in the wall at given turgor pressure, hence their elastic modulus must be higher (Steudle and Zimmermann, 1977). In the case of study on 'Stabilstroh' genotype, no significant differences were found either in the diameter of epidermal or sclerenchymal cells, in comparison to the wildtype, suggesting this trait less crucial for the lodging resistance of 'ms 135'.

On the microscopic level, the critical factor responsible for mechanical stability and culm strength is the thickness of the CW, in particular, the secondary CW, which constitutes significantly to the skeletal structures of plant bodies and determines their mechanical strength (Mulder, 1954; Cosgrove, 2005; Aohara *et al.,* 2009). The lodging resistant line was characterised by an almost twice thicker CW of the sclerenchyma and more than half times thicker inner periclinal CW of the epidermis, in comparison to the wildtype, confirming observations by previous authors about the role of this trait in lodging resistance. Importance of the thickness of the secondary CW for plant stability emphasises the *brittle stem* (*bs*) mutant in rye, which recessive gene shows the pleiotropic effect on plant and causes fragility of roots, heads, and leaves, and depresses the general viability of the mutant (Kubicka and Kubicki, 1981). It was shown in anatomical studies that *bs* causes disturbances in the normal lignification of the sclerenchymal and epidermal cells, both in shoots and roots, where the secondary CW was significantly thinner in comparison to the wildtype (Kubicka and Kubicki, 1981). A layer of thick-walled, lignified sclerenchyma on the periphery of the stem significantly increases mechanical strength and lodging resistance (Mulder, 1954; Jellum, 1962; Cosgrove, 2005; Kong *et al.,* 2013), supporting the observations for 'Stabilstroh', the lodging resistant line. Not only the thickness of the CW has a crucial role in plant stability, but also its composition and dynamics: xyloglucan – cellulose interactions are important determinants of the mechanical and growth properties of the CW (Cosgrove, 2005). Another evidence

for the importance of CW components interactions for maintaining organ flexibility and plant stability was presented by Sindhu *et al.,* (2007) in studies on maize *brittle stalk2* (*bs2*) recessive mutant, which aerial parts are fragile and easy to break. This mutant is characterised by cellulose content lowered by 40% in the mature zones and by the increase in the content of xylans, phenolic ester, and saponifiable hydroxycinnamates, in comparison to the wildtype (Sindhu *et al.,* 2007). Additionally, *bs2* is characterised by thinner secondary CW of scleroids surrounding vascular bundles lying under the epidermis (Sindhu *et al.,* 2007). The brittleness of *bs2* mutant does not result from loss of tensile strength, but from loss in flexibility of the CW by an aberrant lignin polymerisation, caused by lack of proper cellulosic matrix in the secondary CW, since the product of *Bk2* gene functions in a pattering of lignin-cellulose interactions maintaining CW flexibility (Sindhu *et al.,* 2007). Hydroxyl radical (•OH) harnessed by growing cells can also modify CW physical properties since it loosens them by nonenzymatically removing a hydrogen atom from polysaccharides (Fry *et al.,* 2002). It was shown that this endogenous •OH could be produced from the superoxide anion and hydrogen peroxide by copper ions that are bound to CW components or peroxidases, which are also deciding about CW stability (Fry *et al.,* 2002; Cosgrove, 2005). Interestingly, •OH treatment experiments led to wall breakage (Cosgrove, 2005), suggesting this process has to be carefully regulated to target hydroxyl radicals reactivity to xyloglucan and other polysaccharides and to remain integrity and elastic properties of the CW. Finally, one must not forget about the process of silicification of sclerenchymal and epidermal CW (Yoshida *et al.,* 1962), which is also contributing to lodging resistance of the plant (Ma and Yamaji, 2006; Kashiwagi *et al.,* 2008).

5.1.3 | Elements and lodging resistance

Although iron, molybdenum, and nickel are necessary for biomass production being involved in processes like the formation of photosynthetic apparatus, respiration, photosynthesis, hydrogen metabolism, nitrogen fixation, and nitrate reduction (Raven *et al.* 1999; Curie and Briat, 2003; Bernal *et al.,* 2006; Ahmad and Ashraf, 2011; Mendel and Kruse, 2012), in this study both parental lines were characterised by a similar content of those elements in the basal internodes, implying them less crucial for biomass production and lodging resistance of 'ms 135' parental line. It is worth to mention that all those elements content has to be precisely regulated, since their deficiency may be lethal for a plant causing symptoms such as chlorosis, induction of senescence, and the reduction of plant growth and crop yields (Curie and Briat, 2003; Ahmad and Ashraf, 2011; Mendel and Kruse, 2012). On the other hand, their excess accumulation

results in toxicity symptoms (Halliwell and Gutteridge, 1992; Ahmad and Ashraf, 2011; Mendel and Kruse, 2012). Nevertheless, precaution has to be taken about the thickness of the secondary CWs in 'ms 135' parental line, which contributes most to the dry mass of the internode and may bias the final content of the element present in the cell body.

Boron and calcium ions have been termed as apoplastic elements, not only because of their localisation in the CW but also because of their contribution to the integrity of the CW through binding to pectic polysaccharides (Kouchi and Kumazawa, 1976; Gupta, 1979; Dugger, 1983; Hu and Brown, 1994; Matoh and Kobayashi, 1998; Cosgrove, 2005). The linkage of pectins involving boron and calcium are essential crosslinking mechanisms in the plant CW (Dugger, 1983; Hu and Brown, 1994; Matoh and Kobayashi, 1998; Cosgrove, 2005). Boron in the CW forms a complex with rhamno-galacturonan II through borate esters necessary for normal wall formation, as well as for the control of wall porosity and its thickness (Hu and Brown, 1994; Ishii and Matsunaga, 1996; Matoh and Kobayashi, 1998; Cosgrove, 2005). Moreover, calcium ions are also necessary to form this complex, cross-linking homogalacturonans in the middle lamella and other CW layers through ionic and coordinate bonds, necessary for CW flexibility and stabilization of those complexes by gel formation when growth ceases (Inanaga and Okasaka, 1995; Matoh and Kobayashi, 1998; Cosgrove, 2005). On the other hand, a considerable amount of calcium can be found in the lignin fraction of the CW of mature leaves (Ito and Fujiwara, 1968). Calcium is also involved in the control of acidic growth, ion exchange properties, and the activities of wall enzymes (Demarty et al., 1984), as well as for the signal transduction as a secondary messenger (Matoh and Kobayashi, 1998). Interestingly, there were no statistically significant differences in the content of boron between wildtype and lodging resistant line (16.15 ± 8.259 µg/g and 13.15 ± 5.301 µg/g, respectively). In the case of the content of calcium, the wildtype was characterised by its higher content in dry weight of basal internodes (14,686 ± 4,245 µg/g), in comparison to the lodging resistant genotype (4,835 ± 2,460 µg/g). However, it has to be mentioned that pectins building complexes with these elements are mostly present in the primary CW and middle lamella (Knox et al., 1990; Freshour et al., 1996; Williams et al., 1996; Matoh and Kobayashi, 1998). Since the lodging resistant line was characterised by a thicker secondary CW, the content of boron and calcium per g of dry weight could be affected by a higher ratio of secondary to primary CW thickness in 'ms 135'.

The mechanical strength of basal internodes of phosphate-deficient barley was almost twice higher than control plants (Tubbs, 1930). Likewise, Mulder (1954) observed phosphorus-deficient plants lodged less severely than those supplied with phosphate, although did not observe any particular effect of phosphorus supply on the standing

capacity of oats and wheat. Moreover, the yields of phosphorus-deficient wheat and oats were approximately 30 - 60% of the yields of plants treated with adequate phosphorus. On the other hand, high levels of bioavailable phosphorus induced zinc and copper deficiency (Spencer, 1960; Bingham, 1963; Stuckenholtz *et al.,* 1966). The inactivated iron by decreased plant capacity to absorb and hold iron in a soluble mobile form as phosphorus tissue content increases leads to precipitation of iron phosphate on or in the roots (Biddulph and Woodbridge, 1952; Watanabe *et al.,* 1965). Nevertheless, the content of phosphorus in two parental lines was similar, implying this element of less importance for 'Stabilstroh' plant stability.

Sodium also seems to be of less importance for the lodging resistant genotype. The content of this element in the basal internodes was comparable between two parental lines; reaching mean values of 3,142 and 2,923 µg/g in 'ms 135' and 'R1124' respectively. Moreover, literature studies show sodium less essential for plant growth and development, except C4 grasses, which require sodium for the uptake of pyruvate into chloroplasts by Na^+-pyruvate cotransporter, which function is mediated by an H^+ coupled pyruvate carrier in other plants (Furumoto *et al.,* 2011). Nevertheless, Na^+ can be beneficial for the C3 plants, especially during K^+ deficiency, and for salt-tolerant plants, it can promote growth (Amtmann and Sanders, 1999; Subbarao *et al.,* 2003). On the other hand excess of sodium in the soil, especially present as sodium chloride, lowers the water potential and creates at first osmotic stress, and afterwards increases cellular ion contents negatively affecting cellular biochemistry (Maathuis, 2013). The effectiveness of sodium uptake in both parental lines in this study seems comparable and conserved between these two rye genotypes.

Copper is involved in many physiological processes during plant growth and development (Bernal *et al.,* 2006; Burkhead *et al.,* 2009; Printz *et al.,* 2016). Its deficiency causes growth defects, such as sinuous stems and branches (Fry *et al.,* 2002), decreased growth rate, chlorosis of young leaves, damage to the apical meristems, as well as insufficient water transport caused by a decrease in CW formation and lignification in several tissues, including xylem tissue (Marschner, 1995; Burkhead *et al.,* 2009). Yet at the concentrations above those required for optimal growth, it interferes with important cellular processes, such as photosynthesis (it targets especially photosystem), and respiration, inhibiting plant growth (Marschner, 1995; Bernal *et al.,* 2006; Burkhead at al., 2009). Copper is an essential redox-active transition metal involved in photosynthetic electron transport, mitochondrial respiration, CW metabolism, scavenging of oxidative stress, response to pathogens, and hormone signalling, as it is involved in the perception of ethylene (Marschner, 1995; Yruela, 2005; Bernal *et al.,* 2006; Burkhead

et al., 2009; Jung *et al.,* 2014; Printz *et al.,* 2016). The major sites of copper accumulation in plants are: the chloroplast (the most abundant Cu protein is plastocyanin, a photosynthesis-related protein involved in the transfer of electrons from cytochrome f to P700+), the vacuole, the cytoplasm and the CW (Bernal *et al.,* 2006; Printz *et al.,* 2016). In the CW copper (II) complexed with CW polymers can be reduced to copper (I) by apoplastic electron donors, such as ascorbate and superoxide, and then undergo a reaction with apoplastic hydrogen peroxide to generate hydroxyl radicals (Fry *et al.,* 2002). These can cause non-enzymatic scission of CW polysaccharides, resulting in loosening of the CW and solubilising of pectins (Fry *et al.,* 2002). Copper is also present in enzymes, such as laccases, which are responsible for the metabolism of phenolic compounds like anthocyanins and lignins (Burkhead *et al.,* 2009; Tomková *et al.,* 2012), contributing to CW remodelling during lignification, although the effect on lignin, cellulose, hemicellulose, and acetyl contents of the CW was only observed in severely-deficient plants (Robson *et al.*, 1981). It is known that plants thoroughly regulate copper homeostasis to prevent its deficiency and avoid the toxicity by transcriptional control of genes encoding COPT proteins involved in its uptake, trafficking, and tissue partitioning (Burkhead *et al.,* 2009; Jung *et al.,* 2014; Printz *et al.,* 2016). Additionally, copper can also be relocated in the cell among Cu requiring enzymes (Burkhead *et al.,* 2009; Jung *et al.,* 2014; Printz *et al.,* 2016). Both parental lines had comparable copper content in the internodes to data observed for wheat, where stems were characterised by 3.7 ppm of this element (Hooper and Davies, 1968). Moreover, 4.554 µg/g (± 2.29) was enough for the lodging resistant genotype to develop a thicker and more lignified CW than the other parental line, which interestingly was characterised by a higher content of copper (8.211 ± 3.406 µg/g), suggesting more efficient process of lignification in 'ms 135' parental line. Considering the fact that rye is the least sensitive to Cu deficiency among other cereal crops (Solberg *et al.,* 1999; Jung *et al.,* 2014), the results obtained in this study suggest that this element can play a smaller role in the lodging resistance of 'ms 135'. Nonetheless, one should not forget about the effect of a thicker secondary CW on the content of elements in 'ms 135', which could be verified by energy-dispersive X-ray spectroscopy.

The mechanical strength of basal internodes of potassium deficient barley was more than twice lower than control plants (Tubbs, 1930). The loss of mechanical strength of potassium deficient plants was due to the reduced thickness of the internode wall and reduced lignifications of the CW (Tubbs, 1930). Same results were shown for rye, wheat, and oats, where potassium deficiency caused brittleness of all internodes of stems, as well as reduction of the thickness of lignified cell walls (Mulder, 1954). On the other hand, the lodging resistant sorghums contained lower stalk potassium (Esechie *et al.,* 1976),

which is in line with data obtained in this study for the lodging resistant line containing 25% less of this element in the basal internodes in comparison to the wildtype.

Magnesium plays a role in photosynthesis as a central atom in the tetrapyrrole ring of chlorophyll a and b molecules (Wilkinson *et al.*, 1990). It is also involved in the regulation of cell proliferation, the formation of the mitotic spindle and cytokinesis (Maier, 2013), as well as in a wide variety of biochemical reactions activating a number of enzymes (Wolf and Trapani, 2008), and is required for the stability of ribosomal particles (Wilkinson *et al.*, 1990). The presence of magnesium ions in the CW makes it more extensible due to ion exchange with calcium and changes of stereochemical properties of pectins (Morikawa and Senda, 1974; Nakajima *et al.*, 1981). In the case of wildtype, magnesium was more abundantly distributed in comparison to the lodging resistant line, suggesting this element not be responsible for lodging resistance in 'ms 135', or similar to other ions its content was biased by the thickness of the secondary CW.

Manganese is necessary for the metabolism of organic acids, activates the reduction of nitrate and hydroxylamine to ammonia, plays a role in enzymes involved in respiration and enzyme synthesis, activates enzyme reactions such as oxidation/reduction and hydrolysis, and has a direct influence on sunlight conversion in the chloroplast (Hakala *et al.*, 2006; Alloway, 2008; Hebbern *et al.*, 2009). Manganese deficiency often occurs on sandy soils (Alloway, 2008; Hebbern *et al.*, 2009), which rye has no problem to grow on, suggesting a strategy to overcome those adverse effects. Nevertheless, the lodging resistant line was characterised by a significantly lower content of this element in the basal internodes in comparison to 'R 1124', suggesting either the lesser role of manganese on lodging resistance of 'ms 135', or again the dilution factor of the secondary CW influences its content in the basal internodes.

Sulfur was another element, which was less abundant in the lodging resistant line, what can be explained by the effect of a thick secondary CW of sclerenchymal and epidermal cells upon the dry weight of the internode. Sulfur, as an integral part of cysteine and methionine, is required for protein synthesis in the cell, and additionally is present in a variety of metabolites (Leustek and Saito, 1999). That is why sulfur deficient plants have severely affected photosynthetic apparatus, lowered chlorophyll and Rubisco content, and overall generate lower yield and biomass (Yoshida and Chaudhry, 1979; Lunde *et al.*, 2008). It can be concluded that both parental lines, having sufficient access to this element, accumulated it in the amount adequate for their biomass production.

The lodging resistant line was characterised by a significantly higher content of zinc in the basal internodes in comparison to the wildtype. It is known that zinc is necessary for dimerization of cellulose synthase (CESA), required for further assembly into hexamers

in the plasma membrane of the CESA subunits, involving oxidatively reversible disulphide bond formation between cysteines in the N-terminal zinc finger region in CESA, which is necessary for synthesis of cellulose microfibrils (Kurek *et al.,* 2002; Cosgrove, 2005). The undesirable effects of zinc deficiency appear mainly in the meristematic tissues (Broadley *et al.,* 2007), since dividing cells are in great need of zinc, not only for dimerisation of CESA, but also for protein synthesis (Kitagishi and Obata, 1986) and for the activity of many enzymes and processes, like the formation of auxin, which could explain the outstanding plant height of 'ms 135'. The results obtained for the lodging resistant line also suggest a more efficient mechanism of uptake or/and transport of zinc ions required for biomass production in 'Stabilstroh'.

Silicon in grasses is a quantitatively major inorganic constituent, and it is present in amounts equivalent to macronutrient elements, such as calcium, magnesium, and phosphorus, although it is considered as 'quasi-essential' for plants (Epstein, 1994; Epstein, 1999). Likewise, the internodes of two parental lines in this study showed its abundance in the basal internodes (4,903 ± 1,803 µg/g for 'R 1124' and 6,960 ± 1,805 µg/g for 'ms 135'). The function of silicon is to enhance resistance of plants to various biotic and abiotic stresses, including lodging, drought, UV radiation, heat, cold, and salt stress (Epstein, 1994; Liang *et al.,* 1994; Epstein, 1999; Ma and Yamaji, 2006; Waseem *et al.,* 2016). This element plays a significant role in plant growth and plant mechanical strength (Epstein, 1994). It is also known that rice and wheat plants grown on soils rich with bio-available silicon (in the form of H_4SiO_4) are characterised by markedly increased yield, spike number, filled grain percentage, and the grain/shoot ratio, compared to the control (Liang *et al.,* 1994). Addition of silicon not only significantly increases the rigidity of rice stalk, which is remarkably higher at a lower dose of nitrogen (Idris *et al.,* 1975), but also significantly increases its root weight (Vaculík *et al.,* 2012). In grasses, silicon is an essential component, which strengthens the CW and enhances its rigidity, especially of epidermal cells (Rafi and Epstein, 1997; Neumann, 2003; Ma and Yamaji, 2006; Ma and Yamaji, 2008) and vascular bundles (Ma and Yamaji, 2006). Moreover, in rice, the evidence was presented that silicon is involved in Si-aromatic ring associations between lignin and carbohydrates (Inanaga and Okasaka, 1995). 'ms 135', the lodging resistant genotype, accumulated significantly higher amounts of silicon in comparison to the wild-type, indicating its role in the resistance to lodging. In addition, silicon promotes plant growth, as it was shown for rice (Ma and Takahashi, 1990), what could also explain the impressive plant height of lodging resistant line.

5.2| Development of a genetic map

For QTL mapping of the traits described in the paragraph above, a linkage map was constructed based on 129 F_2 individuals to find out what was the genetic background of the lodging resistance of 'Stabilstroh' spontaneous mutant. Unfortunately, two parental lines were characterised by low polymorphism of SSR markers. Also, the wildtype parent was characterised by unfixed alleles. In the end, the number of polymorphic and segregating markers was not sufficient (in total 45 polymorphic and segregating markers; polymorphism of 16.73 %) for the effective QTL mapping, what forced the change of the genotyping strategy. Other authors also noted that the number of SSR markers was limited in rye, naming it the main cause why genetic studies in rye are not far advanced (Miedaner *et al.*, 2012). Fortunately, a relatively new technique, DArT (Diversity Array Technology), was available. DArTseq markers are a fast and relatively cheap genotyping platform, which profiles the whole genome and effectively target gene space in the large, complex, and repetitive rye genome (Gawroński *et al.*, 2016). Moreover, DArTs represent one of GBS technology and are the first available high-throughput method of genotyping for *Secale cereale* (Jaccoud *et al.*, 2001; Bolibok-Brągoszewska *et al.*, 2009; Milczarski *et al.*, 2011). Till now DArT markers have found a broad application, being used in rye to investigate the genetic diversity (Bolibok-Brągoszewska *et al.*, 2009), create a consensus linkage map (Milczarski *et al.,* 2011), investigate triticale (Badea *et al.,* 2011; Tyrka *et al.*, 2011), develop tightly linked markers for the restoration of male fertility (Stojalowski *et al.,* 2011). The multi-purpose usage and cheap and fast genotyping platform made a choice to genotype the population with DArT markers easy.

8,090 polymorphic and segregating DArT markers and SNPs gave a great possibility to profile the whole genome. The genetic map of 7 chromosomes was constructed basing on 1,041 markers to obtain a map, with an average distance between the markers of 0.75 cM, making the current map one of the most saturated rye maps up to date (in comparison: the map published by Ma *et al.,* 2001 with the average distance of 3.96 cM; by Bolibok-Brągoszewska *et al.,* 2009 with 2.68 cM, by Milczarski *et al.,* 2011 with 1.1 cM, and just recently published map by Milczarski *et al.,* 2016 with 0.47 cM; Table 16). When the map developed in this study is compared with one of the earliest linkage maps of rye (Senft and Wricke, 1996), it can be seen that there is a 10-fold increase of the number of mapped markers, while the estimated map length stays roughly the same. This comparison also illustrates that there is no clear relationship between the number of markers mapped and the total map length. What is interesting to notice though, is that maps created based on RFLP or SSR markers hardly contain more than 500

mapped markers, while the most recent maps based on DArT markers show easily 1000 markers mapped. However, the two DArT maps by Bolibok-Brągoszewska *et al.* (2009) and by Milczarski *et al.* (2016) also show a considerable increase in the map length, which is unexpected, since the other maps have a map length between 700 and 1000cM, which comes down to an individual chromosome length between 100 and 140cM. The population size of the studies are roughly comparable with the present study (ranging from 100 to 200 individuals), thus an additional number of recombinations by large population size is not the explanation of the extraordinary long maps of Bolibok-Bragoszewska *et al.* (2009) and Milczarski *et al.* (2016). However, the position of 279 DArTseq markers in the linkage map developed in this study was corresponding with all the positions present on the high-density map presented by Milczarski *et al.* (2016) for rye. Precisely, the position of 33, 29, 24, 27, 50, 39, and 77 markers corresponded to the positions on 1R, 2R, 3R, 4R, 5R, 6R, and 7R, respectively, described by Milczarski *et al.* (2016). The positions of the rest of DArTseq markers were unique and anchored for the first time on rye chromosomes, thus can be useful for the further studies on rye genome. Moreover, the ability to use DArT markers in rye enabled researchers to map more markers, and the map developed in this study can provide rye breeders and researchers more polymorphic markers in their genetic region of interest.

TABLE 16 Overview of genetic linkage maps of rye for 7 chromosomes found in the literature.

Authors	Publication year	Main marker type	No. of markers	Total length [cM]	Density [N marker/cM]	Av. distance between markers [cM]
Devos *et al.*	1993	RFLP	156			
Senft and Wricke	1996	RFLP	127	760	0.16	5.98
Korzun *et al.*	1998	RFLP	91			
Börner and Korzun	1998	RFLP	413			
Korzun *et al.*	2001	RFLP	183	1063.4	0.17	5.81
Ma *et al.*	2001	RFLP	184	727.3	0.25	3.95
Bednarek *et al.*	2003	RFLP	460	1386	0.33	3.01
Bolibok *et al.*	2007	SSR	99	979.2	0.1	9.89
Bolibok-Brągoszewska *et al.*	2009	DArT	1181	3144.6	0.37	2.66
Milczarski *et al.*	2016	DArT	3397	1593	2.13	0.47
Hackauf *et al.*	2017	DArT	912	964.9	0.95	1.06
A.Muszynska PhD thesis	2018	DArT	1041	783.8	1.33	0.75

5.3| QTL mapping of lodging resistance related traits, development of KASP markers for MAS

The obtained linkage map was subsequently used for QTL mapping for the analysed traits. A single marker regression mapping, followed by a composite interval mapping, allowed

to find QTL associated with: plant height, the length of the second basal internode, the number of tillers, dry weight of culms, the number of epidermal invaginations, the thickness of culm wall and sclerenchymal layer, the number of inner vascular bundles, the diameter of epidermal and sclerenchymal cell, the thickness of sclerenchymal CW and inner periclinal CW of epidermis, the content of molybdenum, nickel, copper, sulfur, and zinc.

The QTL found in this study are mainly novel, primarily due to the fact that rye was lagging far behind other crops in terms of genomic resources. Up to date, many QTL studies in rye were focused mostly on plant height and dwarfing genes (Börner and Korzun, 1998; Miedaner *et al.*, 2012). In the current study, traits on the cellular level were considered, and subsequently many of these QTL were not described before in rye or other cereals. There are just a few reports about QTL for morphological and anatomical traits affecting lodging resistance in rye. One study on morphological traits associated with lodging resistance in rye was presented by Milczarski (2008). In this work, one of two QTL for the length of the second basal internode was localised on the long arm of chromosome 3R, which corresponds to findings in '304/1' F_2 population, but interestingly, this QTL is not overlapping with the two QTL on 1R and 7R found for plant height in this study. It is known that the length of the internodes is determining the plant height (Yang and Hwa, 2008). However, it does not appear so in the case of the studied population. Also, in contrast to tef, where three QTL were found for the length of the basal internode, (Yu *et al.*, 2007), and rice, where two QTL were found for total internode length (Nagai *et al.*, 2014), the length of the basal internode was determined by only one QTL. Additionally, Milczarski (2008) had found two QTL responsible for plant height localised on 7R, which is also in line with data obtained in this project, where one of QTL responsible for this trait was located on 7R. According to the literature studies, QTL for plant height in rye were previously detected on all seven chromosomes, which points to a quantitative trait (Schlegel *at al.,* 1998; Börner *at al.*, 2000; Falke *et al.,* 2009a; Falke *at al.,* 2009b; Miedaner et al., 2011; Miedaner *et al.,* 2012).

In contrast to the previous studies of single dwarfing genes responsible for a difference in plant height, and the current study, which only reveals two QTL, Miedaner *et al.,* (2012) had used a population, where plant height was a very polygenic trait and found additional QTL for plant height on chromosome 2R, 3R, 4R, 5R, and 6R. Nevertheless, the location of previously described dwarfing loci on linkage maps (Table 1) can be a good starting point for the identification of genomic regions, which control plant height in presented studies. The detected QTL on the chromosome 1R may correspond to the location of *dw4*, a recessive dwarfing gene described by Melz (1989; reviewed by

Börner *at al.,* 1996), or a recently identified by Stojałowski *et al.* (2015) *Ddw3* dominant gene. Additionally, on the chromosome 7R a dominant dwarfing gene *Ddw2* was described in the literature (reviewed by Börner *at al.,* 1996), as well as recessive *dw1*, *ct1*, and *ct3* dwarfing genes, which position may be corresponding to another QTL for plant height obtained in this study.

Tillering is not only crucial for biomass production and lodging resistance, but also it is a crucial agronomic trait, since it determines the number of spikes, and thus grain yield (Donald, 1968; Hussien *et al.,* 2014). Effective tiller number is a fundamental trait for crop yield and a high-quality variety can be created by reducing the number of ineffective tillers and increasing the rate of effective tillers, as unproductive tillers consume nutrients and can lead to a decreased grain production (Donald, 1968; Li *et al.,* 2010; Hussien *et al.,* 2014). Plant shoot architecture is based upon the activity of the shoot apical meristems and axillary meristems (Sussex, 1989; Wang and Li, 2006), and key roles in the regulation of branching play auxin, cytokinins, strigolactones, and brassinosteroids (Kebrom *et al.,* 2013; Hussien *et al.,* 2014). The primary tillers develop from axillary meristems in leaf axils of the shoot apical meristem, and secondary tillers develop from axillary meristems in the axils of primary tillers (Counce *at al.,* 1996). The finding of only one QTL is in contrast to rice, barley, and wheat, where numerous QTL have been found for the number of tillers (Yan *et al.,* 1998; Wu *et al.,* 1999; Huang *et al.,* 2003; Li *et al.,* 2010; Naruoka *et al.,* 2011; Honsdorf *et al.,* 2014). This possibly points to the presence of a strong pleiotropic gene or of a group of related genes on 3R that mask weaker effects on other linkage groups.

Nevertheless, in wheat Shah *et al.* (1999) mapped a significant QTL for tillering explaining 19.4% of phenotypic variation on the chromosome 3A, which may correspond to the position revealed in this study. In advanced backcross QTL (AB-QTL) analysis of a cross of a German winter wheat cultivar 'Prinz' and a synthetic hexaploid wheat produced from the cross between durum wheat (*Triticum turgidum* L.) and *Triticum tauschii,* Huang *et al.* (2003) found 8 QTL responsible for tiller number/m^2, among which one QTL was located on the chromosome 3B. In later studies on wheat, Kuraparthy *et al.* (2007) located tiller inhibition gene (*tin3*) on 3A and Li *et al.* (2010) found multiple QTL responsible for tillering, where only two QTL: one positioned on chromosome 3A and one on 5A, could be detected under different environments and in different populations. In barley two major QTL, explaining 30.6% and 18.4% of phenotypic variation, were mapped on 3H (Buck-Sorlin, 2002), known to be corresponding to rye chromosome 3R (Martis *et al.,* 2013), and the first QTL was associated by the author with the *low number of tillers1* gene in barley (*Int1*). Other genes responsible for tiller number in barley located on the chromosome 3H were: *als1* (*absent lower laterals1*), *uniculme4* (*cul4*), *semibrachytic*

(*uzu1*), *granum-a1* (*gra-a1*), and *semidwarf1/denso* (*sdw1/denso*), which mutants, except of the latter two genes, are characterized by reduced tillering (Babb and Muehlbauer, 2003; Chono *et al.*, 2003; Rossini *et al.*, 2006; Dabbert *et al.*, 2009; Dabbert *et al.*, 2010; Jia *et al.*, 2011). It is known that the *Uzu* gene encodes a putative brassinosteroid receptor HvBRI1, indicating its role not only in tillering but also in the regulation of stem elongation (Chono *et al.*, 2003), which could explain the overlapping position of the QTL found for the length of the basal internode and the number of tillers on chromosome 3R. Moreover, the *semidwarf1/denso* dwarfing gene mapped on 3H has a pleiotropic effect on tillering in barley (Jia *et al.*, 2011). Additionally, in a previous study on barley, QTL for the number of tillers and plant dry weight colocalised (Honsdorf *et al.*, 2014), which is in line with data obtained in this study and also agrees with the correlations found between those traits in the F_2 population. In wheat, a QTL for the number of tillers was found to be linked to a late-flowering allele (Kato *et al.*, 2000). Although in sugarcane (Remison and Akinleye, 1978), earliness is not correlating with lodging, it would still be interesting to examine the correlation in rye. It is not easy and straightforward to figure out which gene or QTL corresponds to the QTL for tillering found in this study. Therefore further research is required to fine map the exact location of the tillering QTL and unreveal the genomic function.

As it was mentioned before, in the same interval on chromosome 3R also a QTL for dry weight of culms was found. In previous studies on F_3 plants originating from two mapping populations of rye, Korzun *et al.* (2001) found two QTL responsible for straw yield: one localised on chromosome 5R, and one on 6R. In rice and barley, 4 QTL on 3 different chromosomes were found for above-ground biomass (Zhang *et al.*, 2004; Honsdorf *et al.*, 2014). One QTL in the mentioned study on barley (Honsdorf *et al.*, 2014) was localised on chromosome 3H, which is corresponding to rye chromosome 3R (Martis *et al.*, 2013). In the previous study on barley even 6 QTL responsible for the vegetative dry mass in the BC_2DH population derived from a cross between the spring barley cultivar 'Scarlett' and the wild barley *Hordeum vulgare* ssp. *spontaneum* (von Korff *et al.*, 2006). 4 QTL for shoot dry weight were found on 1B, 2B, 5D, and 7B in 120 double haploid lines derived from winter wheat varieties (An *et al.*, 2006). It can be speculated, that the QTL for dry weight of the culms and number of tillers points out the presence of a strong gene/s, which mask weaker effects on the other linkage groups. Further analyses combined with fine mapping of this QTL region will provide clear answers to this hypothesis.

In the present study, two QTL for culm wall thickness were localised on chromosome 4R and 7R. In wheat, on the chromosome 2D, one QTL was detected for culm wall thickness (Hai *et al.*, 2005). On the other hand, in rice a QTL for culm wall thickness was found on the chromosome 1, and a QTL on the chromosome 6 increasing the culm

diameter, culm strength, as well as the spikelet number of the panicle, and grain yield as a pleiotropic effect (Ookawa *et al.,* 2010). In wheat, there is known a genotype, which is resistant to *Cephus cinctus*, an economically important pest in wheat, and it is characterised by a solid stem. This trait was previously linked to the microsatellite marker *Xgwm340* on the long arm of 3B, which controlled the majority of variation for the stem solidness in a cross between solid- and hollow-stemmed wheat cultivars (Cook *et al.,* 2004), which is very unlikely to be orthologous to the QTL found in the present study. Further genetic studies could give the answer to the question if other QTL in wheat and rice are targeting the same, but orthologous genes in rye. Finding these genes would ultimately speed up marker development for this interesting from the mechanical point of view trait.

The thickness of the sclerenchymal layer, the morphology of its cells, and its cell wall components are critical factors for resisting bending stress (Matsuda *et al.,* 1983; Ookawa and Ishihara, 1993). A QTL responsible for the thickness of sclerenchymal layer found in this study colocalised with a QTL responsible for the thickness of culm wall on 7R, but interestingly its position did not overlap with the thickness of sclerenchymal CW (localised on 1R), suggesting different genes regulating the thickness of these traits. In rye, *brittle stem* (*bs*) mutant was characterised by a significantly thinner sclerenchymal layer, in comparison to the wildtype (Kubicka and Kubicki, 1981). The gene, later on, was localised on the chromosome 5R (Schlegel *et al.,* 1986), which differ from the results obtained in this project. In studies on solid-stemmed wheat line, 99% of the variation in lodging resistance could be explained by the width of the mechanical tissue (Kong *et al.,* 2013). The first report about QTL for the thickness of the sclerenchymal layer was provided by Ookawa *et al.,* (2016) in a study on rice using reciprocal chromosome segment substitution lines (CSSLs) derived from the cross between 'Koshihikari' and 'Takanari' varieties. In mentioned study the QTL for the thickness of sclerenchymatous fibre tissue were detected in the genomic regions of chromosomes 2, 7, and 9 on both, 'Koshihikari' and 'Takanari', genetic backgrounds of CSSLs (Ookawa *et al.,* 2016). The positions of these QTL, according to the high-density comparative analysis of the linear gene order of the barley genome zippers versus the sequenced genome of rice by Mayer *et al.* (2011), may correspond to 6H, 2H, and 5H barley chromosomes, respectively, from which the positions of two latter ones could explain the results obtained in the present study. No other QTL associated with the thickness of sclerenchymal layer have been reported so far in monocots, although this trait is essential from the mechanical point of view and significantly improves lodging resistance. Thus more effort should be undertaken to understand the genetic background of that trait fully.

The vascular system provides transport of water, elements, and assimilates to the developing organs and caryopses, as well as mechanical stiffness (Rich, 1986; Rich, 1987a; Rich, 1987b; Rüggeberg et al., 2009). Additionally, a strong correlation between mechanical stiffness and the number/volume fraction of vascular bundles was found in studies on palms, wheat, triticale, oats, and rye (Brady, 1934; Mulder, 1954; Rich, 1986; Rich, 1987a; Rich, 1987b; Khanna, 1991; Żebrowski, 1992; Zuber et al., 1999; Wang et al., 2006; Packa et al., 2015), nevertheless information about the genetic background of that trait is still scarce. In rye, a mutant brittle stem (bs), characterised by the brittleness of the stem and fragility of roots, heads, and leaves, was shown to have significantly decreased number of inner vascular bundles in the lower internodes of culm (Kubicka and Kubicki, 1981). The gene was mapped on chromosome 5R by Dr. Melz (Schlegel et al., 1986), which is not in line with the position of QTL responsible for the number of inner vascular bundles obtained in the present study. In rice, two QTL regulating panicle branches, Dense and Erect Panicle1 (DEP1) and Ideal Plant Architecture1 (IPA1)/Wealthy Farmer's Panicle (WFP), have been shown to affect the rice vascular system. The dep1 and ipa1 mutants display an increased number of vascular bundles in internodes, which may contribute to the improved water/nutrients transport and lodging resistance, and eventually enhance grain yields (Huang et al., 2009; Jiao et al., 2010; Miura et al., 2010; Wang and Li, 2011). Additionally, it was shown that IPA1/WFP encodes OsSPL14, an SBP-box (SQUAMOSA promoter binding protein-like) protein, which is the target of miRNA156, and the ipa1 allele harbours a point mutation within the miRNA156 target site, perturbing the miRNA156-directed regulation of IPA1 in rice (Jiao et al., 2010). The point mutation in the miRNA156 target site of OsSPL14 also leads to a reduced number of tillers, which appears to result neither from the formation of fewer tiller buds, nor from the defect in tiller bud outgrowth, but from the prolonged plastochron (Jiao et al., 2010; Wang and Li, 2011). Nevertheless, in the present study, a detected QTL for the number of vascular bundles does not overlap with the QTL for the number of tillers, suggesting different genetic background than the one mentioned for rice.

The plant cell size and shape is determined by the plane of cell division and the rate and orientation of expansion (Keyes et al., 1990). The rate of plant cell expansion depends on: cell wall extensibility, the yield threshold of the wall, hydraulic conductance, and the difference in water potential between the cell and extracellular space (Lockhart, 1965; Keyes et al., 1990), indicating the regulation of cell size very complex. Kubicka and Kubicki (1981) noticed the abnormal shape of sclerenchymal cells in the rye bs mutant. Namely, in the transverse sections of basal internodes, sclerenchymal cells were radially elongated in both: subepidermal and in the vascular bundle zone

(Kubicka and Kubicki, 1981). The localisation of QTL responsible for the diameter of sclerenchymal and epidermal cells found in the present study is not in line with the localisation of *bs* allele (5R; Schlegel *et al.,* 1986), thus implying different genes responsible for the regulation of these traits in *bs* mutant and 304/1 F_2 population analysed in this study. The present study is the first report about the QTL underlying culm epidermal and sclerenchymal cell diameter, which were co-localising on chromosome 4R, suggesting a same genetic mechanism for the regulation of both of the traits. Although there were no statistically significant differences in the diameter of epidermal and sclerenchymal cells between the lodging resistant line and the wildtype, these QTL still may be interesting because of their co-localisation with a QTL for culm wall thickness.

Genetic variation of the CW thickness is poorly investigated in populations since such studies demand special equipment, are laborious, and time-consuming. Most of the knowledge about possible genes regulating this factor comes from the analysis of mutants, which show differences in the thickness of CW as a pleiotropic effect of a gene influencing morphological traits. Already mentioned rye *brittle stem* (*bs*) mutant is characterised by disturbances in the normal lignification of sclerenchymal cells, which CWs are significantly thinner than the wildtype (Kubicka and Kubicki, 1981). The localisation of *bs* allele (Schlegel *et al.,* 1986) is in line with one of QTL found for the thickness of inner periclinal CW of epidermis localised on 5R but does not explain the QTL on 1R for the thickness of sclerenchymal CW and inner periclinal CW of the epidermis. Study of the literature suggests, that the marker with the highest LOD detected for the thickness of the sclerenchymal CW on 1R can be the possible localisation of ferulate 5-hydroxylase, one of the enzymes responsible for the synthesis of lignins (Boerjan *et al.,* 2003; Ralph *et al.,* 2004; Barrière *et al.,* 2007; Andersen *et al.,* 2008). Fine mapping of that trait followed by functional analysis of the gene/s will be necessary to confirm this hypothesis. And since it is known that CWs are dynamic structures representing critical determinants of plant architecture, growth and development, and the thickening of the CW is a direct consequence of lignin, cellulose, and matrix phase polysaccharides deposition is depending on the genotype and its growth stage (Bidlack and Buxton, 1992; Farrokhi *et al.,* 2006; Vogel, 2008; Begović *et al.,* 2015), it would be interesting to evaluate CW composition in two parental lines and the mapping population. The use of genes involved in the production of a thicker CW of 'Stabilstroh', and overall stronger culms, can be used in breeding for increased lodging resistance in rye and closely related crops.

Plants have evolved a complex regulation network controlling mineral homeostasis based on strictly controlled uptake, translocation, redistribution, and sequestration to fulfil their mineral need and simultaneously avoid the possible toxic effects (Ghandilyan *et al.,*

2006). This network includes genes encoding various membrane transporters, reductive agents, storage proteins, metal ligands, and regulatory proteins, such as transcription factors, protein kinases, and receptors (Ghandilyan *et al.,* 2006). Although it is known that improvement of lodging resistance may be obtained by alteration of the content and ratios of minerals in grasses (Tubbs, 1930; Mulder, 1954; Miller and Anderson, 1963; Bremner, 1969; Pinthus, 1973; White, 1991; Easson *et al.,* 1993; Chalmers *et al.,* 1998), there are only few reports about QTL associated with elements content, and mostly only their grain content was investigated. There were two QTL detected for zinc content in this study: one on the chromosome 1R, and one on 2R. Interestingly, one of the QTL found in the present study overlapped with the QTL detected for the content of nickel, although no statistically significant correlation was observed in 304/1 F_2 population between these two traits (Fig.39). Vreugdenhil *et al.* (2004) identified four QTL on chromosomes 1, 2, 3, and 5, which are involved in seed Zn content and explained up to 42% of the variation in *Arabidopsis,* proving it to be a polygenic trait. In wheat, using RILs, one QTL controlling shoot Zn content localised on 3AL was identified for the control plants and one QTL localised on 7A for Cu-treated plants (Balint *et al.,* 2007).

On the other hand, the presence of the 1B/1R translocation in the germplasm of CIMMYT wheat had a positive effect on the concentration of zinc in the grain (Monasterio and Graham, 2000), which can be in line with the QTL observed on 1R. In barley, Lonergan *et al.* (2001) identified a region on the long arm of chromosome 4H associated with shoot Zn content. Additionally, Sadeghzadeh *et al.* (2015) identified four regions in barley, located on the long arm of chromosomes 3H, on the short arm of 4H, and finally on short and long arms of chromosome 2H, associated with seed Zn concentration, which according to the synteny map between barley and rye (Martis *et al.,* 2013) would correspond to the position of QTL on the chromosome 2R obtained in this study. Finally, Yun *et al.* (2015) revealed 4 QTL: on 1a, 2b, 5Ns, and 5Xm in a population derived from two perennial wildrye species, *Leymus cinereus* and *Leymus triticoides*, grown in the soil contaminated with trace elements. This perennial wildrye QTL for Zn content on 1a aligned to four barley *metallothionine* (*MT*) genes, whereas the QTL located on 2a aligned to two *yellow stripe-like* loci, which include one of the heavy metal transporter genes identified and affect Cu, Fe, Mn, and Zn accumulation (Curie *et al.,* 2001; Yun *et al.,* 2015). Taking in count the homology of this allotetraploid *Leymus* species chromosomes to barley and wheat, the QTL described by Yun *et al.,* (2015) can correspond to the QTL found in the present study.

In studies on the natural variation of shoot sulfate content in *Arabidopsis thaliana*, Loudet *et al.* (2007) found out that this trait is highly controlled by APR2, a key enzyme

of the assimilatory sulfate reduction pathway, adenosine 5'-phosphosulfate reductase. Additionally, authors showed that a single–amino acid substitution was responsible for a decrease in enzyme activity, leading to sulfate accumulation in the plant. Moreover, for *Arabidopsis*, the analysis of knockout mutants confirmed that two high-affinity sulfate transporters: SULTR1;1 and SULTR1;2, facilitate uptake of sulfate into roots, especially under sulfur deficiency (Yoshimoto *et al.,* 2007; Barberon *et al.,* 2008). SULTR2;1, a low-affinity sulfate transporter expressed in the central cylinder, has been postulated to mediate the influx of sulfate in the xylem parenchyma cells, where the concentration of sulfate in the symplast needs to be elevated (Takahashi, 2010). In barley, a high-affinity sulfate transporter, HVST1, expressed in pericycle and xylem parenchyma cells, is likely involved in the retrieval process in the central cylinder (Smith *et al.,* 1997). Moreover, the gene was mapped to the chromosome 4H (Pillen *et al.,* 2000), which can correspond to the position of one of the QTL described for sulfur content in 304/1 population. Yet, more investigation about tissue and cellular distribution of sulfur by energy-dispersive X-ray spectroscopy should answer the question if genes involved in the transport of this element can be good candidates for the obtained QTL.

In 304/1 F_2 mapping population, only one QTL for the content of molybdenum was found on the chromosome 7R, which colocalised with the QTL for copper. It has been shown for *Arabidopsis thaliana* that *molybdate transporter1* (*MOT1*) gene coding a mitochondrial molybdenum transporter is associated with natural genetic variation of the content of molybdenum (Baxter *et al.,* 2008). Moreover, barley *molybdate transporter1* gene was located on an unmapped scaffold of barley 7HL and the rice *MOT1* gene maps to the rice Chromosome 8, which aligns with the perennial wildrye QTL for molybdenum content on 7a and 7b (Yun *et al.,* 2015). Therefore, *MOT1* can be a good candidate gene for a QTL detected for molybdenum content in rye 304/1 F_2 population.

In the case of copper content in the present study, only one QTL was detected on 7R, explaining around 14.5% of the phenotypic variance. In contrast, in wheat-rye addition lines, the role of chromosome 5R was reported to affect the shoot Cu-concentration (Schlegel *et al.,* 1993). In later studies on wheat seedlings (Balint *et al.,* 2007), also only one QTL could be detected for the content of this element in Cu-treated plants, located on the chromosome 1BL and explaining twice much phenotypic variance than observed for the present study. Additionally, the authors were able to determine the position of QTL for Cu-tolerance index (the ratios of shoot dry masses under Cu-stress and non-stress conditions) and Cu-accumulation on 5D and 5A respectively, which according to the synteny maps could correspond to the findings obtained in 304/1 F_2 population. In the studies in *Brachypodium distachyon* on CTR/COPT family of Cu transporters, involved

either in Cu uptake from the soil into epidermal cells in the root, or long-distance transport and distribution of Cu in photosynthetic tissues, 5 genes could be identified (Jung *et al.,* 2014). *BdCOPT1* and *BdCOPT2* were located on chromosome 1, while *BdCOPT3*, *BdCOPT4*, and *BdCOPT5* are found on chromosome 2, 4, and 5, respectively (Jung *et al.,* 2014), and according to synteny maps by Martis *et al.,* (2013), the position of the QTL detected for the content of copper in 304/1 population can correspond to the positions of 3 of these genes (*BdCOPT1*, *BdCOPT2,* and *BdCOPT5*). Nevertheless, the methods involving energy-dispersive X-ray spectroscopy should be employed in the further phenotyping to answer the question if the parental lines differed in the efficiency of copper uptake and if *COPTs* could be good candidate genes.

Finally, the DArT markers linked to: the thickness of the sclerenchymal CW and inner periclinal CW of the epidermis, as well as the content of Zn and plant height, localised at the position of 11.7 and 25 cM on 1R (SNP 5218584 and 3353579); the thickness of sclerenchymal tissue and culm wall, the content of Mo and Cu, as well as plant height, localized on chromosome 7R at the position of 35.1 and 43.2 cM (SNP 3349542 and 5224120), were successfully applied for the development of KASPs, PCR-based markers, which can be useful for marker-assisted selection. Two markers used simultaneously can increase the efficiency of marker-assisted selection and thus improve the breeding process (Milczarski *et al.,* 2016).

Ad summam, in this study using the segregating F_2 population of outstanding rye spontaneous lodging resistant mutant and wildtype, quantitative trait loci were identified for traits associated with lodging resistance. Moreover, for the first time, a detailed analysis of plant phenotype on the cellular and elemental level was conducted in regards to lodging resistance. In the past, rye geneticists and breeders have collected, analysed, and developed many lines characterised by greater lodging resistance, however, most of these lines were characterised by dwarf phenotype. The phenotypic and genotypic characterisation of the lodging resistant line used in this study, combined with marker-assisted selection using KASP markers developed in this project, opens possibilities for finding and breeding superior and more suitable genotypes characterised by higher biomass production and greater lodging resistance. Additionally, further genetic studies, including genetic fine mapping, will allow the identification of the genes increasing rye productivity.

6. Summary

Lodging, the state of permanent displacement of the tillers from their upright position, is the main concern in crop production. It can decrease the final yield of grain by up to 80% and causes additional economic losses and other undesirable effects, including reduced grain quality, greater drying costs, and problematic harvest. Lodging can be a result of buckling or breaking of the basal internodes, typically near the base of the stem, described as stem lodging, or can result from failure of the anchorage system and is characterised by permanent displacement of the stem without any observable stem buckling involving a specific disturbance of the root system, known as root lodging. In small-grained crops lodging is usually caused by one of the bottom two internodes buckling rather than by the loss of anchorage, especially in rye, which has a larger proportion of root dry weight in the upper soil layer than other cereal crops. Hence, the development of varieties resistant to lodging, characterised by strong culms, is an important objective in most breeding programs.

Although 'Stabilstroh' ('Stable straw'), a recently identified genotype of rye, is characterized by lodging resistance, its increased plant height and biomass production is outstanding among German collection of rye hybrids. To answer the question about the genetic background of 'Stabilstroh' lodging resistance, detailed phenotyping using histological and ultrastructural techniques, such as: light, scanning electron, and transmission electron microscopy, was performed on the basal internodes of the parental lines: 'ms 135' (bearing 'Stabilstroh' traits) and 'R 1124' (wildtype). For the first time, a detailed analysis of plant phenotype on the cellular and elemental level was conducted in regards to lodging resistance. The characterisation of traits at the ultrastructural and physiological level was performed to identify trait interactions and indirect selection criteria to accelerate breeding progress. Additionally, easily measurable culm traits related to lodging resistance were identified to simplify the selection process, to reduce selection time and financial effort, and to significantly improve the straw mechanical stability of new rye varieties, which is of great importance for yield quality and quantity, especially in organic cultivation. The tillers of 'ms 135' in comparison to the wildtype were characterised by a significantly higher ratio of the thickness of sclerenchyma to the diameter. The sclerenchymal cell walls and inner periclinal cell walls of the epidermis were distinctly thickened in the lodging resistant parent.

In comparison to 'R 1124', 'ms 135' was also characterised by a higher number of tillers, increased dry weight of culms, a higher number of stalk invaginations, and outer vascular bundles, an important factor enhancing the mechanical stability of the plant. Interestingly, 'Stabilstroh' was characterised by a significantly smaller diameter of the second basal internode and reduced thickness of the culm wall, an extraordinary aspect of this genotype. Inductively Coupled Plasma Mass Spectrometry (ICPOES) was used to analyse the content of elements influencing physical properties of cell walls, or having direct or indirect control upon biosynthesis of primary or secondary cell wall components. The analysis of elements revealed the higher content of calcium, copper, potassium, magnesium, manganese, and sulfur in 'R 1124', while 'ms 135' showed a higher content of zinc and silicon, elements associated with cell walls strength.

Subsequently '304/1', segregating F_2 population, was phenotyped using the described anatomical, ultrastructural, and elemental traits to detect QTL underlying these characters and to elucidate the genetic basis of the lodging resistance in rye. In order to detect QTL responsible for traits related to lodging resistance and develop PCR-based molecular markers for marker-assisted selection (MAS), parental lines and F_2 population were genotyped with SSR and DArTseq markers. The genetic map of 7 chromosomes with an average density of 0.75 cM was constructed basing on 1,041 markers, which made the presented map one of the most saturated rye maps up to date. The obtained linkage map was subsequently used for QTL mapping for the analysed traits. A single marker regression mapping, followed by a composite interval mapping, allowed to find 22 determined regions on 6 chromosomes associated with: plant height, the length of the second basal internode, the number of tillers, dry weight of culms, the number of epidermal invaginations, the thickness of culm wall and sclerenchymal layer, the number of inner vascular bundles, the diameter of the epidermal and sclerenchymal cell, the thickness of sclerenchymal and inner periclinal cell walls of the epidermis, and the content of molybdenum, nickel, copper, sulfur, and zinc. The QTL found in this study were mainly novel, mostly due to the fact that rye was lagging far behind other crops in terms of genomic resources. In the current study, traits on the cellular level were considered, and subsequently many of these QTL were not described before in rye or other cereals.

For the selection of SNPs associated with at least four traits, KASP primers were designed, which can be used for marker-assisted selection process in the development of new rye varieties characterised by higher biomass production and greater lodging resistance to complement empirical breeding and hasten progress to increased rye production. Additionally, these markers used simultaneously can increase the efficiency of marker-assisted selection and thus improve the breeding process.

7. Zusammenfassung

Lager, ein Zustand der permanenten Veränderung der Halme aus ihrer aufrechten Position (Umfallen), ist eines der Hauptprobleme in der Pflanzenproduktion, da es die endgültige Ertragsmenge um bis zu 80% verringern kann. Es verursacht auch zusätzliche wirtschaftliche Verluste und Probleme, wie reduzierte Korngröße und -zahl, reduzierte Kornqualität, höhere Trocknungskosten und eine schwierige Ernte. Lager kann ein Ergebnis des Knickens oder Brechens der Basal-Internodien sein, typischerweise in der Nähe der Basis des Halmes, beschrieben als Halmbruch oder es kann aus dem Versagen des Verankerungssystems der Wurzeln resultieren und ist dabei durch ein Umfallen der Pflanze ohne Bruch des Halmes gekennzeichnet, auch bekannt als Wurzellager. Bei den Gertreiden wird das Lager in der Regel durch ein Abknicken eines der unteren zwei Internodien hervorgerufen, anstatt durch Verlust der Verankerung. Das ist vor allem bei Roggen der Fall, der einen größeren Anteil von Wurzeltrockengewicht in der oberen Bodenschicht hat, verglichen mit anderen Getreidearten. Daher ist die Entwicklung von lagerresistenten Sorten vor allem mit stabilen Halmen verbunden, ein wichtiges Ziel in den meisten Zuchtprogrammen

"Stabilstroh", ein kürzlich identifizierter Genotyp im Roggen, der durch die Resistenz gegenüber Lager charakterisiert ist, zeichnet sich durch eine erhöhte Pflanzenlänge und Biomasseproduktion im Vergleich zu anderen deutschen Roggenhybriden aus. Um die Frage nach dem genetischen Hintergrund der "Stabilstroh" - Lagerresistenz zu beantworten, wurde eine detaillierte Phänotypisierung der Basal-Internodien der Elternlinien ('ms 135', 'Stabilstroh' und 'R 1124', Wildtyp) unter Verwendung von histologischen und ultrastrukturellen Techniken wie: Licht-, Rasterelektronen- und Transmissionselektronenmikroskopie durchgeführt. Zum ersten Mal wurde eine detaillierte Analyse von Pflanzenphänotypen unterschiedlicher Lagerneigung auf zellulärer und chemisch-elementarer Ebene ausgeführt. Die Charakterisierung von Merkmalen auf der ultrastrukturellen und physiologischen Ebene wurde initiiert, um Merkmals-Interaktionen und indirekte Selektionskriterien herauszufinden, die den Zuchtfortschritt beschleunigen können. Es sollten insbesondere leicht messbare Halmmerkmale für Lagerresistenz identifiziert werden, um das Auswahlverfahren im Zuchtprozess zu vereinfachen, die Selektionszeit und den finanziellen Aufwand zu reduzieren und die mechanische Stabilität neuer Roggensorten bei gleichzeitig hohem Ertrag deutlich zu verbessern, so dass sich diese auch für den organischen Anbau eignen.

Die Halme von 'ms 135' waren durch ein deutlich höheres Verhältnis der Dicke des Sklerenchyms zum Halmdurchmesser gekennzeichnet. Gleichzeitig waren sklerenchymale und innere periklinale Zellwände der Epidermis eindeutig verdickt. Im Vergleich zu 'R 1124' war die Mutante 'ms 135' auch durch eine höhere Anzahl und ein erhöhtes Trockengewicht der Halme sowie eine höhere Anzahl von Stengel-Invaginationen (Einbuchtungen) und äußeren Gefäßbündeln gekennzeichnet, wichtige Faktoren, welche die mechanische Stabilität der Pflanze erhöhen. Interessanterweise war "Stabilstroh" zusätzlich durch einen deutlich kleineren Durchmesser des zweiten Basal Internodiums und eine reduzierte Dicke der Halmwand gekennzeichnet, ein außergewöhnlicher Aspekt dieses Genotyps. Induktiv gekoppelte Plasma-Massenspektrometrie (Inductively Coupled Plasma Mass Spectrometry, ICPOES) wurde verwendet, um den Gehalt an chemischen Elementen zu analysieren, welche die physikalischen Eigenschaften von Zellwänden beeinflussen oder einen direkten oder indirekten Einfluss auf die Biosynthese von primären oder sekundären Zellwandkomponenten haben. Die Elementanalyse ergab einen höheren Gehalt an Kalzium, Kupfer, Kalium, Magnesium, Mangan und Schwefel in 'R 1124', während 'ms 135' einen höheren Gehalt an Zink und Silizium zeigte, Elemente, welche die Zellwandstabilität beeinflussen.

Neben der Analyse der Eltern, wurde die segregierende F$_2$-Population phänotypisiert, indem sie für die anatomischen, ultrastrukturellen und chemisch-elementaren Merkmale untersucht wurde. Ziel war es, genetische Loci (Quantitatve Trait Loci, QTL) zu erkennen, die diesen Merkmalen zugrunde liegen, um damit die genetische Grundlage der Resistenz in Roggen aufzuklären. Um entsprechende QTL zu identifizieren und darauffolgend PCR-basierte molekulare Marker für eine künftige Marker-gestützte Selektion (Marker Asisted Selection, MAS) zu entwickeln, wurden die Elternlinien und die F$_2$-Population mit SSR- und DArTseq-Markern genotypisiert. Dabei wurde eine genetische Karte für 7 Chromosomen mit insgesamt 1.041 genetischen Markern und einer durchschnittlichen Markerdichte von 0,75 cM konstruiert. Die hier entwickelte Karte ist damit eine der am meisten gesättigten Roggenkarten, die bisher beschreiben wurden. Die erhaltene Kopplungskarte wurde anschließend für die QTL-Kartierung der analysierten Merkmale verwendet. Die Durchführung einer Single-Marker-Regressionskartierung gefolgt von einer Composite Interval Kartierung führte zur Identifizierung von insgesamt 22 Genomregionen auf 6 Chromosomen, welche die Merkmale Pflanzenhöhe, Länge des zweiten Basal-Internodiums, Anzahl der Halme, Trockengewicht der Halme, Anzahl der Epidermis Invaginationen, Dicke der Halmwand, Dicke der sklerenchymalen Schicht, Anzahl der inneren Gefäßbündel, Durchmesser der epidermalen und sklerenchymalen Zellen, Dicke der sklerenchymalen und inneren periklinalen Zellwände der Epidermis und

die Gehalte an Molybdän, Nickel, Kupfer, Schwefel, und Zink steuern. Die QTL, die in dieser Studie gefunden wurden, waren vorwiegend bisher unbeschrieben, vor allem wegen der Tatsache, dass Roggen in Bezug auf genomische Ressourcen weit hinter anderen Kulturen zurückliegt. Ein weiterer Grund dafür liegt darin begründet, dass in der aktuellen Studie vor allem Untersuchungen auf zellulärer Ebene durchgeführt wurden, die zuvor in Roggen oder anderen Getreiden nicht beschrieben waren.

Für eine Auswahl von SNPs, die mit mindestens je vier Merkmalen assoziiert sind, wurden KASP-Primer entworfen, die für den markergestützten Selektionsprozess bei der Entwicklung neuer, lagerresistenter Roggensorten, die gleichzeitig durch eine höhere Biomasseproduktion gekennzeichnet sind, verwendet werden können. Diese Marker können die Effizienz der markergestützten Selektion erhöhen und damit den Zuchtprozess beschleunigen.

8. References

Ahmad MS, **Ashraf** M, **2011**. Essential roles and hazardous effects of nickel in plants. *Reviews of Environmental Contamination and Toxicology,* 214: 125-167.

Allan RE, **1986**. Agronomic comparisons among wheat lines nearly isogenic for three reduced height genes. *Crop Science,* 26: 707-710.

Alloway, **2008**. *Micronutrient Deficiencies in Global Crop Production.* Springer Netherlands.

Amtmann A, **Sanders** D, **1999**. Mechanisms of Na⁺ uptake by plant cells. *Advances in Botanical Research,* 29: 75-112.

An D, Su J, Liu Q, Zhu Y, Tong Y, Li J, Jing R, Li B, Li Z, **2006**. Mapping QTLs for nitrogen uptake in relation to the early growth of wheat (*Triticum aestivum* L.). *Plant and Soil,* 284: 73–84.

Andersen JR, Zein I, Wenzel G, Darnhofer B, Eder J, Ouzunova M, Lübberstedt T, **2008**. Characterization of phenylpropanoid pathway genes within European maize (Zea mays L.) inbreds. *BMC Plant Biology,* 8:2.

Aohara T, Kotake T, Kaneko Y, Takatsuji H, Tsumuraya Y, Kawasaki S, **2009**. Rice *BRITTLE CULM 5* (*BRITTLE NODE*) is involved in secondary cell wall formation in the sclerenchyma tissue of nodes. *Plant & Cell Physiology,* 50(11): 1886-1897.

Atkins IM, **1938**. Relation of certain plant characters to strength of straw and lodging in winter wheat. *Journal of Agricultural Research,* 56: 99-120.

Aubertin-Leheudre M, Gorbach S, Woods M, Dwyer J T, Goldin B, Adlercreutz H, **2008**. Fat/Fiber intakes and sex hormones in healthy premenopausal women in USA. *Journal of Steroid Biochemistry and Molecular Biology,* 112: 32–39.

Babb S, **Muehlbauer** GJ, **2003**. Genetic and morphological characterization of the barley *uniculm2* (*cul2*) mutant. *Theoretical and Applied Genetics*, 106:846-857.

Backes G, Graner A, Foroughi-Wehr B, Fischbeck G, Wenzel G, Jahoor A, **1995**. Localization of quantitative trait loci (QTLs) for agronomically important characters by the use of a RFLP map in barley (*Hordeum vulgare* L.). *Theoretical and Applied Genetics,* 90: 294-302.

Badea A, Eudes F, Salmon D, Tuvesson S, Vrolijk A, Larsson CT, Caig V, Huttner E, Kilian A, Laroche A, **2011**. Development and assessment of DArT markers in triticale. *Theoretical and Applied Genetics,* 122: 1547–1560.

Baethgen WE, **Alley** MM, **1989**. Optimizing soil and fertilizer nitrogen use for intensively managed winter wheat. II. Critical levels and optimum rates of nitrogen fertilizer. *Agronomy Journal,* 81: 120-125.

Baethgen WE, Christianson CB, Lamothe AG, **1995**. Nitrogen fertilizer effects on growth, grain yield, and yield components of malting barley. *Field Crops Research,* 43: 87-99.

Baker CJ, **1995**. The development of theoretical model for the windthrow of plants. *Journal of Theoretical Biology,* 175: 355-372.

Baker CJ, Berry PM, Spink JH, Sylvester-Bradley R, Clare RW, Scott RK, Griffin JM, **1998**. A method for the assessment of the risk of wheat lodging. *Journal of Theoretical Biology,* 194: 587-603.

Balint AF, Roder M., Hell R, Galiba G, Borner A, **2007**. Mapping of QTLs affecting copper tolerance and the Cu, Fe, Mn and Zn contents in the shoots of wheat seedlings. *Biologia Plantarum,* 51: 129-134.

Balyan HS, **Singh** O, **1994**. Pleiotropic effects of GA-insensitive *Rht* genes on grain yield and its component characters in wheat. *Cereal Research Communications,* 22: 195-200.

Barberon M, Berthomieu P, Clairotte M, Shibagaki N, Davidian JC, Gosti F, **2008**. Unequal functional redundancy between the two *Arabidopsis thaliana* high-affinity sulphate transporters SULTR1;1 and SULTR1;2. *New Phytologist,* 180: 608–619.

Barnes JP, **Putnam** AR, **1986**. Evidence for Allelopathy by Residues and Aqueous Extracts of Rye (*Secale cereale*). *Weed Science,* 34: 384-390.

Barrière Y, Riboulet C, Méchin V, Maltese S, Pichon M, Cardinal A, Lapierre C, Lübberstedt T, Martinant JP, **2007**. Genetics and genomics of lignification in grass cell walls based on maize as model species. Genes, *Genomes and Genomics,* 1: 133-156.

Baxter I, Muthukumar B, Park HC, Buchner P, Lahner B, Danku J, Zhao K, Lee J, Hawkesford MJ, Guerinot ML, Salt DE, **2008**. Variation in molybdenum content across broadly distributed populations in *Arabidopsis thaliana* is controlled by a mitochondrial molybdenum transporter (*MOT1*). *PLoS Genetics,* https://doi.org/10.1371/journal.pgen.1000004

Bednarek PT, Masojć P, Lewandowska R, Myśków B, **2003**. Saturating rye genetic map with amplified fragment length polymorphism (AFLP) and random amplified polymorphic DNA (RAPD) markers. *Journal of Applied Genetics*, 44(1): 21-33.

Begović L, Ravlić J, Lepeduš H, Leljak-Levanić D, Cesar V, **2015**. The pattern of lignin deposition in the cell walls of internodes during barley (*Hordeum vulgare* L.) development. *Acta Biologica Cracoviensia,* 57: 55-66.

Bernal M, Ramiro MV, Cases R, Picorel R, Yruela I, **2006**. Excess copper effect on growth, chloroplast ultrastructure, oxygen-evolution activity and chlorophyll fluorescence in *Glycine max* cell suspensions. *Physiologia Plantarum,* 127: 312–325.

Berry PM, Griffin JM, Sylvester-Bradley R, Scott RK, Spink JH, Baker CJ, Clare RW, **2000**. Controlling plant form through husbandry to minimise lodging in wheat. *Field Crops Research*, 67(1): 59-81.

Berry PM, Sterling M, Baker CJ, Spink J, Sparkes DL, **2003**. A calibrated model of wheat lodging compared with field measurements. *Agricultural and Forest Meteorology,* 119: 167-180.

Berry PM, Sterling M, Spink JH, Baker CJ, Sylvester-Bradley R, Mooney SJ, Tams AR, Ennos AR, **2004**. Understanding and Reducing Lodging in Cereals. *Advances in Agronomy*, 84: 217-271.

Beschreibende Sortenliste, 2009. Bundessortenamt, Landbuch-Verlag, Hannover, Germany.

Biddulph O, **Woodbridge** CG, **1952**. The Uptake of Phosphorus by Bean Plants with Particular Reference to the Effects of Iron. *Plant Physiology*, 27(3): 431–444.

Bidlack J, **Buxton** D, **1992**. Content and deposition rates of cellulose, hemicellulose, and lignin during regrowth of forage grasses and legumes. *Canadian Journal of Plant Science,* 72: 809-818.

Bingham FT, **1963**. Relation Between Phosphorus and Micronutrients in Plants1. *Soil Science Society of America Journal,* 27: 389-391.

Boer MP, Malosetti M, Welham SJ, Thissen JTNM, **2014**. Part 2: Statistical genetics and QTL estimation. In: Payne RW, Harding SA, Murray DA, Soutar DM, Baird DB, Glaser AI, et al., editors. *The guide to GenStat release 17.* Hemel Hempstead, UK: VSN International.

Boerjan W, Ralph J, Maucher M, **2003**. Lignin biosynthesis. *Annual Review of Plant Biology,* 54: 519-546.

Bolibok H, Gruszczyńska A, Hromada-Judycka A, Rakoczy-Trojanowska M, **2007**. The Identification of QTLs Associated with the *in vitro* Response of Rye (*Secale cereale* L.). *Cellular and Molecular Biology Letters,* 12: 523 – 535.

Bolibok-Brągoszewska H, Heller-Uszyńska K, Wenzl P, Uszyński G, Kilian A, Rakoczy-Trojanowska M, **2009**. DArT markers for the rye genome - genetic diversity and mapping. *BMC Genomics,* 10:578, https://doi.org/10.1186/1471-2164-10-578

Bolibok-Brągoszewska H, Targońska M, Bolibok L, Kilian A, Rakoczy-Trojanowska M, **2014**. Genome-wide characterization of genetic diversity and population structure in *Secale. BMC Plant Biology,* 14: 184.

Börner A, **1991**. Genetical Studies of Gibberellic Acid Insensitivity in Rye (*Secale cereale* L.). *Plant Breeding,* 106: 53–57.

Börner A, **Korzun** V, **1998**. A consensus linkage map of rye (*Secale cereale* L.) including 374 RFLPs, 24 isozymes and 15 gene loci. *Theoretical and Applied Genetics,* 97: 1279—1288.

Börner A, **Melz** G, **1988**. Response of rye genotypes differing in plant height to exogenous gibberellic acid application. *Archiv für Züchtungsforschung,* 18: 79-82.

Börner A, Plaschke J, Korzun V, Worland AJ, **1996**. The relationships between the dwarfing genes of wheat and rye. *Euphytica,* 89: 69-75.

Börner A, Korzun V, Worland AJ, **1998**. Comparative genetic mapping of loci affecting plant height and development in cereals. *Euphytica,* 100: 245-248.

Börner A, Korzun V, Voylokov AV, Weber WE, **1999**. Detection of quantitative trait loci on chromosome 5R on rye (*Secale cereale* L.). *Theoretical and Applied Genetics,* 98: 1087-1090.

Börner A, Korzun V, Voylokov AV, Worland AJ, Weber WE, **2000**. Genetic mapping of quantitative trait loci in rye (*Secale cereale* L.). *Euphytica,* 116: 203–209.

Börner A, Schumann E, Fürste A, Cöster H, Leithold B, Röder MS, Weber WE, **2002**. Mapping of quantitative trait loci determining agronomic important characters in hexaploid wheat (*Triticum aestivum* L.). *Theoretical and Applied Genetics,* 105: 921-936.

Brady J, **1934**. Some factors influencing lodging in cereals. *Journal of Agricultural Science,* 24: 209-232.

Bremner PM, **1969**. Effects of time and rate of nitrogen application on tillering, 'sharp eyespot' (*Rhizoctonia solani*) and yield in winter wheat. *Journal of Agricultural Science,* 87: 1198-1206.

Broadley MR, White PJ, Hammond JP, Zelko I, Lux A, **2007**. Zinc in plants. *New Phytologist,* 173 (4): 677-702.

Buck-Sorlin GH, **2002**. The search for QTL in barley (*Hordeum vulgare* L.) using a new mapping population. *Cellular and Molecular Biology Letters,* 7: 523 – 535.

Burkhead JL, Reynolds KA, Abdel-Ghany SE, Cohu CM, Pilon M, **2009**. Copper homeostasis. *New Phytologist,* 182: 799-816.

Bushuk W, **2001**. Rye production and uses worldwide. *Cereal Foods World,* 46: 70-73.

Burton RA, Wilson SM, Hrmova M, Harvey AJ, Shirley NJ, Medhurst A, Stone BA, Newbigin EJ, Bacic A, Fincher GB, **2006**. Cellulose Synthase-Like CslF Genes Mediate the Synthesis of Cell Wall (1,3;1,4)-ß-d-Glucans. *Science*, 311(5769): 1940-1942.

Cade JE, Burley VJ, Greenwood DC, **2007**. Dietary fibre and risk of breast cancer in the UK Women's Cohort Study. *International Journal of Epidemiology,* 36: 431-438.

Carpita NC, **1989**. Pectic polysaccharides of maize coleoptiles and proso millet cells in liquid culture. *Phytochemistry,* 28: 121-125.

Carpita NC, **1996**. Structure and biogenesis of the cell walls of grasses. *Annual Review of Plant Physiology and Plant Molecular Biology,* 47: 445-476.

Carpita NC, **Gibeaut** DM, **1993**. Structural models of primary cell walls in flowering plants: consistency of molecular structure with the physical properties of the walls during growth. *Plant Journal*, 3: 1-30.

Cassab GI, **Varner** JE, **1988**. Cell wall proteins. *Annual Review of Plant Physiology and Plant Molecular Biology,* 39: 321-353.

Cenci CA, Grando S, Ceccarelli S, **1984**. Culm anatomy of barley (*Hordeum vulgare*). *Canadian Journal of Botany,* 62: 2023-2027.

Chalmers AG, Dyer CJ, Sylvester-Bradley R, **1998**. Effects of nitrogen fertilizer on the grain yield and quality of winter oats. *Journal of Agricultural Science,* 131: 395-407.

Chebotar S, Röder MS, Korzun V, Saal B, Weber WE, Börner A, **2003**. Molecular studies on genetic integrity of open pollinating species rye (*Secale cereale* L.) after long-term genebank maintenance. *Theoretical and Applied Genetics*, 107: 1469–1476.

Chono M, Honda I, Zeniya H, Yoneyama K, Saisho D, Takeda K, Takatsuto S, Hoshino T, Watanabe T, **2003**. A semidwarf phenotype of barley *uzu* results from a nucleotide substitution in the gene encoding a putative brassinosteroid receptor. *Plant Physiology,* 133: 1209-1219.

Clark ER, **Wilson** HK, **1933**. Lodging in small grains. *Journal of the American Society of Agronomy,* 25 (9): 561-572.

Cook JP, Wichman DM, Martin JM, Bruckner PL, Talbert LE, **2004**. Identification of microsatellite markers associated with a stem solidness locus in wheat. *Crop Science,* 44: 1397-1402.

Cosgrove DJ, **2005**. Growth of the plant cell wall. *Nature Reviews Molecular Cell Biology,* 6: 850-861.

Cosgrove DJ, **2014**. Re-constructing our models of cellulose and primary cell wall assembly. *Current Opinion in Plant Biology,* 22: 122-131.

Counce PA, Siebenmorgen TJ, Poag MA, Holloway GE, Kocher MF, Lu RF, **1996**. Panicle emergence of tiller types and grain yield of tiller order for direct-seeded rice cultivars. *Field Crops Research,* 47: 235-242.

Crook MJ, **Ennos** AR, **1993**. The mechanics of root lodging in winter wheat (*Triticum aestivum* L). *Journal of Experimental Botany*, 44: 1219-1224.

Crook MJ, **Ennos** AR, **1994**. Stem and root characteristics associated with lodging resistance in four winter wheat cultivars. *Journal of Agricultural Science,* 123 (2): 167-174.

Crook MJ, **Ennos** AR, **1995**. The effects of nitrogen and growth regulators on stem and root characteristics associated with lodging in two cultivars of winter wheat. *Journal of Experimental Botany,* 46: 931-938.

Curie C, **Briat** JF, **2003**. Iron transport and signalling in plants. *Annual Review of Plant Biology,* 54: 183-206.

Curie C, Panaviene Z, Loulerue C, Dellaporta SL, Briat JF, Walker EL, **2001**. Maize *yellow stripe1* encodes a membrane protein directly involved in Fe (III) uptake. *Nature,* 409: 346-349.

Dabbert T, Okagaki RJ, Cho S, Boddu J, Muehlbauer GJ, **2009**. The genetics of barley low-tillering mutants: Absent lower laterals (als). *Theoretical and Applied Genetics,* 118: 1351-1360.

Dabbert T, Okagaki RJ, Cho S, Heinen S, Boddu J, Muehlbauer GJ, **2010**. The genetics of barley low-tillering mutants: Low number of tillers-1 (lnt1). *Theoretical and Applied Genetics,* 121: 705-715.

Davy H, **1836**. *Elements of agricultural chemistry in a course of lectures for the board of agriculture delivered between 1802 and 1812*. A.Spottiswoode, London.

Day AD, **Dickson** AD, **1958**. Effect of artificial lodging on grain and malt quality of fall-sown irrigated barley. *Agronomy Journal,* 50: 338-340.

De Baets S, Poesen J, Meersmans J, Serlet L, **2011**. Cover crops and their erosion-reducing effects during concentrated flow erosion. *Catena,* 85: 237-244.

De Vries JN, **Sybenga** J, **1984**. Chromosomal location of 17 monogenically inherited morphological markers in rye (*Secale cereale* L.) using the translocation tester set. *Zeitschrift fuŕ Pflanzenzu̇chtung,* 92: 117 - 139.

Demarty M, Morvan C, Thellier M, **1984**. Calcium and the cell wall. *Plant Cell Environ.,* 7: 441–448.

Devos KM, Atkinson MD, Chinoy CN, Francis HA, Harcourt RT, Koebner RL, Liu CJ, Masojc P, Xie DX, Gale MD, **1993**. Chromosomal rearrangements in the rye genome relative to that of wheat. *Theoretical and Applied Genetics,* 85: 673-680.

Dharmawardhana DP, Ellis BE, Carlson JE, **1992**. Characterization of vascular lignification in *Arabidopsis thaliana*. *Canadian Journal of Botany,* 70: 2238-2244.

Donald CM, **1968**. The breeding of crop ideotypes. *Euphytica,* 17: 385-403.

Dugger WM, **1983**. Boron in plant metabolism. In: Läuchli A & Bieleski L (eds) *Encyclopedia of Plant Physiology, New Series Vol. 15B*. Springer, Berlin (pp 626–650).

Easson DL, White EM, Pickles SJ, **1993**. The effects of weather, seed rate and cultivar on lodging and yield in winter wheat. *Journal of Agricultural Science,* 121: 145-156.

Epstein E, **1994**. The anomaly of silicon in plant biology. *Proceedings of the National Academy of Sciences,* 91: 11-17.

Epstein E, **1999**. Silicon. *Annual Review of Plant Physiology and Plant Molecular Biology,* 50: 641-664.

Esechie HA, Maranville JW, Ross WM, **1976**. Relationship of Stalk Morphology and Chemical Composition to Lodging Resistance in Sorghum. *Crop Science,* 17: 609-612.

Falke KC, Wilde P, Wortmann H, Geiger HH, Miedaner T, **2009a**. Identification of genomic regions carrying QTL for agronomic and quality traits in rye (*Secale cereale*) introgression lines. *Plant Breeding,* 128: 615-623.

Falke KC, Sušić Z, Wilde P, Wortmann H, Möhring J, Piepho HP, Geiger HH, Miedaner T, **2009b**. Testcross performance of rye introgression lines developed by marker-assisted backcrossing using Iranian accession as donor. *Theoretical and Applied Genetics,* 118: 1225-1238.

FAOSTAT, **2016**. Food and Agriculture Organization of the United Nations: Statistics Division. http://faostat3.fao.org/

Farrokhi N, Burton RA, Brownfield L, Hrmova M, Wilson SM, Bacic A, Fincher GB, **2006**. Plant cell wall biosynthesis: genetic, biochemical and functional genomics approaches to the identification of key genes. *Plant Biotechnology Journal,* 4: 145-167.

Fincher GB, **2009**. Revolutionary times in our understanding of cell wall biosynthesis and remodelling in the grasses. *Plant Physiology,* 149: 27-37.

Fischer RA, **Stapper** M, **1987**. Lodging effects on high-yielding crops of irrigated semidwarf wheat. *Field Crops Research,* 17: 245-248.

Flintham JE, Börner A, Worland AJ, Gale MD, **1997**. Optimizing wheat grain yield: effects of *Rht* (gibberellin-insensitive) dwarfing genes. *Journal of Agricultural Science,* 128: 11-25.

Ford MA, Blackwell RD, Parker ML, Austin RB, **1979**. Associations Between Stem Solidity, Soluble Carbohydrate Accumulation and Other Characters in Wheat. *Annals of Botany,* 44: 731-738.

Foulkes MJ, Slafer GA, Davies WJ, Berry PM, Sylvester-Bradley R, Martre P, Calderini DF, Griffiths S, Reynolds MP, **2011**. Raising yield potential of wheat. III. Optimizing partitioning to grain while maintaining lodging resistance. *Journal of Experimental Botany,* 62: 469-486.

Freeman S, **2005**. *Biological Science.* Pearson Prentice Hall, Upper Saddle River, New Jersey.

Freshour G, Clay RP, Fuller MS, Albersheim P, Darvill AG, Hahn MG, **1996**. Developmental and tissue-specific structural alternations of the cell-wall polysaccharides of *Arabidopsis thaliana* roots. *Plant Physiology,* 110: 1413-1429.

Fry SC, Miller JG, Dumville JC, **2002**. A proposed role for copper ions in cell wall loosening. *Plant Soil,* 247: 57-67.

Furumoto T, Yamaguchi T, Ohshima-Ichie Y, Nakamura M, Tsuchida-Iwata Y, Shimamura M, Ohnishi J, Hata S, Gowik U, Westhoff P, Bräutigam A, Weber AP, Izui K, **2011**. A plastidal sodium-dependent pyruvate transporter. *Nature,* 476: 472-475.

Gale MD, **Youssefian** S, **1985**. Dwarfing genes in wheat. In: GE Russel (Ed.) *Progress in Plant Breeding*, University Press, Cambridge, UK.

Garber RJ, **Olson** PJ, **1919**. A study of the relation of some morphological characters to lodging in cereals. *Journal of the American Society of Agronomy,* 11: 173-186.

Gardner CA, **1952**. Flora of Western Australia: Gramineae. Govt. Printer, Perth.

Gawroński P, Pawełkowicz M, TofilK, UszyńskiG, Sharifova S, Ahluwalia S, Tyrka M, Wędzony M, Kilian A, Bolibok-Brągoszewska H, **2016.** DArT Markers Effectively Target Gene Space in the Rye Genome. *Frontiers in Plant Science,* doi: 10.3389/fpls.2016.01600.

Geiger HH, **Miedaner** T, **1996**. Genetic basis and phenotypic stability of male fertility restoration in rye. *Vorträge für Pflanzenzüchtung,* 35: 27–38.

Geiger HH, **Miedaner** T, **2009**. Rye (*Secale cereale* L.). In: MJ Carena (Ed.) *Cereals.* Springer-Verlag, New York, USA.

Ghandilyan A, Vreugdenhil D, Aarts GM, **2006**. Progress in the genetic understanding of plant iron and zinc nutrition. *Physiologia Plantarum,* 126: 407-417.

Guntzer F, Keller C, Meunier JD, **2010**. Determination of the silicon concentration in plant material using Tiron extraction. *New Phytologist*, 188: 902–906.

Gupta UC, **1979**. Boron nutrition of crops. *Advances in Agronomy,* 31: 273-307.

Hackauf B, **Wehling** P, **2002**. Identification of microsatellite polymorphisms in expressed portion of the rye genome. *Plant Breeding,* 121: 17-25.

Hackauf B, Haffke S, Fromme F, Roux SR, Kusterer B, Musmann D, Kilian A, Miedaner T, **2017**. QTL mapping and comparative genome analysis of agronomic traits including grain yield in winter rye. *Theoretical and Applied Genetics*, 130(9):1801-1817.

Hai L, Guo H, Xiao S, Jiang G, Zhang X, Yan C, Xin Z, Jia J, **2005**. Quantitative trait loci (QTL) of stem strength and related traits in a doubled-haploid population of wheat (*Triticum aestivum* L.). *Euphytica,* 141: 1-9.

Hakala M, Rantamaki S, Puputti EM, Tyystjarvi T, Tyystjarvi E, **2006**. Photoinhibition of manganese enzymes: insights into the mechanism of photosystem II photoinhibition. *Journal of Experimental Botany,* 57: 1809-1816.

Halliwell B, **Gutteridge** JMC, **1992**. Biologically relevant metal ion-dependent hydroxyl radical generation. *FEBS Letters,* 307: 108-112.

Hayes PM, Liu BH, Knapp SJ, Chen F, Jones B, Blake T, Franckowiak J, Rasmusson D, Sorrells M, Ullrich SE, Wesenberg D, Kleinhofs A, **1995**. Quantitative trait locus effects and environmental interaction in a sample of North American barley germ plasm. *Theoretical and Applied Genetics,* 87: 392-401.

Hayward HE, **1938**. The Structure of Economic Plants. THE MACMILLAN COMPANY, New York.

Hebbern CA, Laursen KH, Ladegaars AH, Schmidt SB, Pedas P, Bruhn D, Schjoerring JK, Wulfsohn D, Husted S, **2009**. Latent manganese deficiency increases transpiration in barley (*Hordeum vulgare*). *Physiologia Plantarum,* 135: 307-316.

Hill MJ, **1997**. Cereals, cereal fibre and colorectal cancer risk: a review of the epidemiological literature. *European Journal of Cancer Prevention,* 6: 219-225.

Hood KR, Baasiri RA, Fritz SE, Hood EE, **1991**. Biochemical and tissue print analyses of hydroxyproline-rich glycoproteins in cell walls of sporophytic maize tissues. *Plant Physiology,* 96: 1214-1219.

Hooper LJ, **Davies** DB, **1968**. Melanism and associated symptoms in wheat grown on copper-responsive chalkland soils. *Journal of the Science of Food and Agriculture,* 19: 733–739.

Honsdorf N, March TJ, Berger B, Tester M, Pillen K, **2014**. High-Throughput Phenotyping to Detect Drought Tolerance QTL in Wild Barley Introgression Lines. *PLoS ONE,* 9(5): e97047.

Hu H, **Brown** PH, **1994**. Localization of Boron in Cell Walls of Squash and Tobacco and Its Association with Pectin (Evidence for a Structural Role of Boron in the Cell Wall). *Plant Physiology,* 105 (2): 681-689.

Huang XQ, Cöster H, Ganal MW, Röder MS, **2003**. Advanced backcross QTL analysis for the identification of quantitative trait loci alleles from wild relatives of wheat (*Triticum aestivum* L.). *Theoretical and Applied Genetics,* 106:1379–1389.

Huang X, Qian Q, Liu Z, Sun H, He S, Luo D, Xia G, Chu C, Li J, Fu X, **2009**. Natural variation at the *DEP1* locus enhances grain yield in rice. *Nature Genetics,* 41: 494 – 497.

Hussien A, Tavakol E, Horner DS, Muñoz-Amatriaín M, Muehlbauer GJ, Rossini L, **2014**. Genetics of tillering in rice and barley. *Plant Genome,* doi: 10.3835/plantgenome2013.10.0032

Idris M, Hossain MM, Choudhury FA, **1975**. The effect of silicon on lodging of rice in presence of added nitrogen. *Plant and Soil,* 43: 691–695.

Iiyama K, Lam TBT, Stone BA, **1990**. Phenolic acid bridges between polysaccharides and lignin in wheat internodes. *Phytochemistry,* 29: 733-737.

Iiyama K, Lam TBT Stone BA, **1994**. Covalent cross-links in the cell wall. *Plant Physiology,* 104: 315-320.

Inanaga S, **Okasaka** A, **1995**. Calcium and silicon binding compounds in cell walls of rice shoots. *Soil Science and Plant Nutrition,* 41 (1): 103-110.

Ishii T, **Matsunaga** T, **1996**. Isolation and characterization of a boron-rhamnogalacturonan-II complex from cell walls of sugar beet pulp. *Carbohydrate Research,* 284 (1): 1–9.

Ito A, **Fujiwara** A, **1968**. The relation between calcium and cell wall in growing rice leaf. *Plant Cell Physiol.,* 9: 433-439.

Jaccoud D, Peng K, Feinstein D, Kilian A, **2001**. Diversity arrays: a solid state technology for sequence independent genotyping. *Nucleic Acids Res,* 29:e25.

Jarvis MC, **1984**. Structure and properties of pectin gels in plant cell walls. *Plant Cell Environment,* 7: 153-164.

Jellum MD, **1962**. Relationships between lodging resistance and certain stem characters in oats. *Crop Science,* 2: 263-267.

Jia Q, Zhang XQ, Westcott S, Broughton S, Cakir M, Yang J, Lance R, Li C, **2011**. Expression level of a gibberellin 20-oxidase gene is associated with multiple agronomic and quality traits in barley. *Theoretical and Applied Genetics,* 122: 1451-1460.

Jiao Y, Wang Y, Xue D, Wang J, Yan M, Liu G, Dong G, Zeng D, Lu Z, Zhu X, Qian Q, Li J, **2010**. Regulation of *OsSPL14* by OsmiR156 defines ideal plant architecture in rice. *Nature Genetics,* 42: 541–544.

Joehanes R, **Nelson** JC, **2008**. QGene 4.0, an extensible Java QTL-analysis platform. *Bioinformatics,* 24 (23): 2788-2789.

Jones L, Ennos AR, Turner SR, **2001**. Cloning and characterization of *irregular xylem4* (*irx4*): a severely lignin-deficient mutant of *Arabidopsis*. *Plant Journal,* 26: 205-216.

Jung H, Gayomba SR, Yan J, Vatamaniuk OK, **2014**. *Brachypodium distachyon* as a model system for studies of copper transport in cereal crops. *Frontiers in Plant Science,* doi: 10.3389/fpls.2014.00236.

Karpenstein-Machan M, **Maschka** R, **1996**. Progress in rye breeding. *Vorträge für Pflanzenzüchtung,* 35: 7-13.

Kashiwagi T, Togawa E, Hirotsu N, Ishimaru K, **2008**. Improvement of lodging resistance with QTLs for stem diameter in rice (*Oryza sativa* L.). *Theoretical and Applied Genetics,* 117: 749-757.

Kato K, Miura H, Sawada S, **2000**. Mapping QTLs controlling grain yield and its components on chromosome 5A of wheat. *Theoretical and Applied Genetics,* 101: 1114-1121.

Kebrom TH, Spielmeyer W, Finnegan EJ, **2013**. Grasses provide new insights into regulation of shoot branching. *Trends in Plant Science,* 18: 41-48.

Kelbert AJ, Spanr D, Briggs KG, King JR, **2004**. The association of culm anatomy with lodging susceptibility in modern spring wheat genotypes. *Euphytica,* 136: 211-221.

Keller M, Karutz C, Schmid JE, Stamp P, Winzeler M, Keller B, Messmer MM, **1999**. Quantitative trait loci for lodging resistance in a segregating wheat x spelt population. *Theoretical and Applied Genetics,* 98: 1171-1182.

Kertesz Z, Flintham JE, Gale MD, **1991**. Effects of *Rht* dwarfing genes on wheat grain yield and its components under Eastern European conditions. *Cereal Research Communications,* 19: 297-304.

Keyes G, Sorrels ME, Setter TL, **1990**. Gibberellic acid regulates cell wall extensibility in wheat (*Triticum aestivum* L.). *Plant Physiology,* 92: 242-245.

Khanna VK, **1991**. Relationship of lodging resistance and yield to anatomical characters of stem in wheat, triticale and rye. *Wheat Information Service*, 73: 19-24.

Khlestkina EK, Than MHM, Pestsova EG, Röder MS, Malyshev SV, Korzun V, Börner A, **2004**. Mapping of 99 new microsatellite-derived loci in rye (*Secale cereale* L.) including 39 expressed sequence tags. *Theoretical and Applied Genetics,* 109: 725–732.

Kieliszewski MJ, **Lamport** DTA, **1994**. Exstensin: repetitive motifs, functional sites, post-translocational codes, and phylogeny. *Plant Journal,* 5: 157-172.

Kirby EJM, **1967**. The effect of plant density upon the growth and yield of barley. *Journal of Agricultural Science,* 68: 317-324.

Kitagishi K, **Obata** H, **1986**. Effects of Zinc Deficiency on the Nitrogen Metabolism of Meristematic Tissues of Rice Plants with Reference to Protein Synthesis. *Soil Science and Plant Nutrition,* 32: 397-405.

Knox JP, Linstead PJ, King J, Cooper C, Roberts K, **1990**. Pectin esterification is spatially regulated both within cell walls and between developing tissues of root apices. *Planta,* 191: 512-521.

Kobyljanski VD, **1972**. On genetics of the dominant factor of short straw rye. *Genetika,* 8: 12-17.

Kobyljanski VD, **1975**. Genetic resources of worlds rye collection for solving of more important breeding problems. *Hodowla Roślin, Aklimatyzacja i Nasiennictwo,* 19: 439–446.

Kong E, Liu D, Guo X, Yang W, Sun J, Li X, Zhan K, Cui D, Lin J, Zhan A, **2013**. Anatomical and chemical characteristics associated with lodging resistance in wheat. *Crop Journal,* 1: 43-49.

Korzun V, Börner A, Melz G, **1996**. RFLP mapping of the dwarfing (*Ddw1*) and hairy peduncle (*Hp*) genes on chromosome 5 of rye (*Secale cereale* L.). *Theoretical and Applied Genetics,* 92: 1073–1077.

Korzun V, Malyshev S, Kartel N, Westermann T, Weber WE, Börner A, **1998**. A genetic linkage map of rye (*Secale cereale* L.). *Theoretical and Applied Genetics,* 95 : 468—473.

Korzun V, Malyshev S, Voylokov AV, Börner A, **2001**. A genetic map of rye (*Secale cereale* L.) combining RFLP, isozyme, protein, microsatellite and gene loci. *Theoretical and Applied Genetics,* 102: 709–717.

Kosambi DD, **1943**. The estimation of map distances from recombination values. *Annals of Human Genetics*, 12(1): 172-175.

Kouchi H, **Kumazawa** K, **1976**. Anatomical responses of root tips to boron deficiency. *Soil Science and Plant Nutrition,* 22 (1): 53-71.

Kowalski AM, Gooding M, Ferrante A, Slafer GA, Orford S, Gasperini D, Griffiths S, **2016**. Agronomic assessment of the wheat semi-dwarfing gene *Rht8* in contrasting nitrogen treatments and water regimes. *Field Crops Research,* 191: 150-160.

Kraus JE, de Sousa HC, Rezende MH, Castro NM, Vecchi C, Luque R, **1998**. Astra blue and basic fuchsin double staining of plant materials. *Biotechnic & Histochemistry,* 73: 235-243.

Kubicka H, **Kubicki** B, **1981**. Genetical and anatomical analysis of brittleness of stems in rye (*Secale cereale* L.). *Acta Societatis Botanicum Poloniae,* 50 (4): 567-574.

Kubicka H, **Kubicki** B, **1988**. Charakterystyka składu chemicznego dwóch form żyta o łamliwym źdźble warunkowanym genami bs_1 lub bs_2. *Hodowla Roślin Aklimatyzacja i Nasiennictwo,* 32:1-7.

Kuraparthy V, Sood S, Dhaliwal HS, Chhuneja P, Gill BS, **2007**. Identification and mapping of a tiller inhibition gene (tin3) in wheat. *Theoretical and Applied Genetics,* 114(2): 285-94.

Kurek I, Kawagoe Y, Jacob-Wilk D, Doblin M, Deimer D, **2002**. Dimerization of cotton fiber cellulose synthase catalytic subunits occurs via oxidation of the zinc-binding domains. *PNAS,* 99: 11109-11114.

Kutschera L, Lichtenegger E, Sobotik M, **2009**. Wurzelatlas der Kulturpflanzen gemäßigter Gebiete mit Arten des Feldgemüsebaues. DLG-Verlag, Germany.

Lam TBT, Iiyama K, Stone BA, **1992**. Cinnamic acid bridges between cell wall polymers in wheat and phalaris internodes. *Phytochemistry*, 32: 1179-1183.

Lam TBT, Iiyama K, Stone BA, **1994**. An approach to the estimation of ferulic acid bridges in unfractionated cell walls of wheat internodes. *Phytochemistry,* 37: 327-333.

Larson SR, Kadyrzhanova D, McDonald C, Sorrells M, Blake TK, **1996**. Evaluation of barley chromosome-3 yield QTLs in a backcross F_2 population using STS-PCR. *Theoretical and Applied Genetics,* 98: 1171-1182.

Leinonen KS, Poutanen KS, Mykkänen HM, **2000**. Rye bread decreases serum total and LDL cholesterol in men with moderately elevated serum cholesterol. *Journal of Nutrition,* 130: 164-170.

Lerouxel O, Cavalier DM, Liepman AH, Keegstra K, **2006**. Biosynthesis of plant cell wall polysaccharides – a complex process. *Current Opinion in Plant Biology,* 9: 621-630.

Leustek T, **Saito** K, **1999**. Sulfate transport and assimilation in plants. *Plant Physiology,* 120: 637-644.

Li Z, Peng T, Xie Q, Han S, Tian J, **2010**. Mapping of QTL for tiller number at different stages of growth in wheat using double haploid and immortalized F_2 populations. *Journal of Genetics,* 89: 409-415.

Liang YC, Ma TS, Li FJ, Feng YJ, **1994**. Silicon availability and response of rice and wheat to silicon in calcareous soils. *Communications in Soil Science and Plant Analysis,* 25: 2285-2297.

Liebig J, **1843**. *Chemistry in its application to agriculture and physiology.* James M. Campbell & Co., New York, USA.

Lockhart JA, **1965**. An analysis of irreversible plant cell elongation. *Journal of Theoretical Biology,* 8: 264-275.

Lonergan PF, Graham RD, Barker SJ, Paull JG, **2001**. Mapping of chromosome regions associated with increased vegetative zinc accumulation using a barley doubled haploid population. *Developments in Plant and Soil Sciences,* 92: 84-85.

Loudet O, Saliba-Colombani V, Camilleri C, CalengeF, Gaudon V, Koprivova A, North KA, Kopriva S, Daniel-Vedele F, **2007**. Natural variation for sulfate content in Arabidopsis thaliana is highly controlled by APR2. *Nature Genetics,* 39: 896 – 900.

Lunde C, Zygadlo A, Simonsen HT, Nielsen PL, Blennow A, Haldrup A, **2008**. Sulfur starvation in rice: the effect on photosynthesis, carbohydrate metabolism, and oxidative stress protective pathways. *Physiologia Plantarum,* 134: 508-521.

Lynch M, **Walsh** B, **1998**. *Genetics and Analysis of Quantitative Traits.* Sinauer Associates, Sunderland, MA.

Ma J, **Takahashi** E, 1990. Effect of silicon on the growth and phosphorus uptake of rice. *Plant and Soil*, 126(1): 115–119.

Ma QH, **Xu** Y, **2008**. Characterization of a caffeic acid 3-O-methyltransferase from wheat and its function in lignin biosynthesis. *Biochimie,* 90: 515-524.

Ma JF, **Yamaji** N, **2006**. Silicon uptake and accumulation in higher plants. *Trends in Plant Science,* 11: 392-397.

Ma JF, **Yamaji** N, **2008**. Functions and transport of silicon in plants. *Cellular and Molecular Life Sciences,* 65: 3049-3057.

Ma XF, Wanous MK, Houchins K, Rodriguez Milla MA, Goicoechea PG, Wang Z, Xie M, Gustafson JP, **2001**. Molecular linkage mapping in rye (*Secale cereale* L.). *Theoretical and Applied Genetics*, 102(4): 517–523.

Ma QH, Xu Y, Lin ZB, He P, **2002**. Cloning of cDNA encoding COMT from wheat which is differentially expressed in lodging sensitive and resistant cultivars. *Journal of Experimental Botany,* 53: 2281-2282.

Maathuis FJM, **2013**. Sodium in plants: perception, signalling, and regulation of sodium fluxes. *Journal of Experimental Botany,* 65: 849-858.

Madej LJ, **1996**. Worldwide trends in rye growing and breeding. *Vorträge für Pflanzenzüchtung,* 35: 1-6.

Mahmud I, **Kramer** HH, **1951**. Segregation for yield, height, and maturity following a soybean cross. *Agronomy Journal,* 43 (12): 605-608.

Maier JA, **2013**. Magnesium and Cell Cycle. In: Kretsinger RH, Uversky VN, Permyakov EA (eds) *Encyclopedia of Metalloproteins.* Springer, New York.

Malyshev S, Korzun V, Voylokov A, Smirnov V, Börner A, **2001**. Linkage mapping of mutant loci in rye (*Secale cereale* L.). *Theoretical and Applied Genetics*, 103: 70–74.

Marschner H, **1995**. *Mineral nutrition of higher plants.* Academic Press, London.

Martis MM, Zhou R, Haseneyer G, Schmutzer T, Vrána J, Kubaláková M, König S, Kugler KG, Scholz U, Hackauf B, Korzun V, Schön CC, Dolezel J, Bauer E, Mayer KFX, Stein N, **2013**. Reticulate Evolution of the Rye Genome. *Plant Cell*, 25 (10): 3685-3698, DOI: 10.1105/tpc.113.114553.

Marzec M, Szarejko I, Melzer M, **2015**. Arabinogalactan proteins are involved in root hair development in barley. Journal of Experimental Botany, 66: 1245-1257.

Matoh T, **Kobayashi** M, **1998**. Boron and calcium, essential inorganic constituents of pectic polysaccharides in higher plant cell walls. *Journal of Plant Research,* 111: 179-190.

Matsuda T, Kawahara H, Chonan N, **1983**. Histological studies on breaking resistance of lower internodes in rice culm. IV The role of each tissue of internode and leaf sheath in breaking resistance. *Japanese Journal of Crop Science,* 52: 355-361.

Mayer KFX, Martis M, Hedley PE, Šimková H, Liu H, Morris JA, Steuernagel B, Taudien S, Roessner S, Gundlach H, Kubaláková M, Suchánková P, Murat F, Felder M, Nussbaumer T, Graner A, Salse J, Endo T, Sakai H, Tanaka T, Itoh T, Sato K, Platzer M, Matsumoto T, Scholz U, Doležel J, Waugh R, Stein N, **2011**. Unlocking the Barley Genome by Chromosomal and Comparative Genomics. *Plant Cell,* DOI: https://doi.org/10.1105/tpc.110.082537.

McCarthy JL, **Islam** A, **1999**. Lignin Chemistry, Technology, and Utilization: A Brief History. In: Glasser WG, Northey RA, Schultz TP (Eds.) *Lignin: Historical, Biological, and Materials Perspectives.* American Chemical Society, Washington, DC, USA.

Melz G, **1989**. Beitrfige zur Genetik des Roggens (*Secale cereale* L.). PhD thesis, AdL, Berlin, Germany.

Melz G, Schlegel R, Thiele V, **1992**. Genetic linkage map of rye (*Secale cereale* L.). *Theoretical and Applied Genetics,* 85: 33-45.

Mendel RR, **Kruse** T, **2012**. Cell biology of molybdenum in plants and humans. *Biochimica et Biophysica Acta*, 1823: 1568-1579.

Metcalfe CR, **1960**. *Anatomy of the Monocotyledons: I. Gramineae.* AT THE CLARENDON PRESS, Oxford.

Miedaner T, Müller BU, Piepho HP, Falke KC, **2011**. Genetic architecture of plant height in winter rye introgression libraries. *Plant Breeding,* 130: 209-216.

Miedaner T, Hübner M, Korzun V, Schmiedchen B, Bauer E, Haseneyer G, Wilde P, Reif JC, **2012**. Genetic architecture of complex agronomic traits examined in two testcross populations of rye (*Secale cereale* L.). *BMC Genomics,* 13: 706.

Milach SCK, **Federizzi** LC, **2001**. Dwarfing genes in plant improvement. *Advances in Agronomy,* 73: 35-63.

Milczarski P, **2008**. Identyfikacja QTL wybranych cech morfologicznych związanych z wyleganiem u żyta (*Secale cereale* L.). *Biuletyn Instytutu Hodowli i Aklimatyzacji Roślin,* 250: 211-216.

Milczarski P, **Masojć** P, **2002**. The mapping of QTLs for chlorophyll content and responsiveness to gibberellic (GA3) and abscisic (ABA) acids in rye. *Cellular & Molecular Biology Letters,* 7: 449-455.

Milczarski P, Bolibok-Brągoszewska H, Myśków B, Stojałowski S, Heller-Uszyńska K, Góralska M, Brągoszewski P, Uszyński G, Kilian A, Rakoczy-Trojanowska M, **2011**. A High Density Consensus Map of Rye (*Secale cereale* L.) Based on DArT Markers. *PLoS ONE,* 6(12): e28495.

Milczarski P, Hanek M, Tyrka M, Stojałowski S, **2016**. The application of GBS markers for extending the dense genetic map of rye (*Secale cereale* L.) and the localization of the *Rfc1* gene restoring male fertility in plants with the C source of sterility-inducing cytoplasm. *Journal of Applied Genetics,* 57: 439-451.

Miller FL, **Anderson** L, **1963**. Relationship in winter wheat between lodging physical properties of stems and fertilizer treatments. *Crop Science,* 42: 1147-1154.

Miralles DJ, **Slafer** GA, **1995**. Individual grain weight responses to genetic reduction in culm length in wheat as affected by source-sink manipulations. *Field Crops Research,* 43: 55-66.

Miura K, Ikeda M, Matsubara A, Song XJ, Ito M, Asano K, Matsuoka M, Kitano H, Ashikari M, **2010**. *OsSPL14* promotes panicle branching and higher grain productivity in rice. *Nature Genetics,* 42: 545-549.

Monasterio I, **Graham** RD, **2000**. Breeding for trace minerals in wheat. *Food and Nutrition Bulletin,* 21: 392-396.

Monna L, Kitazawa N, Yoshino R, Suzuki J, Masuda H, Maehara Y, Tanji M, Sato M, Nasu S, Minobe Y, **2002**. Positional Cloning of Rice Semidwarfing Gene, *sd-1:* Rice "Green Revolution Gene" Encodes a Mutant Enzyme Involved in Gibberellin Synthesis. *DNA Research,* 9(1): 11–17.

Montfort F, Klepper BL, Smiley RW, **1996**. Effects of two triazole seed treatments, triticonazole and Triadimenol, on growth and development of wheat. *Pesticide Science,* 46(4): 315-322.

Morikawa H, **Senda** M, **1974**. Oriented structure of matrix polysaccharides in and extension growth of *Nitella* cell wall. *Plant and Cell Physiology,* 15: 1139–1142.

Mulder EG, **1954**. Effect of mineral nutrition on lodging of cereals. *Plant and Soil,* 5: 246-306.

Murthy BN, **Rao** MV, **1980**. Evolving suitable index for lodging resistance in barley. *Indian Journal of Genetics and Plant Breeding,* 40: 253-261.

Nagai K, Kondo Y, Kitaoka T, Noda T, Koruha T, Angeles-Shim RB, Yasui H, Yoshimura A, Ashikari M, **2014**. QTL analysis of internode elongation in response to gibberellin in deepwater rice. *AoB PLANTS,* 6: plu028.

Nakajima N, Morikawa H, Igarashi S, Senda M, **1981**. Differential effect of calcium and magnesium on mechanical properties of pea stem walls. *Plant and Cell Physiology,* 22(7): 1305-1315.

Naruoka Y, Talbert LE, Lanning SP, Blake NK, Martin JM, Sherman JD, **2011**. Identification of quantitative trait loci for productive tiller number and its relationship to agronomic traits in spring wheat. *Theoretical and Applied Genetics,* 123(6): 1043-53.

Neenan M, **Spencer-Smith** JL, **1975**. An analysis of the problem of lodging with particular reference to wheat and barley. *Journal of Agricultural Science,* 85: 495-507.

Nelson JC, **1997**. QGENE: software for marker-based genomic analysis and breeding. *Molecular Breeding,* 3: 239-245.

Neumann D, **2003**. Silicon in Plants. *Progress in Molecular and Subcellular Biology,* 33: 149-160.

Newman AM, **Cooper** JB, **2011**. Global Analysis of Proline-Rich Tandem Repeat Proteins Reveals Broad Phylogenetic Diversity in Plant Secretomes. PLoS ONE, 6 (8): e23167.

Nilsson M, Åman P, Härkönen H, Hallmans G, Bach Knudsen KE, Mazur W, Adlercreutz H, **1997**. Content of Nutrients and Lignans in Roller Milled Fractions of Rye. *Journal of the Science of Food and Agriculture,* 73: 143-148.

Oehme F, **1989**. Studies of lodging resistance in winter rye: testing plant characters for evaluation of lodging resistance. *Archiv für Züchtungsforschung,* 19: 407-414.

Okuno A, Hirano K, Asano K, Takase W, Masuda R, Morinaka Y, Ueguchi-Tanaka M, Kitano H, Matsuoka M, **2014**. New approach to increasing rice lodging resistance and biomass yield through the use of high gibberellin producing varieties. *PLoS One,* 9: e86870.

Ookawa T, **Ishihara** K, **1993**. Varietal difference of the cell wall components affecting the bending stress of the culm in relation to the lodging resistance in paddy rice. *Jpn J. Crop Sci,* 62: 378-384.

Ookawa T, Hobo T, Yano M, Murata K, Ando T, Miura H, Asano K, Ochiai Y, Ikeda M, Nishitani R, Ebitani T, Ozaki H, Angeles ER, Hirasawa T, Matsuoka M, **2010**. New approach for rice improvement using a pleiotropic QTL gene for lodging resistance and yield. *Nature Communications,* 1: Article number 132, doi:10.1038/ncomms1132.

Ookawa T, Aoba R, Yamamoto T, Ueda T, Takai T, Fukuoka S, Ando T, Adachi S, Matsuoka M, Ebitani T, Kato Y, Mulsanti IW, Kishii M, Reynolds M, Piñera F, Kotake T, Kawasaki S, Motobayashi T, Hirasawa T, **2016**. Precise estimation of genomic regions controlling lodging resistance using a set of reciprocal chromosome segment substitution lines in rice. *Scientific Reports*, 6: Article number 30572.

Packa D, Wiwart M, Suchowilska E, Bieńkowska E, **2015**. Morpho-anatomical traits of two lowest internodes related to lodging resistance in selected genotypes of *Triticum*. *International Agrophysics,* 29: 275-483.

Pear JR, Kawagoe Y, Schreckengost WE, Delmer DP, Stalker DM, **1996**. Higher plants contain homologs of the bacterial *celA* genes encoding the catalytic subunit of cellulose synthase. *PNAS,* 93: 12637-12642.

Peng J, Richards DE, Moritz T, Caño-Delgado A, Harberd NP, **1999**. Extragenic Suppressors of the Arabidopsis *gai*Mutation Alter the Dose-Response Relationship of Diverse Gibberellin Responses. *Plant Physiology,* 119: 1199–1207.

Pillen K, Binder A, Kreuzkam B, Ramsay L, Waugh R, Förster J, Léon J, **2000**. Mapping new EMBL-derived barley microsatellites and their use in differentiating German barley cultivars. *Theor Appl Genet*, 101:652–660.

Pinthus MJ, **1967**. Spread of the root system as an indicator for evaluating lodging resistance in wheat. *Crop Science,* 7: 107-110.

Pinthus MJ, **1973**. Lodging in wheat, barley and oats: the phenomenon, its causes and preventative measures. *Advances in Agronomy,* 25: 209-263.

Pinthus MJ, **Gale** MD, **1990**. The effects of 'gibberellin-insensitive' dwarfing alleles in wheat on grain weight and protein content. *Theoretical and Applied Genetics,* 79: 108-112.

Pinthus MJ, **Levy** AA, **1983**. The relationship between the *Rht1* and *Rht2* dwarfing genes and grain weight in *Triticum aestivum* L. spring wheat. *Theoretical and Applied Genetics,* 66: 153-157.

Plaschke J, Börner A, Xie DX, Koebner RMD, Schlegel R, Gale MD, **1993**. RFLP mapping of genes affecting plant height and growth habit in rye. *Theoretical and Applied Genetics,* 85: 1049-1054.

Plaschke J, Ganal MW, Röder MS, **1995a**. Detection of genetic diversity in closely related bread wheat using microsatellite markers. *Theoretical and Applied Genetics,* 91: 1001-1007.

Plaschke J, Korzun V, Koebner RMD, Börner A, **1995b**. Mapping the GA$_3$-insensitive dwarfing gene *ct1* on chromosome 7 in rye. *Plant Breeding,* 114: 113–116.

Printz B, Lutts S, Hausman J-F, Sergeant K, **2016**. Copper Trafficking in Plants and Its Implication on Cell Wall Dynamics. *Frontiers in Plant Science,* https://doi.org/10.3389/fpls.2016.00601

Rademacher W, **2000**. Growth retardants: effects on gibberellin biosynthesis and other metabolic pathways. *Annual Review of Plant Physiology and Plant Molecular Biology,* 51: 501-531.

Rafi MM, **Epstein** E, **1997**. Silicon deprivation causes physical abnormalities in wheat (*Triticum aestivum* L.). *Journal of Plant Physiology,* 151: 497-501.

Rakowska M, **1996**. The nutritive quality of rye. *Vorträge für Pflanzenzüchtung,* 35: 85-95.

Ralph J, Lundquist K, Brunow G, Lu F, Kim H, Schatz PF, Marita JM, Hatfield RD, Ralph SA, Christensen JH, Boerjan W, **2004**. Lignins: Natural polymers from oxidative coupling of 4-hydroxyphenyl-propanoids. *Phytochemistry Reviews,* 3: 29-60.

Raven JA, Evans MCW, Korb RE, **1999**. The role of trace metals in photosynthetic electron transport in O$_2$-evolving organisms. *Photosynthesis Research,* 60: 111–149.

Remison SU, **Akinleye** D, **1978**. Relationship between lodging, morphological characters and yield of variates of maize (Zea mays L.). *Journal of Agricultural Science,* 91: 633-638.

Reynolds ES, **1963**. The Ude of Lead Citrate at High pH as an Electron-Opaque Stain in Electron Microscopy. *Journal of Cell Biology*, 17(1): 208–212.

Rich PM, **1986**. Mechanical architecture of arborescent rain forest palms. *Principes,* 30: 117–131.

Rich PM, **1987a**. Mechanical structure of the stem of arborescent palms. *Botanical Gazette,* 148: 42–50.

Rich PM, **1987b**. Developmental anatomy of the stem of *Welfia georgii, Iriartea gigantea*, and other arborescent rainforest palms: implications for mechanical support. *American Journal of Botany,* 74: 792–802.

Robson AD, Hartley RD, Jarvis SC, **1981**. Effect of copper deficiency on phenolic and other constituents of wheat cell walls. *New Phytologist*, 89: 361-371.

Röder MS, Korzun V, Wendehake K, Plaschke J, Tixier MH, Leroy P Martin W. Ganal MW, **1998**. A Microsatellite Map of Wheat. *Genetics,* 149(4): 2007-2023.

Rossini LA, Vecchietti A, Nicoloso L, Stein N, Franzago S, Salamini F, Pozzi C, **2006**. Candidate genes for barley mutants involved in plant architecture: An *in silico* approach. *Theoretical and Applied Genetics,* 112: 1073-1085.

Roudier F, Fernandez AG, Fujita M, Himmelspach R, Borner GHH, Schindelman G, Song S, Baskin TI, Dupree P, Wasteneys GO, Benfey PN, **2005**. COBRA, an Arabidopsis extracellular glycosyl-phosphatidyl inositol-anchored protein, specifically controls highly anisotropic expansion through its involvement in cellulose microfibril orientation. *Plant Cell,* 17: 1749-1763.

Rovenská B, **1973**. Anatomický atlas žita. ACADEMIA NAKLADATELSTVÍ ČESKOSLOVENSKÉ AKADEMIE VĚD, Praha.

Rudall PJ, **Caddick** LR, **1994**. Investigation of the presence of phenolic compounds in monocotyledonous cell walls using UV fluorescence microscopy. *Annals of Botany,* 74: 483-491.

Rüggeberg M, Speck T, Burgert I, **2009**. Structure–function relationships of different vascular bundle types in the stem of the Mexican fanpalm (*Washingtonia robusta*). *New Phytologist,* DOI: 10.1111/j.1469-8137.2008.02759.x.

Saal B, **Wricke** G, **1999**. Development of simple sequence repeat markers in rye (*Secale cereale* L.). *Genome*, 42(5): 964-972.

Sadeghzadeh B, Rengel Z, Li C, **2015**. Quantitative trait loci (QTL) of seed Zn accumulation in barley population Clipper x Sahara. *Journal of Plant Nutrition*, 38: 1672-1684.

Salmon SC, **1931**. An instrument for determining the breaking strength of straw and a preliminary report on the relation between breaking strength and lodging. *Journal of Agricultural Research,* 43: 73-82.

Sarker ZI, Shamsuddin AKM, Rahman L, Ara R, **2007**. Genotypic and phenotypic correlation and path analysis for lodging resistance traits in bread wheat (Triticum aestivum L.). *Bangladesh J Genet Pl Breed,* 20 (2): 51-57.

Sasaki T, Matsumoto T, Yamamoto K, Sakata K, Baba T, Katayose Y, Wu J, Niimura Y, Cheng Z, Nagamura Y, Antonio BA, Kanamori H, Hosokawa S, Masukawa M, Arikawa K, Chiden Y, Hayashi M, Okamoto M, Ando T, Aoki H, Arita K, Hamada M, Harada C, Hijishita S, Honda M, Ichikawa Y, Idonuma A, Iijima M, Ikeda M, Ikeno M, Ito S, Ito T, Ito Y, Ito Y, Iwabuchi A, Kamiya K, Karasawa W, Katagiri S, Kikuta A, Kobayashi N, Kono I, Machita K, Maehara T, Mizuno H, Mizubayashi T, Mukai Y, Nagasaki H, Nakashima M, Nakama Y, Nakamichi Y, Nakamura M, Namiki N, Negishi M, Ohta I, Ono N, Saji S, Sakai K, Shibata M, Shimokawa T, Shomura A, Song J, Takazaki Y, Terasawa K, Tsuji K, Waki K, Yamagata H, Yamane H, Yoshiki S, Yoshihara R, Yukawa K, Zhong H, Iwama H, Endo T, Ito H, Hahn JH, Kim HI, Eun MY, Yano M, Jiang J, Gojobori T, **2002**. The genome sequence and structure of rice chromosome 1. *Nature*, 420: 312–316.

Scalbert A, Monties B, Lallemand JY, Guittet E, Rolando C, **1985**. Ether linkage between phenolic acids and lignin fractions from wheat straw. *Phytochemistry,* 24: 1359-1362.

Schindelin J, Arganda-Carreras I, Frise E, Kaynig V, Longair M, Pietzsch T, Preibisch S, Rueden C, Saalfeld S, Schmid B, Tinevez JY, White DJ, Hartenstein V, Eliceiri K, Tomancak P, Cardona A, **2012**. Fiji: an open-source platform for biological-image analysis. *Nature Methods,* 9: 676–682.

Schlegel RHJ, **2014**. *Rye: Genetics, Breeding, and Cultivation.* CRC Press, Boca Ranton, USA.

Schlegel R, Melz G, Mettin D, **1986**. Rye cytology, cytogenetics and genetics - Current status. *Theoretical and Applied Genetics,* 72: 721-734.

Schlegel R, Kynast R, Schwarzacher T, Römheld V, Walter A, **1993**. *Plant and Soil.* 154(1): 61-65.

Schlegel R, Melz G, Korzun V, **1998**. Genes, marker and linkage data of rye (*Secale cereale* L.): 5th updated inventory. *Euphytica,* 101: 23–67.

Senft P, **Wricke** G, **1996**. An extended genetic map of rye (*Secale cereale* L.). *Plant Breeding*, 115: 508—510.

Shah MM, Gill KS, Baenzinger PS, Yen Y, Kaeppler SM, Ariyarathne HM, **1999**. Molecular mapping of loci for agronomic traits on chromosome 3A of bread wheat. *Crop Science,* 39: 1728-1732.

Sheng Q, **Hunt** LA, **1991**. Shoot and root dry weight and soil water in wheat, triticale and rye. *Canadian Journal of Plant Science,* 71: 41-49.

Showalter AM, **1993**. Structure and function of plant cell wall proteins. *Plant Cell,* 5: 9-23.

Sindhu A, Langewisch T, Olek A, Multani DS, McCann MC, Vermerris W, Carpita NC, Johal G, **2007**. Maize Brittle stalk2 encodes a COBRA-like protein expressed in early organ development but required for tissue flexibility at maturity. *Plant Physiology,* 145: 1444-1459.

Smallwood M, Martin H, Knox JP, **1995**. An epitope of rice threonine- and hydroxyproline-rich glycoprotein is common to cell wall and hydrophobic plasma-membrane glycoproteins. *Planta,* 196: 510-522.

Smirnov VG, **Sosnichina** SP, **1984**. *Генетика ржи*. Издателство ЛГУ, Ленинград.

Smith FW, Hawkesford MJ, Ealing PM, Clarkson DT, Vanden Berg PJ, Belcher AR, Warrilow AG, **1997**. Regulation of expression of a cDNA from barley roots encoding a high affinity sulphate transporter. *Plant Journal,* 12: 875-84.

Solberg E, Evans I, Penny D, **1999**. Copper deficiency: diagnosis and correction. Agri-facts. Soil fertility/crop nutrition. Alberta agriculture, food and rural development. *Agdex,* 532-533: 1-9.

Spencer WF, **1960**. Effects of heavy applications of phosphate and lime on nutrient uptake, growth, freeze injury, and root distribution of grape fruit trees. *Soil Science*, 89: 311–318.

Spielmeyer W, Ellis MH, Chandler PM, 2002. Semidwarf (*sd-1*), "green revolution" rice, contains a defective gibberellin 20-oxidase gene. *Proceedings of the National Academy of Sciences of the United States of America*, 99(13): 9043-9048.

Steudle E, **Zimmermann** U, **1977**. Effect of turgor pressure and cell size on the wall elasticity of plant cells. *Plant Physiology,* 59: 285-289.

Stiefel V, Ruiz-Avila L, Raz R, Vallés MP, Gómez J, Pagés M, Martinez-Izquierdo JA, Ludevid MD, Langdale JA, Nelson T, **1990**. Expression of a maize cell wall hydroxyproline-rich glycoprotein gene in early leaf and root vascular differentiation. *Plant Cell,* 2: 785-793.

Stojałowski SA, Myśków B, Hanek M, **2015**. Phenotypic effect and chromosomal localization of *Ddw3*, the dominant dwarfing gene in rye (*Secale cereale* L.). *Euphytica,* 201: 43-52.

Stukenholtz DD, Olsen RJ, Gogan G, Olson RA, **1966**. On the mechanism of phosphorus-zinc interaction in corn nutrition. *Soil Science Society of America Proceedings,* 30: 759-763.

Sturaro M, Linnestad C, Kleinhofs A, Olsen OA, Doan DNP, **1998**. Characterization of a cDNA encoding a putative extensin from developing barley grains (Hordeum vulgare L.). Journal of Experimental Botany, 329: 1935-1944.

Sturm W, **Engel** KH, **1980**. Trisomenanalyse des Allels HI für Kurzstrohigkeit bei *Secale cereale* L. *Archiv für Züchtungsforschung,* 10: 31-35.

Sturm W, **Müller** HW, **1982**. Localization of the recessive gene of Moscow dwarf mutant short straw character in *Secale cereale* L. *Цитология и Генетика,* 16: 13-17.

Subbarao GV, Ito O, Berry WL, Wheeler RM, **2003**. Sodium: a functional plant nutrient. *Critical Reviews in Plant Sciences,* 22: 391-416.

Sun Y, **Cheng** JJ, **2005**. Dilute acid pretreatment of rye straw and bermudagrass for ethanol production. *Bioresource Technology,* 96: 1599–1606.

Sussex IM, **1989**. Developmental programming of the shoot meristem. *Cell,* 56: 225-229.

Sybenga J, **Prakken** R, **1963**. Gene analysis in rye. *Genetica,* 33: 95-105.

Takahashi H, Watanabe-Takahashi A, Smith FW, Blake-Kalff M, Hawkesford MJ, Saito K, 2010. The roles of three functional sulphate transporters involved in uptake and translocation of sulphate in *Arabidopsis thaliana*. *Plant Journal,* 23(2): 171-182.

Tang ZX, Ross K, Ren ZL, Yang ZJ, Zhang HY, Chikmawati T, Miftahudin M, Gustafson JP, **2011**. *Secale*. In: Kole C (Ed.) Wild Crop Relatives: Genomic and Breeding Resources. Springer-Verlag, Berlin, Germany.

Tenhola-Roininen T, **Tanhuanpää** P, **2010**. Tagging the dwarfing gene *Ddw1* in a rye population derived from doubled haploid parents. *Euphytica,* 172: 303–312.

Tomková L, Kučera L, Vaculová K, Milotová J, **2012**. Characterization and mapping of a putative laccase-like multicopper oxidase gene in the barley (*Hordeum vulgare* L.). *Plant Science,* 183: 77-85.

Tripathi SC, Sayre KD, Kaul JN, Narang RS, **2003**. Growth and morphology of spring wheat (*Triticum aestivum* L.) culms and their association with lodging: effects of genotypes, N levels and ethephon. *Field Crops Research,* 84: 271–290.

Tubbs FR, **1930**. Physiological studies in plant nutrition. II. The effect of manorial deficiency upon the mechanical strength of barley straw. *Annals of Botany*, 44: 147-160.

Turner SR, **Somerville** CR, **1997**. Collapsed xylem phenotype of Arabidopsis identifies mutants deficient in cellulose deposition in the secondary cell wall. *Plant Cell,* 9: 689-701.

Tyrka M, Bednarek PT, Kilian A, Wędzony M, Hura T, Bauer E, **2011**. Genetic map of triticale compiling DArT, SSR, and AFLP markers. *Genome,* 54: 391-401.

Vaculík M, Landberg T, Greger M, Luxová M, Stoláriková, Lux A, **2012**. Silicon modifies root anatomy, and uptake and subcellular distribution of cadmium in young maize plants. *Annals of Botany*, 110: 433–443.

Verma V, Worland AJ, Savers EJ, Fish L, Caligari PDS, Snape JW, **2005**. Identification and characterization of quantitative trait loci related to lodging resistance and associated traits in bread wheat. *Plant Breeding,* 124: 234-241.

Vogel J, **2008**. Unique aspects of the grass cell wall. *Current Opinion in Plant Biology,* 11: 301–307.

von Korff M, Wang H, Léon J, Pillen K, **2006**. AB-QTL analysis in spring barley: II. Detection of favourable exotic alleles for agronomic traits introgressed from wild barley (*H. vulgare* ssp. *spontaneum*). *Theoretical and Applied Genetics,* 112: 1221–1231.

Voylokov AV, **Priyatkina** SN, **2004**. Linkage of Genes Controlling Morphological Traits with Isozyme Markers of Rye Chromosomes. *Russian Journal of Genetics,* 40: 56–61.

Vreugdenhil D, Aarts MGM, Koornneef M, Nelissen H, Ernst WHO, **2004**. Natural variation and QTL analysis for cationic mineral content in seeds of Arabidopsis thaliana. *Plant, Cell & Environment,* 27: 828-839.

Wang Y, **Li** J, **2006**. Genes controlling plant architecture. *Current Opinion in Biotechnology,* 17: 123-129.

Wang Y, **Li** J, **2011**. Branching in rice. *Current Opinion in Plant Biology,* 14: 94-99.

Wang J, Zhu J, Lin Q, Li X, Teng N, Li Z, Li B, Zhang A, Lin J, **2006**. Effects of the stem structure and cell wall components on bending strength in wheat. *Chinese Science Bulletin,* 51 (7): 815-823.

Waseem M, Ahmad R, Randhawa MA, Aziz T, Mahmood N, **2016**. Influence of silicon application on blast incidence and lodging resistance in rice. *Journal of Agricultural Research,* 54: 435-443.

Watanabe FS, Lindsay WL, Olsen SR. **1965**. Nutrient Balance Involving Phosphorus, Iron, and Zinc. Soil Science Society of America Journal, 29: 562-565.

Webster JR, **Jackson** LF, **1993**. Management practices to reduce lodging and maximize grain yield and protein content of fall-sown irrigated hard red spring wheat. *Field Crops Research,* 33: 240-259.

Weibel RO, **Pendleton** JW, **1964**. Effect of artificial lodging on winter wheat grain yield and quality. *Agronomy Journal,* 56: 487-488.

Welker CM, Balasubramanian VK, Petti C, Rai KM, DeBolt S, Mendu V, **2015**. Engineering Plant Biomass Lignin Content and Composition for Biofuels and Bioproducts. *Energies*, 8: 7654-7676

Welton FA, **1928**. Lodging in Oats and Wheat. *Botanical Gazette*, 85: 121-151.

White EM, **1991**. Response of winter barley cultivars to nitrogen and a plant growth regulator in relation to lodging. *Journal of Agricultural Science,* 116: 191-200.

White EM, McGarel ASL, Ruddle O, **2003**. The influence of variety, year, disease control and plant growth regulator application on crop damage, yield and quality of winter oats (*Avena sativa*). *Journal of Agricultural Science,* 140: 31-42.

Wilkinson SR, Welch RM, Mayland HF, Grunes DL, **1990**. Magnesium in plants: Uptake, distribution, function, and utilization by man and animals. *Metal Ions in Biological Systems,* 26: 33–56.

Williams MNV, Freshour G, Darvill AG, Albersheim P, Hahn MG, **1996**. An antibody Fab selected from a recombinant phage display library detects deestrified pectic polysaccharide rhamnogalacturonan II in plant cells. *Plant Cell,* 8: 673-685.

Wolf FI, **Trapani** V, **2008**. Cell (patho)physiology of magnesium. *Clin Sci (Lond),* 114(1): 27-35.

Wong CL, Tong SM, Fu JL, Ya JF, **1994**. Silicon availability and response of rice and wheat to silicon in calcareous soils. *Communications in Soil Science and Plant Analysis,* 25: 2285-2297.

Worland AJ, Law CN, Shakoor A, **1980**. The genetical analysis of an induced height mutant in wheat. *Heredity,* 45: 61–71.

Wu WR, Li WM, Tang DZ, Lu HR, Worland AJ, **1999**. Time-related mapping of quantitative trait loci underlying tiller number in rice. *Genetics,* 151: 297-303.

Wych RD, Simmons SR, Warner RL, Kirby EJM, **1988**. Physiology and development. In: DC Rasmusson (Ed): *Barley. Agronomical Monographs 26.* ASA, Madison, WI.

Yan JQ. Zhu J, He CX, Benmoussa M, Wu P, **1998**. Quantitative trait loci analysis for the developmental behaviour of tiller number in rice (*Oryza sativa* L.). *Theoretical and Applied Genetics*, 97: 267-274.

Yang XC, **Hwa** CM, **2008**. Genetic modification of plant architecture and variety improvement in rice. *Heredity,* 101: 396–404.

Yruela I, **2005**. Copper in plants. *Brazilian Journal of Plant Physiology,* 17 (1): 145-156.

Yoshida S, **Chaudhry** MR, **1979**. Sulfur nutrition of rice. *Soil Science and Plant Nutrition,* 25: 121-134.

Yoshida S, Ohnishi Y, Kitagishi, **1962**. Histochemistry of silicon in rice plant. *Soil Science and Plant Nutrition,* 8: 36-41.

Yoshimoto N, Inoue E, Watanabe-Takahashi A, Saito K, Takahashi H, **2007**. Posttranscriptional regulation of high-affinity sulfate transporters in Arabidopsis by sulfur nutrition. *Plant Physiology,* 145: 378–88.

Yu JK, Graznak E, Breseghello F, Tefera H, Sorrells ME, **2007**. QTL mapping of agronomic traits in tef [*Eragrostis tef* (Zucc) Trotter]. *BMC Plant Biology*, 7:30, doi:10.1186/1471-2229-7-30.

Yun L, Larson SR, Jensen KB, Staub JE, Grossl PR, **2015**. Quantitative trait loci (QTL) and candidate genes associated with trace element concentrations in perennial grasses frown on phytotoxic soil contaminated with heavy metals. *Plant Soil,* 396: 277-296.

Zhang ZH, Li P, Wang LX, Hu ZL, Zhu LH, Zhu YG, **2004**. Genetic dissection of the relationships of biomass production and partitioning with yield and yield related traits in rice. *Plant Science,* 167: 1-8.

Zuber U, Winzeler H, Messmer MM, Keller M, Keller B, Schmid JE, Stamp P, **1999**. Morphological traits associated with lodging resistance of spring wheat (*Triticum aestivum* L.). *Journal of Agronomy and Crop Science,* 182: 17-24.

Żebrowski J, **1992**. Structural and mechanical determinants and methods of lodging resistance estimation in cereals. Part I. Morphological and anatomical traits of stem. *Biuletyn IHAR,* 183: 73-82.
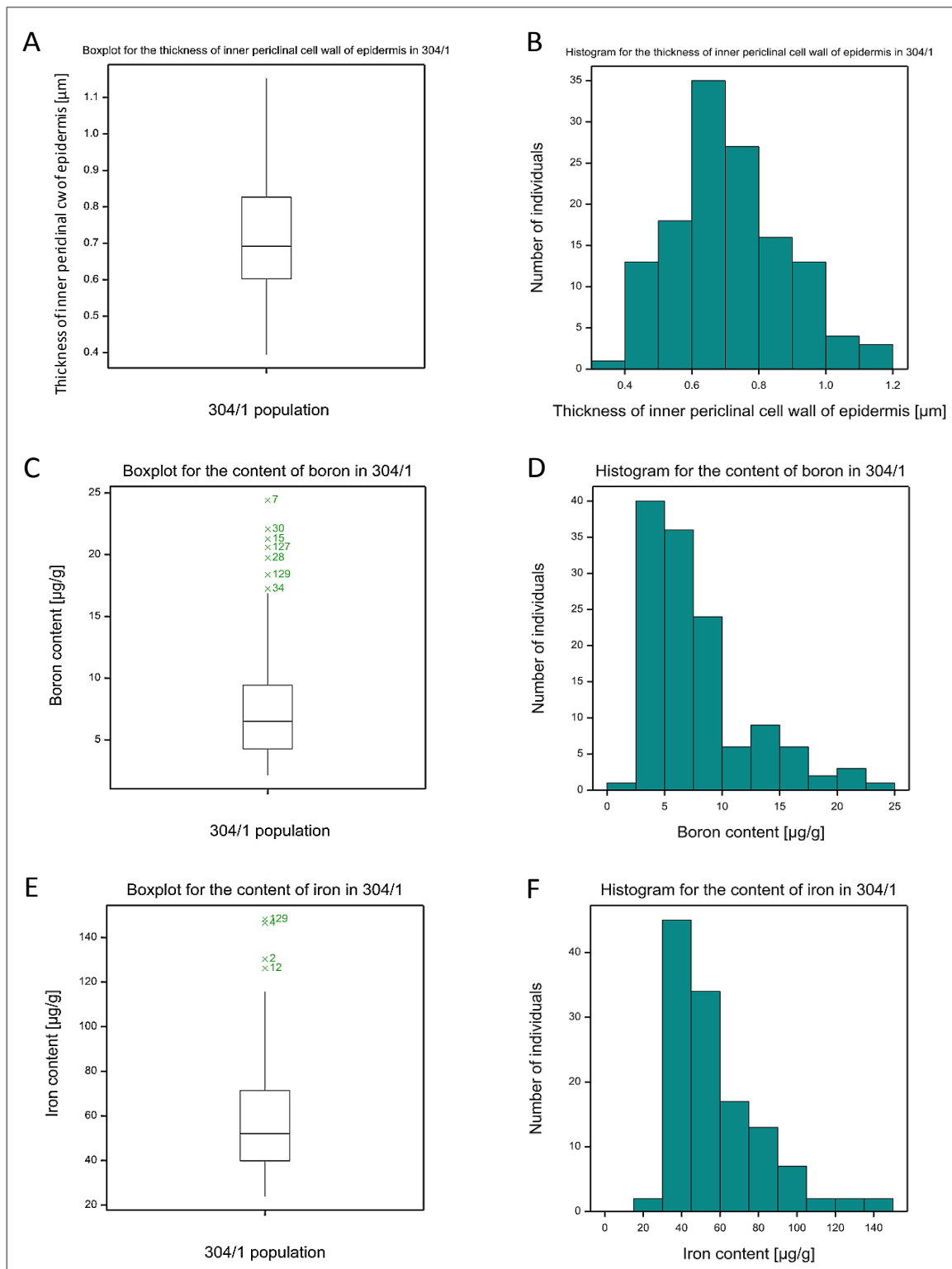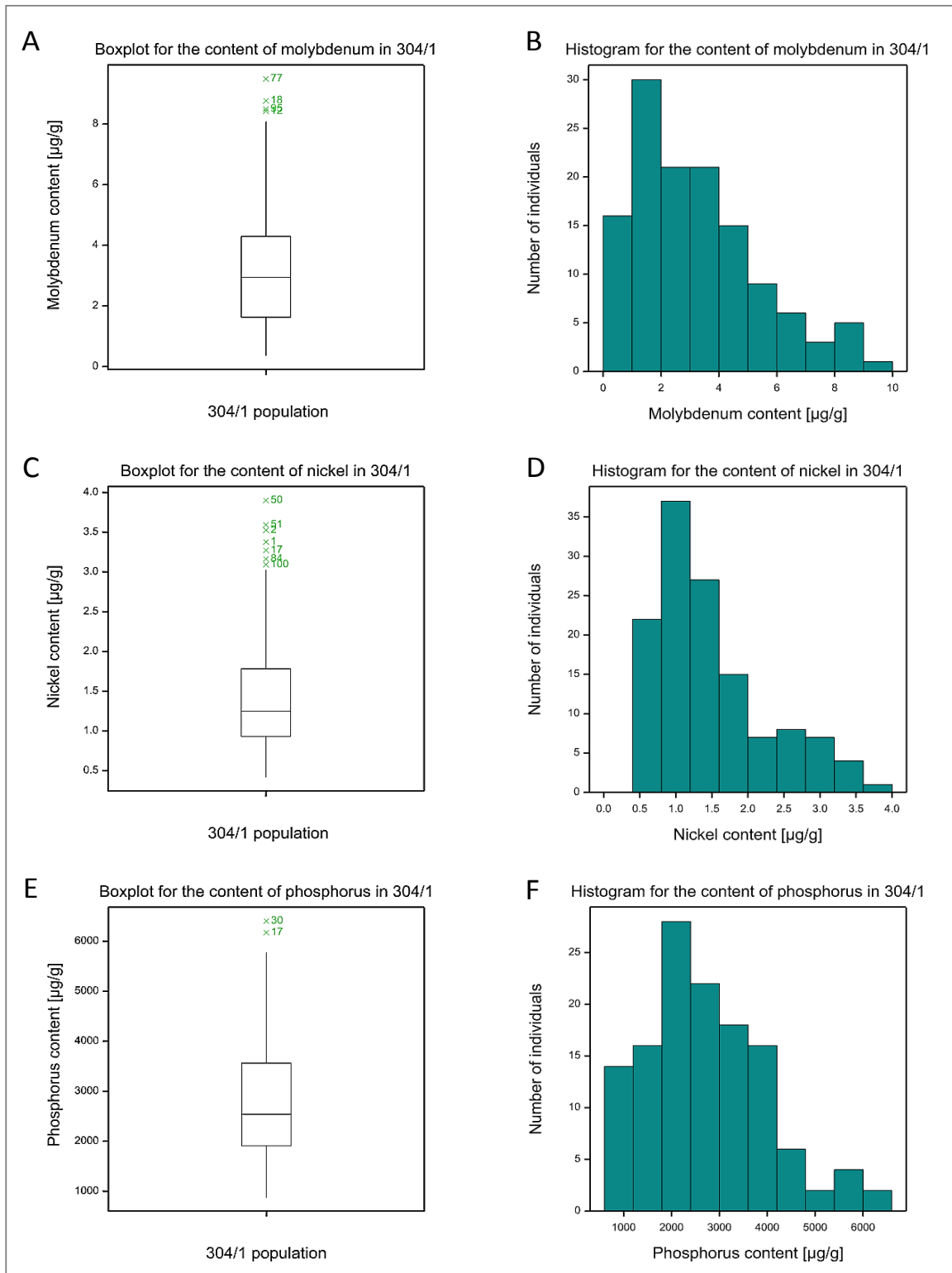
9. Supplementary data
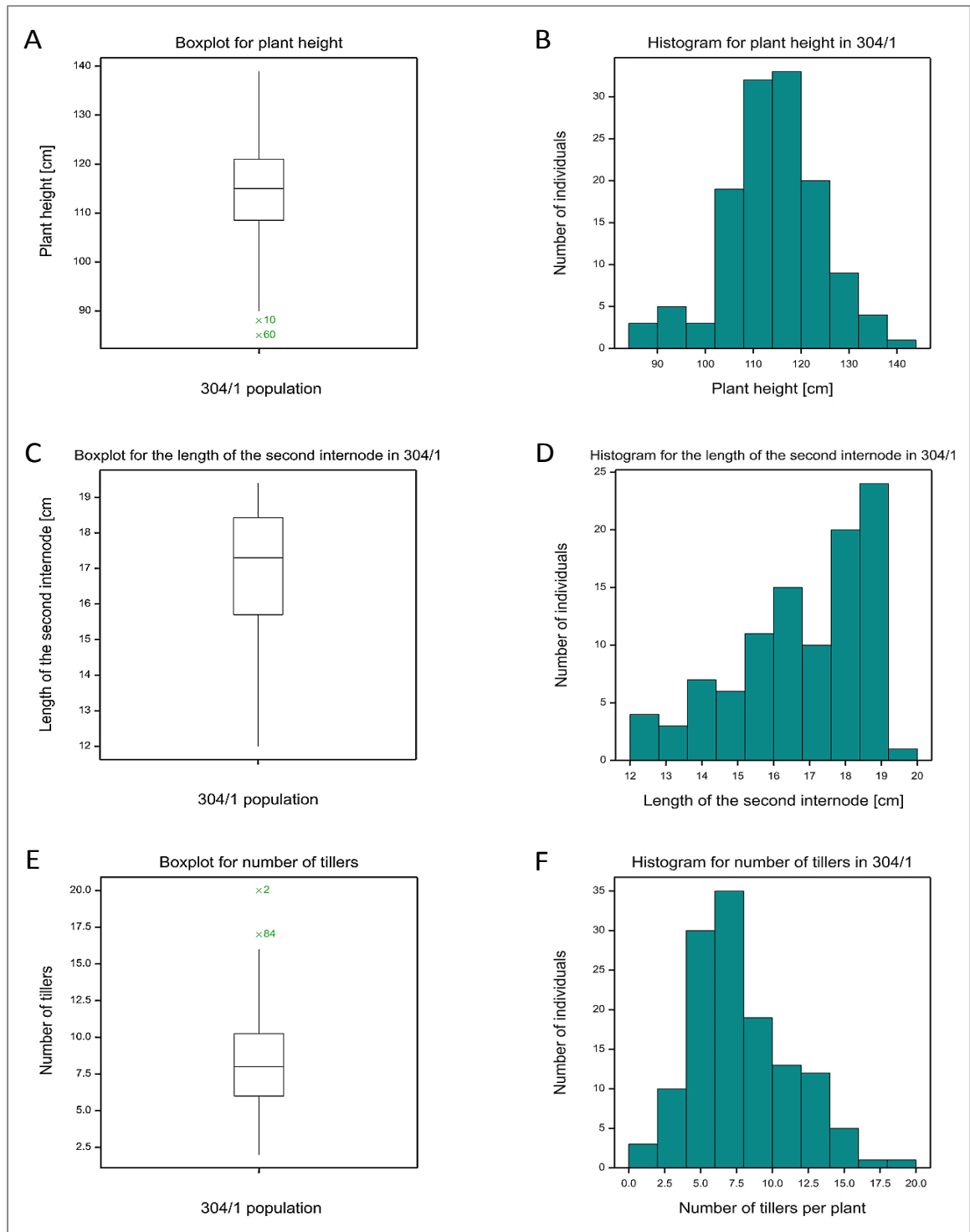
FIGURE 45 Boxplots showing median value with whiskers indicating variability outside the upper and lower quartiles in '304/1' F_2 population for plant height (A), the length of the second basal internode (C), and the number of tillers (E). The distribution of traits in F_2 population: plant height (B), the length of the second basal internode (D), the number of tillers (F).
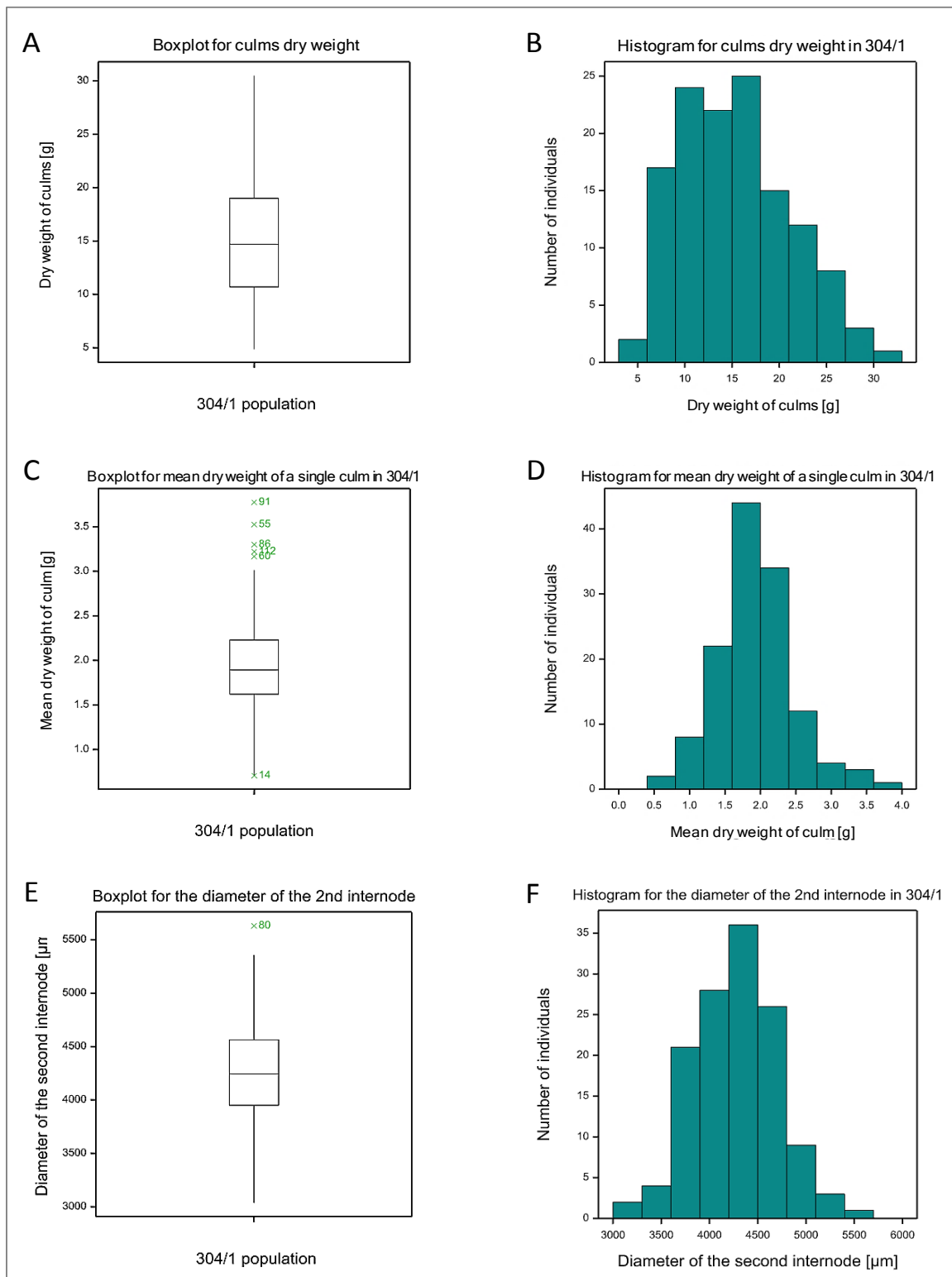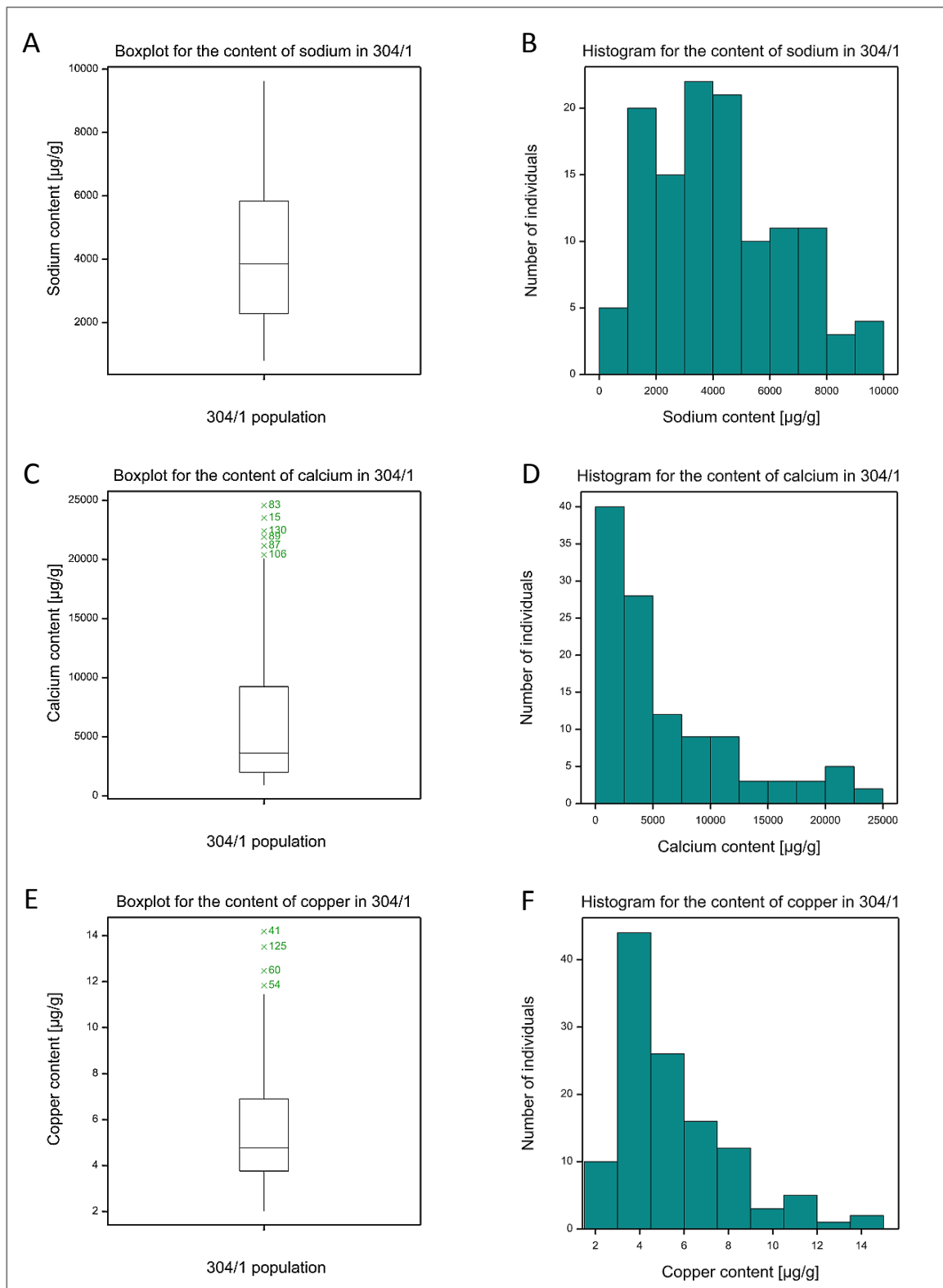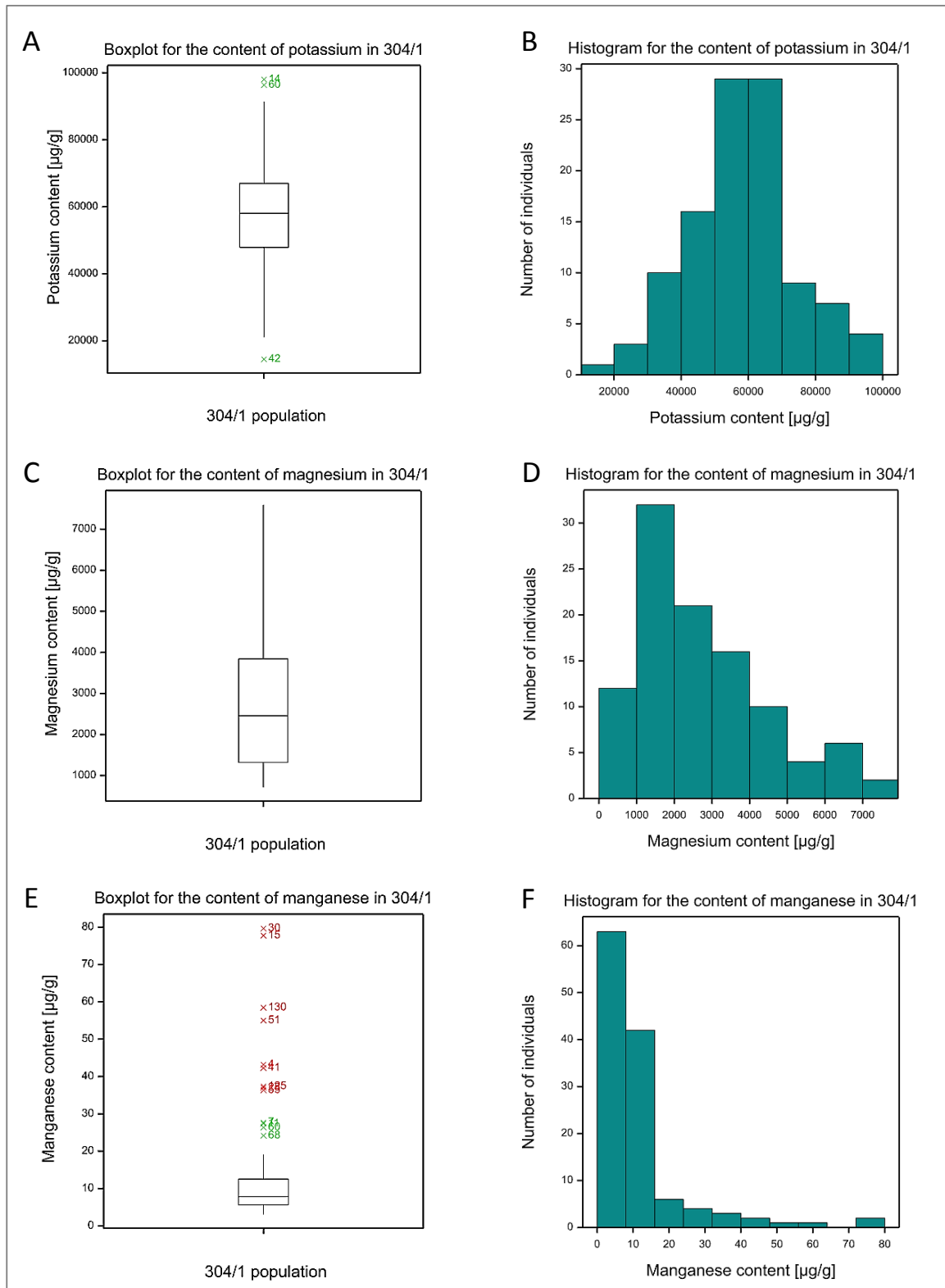
FIGURE 46 Boxplots showing median value with whiskers indicating variability outside the upper and lower quartiles in '304/1' F_2 population for total culms dry weight (A), mean dry weight of a single culm (C), and the diameter of the second basal internode (E). The distribution of traits in F_2 population: total culms dry weight (B), mean dry weight of a single culm (D), the diameter of the second basal internode (F).
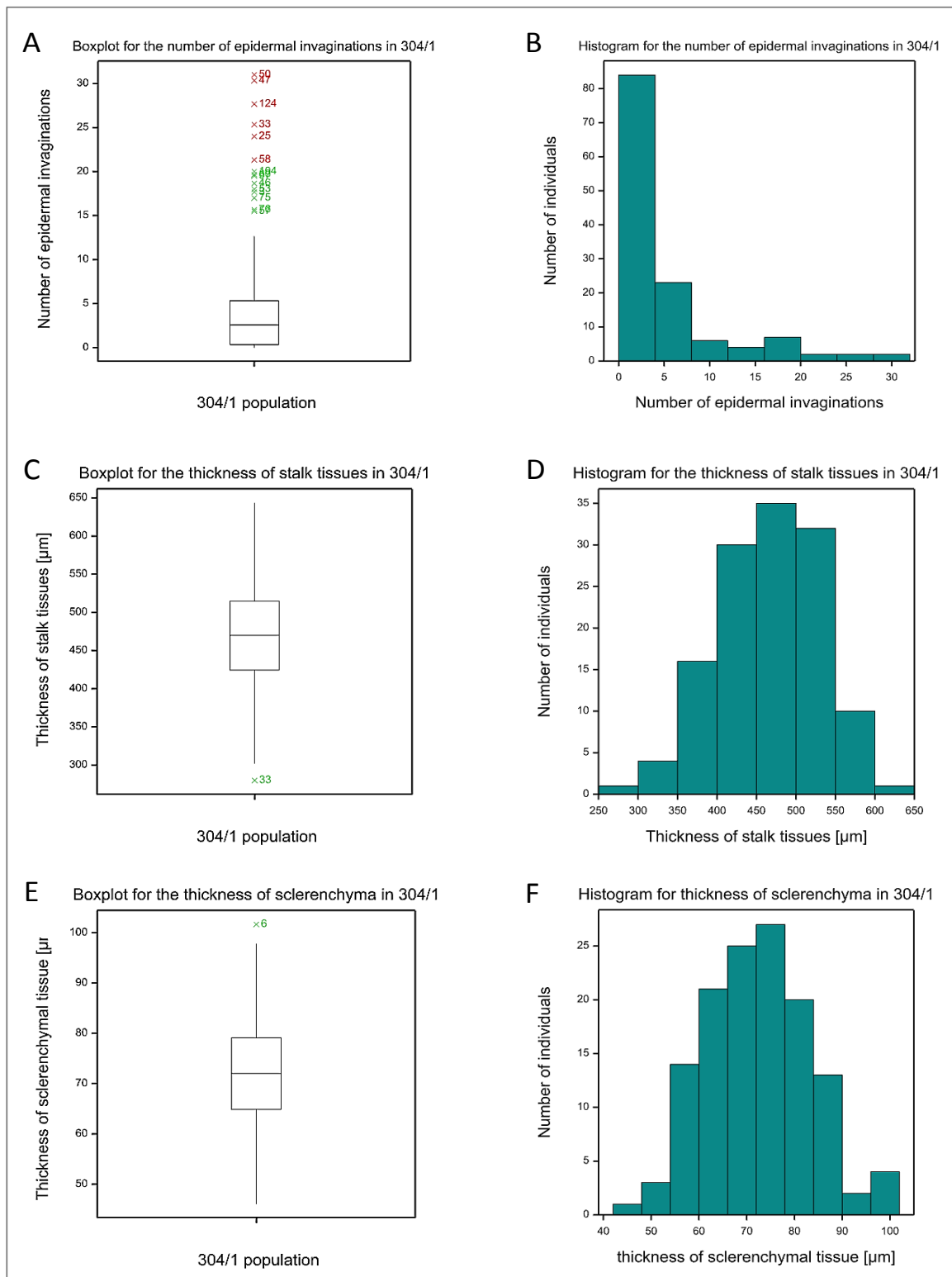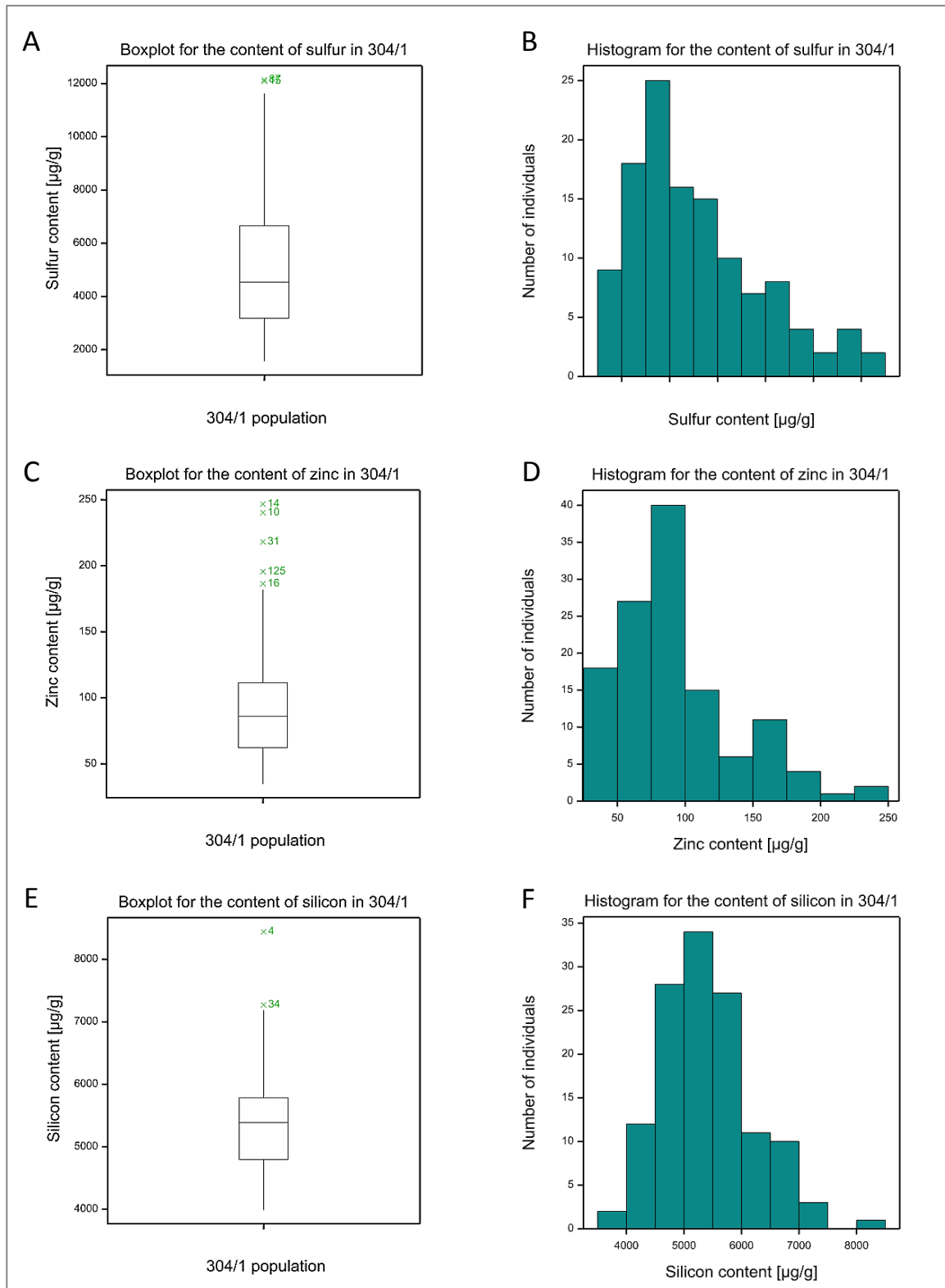
FIGURE 47 Boxplots showing median value with whiskers indicating variability outside the upper and lower quartiles in '304/1' F₂ population for the number of epidermal invaginations (A), the thickness of stalk tissues (C), and the thickness of sclerenchyma (E). The distribution of traits in F₂ population: the number of epidermal invaginations (B), the thickness of stalk tissues (D), the thickness of sclerenchyma (F).
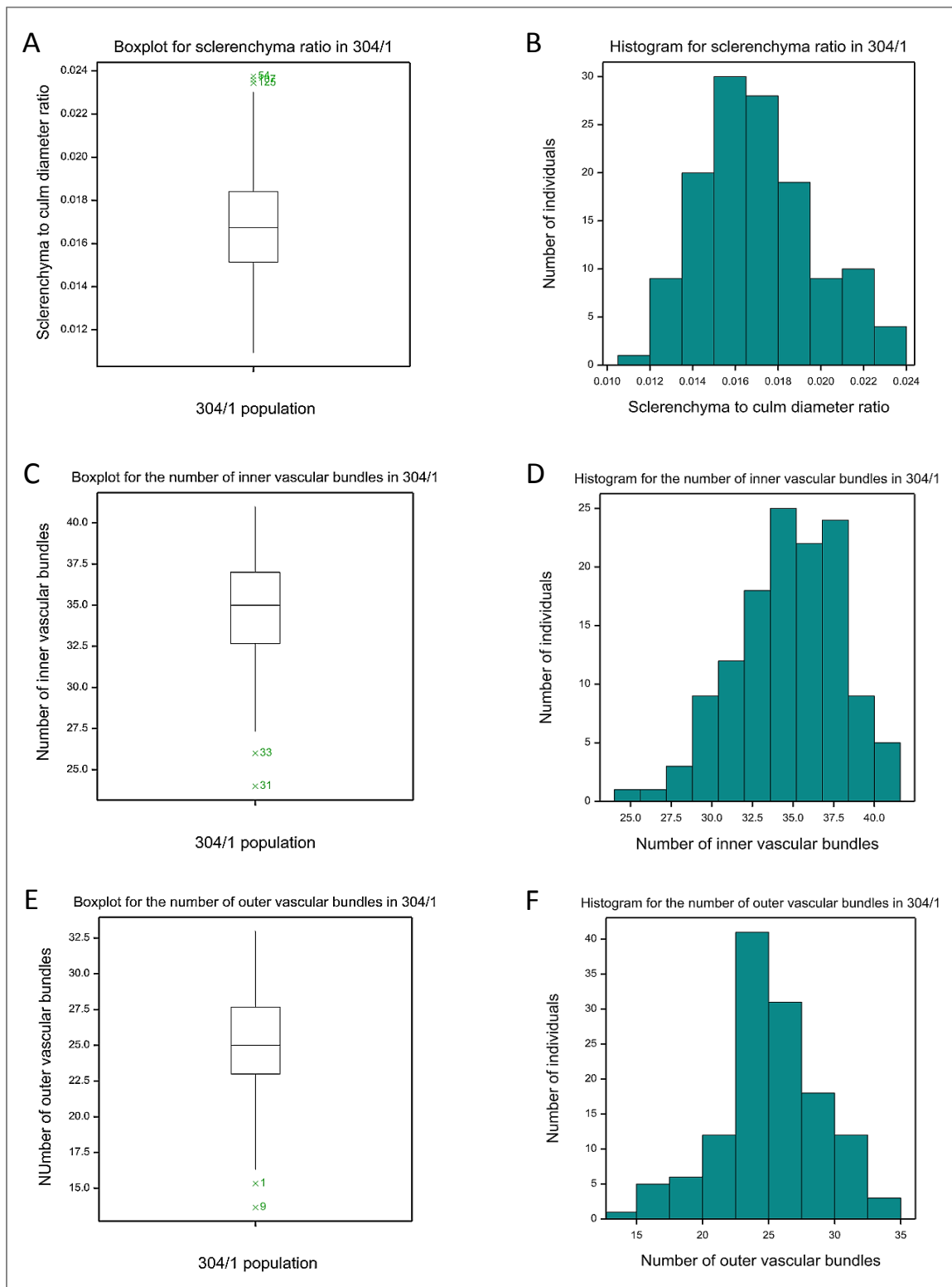
FIGURE 48 Boxplots showing median value with whiskers indicating variability outside the upper and lower quartiles in '304/1' F_2 population for the sclerenchyma to diameter ratio A), the number of inner vascular bundles (C), and the number of outer vascular bundles (E). The distribution of traits in F_2 population: the sclerenchyma to diameter ratio (B), the number of inner vascular bundles (D), the number of outer vascular bundles (F).
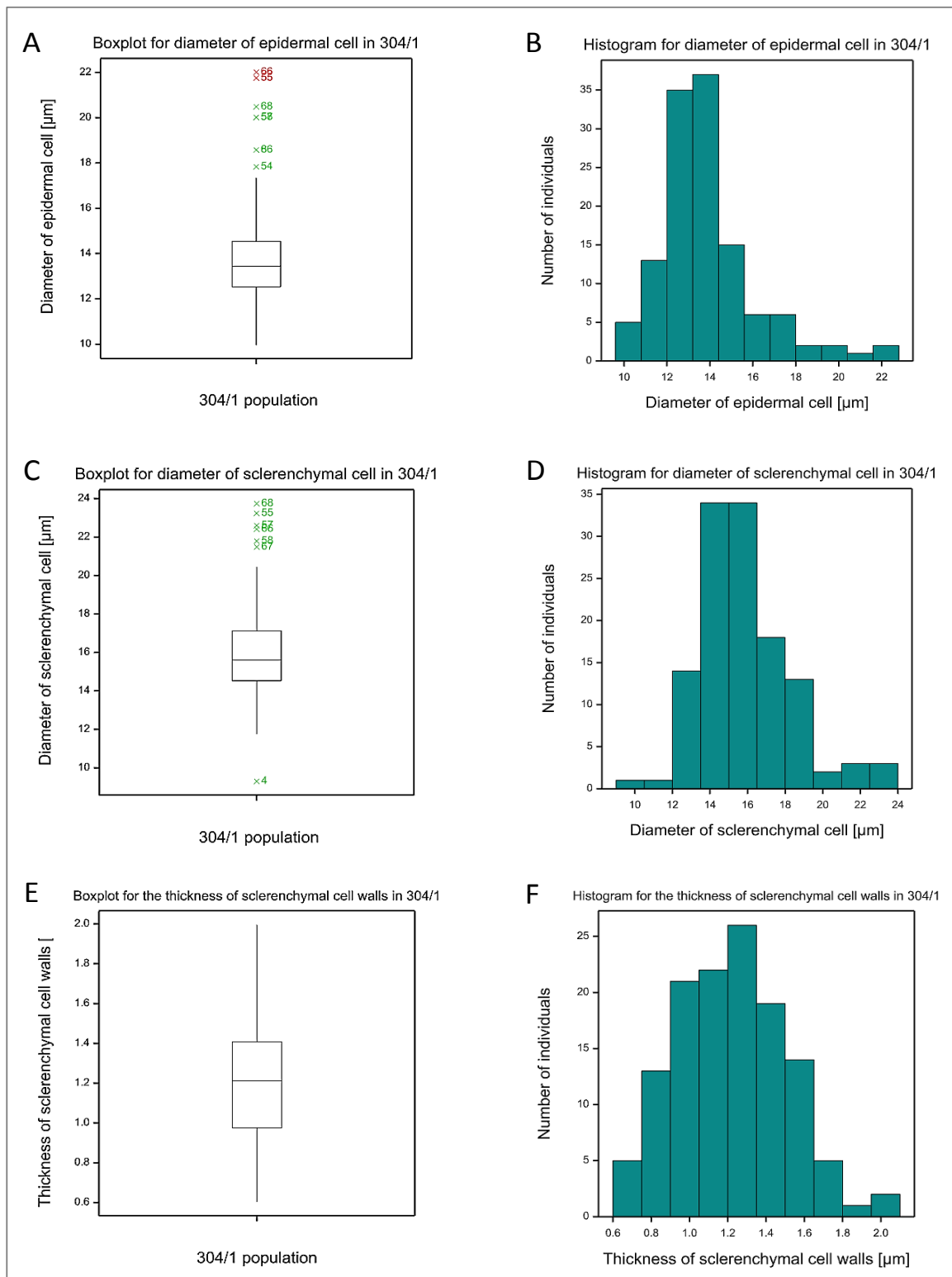
FIGURE 49 Boxplots showing median value with whiskers indicating variability outside the upper and lower quartiles in '304/1' F₂ population for the diameter of the epidermal cell (A), the diameter of the sclerenchymal cell (C), and the thickness of sclerenchymal cell wall (E). The distribution of traits in F₂ population: the diameter of the epidermal cell (B), the diameter of the sclerenchymal cell (D), the thickness of sclerenchymal cell wall (F).

FIGURE 50 Boxplots showing median value with whiskers indicating variability outside the upper and lower quartiles in '304/1' F_2 population for the thickness of inner periclinal cell wall of the epidermis (A), the content of boron (C), and the content of iron (E). The distribution of traits in F_2 population: the thickness of inner periclinal cell wall of the epidermis (B), the content of boron (D), the content of iron (F).

FIGURE 51 Boxplots showing median value with whiskers indicating variability outside the upper and lower quartiles in '304/1' F_2 population for the content of molybdenum (A), nickel (C), and phosphorus (E). The distribution of traits in F_2 population: the content of molybdenum (B), nickel (D), and phosphorus (F).

FIGURE 52 Boxplots showing median value with whiskers indicating variability outside the upper and lower quartiles in '304/1' F$_2$ population for the content of sodium (A), calcium (C), and copper (E). The distribution of traits in F$_2$ population: the content of sodium (B), calcium (D), copper (F).

FIGURE 53 Boxplots showing median value with whiskers indicating variability outside the upper and lower quartiles in '304/1' F$_2$ population for the content of potassium (A), magnesium (C), and manganese (E). The distribution of traits in F$_2$ population: the content of potassium (B), magnesium (D), manganese (F).

FIGURE 54 Boxplots showing median value with whiskers indicating variability outside the upper and lower quartiles in '304/1' F$_2$ population for the content of sulfur (A), zinc (C), and silicon (E). The distribution of traits in F$_2$ population: the content of sulfur (B), zinc (D), silicon (F).
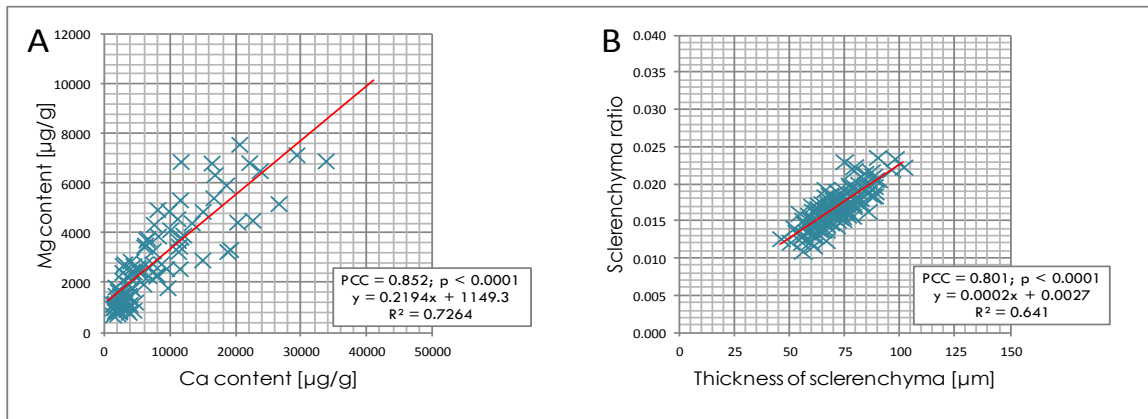
FIGURE 55 Very strong positive correlations between the content of calcium and magnesium (**A**), and sclerenchyma ratio and thickness of sclerenchyma (**B**).
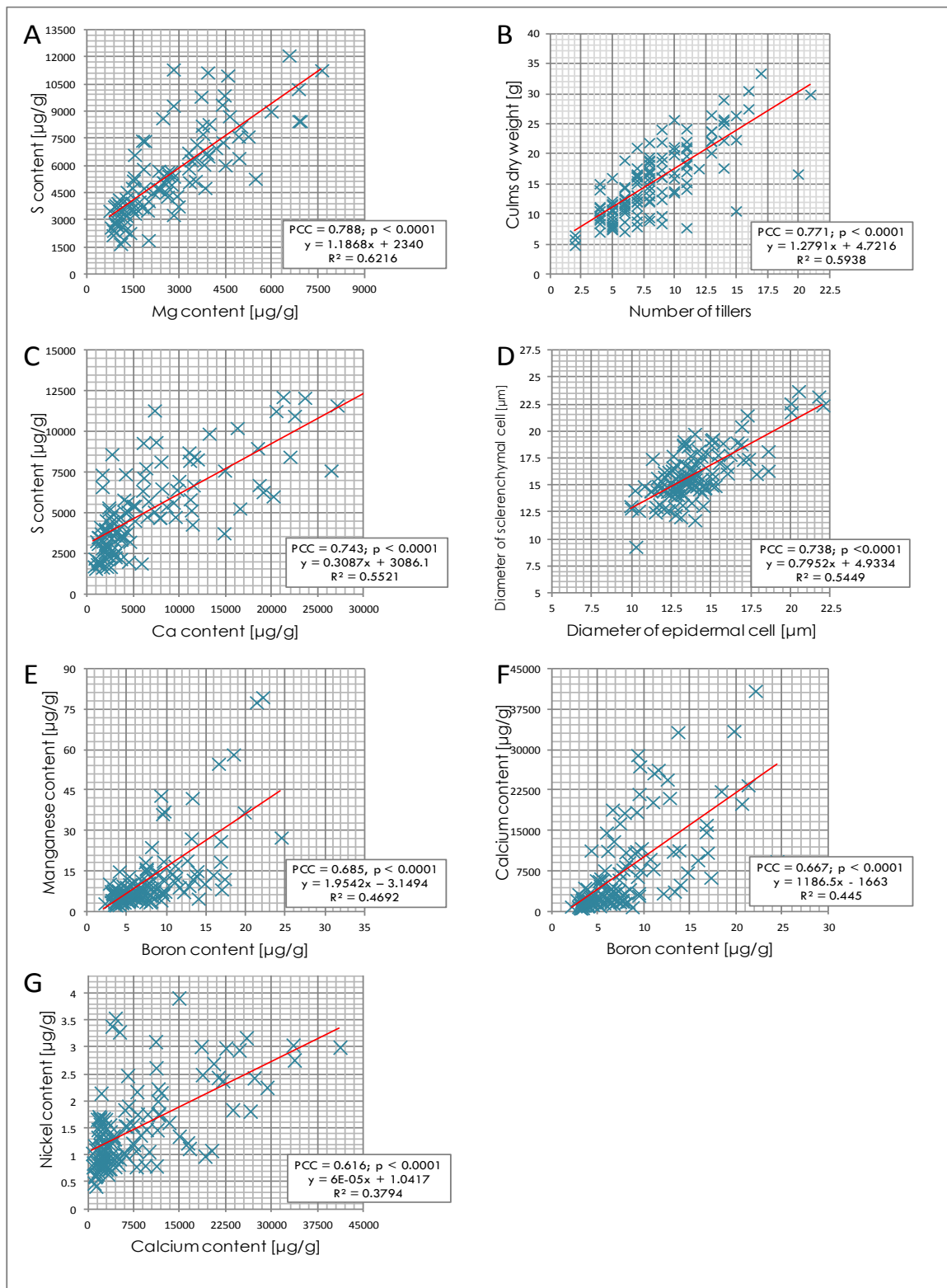
FIGURE 56 Strong positive correlations between: the content of magnesium and sulfur (**A**), the number of tillers and culms dry weight (**B**), the content of calcium and sulfur (**C**), the diameter of epidermal and sclerenchymal cell (**D**), the content of boron and manganese (**E**), the content of boron and calcium (**F**), and the content of calcium and nickel (**G**).
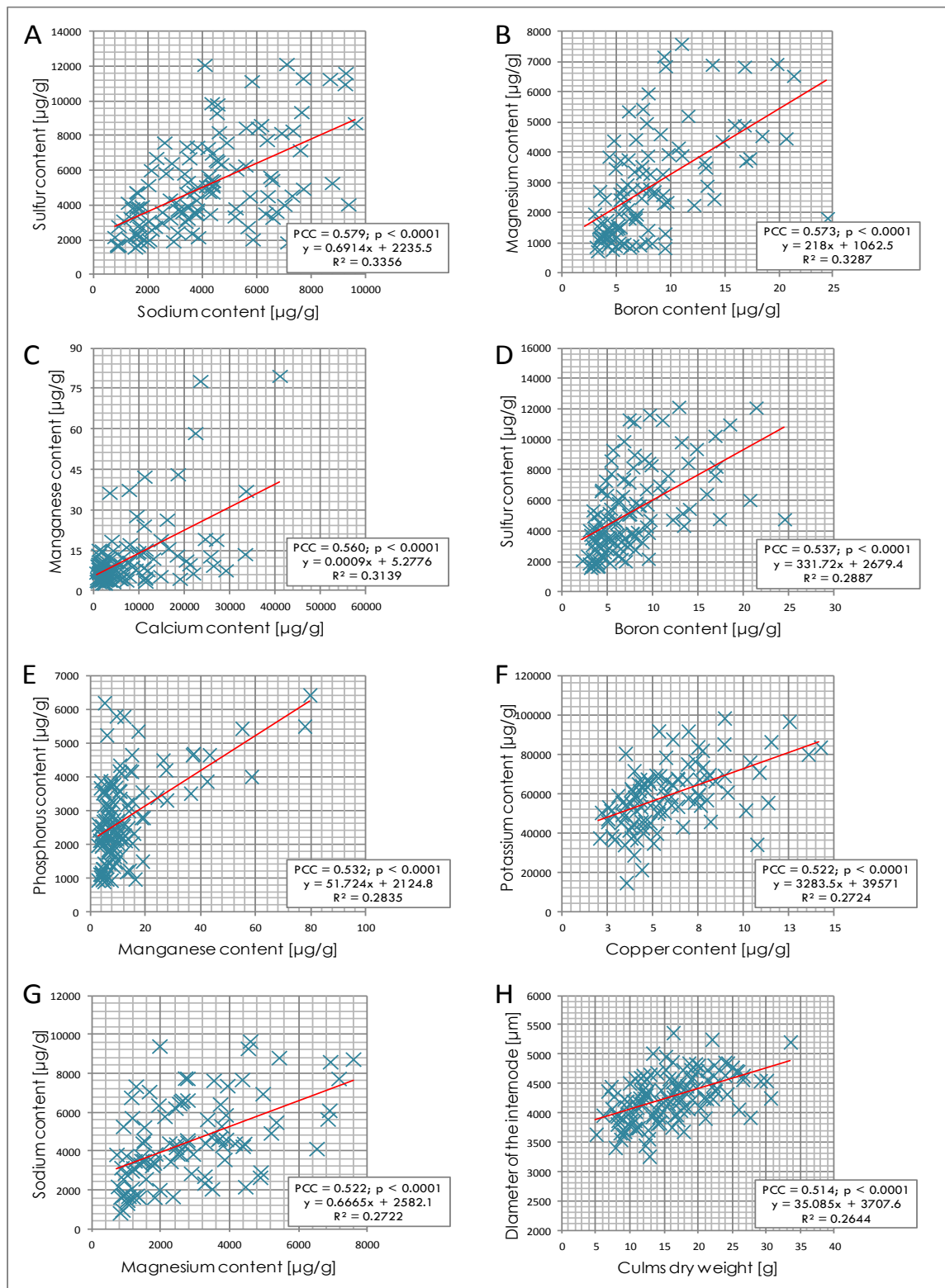
FIGURE 57 Moderate positive correlations between: the content of sulfur and sodium (**A**), the content of boron and magnesium (**B**), the content of manganese and calcium (**C**), the content of boron and sulfur (**D**), the content of manganese and phosphorus (**E**), the content of copper and potassium (**F**), the content of magnesium and sodium (**G**), dry weight of culms and diameter of the second basal internode (**H**).
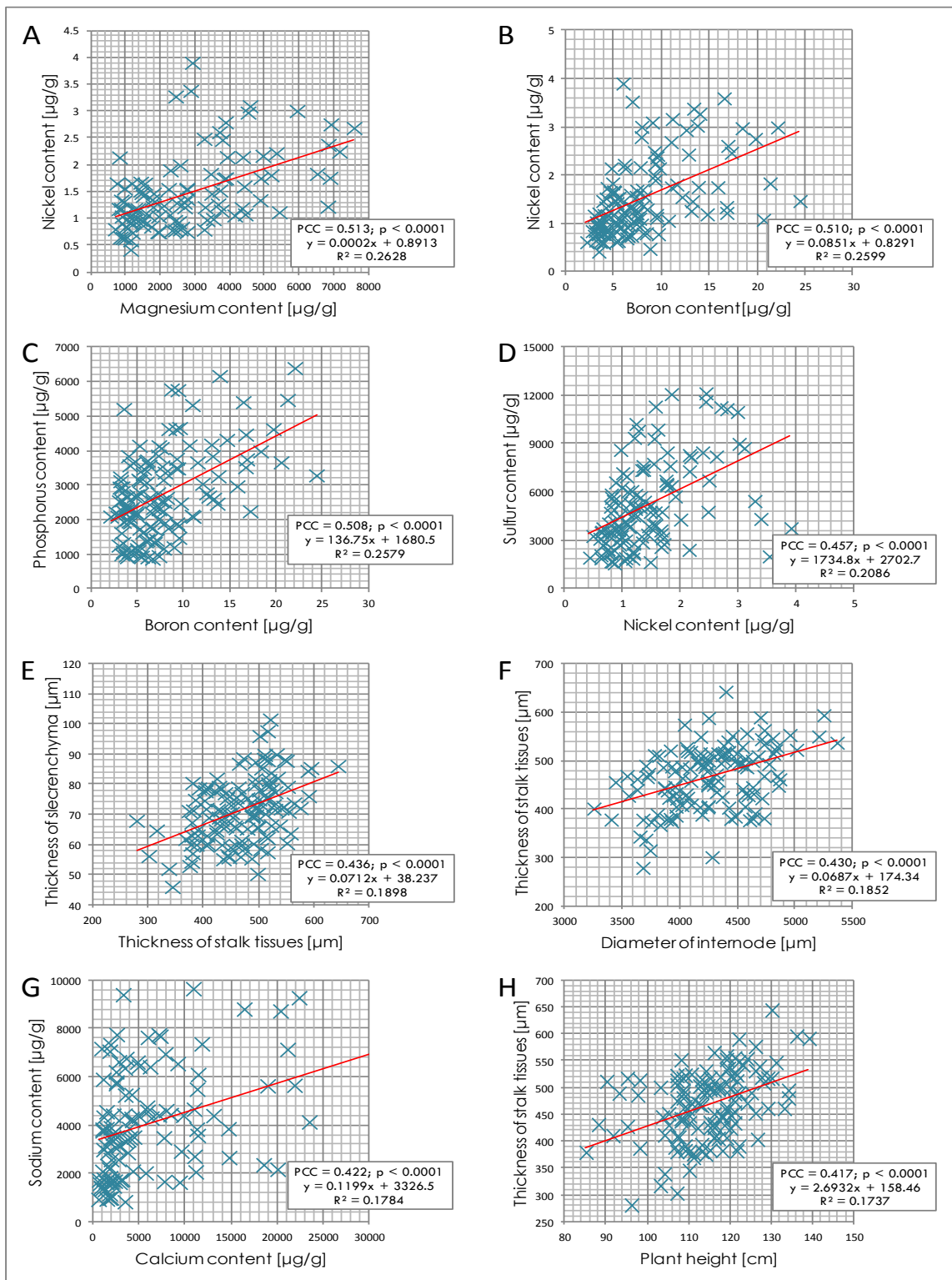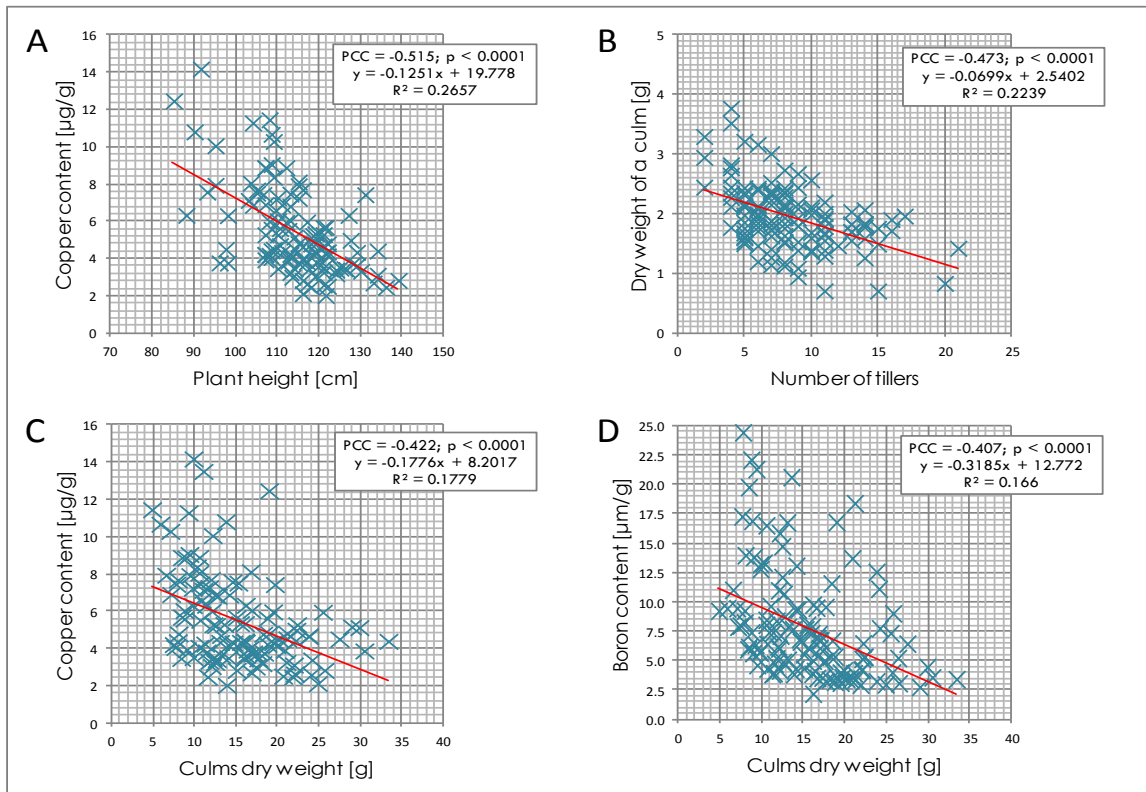
FIGURE 58 Moderate positive correlations between: the content of nickel and magnesium (**A**), the content of boron and nickel (**B**), the content of boron and phosphorus (**C**), the content of nickel and sulfur (**D**), the thickness of stalk tissues and sclerenchymal tissue layer (**E**), the diameter of the second basal internode and the thickness of stalk tissues (**F**), the content of calcium and sodium (**G**), and plant height and the thickness of stalk tissues (**H**).
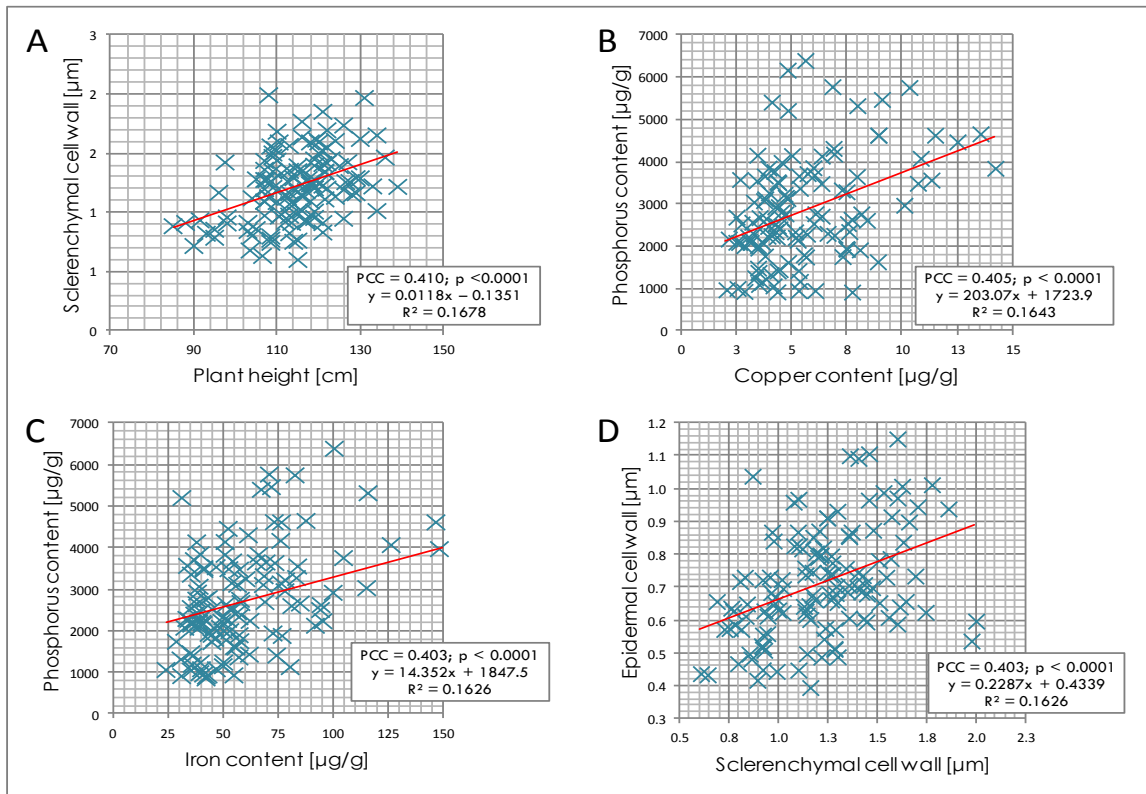
FIGURE 59 Moderate positive correlations between: plant height and the thickness of sclerenchymal cell wall (**A**), the content of copper and phosphorus (**B**), the content of iron and phosphorus (**C**), and the thickness of sclerenchymal and inner periclinal cell wall of the epidermis (**D**).

FIGURE 60 Moderate negative correlations between: plant height and the content of copper (**A**), mean dry weight of a single culm and the number of tillers (**B**), dry weight of culms and the content of copper (**C**), and between dry weight of culms and the content of boron (**D**).
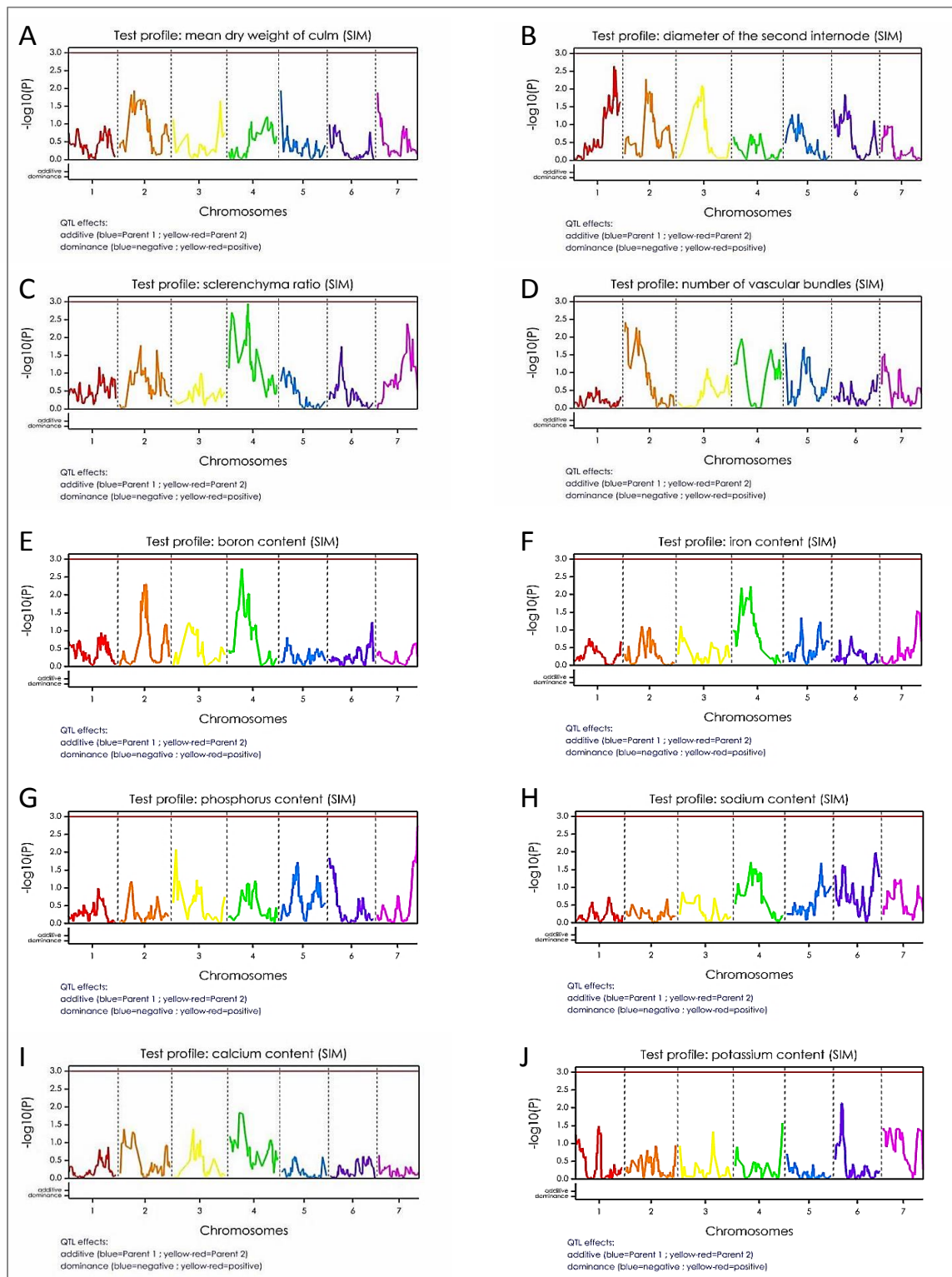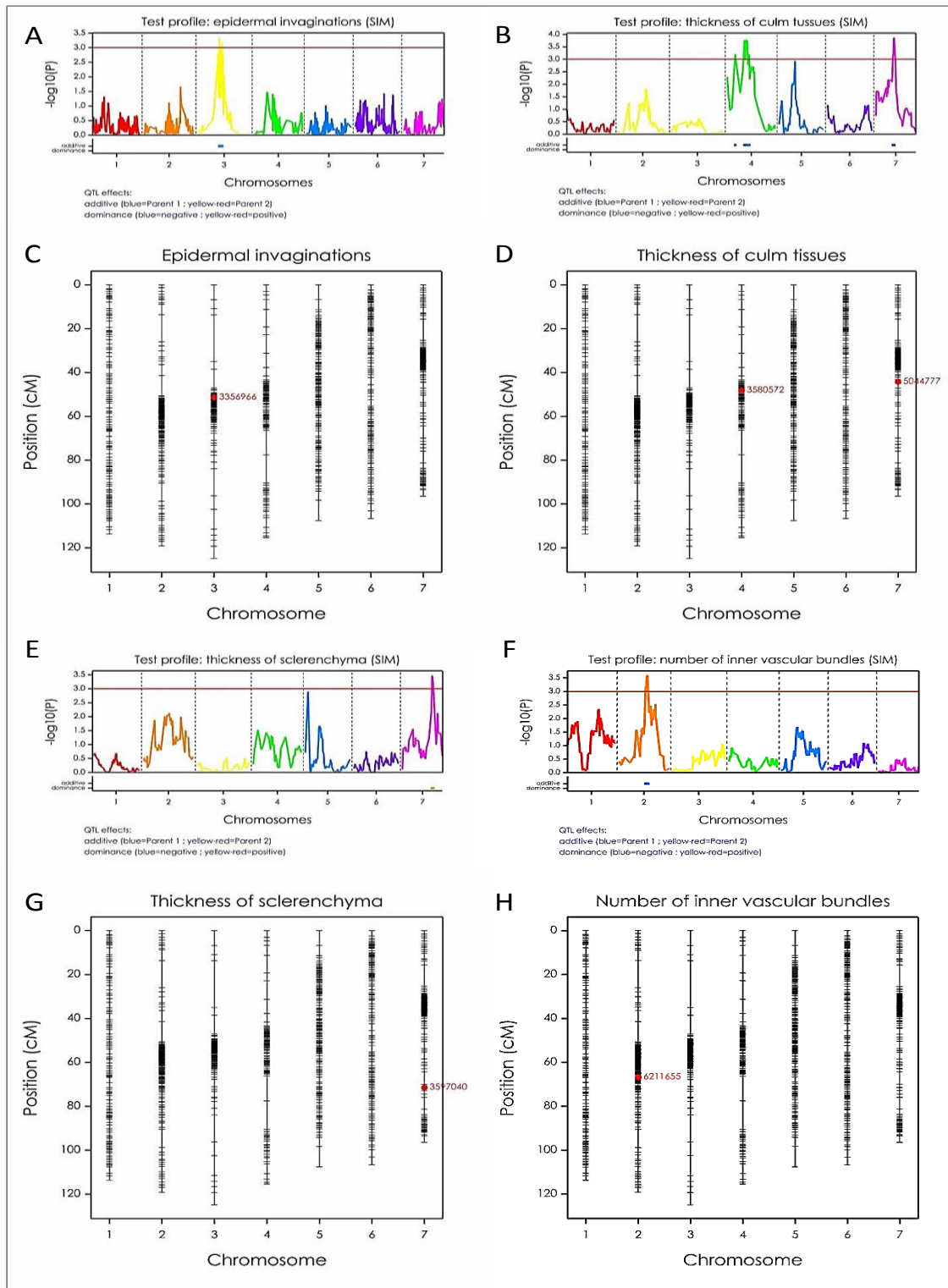
FIGURE 61 Genome-wide Simple Interval Mapping to check association of mapped markers with mean dry weight of a single culm (**A**), the diameter of the second basal internode (**B**), sclerenchyma ratio (**C**), the number of vascular bundles (**D**), boron content (**E**), iron content (**F**), phosphorus content (**G**), sodium content (**H**), calcium content (**I**), and potassium content (**J**).
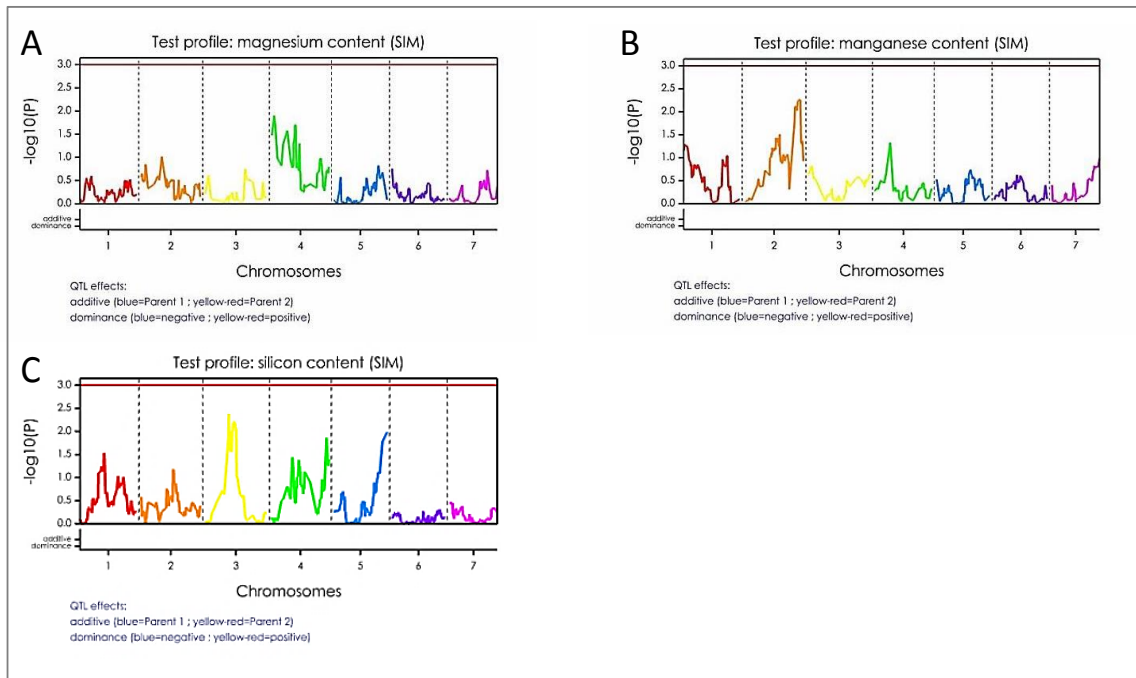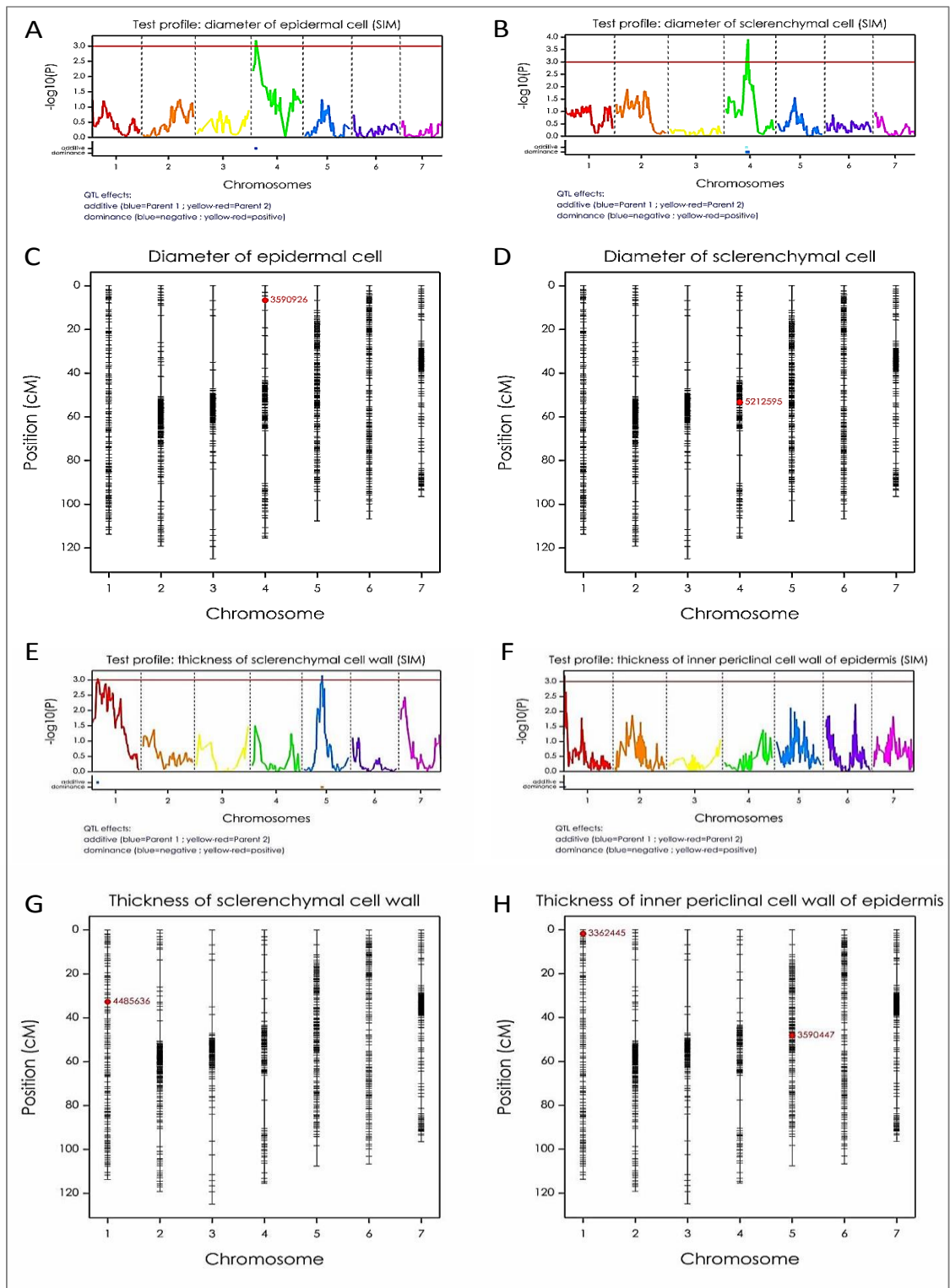
FIGURE 62 Genome-wide Simple Interval Mapping to check association of mapped markers with magnesium content (**A**), manganese content (**B**), and silicon content (**C**).
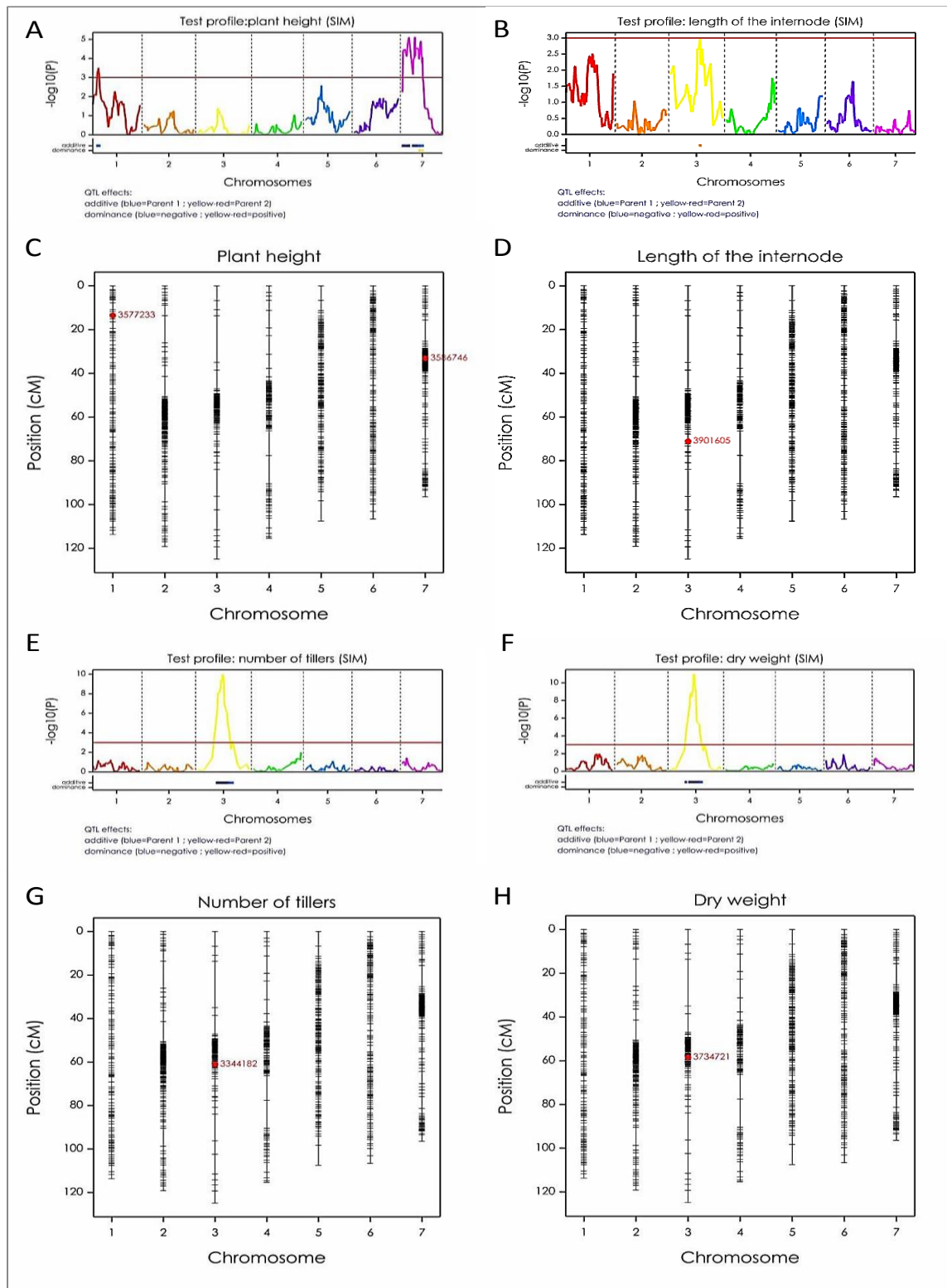
FIGURE 63 Genome-wide Simple Interval Mapping to check association of mapped markers with plant height (**A**) the length of the second basal internode (**B**), the number of tillers (**E**), and dry weight of culms (**F**). The final model of QTL for plant height (**C**), the length of the second basal internode (**D**), the number of tillers (**G**), and dry weight of culms (**H**) based on a set of QTL candidates using backward selection.
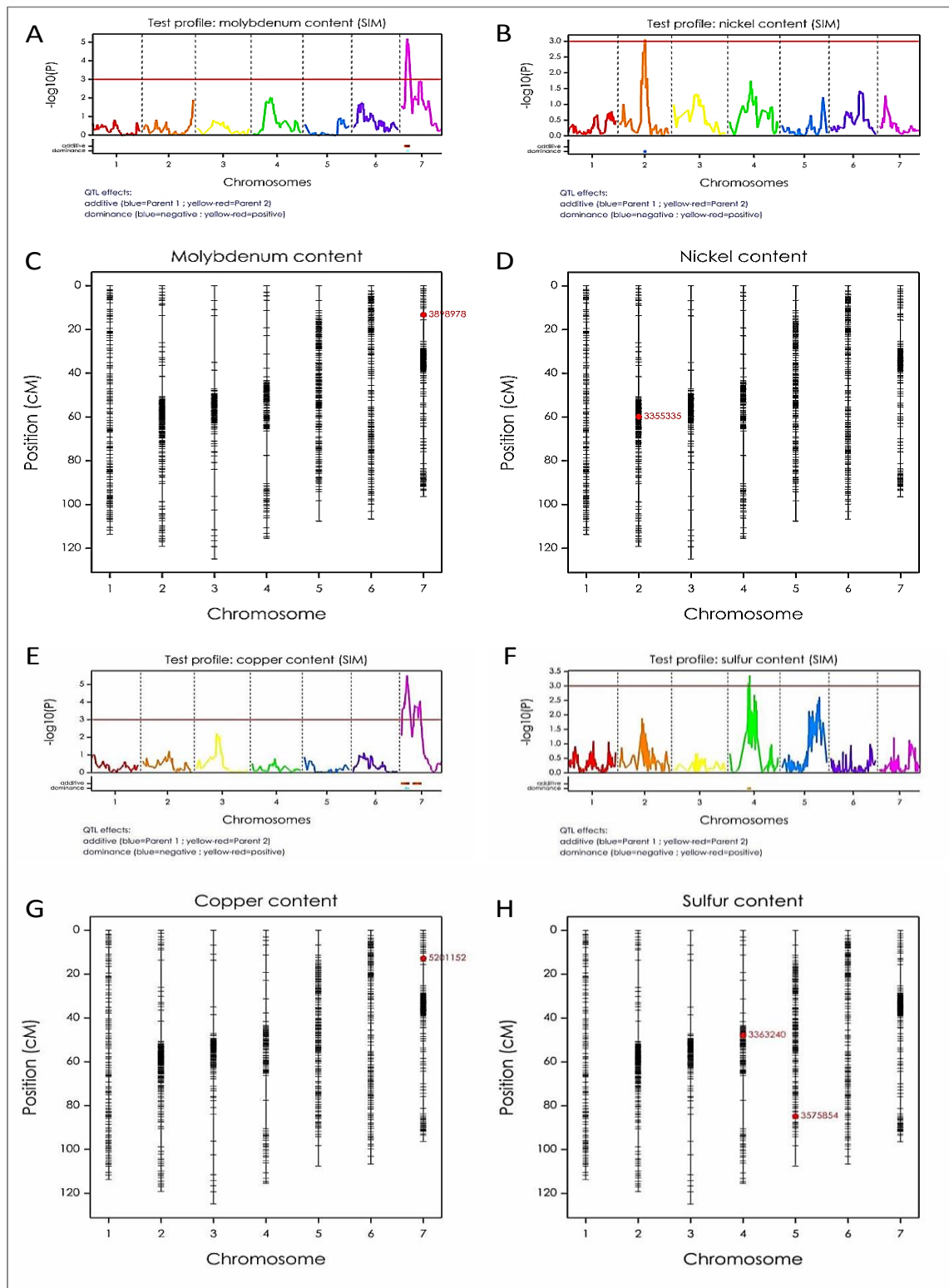
FIGURE 64 Genome-wide Simple Interval Mapping to check association of mapped markers with the number of epidermal invaginations (**A**) the thickness of culm tissues (**B**), the thickness of sclerenchyma (**E**), and the number of inner vascular bundles (**F**). The final model of QTL for the number of epidermal invaginations (**C**), the thickness of culm tissues (**D**), the thickness of sclerenchyma (**G**), and the number of inner vascular bundles (**H**) based on a set of QTL candidates using backward selection.
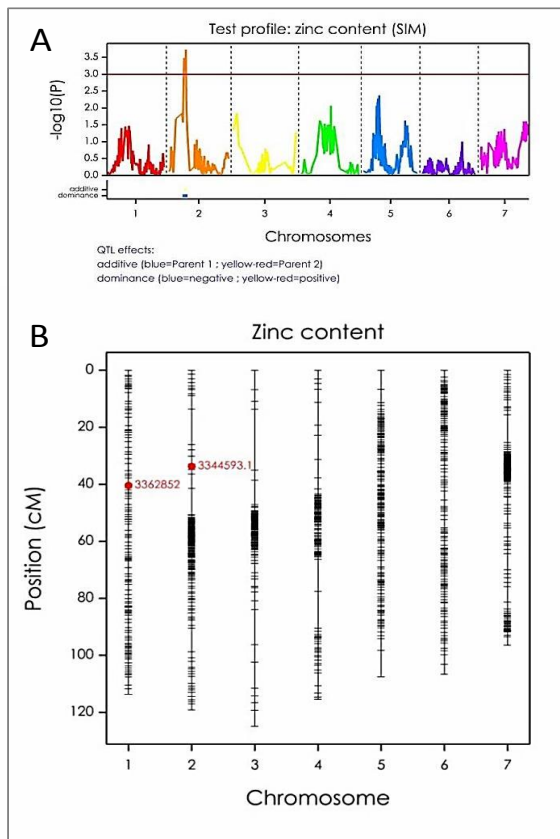
FIGURE 65 Genome-wide Simple Interval Mapping to check association of mapped markers with the diameter of the epidermal cell (**A**) the diameter of the sclerenchymal cell (**B**), the thickness of sclerenchymal cell wall (**E**), and the thickness of the inner periclinal cell wall of the epidermis (**F**). The final model of QTL for the diameter of the epidermal cell (**C**), the diameter of the sclerenchymal cell (**D**), the thickness of sclerenchymal cell wall (**G**), and the thickness of the inner periclinal cell wall of the epidermis (**H**) based on a set of QTL candidates using backward selection.

FIGURE 66 Genome-wide Simple Interval Mapping to check association of mapped markers with the content of molybdenum (**A**), the content of nickel (**B**), the content of copper (**E**), and the content of sulfur (**F**). The final model of QTL for the content of molybdenum (**C**), the content of nickel (**D**), the content of copper (**G**), and the content of sulfur (**H**) based on a set of QTL candidates using backward selection.

FIGURE 67 Genome-wide Simple Interval Mapping to check association of mapped markers with the content of zinc (**A**) and the final model of QTL for the content of zinc (**B**), based on a set of QTL candidates using backward selection.

10. List of Publications

Marzec M, **Muszynska** A. 2015. In Silico Analysis of the Genes Encoding Proteins that Are Involved in the Biosynthesis of the RMS/MAX/D Pathway Revealed New Roles of Strigolactones in Plants. *International Journal of Molecular Sciences*, 16: 6757-6782.

Muszyńska A, Jarocka K, Kurczyńska EU. 2014. Plasma membrane and cell wall properties of an aspen hybrid (*Populus tremula* x *tremuloides*) parenchyma cells under the influence of salt stress. *Acta Physiologiae Plantarum*, 36 (5): 1155-1165.

Marzec M, **Muszynska** A, Melzer M, Sas-Nowosielska H, Kurczynska EU. 2013. Increased symplasmic permeability in barley root epidermal cells correlates with defects in root hair development. *Plant Biology*, 16: 476-484.

Marzec M, **Muszynska** A, Gruszka D. 2013. The Role of Strigolactones in Nutrient-Stress Responses in Plants. *International Journal of Molecular Sciences*, 14: 9286-9304.

Marzec M, **Muszynska** A. 2012. Strigolactones - new candidates for plant hormones. *Postępy Biologii Komórki*, 39: 63-86.

Przedpełska E, **Muszyńska** A, Polatajko A, Kurczyńska EU, Wierzbicka M. 2008. Influence of cadmium stress on aquaporins activity in *Arabidopsis halleri* (L.) O`Kane & Al-Shehbaz ssp *halleri* cells. Volume X of Metal Ions in Biology and Medicine (John Libbey Eurotext, Paris).

11. List of Proceedings

Muszynska A., A. Börner, G. Melz, M. S. Röder, M. Melzer. Poster: Survival of the fittest: how 'Stabilstroh' became lodging resistant. Plant Biology 2017, Honolulu, Hawaii, USA, June 24th-28th, 2017.

Muszynska A, Röder MS, Börner A, Melz G, Rutten T, Melzer M. Poster: Identification of the genetic traits responsible for 'Stabilstroh' phenotype. EUCARPIA Cereals Section: International Conference on Rye Breeding and Genetics, Wrocław, Poland, June 24th-26th, 2015.

Muszynska A, Röder MS, Börner A, Melz G, Rutten T, Melzer M. Poster: QTL mapping of traits responsible for 'Stabilstroh' phenotype. 11th Plant Science Student Conference, Leibniz Institute of Plant Biochemistry, Halle, Germany, June 2nd -5th, 2015.

Muszynska A, Börner A, Melz G, Röder M, Rutten T, Hoffie K, Benecke M, Melzer M. Poster: Identification of the genetic traits responsible for 'Stabilstroh' phenotype. 18th International Microscopy Congress, Prague, Czech Republic, September 7th- 12th, 2014.

Marzec M, **Muszynska** A, Melzer M, Kurczynska E. Poster: Callose deposition plays a crucial role in barley rhizodermis cell differentiation. 18th International Microscopy Congress, Prague, Czech Republic, September 7th- 12th, 2014.

Muszynska A, Melzer M, Melz G, Röder M, Rutten T, Hoffie K, Benecke M, Börner A. Poster: 'Stabilstroh': A new hope for lodging resistance. Joint Eucarpia Cereal Section & ITMI Conference, Wernigerode, Germany, June 29th–July 4th, 2014.

Muszynska A, Börner A, Melz G, Röder M, Rutten T, Hoffie K, Benecke M, Melzer M. Poster: 'Stabilstroh': A New Hope for Lodging Resistance. Plant Biology Europe FESPB/EPSO 2014 Congress, Dublin, Ireland, June 22nd-26th, 2014.

Marzec M, **Muszynska** A, Melzer M, Kurczynska E. Poster: Symplasmic Communication during Root Epidermal Cell Differentiation. Plant Biology Europe FESPB/EPSO 2014 Congress, Dublin, Ireland, June 22nd-26th, 2014.

Muszynska A, Börner A, Melz G, Röder M, Rutten T, Hoffie K, Benecke M, Melzer M. Oral presentation: The stronger always succeeds: How 'Stabilstroh' became lodging resistant. 10th Plant Science Student Conference, IPK Gatersleben, Germany, June 2nd-5th, 2014.

Muszynska A, Börner A, Melz G, Röder M, Rutten T, Hoffie K, Benecke M, Melzer M. Poster: Histology and Ultrastructure of a New Lodging Resistant Genotype of Rye. 7th EPSO Conference 'Plants for a Greening Economy', Porto Heli, Greece, September 1st-4th, 2013.

Marzec M, **Muszynska** A, Melzer M, Sas-Nowosielska H, Kurczynska E. Poster: Increased symplasmic permeability in barley root epidermal cells correlates with defects in root hair development. 7th EPSO Conference 'Plants for a Greening Economy', Porto Heli, Greece, September 1st-4th, 2013.

Muszynska A, Börner A, Melz G, Röder M, Rutten T, Hoffie K, Benecke M, Melzer M. Oral presentation: Histological and Ultrastructural Analysis of „Stabilstroh", a new Genotype of Rye (Secale cereale L.). 9th Plant Science Student Conference, Leibniz Institute of Plant Biochemistry, Halle, Germany, May 28th-31st, 2013.

Marzec M, Melzer M, Potocka I, **Muszynska** A, Rutten T, Szarejko I. Poster: Arabinogalactan proteins with epitopes containing glucuronic acid are involved in root hair development in *Hordeum vulgare*. Plant Biology Congress, Freiburg, July 29th- August 3rd, 2012.

Muszynska A, Jarocka K, Kurczynska EU. Poster: „The influence of salt stress on turgor pressure and cell wall properties of an aspen hybrid (*Populus tremula* x *tremuloides*) parenchyma cells. 8th Plant Science Student Conference, June 4th-7th, 2012.

Marzec M, **Muszyńska** A, Sas-Nowosielska H. Poster: Symplasmic isolation plays a key role in differentiation of barley root hairs. 6th Plant Science Student Conference 'All You Need Is Plant', IPK Gatersleben, Germany, June 16th-18th, 2010.

Przedpełska E, **Muszyńska** A, Polatajko A, Kurczyńska EU, Wierzbicka M. Poster: Influence of cadmium stress on aquaporins activity in *Arabidopsis halleri* (L.) O`Kane & Al-Shehbaz ssp *halleri* cells. 10th International Symposium on Metal Ions in Biology and Medicine, Bastia, France, May 19th-22nd, 2008.

Wiera B, **Muszyńska** A. Poster: Water relations in control and mercury treated cortical cells of sunflower hypocotyls (*Helianthus annuus* L.). 14th FESPB Congress, Cracow, August 24th-27th, 2004.

12. Declaration

I hereby declare that this thesis has been written by me without having used other than mentioned references and resources. This thesis has been submitted in neither its original nor similar form for the purpose of academic examination.

Hiermit erkläre ich, dass ich diese Arbeit selbständig und nur unter Zuhilfenahme der angegebenen Hilfsmittel und Literatur angefertigt habe. Ich versichere, dass diese Arbeit von mir bisher weder der Naturwissenschaftliche Fakultät III - Agrar- und Ernährungswissenschaften, Geowissenschaften und Informatik der Martin-Luther-Universität Halle-Wittenberg noch einer anderen wissenschaftlichen Einrichtung zum Zweck der Promotion eingereicht wurde.

Gatersleben, den ....   _____

                                                            Aleksandra Muszynska

13. Curriculum vitae

<u>Personal information:</u>

Name: Aleksandra Muszyńska
Address: 06466, Hans-Stubbe Str. 18, Gatersleben, Germany
Phone/E-mail: +49(0)394825560; aleksandra.muszynska@gmail.com;
muszynska@ipk-gatersleben.de
Date of Birth: November 5, 1981
Place of Birth: Świętochłowice, Poland

Academic education:

PhD (December 2012 – October 2017) Plant Breeding, Institut für Agrar- und
Ernährungswissenschaften, Martin Luther University, Halle, Germany, Thesis
prepared at Leibniz Institute of Plant Genetics and Crop Plant Research
(IPK), Structural Cell Biology group, Gatersleben, Germany

Thesis title: Histological, ultrastructural, elemental, and molecular genetic
characterization of 'Stabilstroh', a complex trait of rye (*Secale cereale* L.)
determining lodging resistance.

M.Sc. (October 2000 – July 2005) University of Silesia in Katowice, Faculty of Biology
and Environmental Protection, Department of Biophysics and Cell Biology,
Katowice, Poland.

Thesis title: Influence of turgor pressure on the aquaporin water channels activity
of sunflower (*Helianthus annuus* L) hypocotyl cortex cells.

Employment:

2016- Researcher at Leibniz Institute of Plant Genetics and Crop Plant
Research (IPK), Assimilate Allocation and NMR Group, Gatersleben,
Germany.

2012-2015 PhD student at Leibniz Institute of Plant Genetics and Crop Plant
Research (IPK), Structural Cell Biology Group, Gatersleben,
Germany.

Project: 'Molecular genetic and histological characterization of the trait
'Stabilstroh' in rye'.

2006 – 2010   Research Assistant at University of Silesia, Faculty of Biology and Environmental Protection, Laboratory of Cell Biology, Poland.

Projects: 'Environmental pollution and the physiological status of plant cells with particular emphasis on the functional state of aquaporin water channels';

'Apoplast of plant cells, the structure and function';

'Analysis of histological changes and symplastic communication during somatic embryogenesis in *Arabidopsis thaliana.'*

2005 – 2006   Research Assistant at University of Silesia, Faculty of Biology and Environmental Protection, Department of Biophysics and Cell Biology, Poland.

Researching the influence of turgor pressure and cadmium stress on aquaporins activity.

Internships and courses:

2014   'Journal of Microscopy Author Workshop', Prague, Czech Republic.

2012   'Map Construction and QTL Analysis in Plants', the course organised by Department of Plant and Environmental Studies, University of Copenhagen, Denmark.

2009   two-month internship in Applied Plant Sciences Group, Technical University in Darmstadt, Germany.

2008   'Genomics and Proteomics', the workshop organised by MBS Molecular Biology Services, Warsaw, Poland.

2008   'Meiosis', the workshop organised jointly by Institute of Biological Sciences, Aberystwyth University (United Kingdom) and the Department of Plant Anatomy and Cytology, University of Silesia in Katowice, Poland.

2005   'Handling of autoclaves', University of Silesia in Katowice, Poland.

2004/05 six-month internship in Pflanzenökologie Group (Prof. Steudle Group), University of Bayreuth, Germany.

2004   International 'Pressure Probe Technique Course' organised by Institute of Plant Ecophysiology (University of Bayreuth) in cooperation with Department of Biophysics and Cell Biology (University of Silesia), Katowice, Poland.

Awards and grants

2014   The Federation of European Societies of Plant Biology (FESPB) Travel Grant for graduate students.

2007-2010 Polish Ministry of Science and Higher Education research grant ('Analysis of histological changes and symplastic communication during somatic embryogenesis in Arabidopsis thaliana", **contractor**).

2009   Two-month internship in the Technical University in Darmstadt funded under UPGOW program (a part of European Structural Funds).

2007-2008 University of Silesia Rector's research grant ('Apoplast of plant cells, the structure and function', **contractor**).

2006   University of Silesia Rector's research grant ('Environmental pollution and the physiological status of plant cells with particular emphasis on the functional state of aquaporin water channels', the **main contractor**).

2004/05 six-month Socrates/Erasmus scholarship (University of Bayreuth, Germany).

2003-05 University of Silesia Rector's scholarships (in the academic year 2003/04 and 2004/05); awarded for the academic achievement.